2011

NUMERICAL INVESTIGATION OF THE UNDRAINED PULLOUT CAPACITY OF ANCHORS EMBEDDED IN CLAY

Ahmed M. Fahmy

NUMERICAL INVESTIGATION OF THE UNDRAINED PULLOUT CAPACITY OF ANCHORS EMBEDDED IN CLAY

(Spine title: Numerical investigation of anchors)

(Thesis format: Integrated Article)

by

Ahmed M. Fahmy

Graduate Program in Engineering Science
Department of Civil and Environmental Engineering

A thesis submitted in partial fulfillment
of the requirements for the degree of
Master of Engineering Science

The School of Graduate and Postdoctoral Studies
The University of Western Ontario
London, Ontario, Canada

THE UNIVERSITY OF WESTERN ONTARIO
SCHOOL OF GRADUATE AND POSTDOCTORAL STUDIES

CERTIFICATE OF EXAMINATION

Supervisors	Examiners
Dr. Timothy A. Newson	Dr. H. El Naggar
Dr. John R. de Bruyn	Dr. J. Q. Shang
	Dr. S. D. Hinchberger

The thesis by

Ahmed M. Fahmy

entitled:

NUMERICAL INVESTIGATION OF THE UNDRAINED PULLOUT CAPACITY OF ANCHORS EMBEDDED IN CLAY

is accepted in partial fulfillment of the
requirements for the degree of
Master of Engineering Science

Date	Chair of the Thesis Examination Board

ABSTRACT

Two dimensional plane strain finite element analysis has been conducted to simulate the pullout behavior of vertical anchors of different shapes when embedded in clay. These shapes include plate anchors, anchors with irregular base shapes, and plate anchors with rectangular openings. For the first two types, the effects on the pullout behavior of embedment depth, overburden pressure, soil-anchor interface strength, anchor thickness, base shape and size, rate of clay strength increase, anchor and load inclination, point of load application and soil disturbance due to anchor installation were all studied. The anchor pullout capacity is shown to be strongly affected by embedment depth, overburden pressure, load inclination angle, rate of clay shear strength increase per depth and soil-anchor interface strength. Similarly, disturbed clay strengths adjacent to the anchor following installation were found to cause a significant reduction in the anchor capacity. The effect of other parameters, such as the anchor thickness and the load application point, were found to be less significant. Among the studied base shapes, the triangular based anchors were found to have the greatest vertical pullout resistance, while the lateral pullout was not significantly improved for any of the studied shapes. This form of anchor was also shown to be the most efficient shape in terms of cross-sectional steel area compared to the pullout capacity. Normal and inclined load vertical and horizontal plate anchors with rectangular openings were studied at different embedment depths for no-breakaway and immediate breakaway conditions. For this anchor type, the embedment depth showed a significant effect on the efficiency for fully bonded conditions, but only a negligible effect for immediate breakaway conditions. The results suggest the feasibility of this anchor type as an alternative to regular plate anchors, especially for shallow offshore conditions, where limitations on cranage capacity exist.

KEYWORDS: Anchors; Pullout; Clay; Undrained; Numerical modeling, Parametric study; Irregular.

CO-AUTHORSHIP

This thesis has been prepared in accordance with the regulations for an Integrated-Article format thesis stipulated by the School of Graduate and Postdoctoral Studies at the University of Western Ontario and has been co-authored as:

Chapter 3: Numerical Investigation of The Undrained Capacity of Plate Anchors Embedded In Clay

All the numerical work was conducted by Ahmed M. Fahmy under close supervision of Dr. John R. de Bruyn and Dr. Timothy A. Newson. A paper co-authored by Ahmed M. Fahmy, John R. de Bruyn and Timothy A. Newson has been submitted to *The International Journal of Geomechanics.*

Chapter 4: Numerical Investigation of The Undrained Capacity of Enlarged Based Anchors Embedded In Clay

All the numerical work was conducted by Ahmed M. Fahmy under close supervision of Dr. Timothy A. Newson and Dr. John R. de Bruyn. A paper co-authored by Ahmed M. Fahmy, Timothy A. Newson and John R. de Bruyn will be submitted to *The Electronic Journal of Geotechnical Engineering.*

Chapter 5: Numerical Investigation of The Undrained Capacity of Anchors With Rectangular Openings Embedded In Clay

All the numerical work was conducted by Ahmed M. Fahmy under close supervision of Dr. Timothy A. Newson and Dr. John R. de Bruyn. A paper co-authored by Ahmed M. Fahmy, Timothy A. Newson and John R. de Bruyn will be submitted to *The International Journal of Offshore and Polar Engineering*

To the memory of my parents

ACKNOWLEDGEMENT

I would like to express my gratitude to all those who helped me throughout the past two years.

First, I am heartily thankful to my supervisor, Dr. Timothy A. Newson, for his continuous guidance, understanding and patience. It has been a privilege to work under his supervision.

Sincere thanks for Dr. John R. de Bruyn for his continuous help and valuable contribution. I wouldn't have finished this thesis without his support.

I would like to thank my parents. I can't find the suitable words to express my gratitude for all what they have done for me throughout their lives; I really wish they were here.

All the love and gratitude go to my adorable wife Sara. For all the time she spent reviewing my work day after day for the past two years, for the affection and care she has provided time and again, for believing in me when I had doubts, and above all, for the fact that she was always there for me.

I also owe my deepest gratitude to my sister Kadria and my brother Omar for their continuous support, encouragement and patience.

Special appreciation for all my friends who supported me and shared their valuable experience with me. Special thanks to Fadi Yassa.

Finally, none of this would have been possible without the love and patience of my family, specially my grandmother, for their continuous support and encouragement.

TABLE OF CONTENTS

LIST OF FIGURES

LIST OF TABLES

LIST OF SYMBOLS

A = Membrane surface area-deflated [m^2]

A' = Membrane surface area-inflated [m^2]

B = Anchor length [m]

b = width of the solid part of plate anchors with intermediate openings [m]

$C_{interface}$ = Shear strength at anchor interface [kN/m^2]

C_u = Clay undrained shear strength [kN/m^2]

C_{uo} = Initial clay undrained shear strength at ground surface [kN/m^2]

D = Caisson diameter [m]

D_s = Shaft diameter [m]

D_u = Underreamed diameter [m]

D_g = Depth to the barycentre of the anchor flukes [m]

E = Young's modulus [kN/m^2]

F_{ui} = Inflatable anchor membrane capacity-inflated membrane [kN]

F_{uo} = Inflatable anchor membrane capacity-deflated membrane [kN]

F_y = Non-dimensional uplift capacity factor

H = Embedment depth (distance from ground surface to anchor tip) [m]

H_c = Critical depth [m]

h = Distance between ground surface and anchor centre of mass [m]

K_o = Lateral earth pressure coefficient

L = Caisson length [m]

L_s = Shaft length [m]

N_c = Breakout factor

$\overline{N_c}$ = Breakout factor for unbonded condition

N_c* = Breakout factor for fully bonded condition

$N_{co\rho}$ = Inhomogeneous breakout factor

$N_{co\psi}$ = Breakout factor for inclined anchor in weightless soil

N_{co90} = Breakout factor for vertical anchor in weightless soil

N_v = Breakout factor in the vertical direction

N_h = Breakout factor in the horizontal direction

P = Ultimate load/unit length [kN/m]

p = Ultimate pullout load [kN]

P_u = Failure load [kN/m]

P_F = Regular plate anchor pullout capacity [kN/m]

P_{FT} = Full capacity of regular plate anchor [kN/m]

P_{Fo} = Full capacity of anchor with rectangular openings [kN/m]

P_o = Plate anchor with rectangular openings pullout capacity [kN/m]

q_h = Overburden pressure [kN/m^2]

q_u = Applied pressure required to cause undrained failure [kN/m^2]

s = Coefficient for the effect of overburden pressure on anchor capacity

S = Spacing [m]

S_t = Soil sensitivity

t = Anchor thickness [m]

W_F = Regular plate anchor weight [kN/m]

W_o = Anchor with rectangular openings weight [kN/m^2]

β = Anchor inclination to the vertical [Degrees]

Δ = Suction caissons rotation angle to the vertical [Degrees]

λ = Embedment ratio

γ = Soil unit weight [kN/m^3]

φ = Angle of internal friction [Degrees]

ρ = Rate of increase of undrained shear strength per unit length [kN/m^2/m]

ν = Poisson's ratio

σ_v = Effective overburden stresses [kN/m^2]

α = Adhesion factor

ψ = The angle between the vertical plane and the pullout direction [Degrees]

θ = Load inclination angle to the vertical [Degrees]

ξ = Efficiency factor (Pullout capacity of plate anchor with opening of width *S*/ pullout capacity of regular plate anchor)

Chapter 1 Introduction

1.1 Background

An anchor is commonly defined as a steel body embedded in the seabed and attached by means of steel chains/wires to a vessel or structure, to ensure its stability against current, wave and wind forces.

While current anchors are normally made of steel; rocks and stone were used as prehistoric alternatives for anchors, which then evolved to wooden anchors, and in latter stages were strengthened by metal sections (Colwill 1996). An illustration of the development of anchorage systems with time is presented in Figure 1. 1.

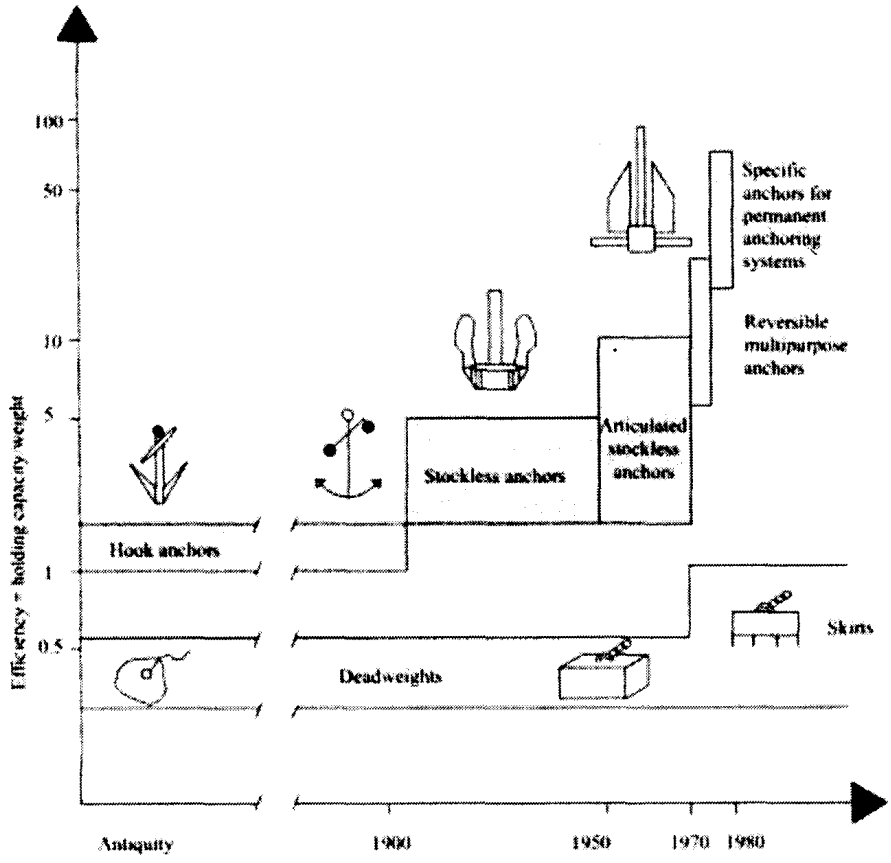

Figure 1. 1: Historical development of the different anchorage systems (Puech 1984).

Nowadays, the definition of soil anchors extends to include the common support systems used in geotechnical engineering to sustain tensile and uplift forces for a range of both onshore and offshore applications. In addition, the use of tension anchors for foundation systems became essential with the expansion of the special lightweight structure construction (Das 1990).

Furthermore, the current trend in the offshore industry is for explorations in waters of more than 500m in depth, rendering conventional piles, mat foundations and gravity structures uneconomic. Consequently, floating structures attached to the sea floor by means of mooring lines anchored to the seabed are becoming more widespread (Jun *et al.* 2006).

A wide range of anchor types were developed for onshore and offshore applications. For onshore applications, plate anchors, screw anchors and cylindrical anchors are mainly used (Liang 2010). For offshore applications, plate anchors are also commonly used, in addition to many other types such as suction caissons, drag anchors and duck-bill anchors (Liang 2010; Veenstra 2005). A schematic presentation of these anchor types are presented in Figure 1. 2. These anchor types have provided successful solutions for a large number of conditions. However, they might not be feasible in projects involving severe conditions (e.g. complex loads, great water depths and very soft/loose soil profiles). Accordingly, many attempts have been made to develop improved anchoring alternatives (e.g. the SEPLA; Song *et al.* 2009).

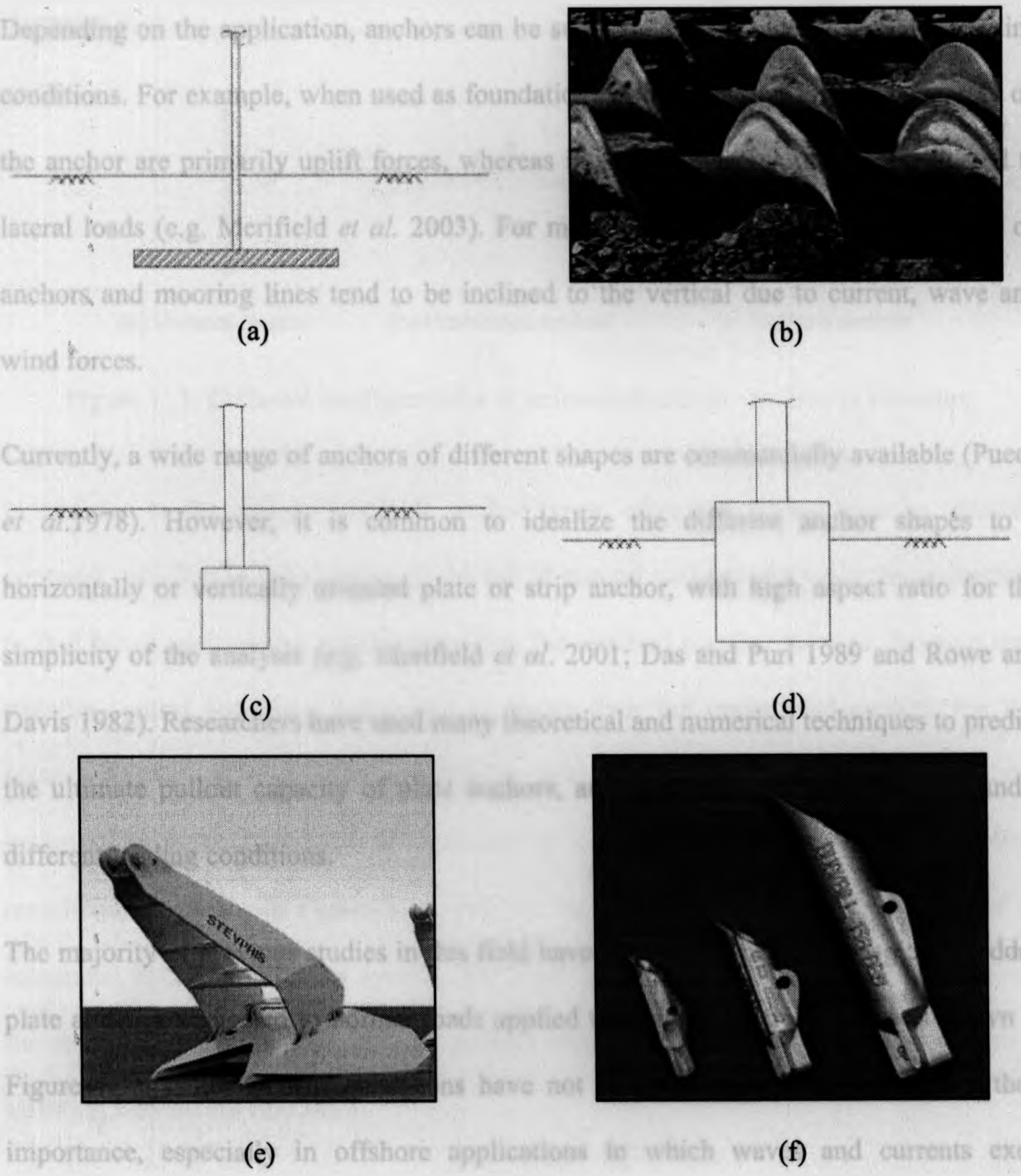

(a) (b) (c) (d) (e) (f)

Figure 1. 2: Common anchor types in onshore and offshore applications

(a) Plate anchors;
(b) Screw anchors (Smyth 2010);
(c) Cylindrical anchors;
(d) Suction caissons;
(e) Drag anchors (Vryhof anchors 2010);
(f) Drug-bill anchors (Duckbill earth anchors 2010).

Depending on the application, anchors can be subjected to a variety of complex loading conditions. For example, when used as foundations of transmission towers, the forces on the anchor are primarily uplift forces, whereas in shoring systems they are subjected to lateral loads (e.g. Merifield *et al.* 2003). For marine applications, the pullout forces on anchors and mooring lines tend to be inclined to the vertical due to current, wave and wind forces.

Currently, a wide range of anchors of different shapes are commercially available (Puech *et al.*1978). However, it is common to idealize the different anchor shapes to a horizontally or vertically oriented plate or strip anchor, with high aspect ratio for the simplicity of the analysis (e.g. Merifield *et al.* 2001; Das and Puri 1989 and Rowe and Davis 1982). Researchers have used many theoretical and numerical techniques to predict the ultimate pullout capacity of plate anchors, and to understand their behavior under different loading conditions.

The majority of previous studies in this field have been concerned with single embedded plate anchors, subjected to normal loads applied through its centre of mass as shown in Figure 1. 3. Other loading conditions have not received much attention despite their importance, especially in offshore applications in which waves and currents exert complicated loading forces on the anchors.

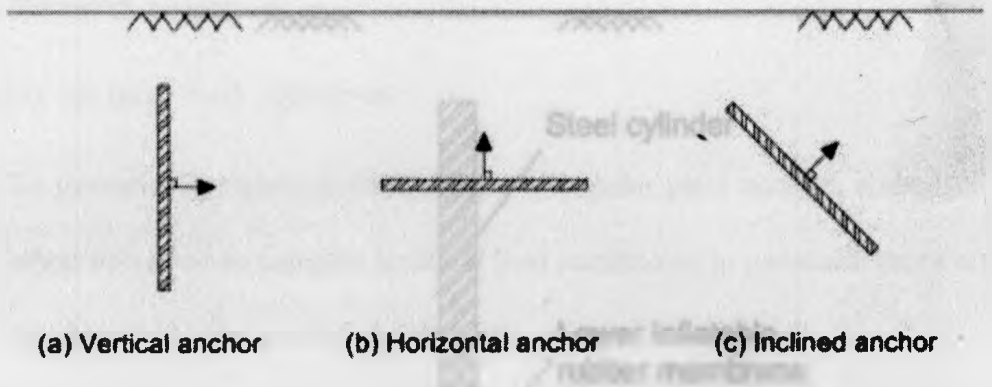

Figure 1. 3: Different configurations of embedded anchors studied in literature.

In addition to the already available anchor types, other techniques, such as remotely operated vehicles (ROVs) relying on the use of ground anchors motivated the researchers to find better anchoring solutions, providing the required reaction force to maintain their stability against buoyancy forces and to ensure their full operational control. For this reason, Newson *et al.* (2003a and 2003b) developed an innovative inflatable anchor system. The proposed system is composed of a steel anchor rod with a lower rubber membrane as shown in Figure 1. 4, that can be inflated and deflated by means of an integrated hydraulic pressure system. The main advantage of the proposed anchor over the existing anchors is its increased pullout resistance, and also the ease of deflation, allowing fast anchor relocation.

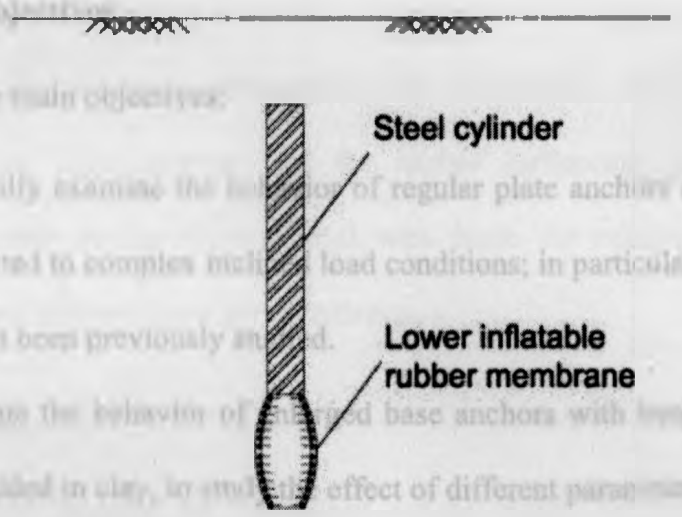

Figure 1. 4: The inflatable anchor configuration.

The numerical models carried out by Liang *et al.* (2008), as well as some experimental studies by Newson *et al.* (2003a and 2003b) have studied the pullout behavior of inflatable anchors. The analyses were a good first start and the parameters studied included inflation pressure, embedment ratio, anchor length, membrane thickness, and membrane surface roughness. Further investigation of the various parameters, such as the anchor and loading inclination and soil-strength interface conditions would provide a better understanding of this type of anchor, and hence lead to better design for this system.

For all the mentioned anchor types, most of the available studies investigate the behavior of a single embedded anchor. However, It is also anticipated that the use of multiple anchors will lead to a combination of compressive, uplift and inclined forces applied at these anchors. Accordingly, simulation of multiple adjacent anchors is essential in order to assess the interaction effect on their ultimate pullout capacities.

1.2 Research objectives

This study has three main objectives:

1. To numerically examine the behavior of regular plate anchors embedded in clay when subjected to complex inclined load conditions; in particular those conditions that have not been previously studied.
2. To investigate the behavior of enlarged base anchors with irregular base shapes when embedded in clay, to study the effect of different parameters on their pullout capacity and determine the most efficient base shape.
3. To investigate the behavior of a novel anchorage solution. Specifically, a plate anchor with intermediate rectangular openings as shown in Figure 1. 5.

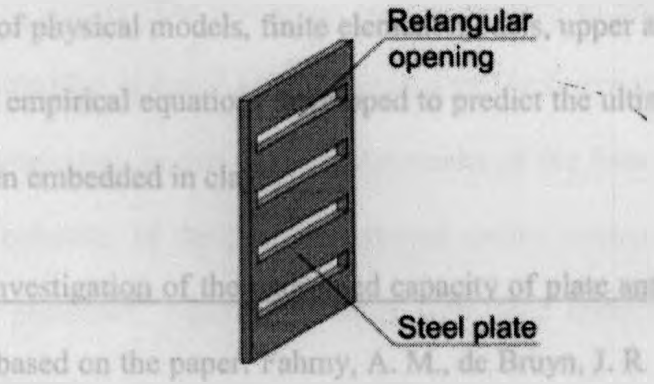

Figure 1. 5: The proposed anchor system: a steel anchor with intermediate rectangular openings.

For each of the before mentioned objectives, addressing the objectives involved the development of two-dimensional plane strain finite element models using the software package Plaxis 2D V8.5. (Plaxis 2006) These models were used to carry out parametric

studies investigating the effect of a variety of factors on the anchor ultimate pullout capacity. The investigated parameters include the soil-anchor interface strength, the anchor thickness, the load direction and the anchor inclination, the point of load application, the increase in clay shear strength with depth, the enlarged base shape and disturbance of the soil following anchor installation.

1.3 Thesis outline

This thesis has been prepared in 'Integrated-Article' format. It is divided into six chapters. A brief description of the following five chapters is as follows:

Chapter 2: Literature survey. This chapter provides a survey of the existing literature on regular plate anchors and enlarged base anchors embedded in clay. It also provides a review of applications and techniques similar to the proposed slotted anchor alternative. These include a review of physical models, finite element models, upper and lower bound plasticity solutions, and empirical equations developed to predict the ultimate capacity of these anchors types when embedded in clay.

Chapter 3: Numerical investigation of the undrained capacity of plate anchors embedded in clay. This chapter is based on the paper: Fahmy, A. M., de Bruyn, J. R. and Newson, T. A. (Submitted 2010). "Numerical investigation of the inclined pullout behavior of vertical anchors embedded in clay," submitted to *The International Journal of Geomechanics.* This chapter summarizes the finite element model created to numerically simulate the pullout behavior of regular plate anchors embedded in clay under plane strain conditions. The results of simulations carried out to assess the effect of the various parameters on regular plate anchors pullout capacity are presented. Where applicable, the results are

compared to results from the literature.

Chapter 4: Numerical investigation of the undrained capacity of enlarged based anchors embedded in clay. This chapter is based on the paper: Fahmy, A. M., Newson, T. A. and de Bruyn, J. R. (2010) "Numerical investigation of the pullout behavior of enlarged base anchors embedded in clay," to be submitted to *The Electronic Journal of Geotechnical Engineering.* In this chapter, the results of the finite element model simulating the pullout behavior of anchors with irregular base shapes embedded in clay are presented. The effects of the different parameters on anchor ultimate capacity are determined. The results are then compared to those for regular plate anchors obtained in Chapter 3.

Chapter 5: Numerical investigation of the undrained capacity of anchors with rectangular openings embedded in clay. This chapter is based on the paper: Fahmy, A. M., Newson, T. A. and de Bruyn, J. R. (2010) "The undrained pullout capacity of plate anchors with rectangular openings embedded in clay," to be submitted to *The International Journal of Offshore and Polar Engineering.* In this chapter, the results of the finite element model simulating the pullout behavior of the proposed slotted anchor system under selected loading conditions are presented. Again the results were then compared to those of regular plate anchors presented in chapter 3, and the feasibility of using the proposed system as an alternative to regular plate anchor was assessed.

Chapter 6: Summary and conclusion. In this chapter, a summary of the results for the three previous chapters is presented and conclusions are drawn from these studies. In addition, suggested recommendations for future study are presented.

1.4 References

Colwill, R. D. (1996). "Marine drag anchor behavior-a centrifuge modeling and theoretical investigation," Degree of doctor of philosophy thesis, The University of Manchester, Manchester, United kingdom

Das, B. M. (1990). "Earth anchors," Elsevier, Amsterdam, Netherlands

Das, B. M., and Puri, V. K. (1989). "Holding capacity of inclined square plate anchors in clay," *Soils and Foundations Journal*, Vol.29,No.3, pp 138-144

Duckbill earth anchors (2010), *http://fptestzone.info/Duckbill_Anchor_Models.html*

Fahmy, A. M., de Bruyn, J. R. and Newson, T. A. (Submitted 2010). "Numerical investigation of the inclined pullout behavior of vertical anchors embedded in clay," *International Journal of Geomechanics.*

Fahmy, A. M., Newson, T. A. and de Bruyn, J. R. (will be submitted 2010) "Numerical investigation of the pullout capacity of plate anchors with intermediate rectangular openings embedded in clay," *Electronic Journal of Geotechnical Engineering*

Fahmy, A. M., Newson, T. A. and de Bruyn, J. R. (will be submitted 2010). "Numerical investigation of the inclined pullout behavior of irregular anchors embedded in clay," *International Journal of Offshore and Polar Engineering*

Jun, L., Li-ling, W. and Yu-xia, H. (2006). "Pullout capacity of circular plate anchors in NC clay," *Journal of Dalian University of technology*, Vol.46, No.5, pp 712-719

Liang, Y. (2010). "The mechanics of inflatable anchors embedded in soils," Degree of doctor of philosophy thesis, The University of Western Ontario, London, Canada

Liang, Y., Newson, T. A. and Hinchberger, S. (2008). "Numerical study of the mechanics of inflatable anchors in clay," *Proceedings of the18th International Offshore and Polar Engineering Conference*, pp 546-551

Merifield, R. S., Lyamin, A.V., Sloan, S. W., and Yu, H. S. (2003). "Three-dimensional lower bound solutions for stability of plate anchors in clay," *Journal of Geotechnical and Geoenvironmental Engineering*, Vol.129, No.3, pp 243-253

Merifield, R. S., Sloan, S. W., and Yu, H. S. (2001). "Stability of plate anchors in undrained clay," *Geotechnique,* Vol.51, No.2, pp 141-153

Newson, T. A., Smith, F. W. and Brunning, P. (2003a). "An experimental study of inflatable offshore anchors in soft clay," *BGA International Conference on Foundations, Innovations, Observations, Design and Practice*, pp 695-704

Newson, T. A., Smith, F. W., Brunning, P. and Gallaher, S. (2003b). "An experimental study of inflatable offshore anchors," *Proceedings of the 13th International Offshore and Polar Engineering Conference, Design and Practice*, pp 1340-1345

Puech, A. (1984). "The use of anchors in offshore petroleum operations," Houston Gulf publications, Paris

Puech, A., Meunnier, J. and Pallard, M. (1978). "Behavior of anchors in different soil conditions," *Proceedings of the 10th Offshore Technology Conference,* Houston, OTC 3204, pp 1321-1329

Rowe, R. K., and Davis, E. H. (1982). "The behavior of plate anchors in clay," *Geotechnique*, Vol.32, No.1, pp 9-23

Smyth, J. (2010), eHow, *http://www.ehow.com/how_7460583_install-ground-anchor.html.*

Song, Z., Hu, Y., O'Loughlin, C. and Randolph, M. F. (2009). "Loss in anchor embedment during plate anchor keying in clay," *Journal of Geotechnical and Geoenvironmental Engineering*,Vol.135, No.10, pp 1475-1485.

Veenstra, E. G. (2005). "Anchor chain cutting through a rock cover," Degree of Master of Science thesis, Delft University of Technology, Netherlands

Vryhof anchors (2010), *http://www.vryhof.com/products/anchors/stevpris_mk6.html*

Chapter 2 Literature Survey

2.1 Introduction

In this chapter, a review of the existing literature on the behavior of soil anchors is presented, highlighting important loading conditions and anchor configurations that have received little prior attention and hence warrant further investigation. This literature review is divided into three sections, dealing with regular plate anchors, enlarged base anchors and anchors with rectangular openings.

2.2 Regular plate anchors

A large body of literature (e.g. Das and Singh 1994; Das and Shin 1993; Das and Puri 1989; El-Khatib and Randolph 2004; El-Khatib *et al.* 2002; Merifield *et al.* 2001; Merifield *et al.* 2003; Merifield *et al.* 2005; O'Neil *et al.* 2003; Rao *et al.* 1997; Rao *et al.* 2006; Rowe and Davis 1982; Song *et al.* 2008) exists on the application and capacity of regular plate anchors in clay soils. The effects of parameters such as embedment depth, overburden pressure, anchor inclination, anchor thickness and shape, change of soil strength with depth, and anchor-soil interface strength on anchor pullout capacity have been considered.

Physical models, finite element models, upper and lower bound plasticity solutions, and empirical equations have been developed to predict the ultimate capacity of horizontal, vertical and inclined plate anchors and to understand their behavior under a range of loading conditions.

Previous studies have mainly investigated the behavior of plate anchors subjected to loads perpendicular to their long dimension and applied through the center of mass, as

shown in Figure 2. 1. This approach is motivated by the fact that when the mooring line attached to the anchor is tensioned after installation, the anchor keys to an orientation perpendicular to the direction of loading (Yu *et al.* 2009).

A wide range of dimensions exists for the different anchor types. For example drag-in plate anchors length could range from 0.31 m to 4.24 m while fluke width varies from 0.43m to 6.86m (Colwill 1996). Similarly, suction embedded plate anchors ranges from 2.5m to 3m width by 6 m to 7.3 m length for anchors used in mobile offshore drilling units, while for permanent installations, double skin or hollow flukes should be used with dimensions up-to 4.5m by 10m (Wilde *et al.* 2001).

Previous work on the effects of the parameters governing the behavior of regular anchors is reviewed in the following subsections.

2.2.1 Effect of embedment depth and overburden pressure

Rowe and co-workers (Rowe 1978, Rowe and Davis 1982) carried out numerical plane strain finite element analyses of both vertical and horizontal anchors, as shown in Figure 2. 1 (a) and (b) respectively. In their study, they classified anchors according to their adhesion to soil. They considered two cases at the anchor-soil interface: the immediate breakaway condition in which the interface cannot sustain any tension, and the "no-breakaway condition, in which a full bond between the anchor and soil was assumed. In practical situations, conditions at the anchor-soil interface will be intermediate between these two extremes.

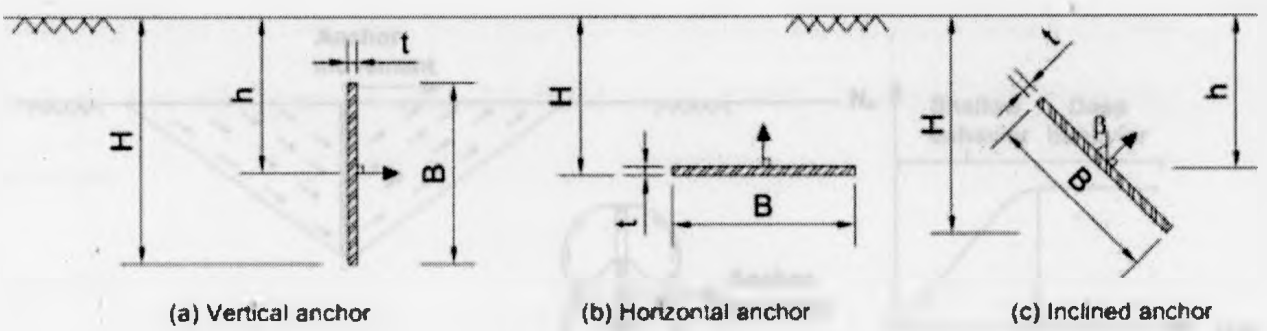

Figure 2. 1: Typical configurations of embedded anchors studied in the literature. Important geometric parameters are indicated.

Rowe and Davis (1982) also classified anchors as shallow or deep depending on whether the anchor capacity was greatly affected by embedment and overburden pressure, and whether the region of plastic deformation around the anchor extended to the ground surface (see Figure 2. 2 (a) and (b)). When the anchor embedment becomes deeper than a critical depth H_c, measured from the ground surface to the bottom of the anchor, its behavior changes from shallow to deep, as illustrated in Figure 2. 2 (c). This is a result of the fact that beyond the critical depth, the undrained shear strength of the clay becomes independent of the mean normal stress (Merifield *et al.*, 2003).

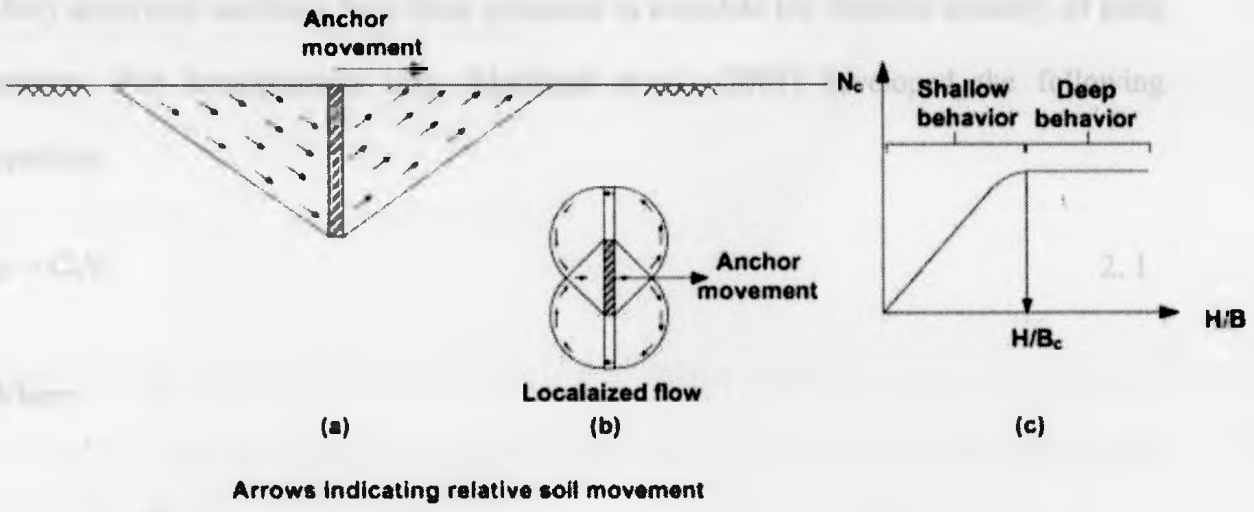

Figure 2. 2: Typical anchor failure mechanisms for horizontally loaded vertical anchors for (a) shallow and (b) deep conditions. (c) illustrates the critical embedment ratio $(H/B)_c$.

The value of the critical depth is influenced by many factors, including load and anchor inclination angles, overburden pressure, anchor surface roughness and the point of load application. The results of Rowe and Davis (1982) indicate that, for horizontal anchors, deep anchor behavior occurs at embedment ratios H/B greater than 4 under immediate breakaway conditions and at an embedment ratio of 3 under no-breakaway conditions. Here B is the total anchor length. On the other hand, vertical anchors exhibit deep behavior at an embedment ratio of 3 for both limiting breakaway conditions (Rowe and Davis, 1982).

Rowe and Davis (1982) also showed that the overburden pressure required to ensure a no-breakaway response for a homogeneous elasto-plastic material is approximately equal to $6C_u$ for horizontal anchors and ranges from $4C_u/K_o$ to $6C_u/K_o$ for vertical anchors, where C_u is clay undrained shear strength and K_o is the lateral earth pressure coefficient.

Many analytical solutions have been proposed to calculate the ultimate capacity of plate anchors. For homogeneous clay, Merifield *et al.* (2001) developed the following equation:

$$q_u = C_u N_c \qquad 2.1$$

Where

$$N_c = N_{co} + \frac{\gamma h}{C_u} \qquad 2.2$$

$$N_{co} = \left(\frac{q_u}{C_u}\right) \text{for } _{\gamma=,\ \rho=0} \qquad 2.3$$

Based on their finite element analyses, Merifield *et al.* (2001) provided the following equations to calculate N_{co} for both vertical and horizontal anchors in homogeneous clay profiles.

For vertical anchors,

$$N_{co} = 2.46 Log_e\left(\frac{2H}{B}\right) + 0.89 \text{ .....(Lower bound)} \qquad 2.4$$

$$N_{co} = 2.58 Log_e\left(\frac{2H}{B}\right) + 0.98 \text{ .....(Upper bound)} \qquad 2.5$$

while for horizontal anchors,

$$N_{co} = 2.56 Log_e\left(\frac{2H}{B}\right) \text{.....(Lower bound)} \qquad 2.6$$

$$N_{co} = 2.76 Log_e\left(\frac{2H}{B}\right) \text{.....(Upper bound)} \qquad 2.7$$

where h is the distance from ground surface to anchor centre of mass, ρ is the rate of increase of undrained shear strength per unit depth, q_u is the average applied pressure required to cause undrained failure, γ is the soil unit weight, N_c is the breakout factor for homogeneous soil and N_{co} is the breakout factor for homogeneous weightless soil. These equations reflect the reliance of the anchor on both overburden pressure and embedment depth. Accordingly, the dimensionless overburden pressure term $\gamma h/C_u$ was introduced to show this dependence. At any constant depth, the anchor behavior changes from shallow to deep at a certain value of $\gamma h/C_u$.

Merifield *et al.* (2001) compared their results to various available laboratory and finite element results. Figure 2. 3 compares several calculations of the breakout factor N_c with embedment ratio H/B under immediate breakaway conditions. This figure shows the upper and lower bound plasticity solutions after Rowe (1978), a five variable upper bound solution after Merifield *et al.*(2001), and the upper and lower bound solutions of Merifield *et al.* (2001) for a vertical anchor loaded horizontally through the centre of mass. The presented results are very similar up to $H/B = 3$. At higher embedment ratios, the results of Rowe (1978) tend to saturate, while the other results show a continuing increase. At the highest embedment ratios, the solutions diverge, giving values of N_c ranging between 5 and 9 for deep embedments of $H/B = 10$. Merifield *et al.* reported that

the five-variable upper bound solution was not capable of determining the true collapse load for all of the studied embedment ratios, and that its values of the breakout factor are over estimated by 25% for $H/B > 3$. A similar plot comparing the upper and lower bounds calcualted by Merifield *et al.*(2001) with several sets of experimental results is presented in Figure 2. 4. The results showed good agreement, however lower values has been shown for experimental results.

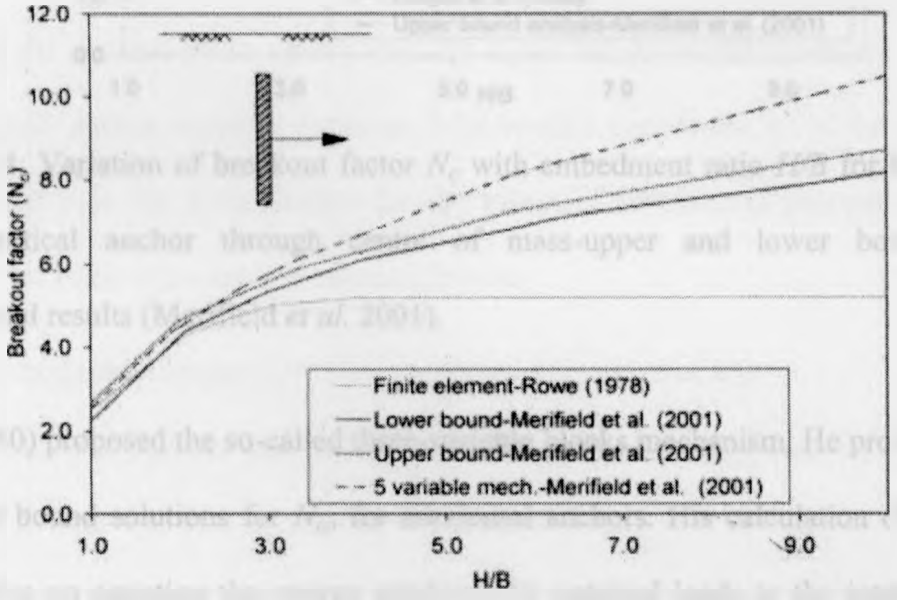

Figure 2. 3: Finite element calculations of the variation of Breakout factor N_c with embedment ratio H/B for a vertical anchor loaded horizontally through its centre of mass. (Merifield *et al.* 2001).

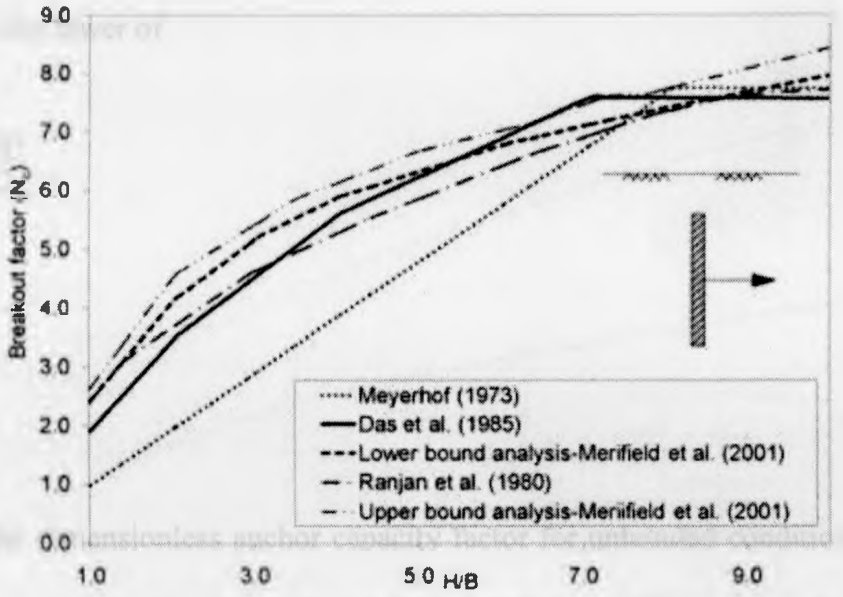

Figure 2. 4: Variation of breakout factor N_c with embedment ratio H/B for horizontally loaded vertical anchor through centre of mass-upper and lower bound versus experimental results (Merifield *et al.* 2001).

Gunn (1980) proposed the so-called three-variable blocks mechanism. He provided upper and lower bound solutions for N_{co} for horizontal anchors. His calculation of the upper bound relies on equating the energy produced by external loads to the internal energy released along discontinuities. For the lower bound calculation, an exact plasticity solution is assumed for the expansion of a thick cylinder embedded in homogeneous clay, leading to the creation of a statically admissible stress field. Figure 2. 5 shows the lower and upper bound values of N_{co} calculated by Gunn (1980) for horizontal anchors over a wide range of embedment ratios.

Rowe and Davis (1982) also estimated the applied pressure required to cause undrained failure of anchors embedded in saturated clays to be

$$q_u = C_u N_c' \qquad 2.8$$

where N_c' is the lower of

$$N_c' = N_c + \frac{sq_h}{C_u} \qquad 2.9$$

and

$$N_c' = N_c^* \quad . \qquad 2.10$$

Here N_c is the dimensionless anchor capacity factor for unbonded conditions, N_c^* is the dimensionless anchor capacity factor at fully bonded conditions, q_h is the overburden pressure and s is the a coefficient for the effect of overburden pressure on anchor capacity. The value of s could be taken as follows

- For horizontal anchors, s= 1 independent of the value of K_o.
- For vertical anchors with hydrostatic initial stress conditions (K_o=1), s varies from 0.5 at H/B=1 to 0.96 at H/B=3.
- For H/B between 1 and 3, the value of S can be obtained by interpolation.
- For H/B>3, s can be taken as unity. For a non-hydrostatic initial stress condition, the value of S can be found by multiplying K_o by the value of s corresponding to a hydrostatic initial stress condition. For deep anchors, although the full collapse load is independent of the initial soil stress state, the pre-failure plastic extent and hence the practical failure load is dependent on the overburden pressure.

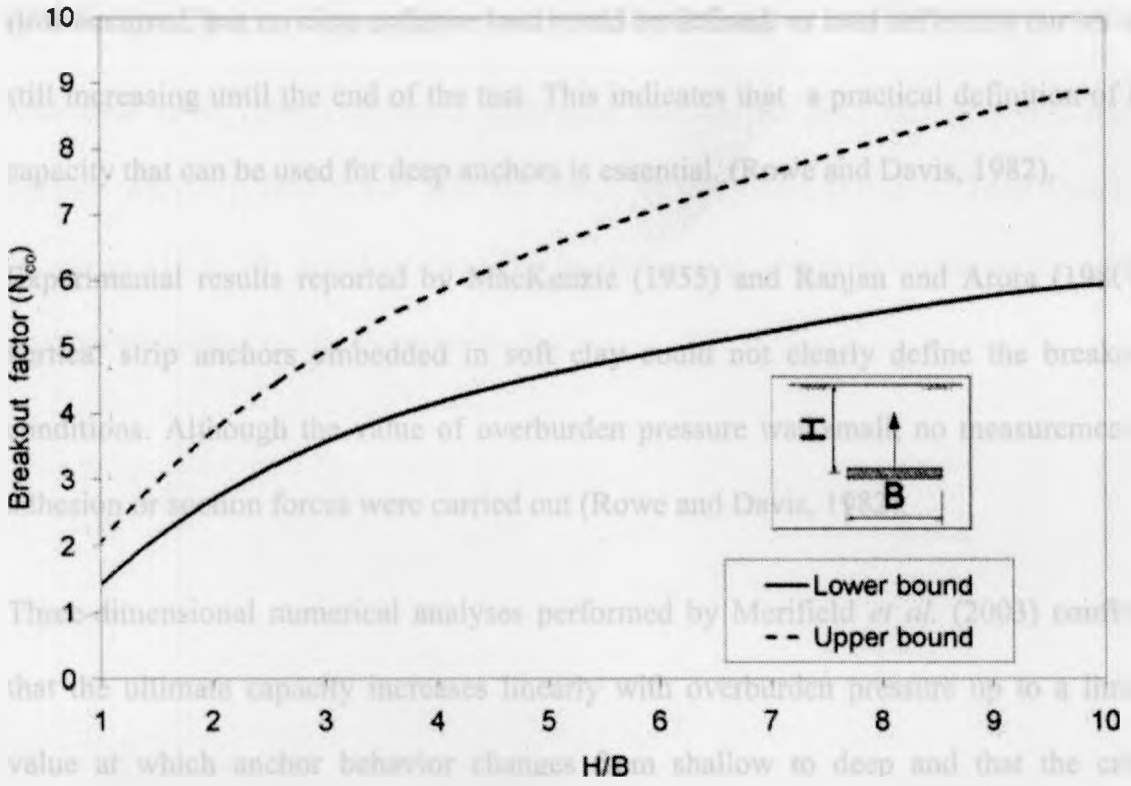

Figure 2. 5: Breakout factors N_{co} provided by Gunn (Merifield *et al.* 2001)

For soil-anchor interface strength intermediate between the immediate an no-breakaway conditions discussed above, anchors will initially behave as fully bonded, then breakaway will occur during loading. Anchor capacity has been shown to increase linearly with overburden pressure between the limits of immediate and no-breakaway (Rowe and Davis, 1982).

Experimental work by the same authors has shown that anchor behavior changes from shallow to deep at an embedment ratio of 4.5. For shallow anchors at $H/B < 2.5$, the collapse load was clearly defined and tension cracks appeared at the surface which might have reduced suction forces as well as anchor capacity. For $2.5 < H/B < 4.5$, no tension cracks were observed (Rowe and Davis 1982). For deep anchors, a noticeable plastic

flow occurred, but no clear collapse load could be defined, as load deflection curves were still increasing until the end of the test. This indicates that a practical definition of load capacity that can be used for deep anchors is essential. (Rowe and Davis, 1982).

Experimental results reported by MacKenzie (1955) and Ranjan and Arora (1980) on vertical strip anchors embedded in soft clay could not clearly define the breakaway conditions. Although the value of overburden pressure was small, no measurements of adhesion or suction forces were carried out (Rowe and Davis, 1982).

Three-dimensional numerical analyses performed by Merifield *et al.* (2003) confirmed that the ultimate capacity increases linearly with overburden pressure up to a limiting value at which anchor behavior changes from shallow to deep and that the critical overburden ratio at which this transition occurs decreases with increasing embedment ratio. Finite element analyses for deep vertical anchors carried out by Merified *et al.* (2001) showed limiting values of the lower and upper bounds for N_c of 10.47 and 11.86 respectively. The upper bound was found to be similar to that for horizontal anchors, while the lower bound value was 6% lower than for horizontal anchors. The analyses also showed that, for vertical anchors horizontally loaded through the centre of mass, an increase of embedment depth increases the plastic zone to include areas above, below and behind the anchor.

2.2.2 Effect of an increase of soil strength with depth

Though most previous work has concentrated on the behavior of anchors embedded in a homogeneous clay layer, normally consolidated clay profiles with a strength that increases with depth have also been studied. This type of strength profile is more

realistic than the constant-strength case, especially for marine clays.

Merrifield *et al.* (2001) derived a theoretical solution for both vertical and horizontal anchors with $1 < H/B < 10$ and for $\rho B/C_u$ varying from 0.1 to 1. They found that equations (1) to (3) could be modified as follows to obtain the ultimate capacity of anchors embedded in inhomogeneous clay:

$$N_c = N_{co\rho} + \frac{\gamma h}{C_{uo}} \qquad 2.11$$

Where

$$N_{co\rho} = \left(\frac{q_u}{C_{uo}}\right)_{\gamma=0,\ \rho\neq 0} \qquad 2.12$$

Here C_{uo} is the initial undrained shear strength at the ground surface and $N_{co\rho}$ is the breakout factor for inhomogeneous, weightless soil.

Merifield *et al.* (2001) formulated charts based on their numerical results, giving breakout factors for both vertical and horizontal anchors in inhomogeneous soils. Figure 2. 6 presents their results on the variation of $N_{co\rho}$ with H/B for vertically embedded anchors.

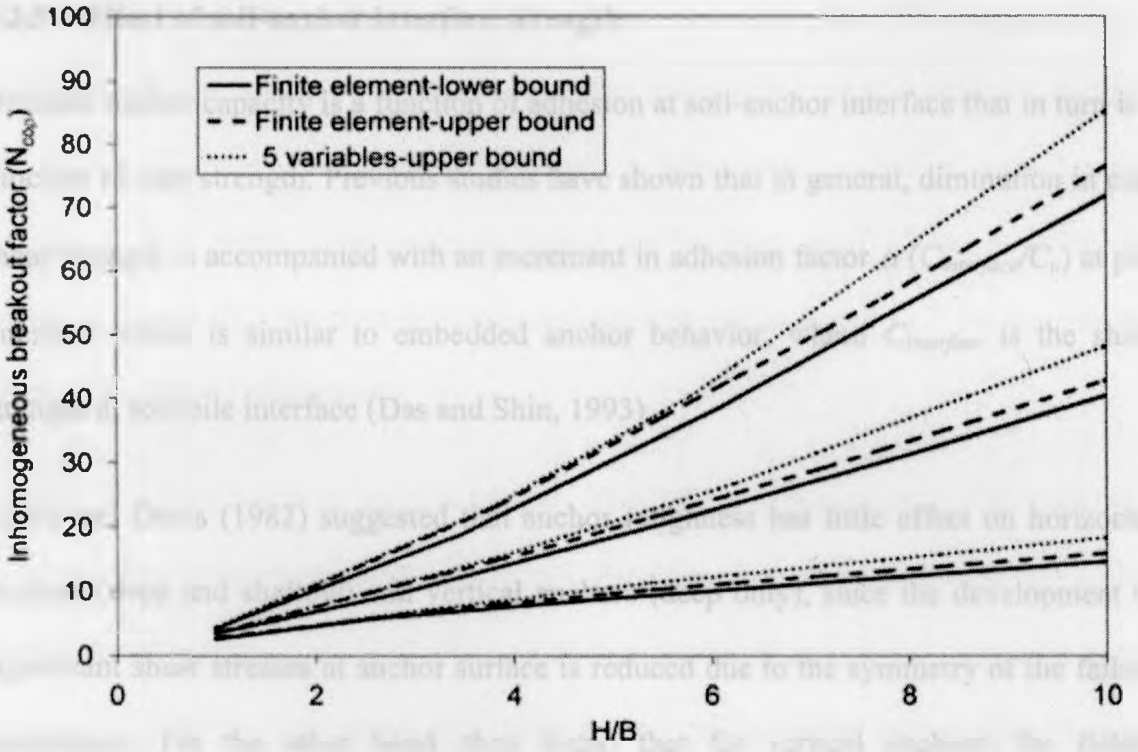

Figure 2. 6: Variation of inhomogeneous breakout for vertical anchors (Merifield *et al.* 2001).

Song *et al.* (2008) studied the behavior of anchors embedded in normally consolidated clays of with a strength that increased linearly with depth. For reasons related to numerical stability, they assumed a constant soil strength for the upper 0.5 m. They considered both immediate and no-breakaway conditions and compared their results with data from centrifuge experiments. The capacities found from their finite element model were about 10% lower than those from the centrifuge tests.

Song *et al.* (2008) also studied the effect of normally consolidated soil profiles on the separation depth of anchors. They found that the separation depth was strongly dependent on the initial clay shear strength at the initial anchor embedment depth. This is because part of the strong soil surrounding the anchor is usually trapped around it during pullout.

2.2.3 Effect of soil-anchor interface strength

Ultimate anchor capacity is a function of adhesion at soil-anchor interface that in turn is a function of clay strength. Previous studies have shown that in general, diminution in clay shear strength is accompanied with an increment in adhesion factor α ($C_{interface}/C_u$) at pile interface which is similar to embedded anchor behavior, where $C_{interface}$ is the shear strength at soil-pile interface (Das and Shin, 1993).

Rowe and Davis (1982) suggested that anchor roughness has little effect on horizontal anchors (deep and shallow) and vertical anchors (deep only), since the development of significant shear stresses at anchor surface is reduced due to the symmetry of the failure mechanism. On the other hand, they found that for vertical anchors, the failure mechanism produced at shallow depths ($H/B<2$) is non-symmetric and high shear stresses might develop at the anchor interface and hence any increase in anchor roughness will lead to an increase in ultimate capacity.

In their study, Merifield *et al.* (2003) suggested that the effect of roughness on the capacity of horizontal anchors could be neglected for different anchor shapes (square, rectangular and circular), whereas for vertical anchors, Merrifield *et al.*(2001) stated that surface roughness has no influence on anchor capacity when the embedment ratio exceeds 2. They also found that changing the roughness of a vertical anchor caused a reduction in N_{co} of up-to 22%. These results conform to those reported by Rowe and Davis (1982) where a reduction of up-to 30% was found. However, these results are based only on numerical analyses, whereas no laboratory testing has been performed to validate them.

Analyses performed by Song *et al.* (2008) demonstrated that surface roughness has a minimal influence in case of horizontal strip plate anchors. For circular anchors, changing the surface roughness state from fully smooth to fully rough resulted in an increase of strength of 4%. Small strain analyses carried out by Song *et al.* (2008) revealed that breakout factors (N_c) for deep fully-attached anchors are 11.6 and 11.7 for smooth and rough strip anchors respectively.

In their Analyses for drag anchors in clay, El-Khatib and Randolph (2004) adopted a finite element plain strain horizontal rectangular plate. Results have shown that anchor surface roughness has a minimal effect on anchor rotational and normal capacities as soil remains attached to both upper and lower surface while sliding occurs only at sides, which has a minimal effect. On the other hand, horizontal capacity is greatly affected by surface friction.

2.2.4 Effect of anchor inclination

Although the work of Rowe and Davis (1982) mainly concentrated on vertical and horizontal anchors. they also suggested solutions for inclined anchors with the load applied through the centre of mass and perpendicular to anchor height, as shown in Figure 2. 1 (c). Their suggestions were based on their own studies and on elastic solutions due to Rowe and Booker (1979, 1980). They suggested that for shallow anchors at inclinations less than 60° to the vertical, their solutions for horizontal anchors could be used, while for angles greater than 60°, their solutions for vertical anchors should be used. For anchors deeper than H/B = 3, solutions for both breakaway conditions are independent of anchor orientation, and for intermediate breakaway conditions, equation

(9) could be used with a value of S ranging from one to K_o depending on anchor inclination.

Das and Puri (1989) studied the effect of inclination on shallow square anchors through laboratory test models. Based on their findings, Das and Puri (1989) developed the following empirical equation for calculating the breakout factor for inclined square anchors:

$$N_c = N_{c(\psi=0^\circ)} + \left[N_{c(\psi=90^\circ)} - N_{c(\psi=0^\circ)}\right]\left(\frac{\psi}{90}\right)^2 \qquad 2.13$$

Where ψ is anchor inclination.

In their study of inclined strip anchors in clay, Merifield *et al.* (2005) used lower and upper bound theorems to investigate the effect of anchor inclination on the breakout factor. They defined the inclination factor as the ratio of the breakout factor for an inclined anchor to that of a vertical one for a weightless soil condition. Figure 2. 7 and Figure 2. 8 show the variation of the inclination factor with anchor inclination ψ determined using the lower bound and solid nonlinear analysis code for anchors embedded in weightless soil. They found that the inclination factor increases in a non-linear way with increasing anchor inclination. These results are consistent with findings of the laboratory study carried out by Das and Puri (1989)

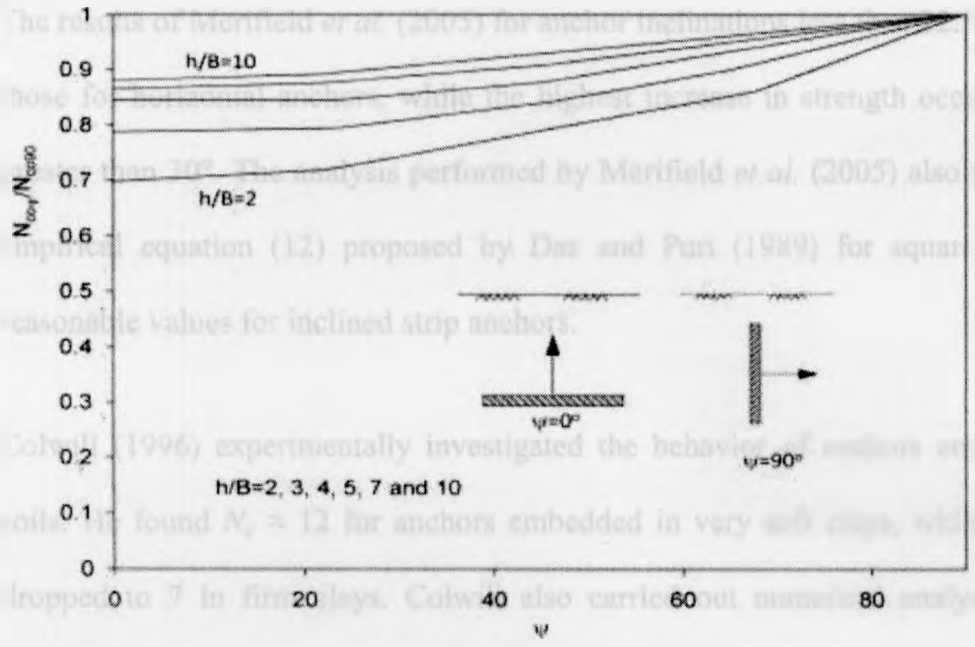

Figure 2. 7: Variation of inclination factor with anchor inclination-lower bound (Merifield *et al.* 2005).

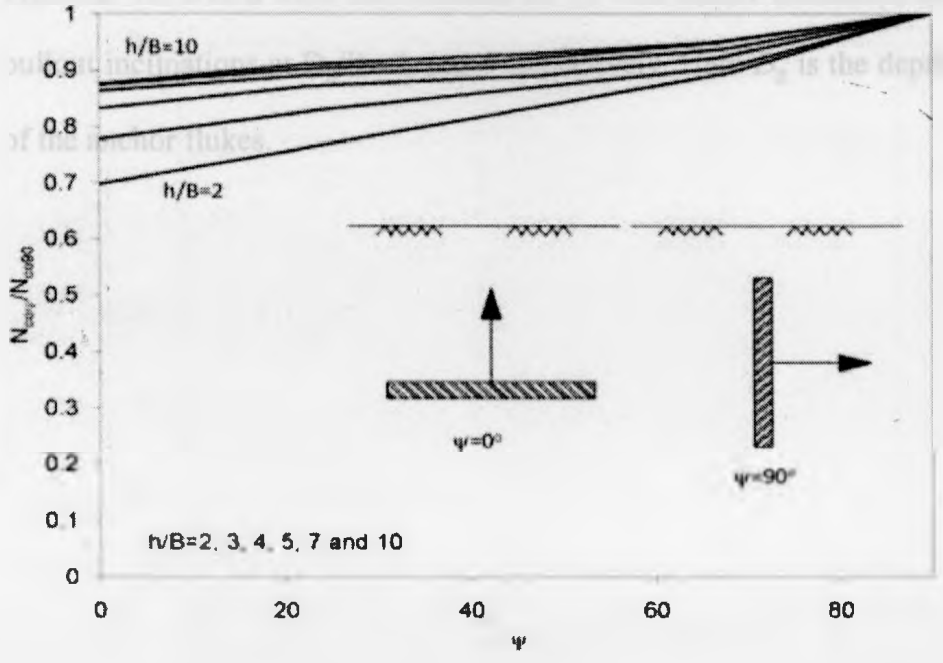

Figure 2. 8: Variation of inclination factor with anchor inclination-solid nonlinear analysis (Merifield *et al.* 2005).

The results of Merifield *et al.* (2005) for anchor inclinations less than 22.5°, are similar to those for horizontal anchors, while the highest increase in strength occurred for angles greater than 30°. The analysis performed by Merifield *et al.* (2005) also showed that the empirical equation (12) proposed by Das and Puri (1989) for square anchors gives reasonable values for inclined strip anchors.

Colwill (1996) experimentally investigated the behavior of anchors embedded in clay soils. He found $N_c \approx 12$ for anchors embedded in very soft clays, while for this value dropped to 7 in firm clays. Colwill also carried out numerical analysis for inclined anchors with a range of pullout inclinations. He attempted to numerically model embedded anchors under un-bonded conditions by inserting a thin layer of low strength and stiffness behind the anchor. The values he reported are presented in Figure 2. 9 and Figure 2. 10, which show the variation of N_c with anchor inclination angle for a range of pullout inclinations at $D_g/B = 1$ and 4 respectively. Here D_g is the depth to the barycentre of the anchor flukes.

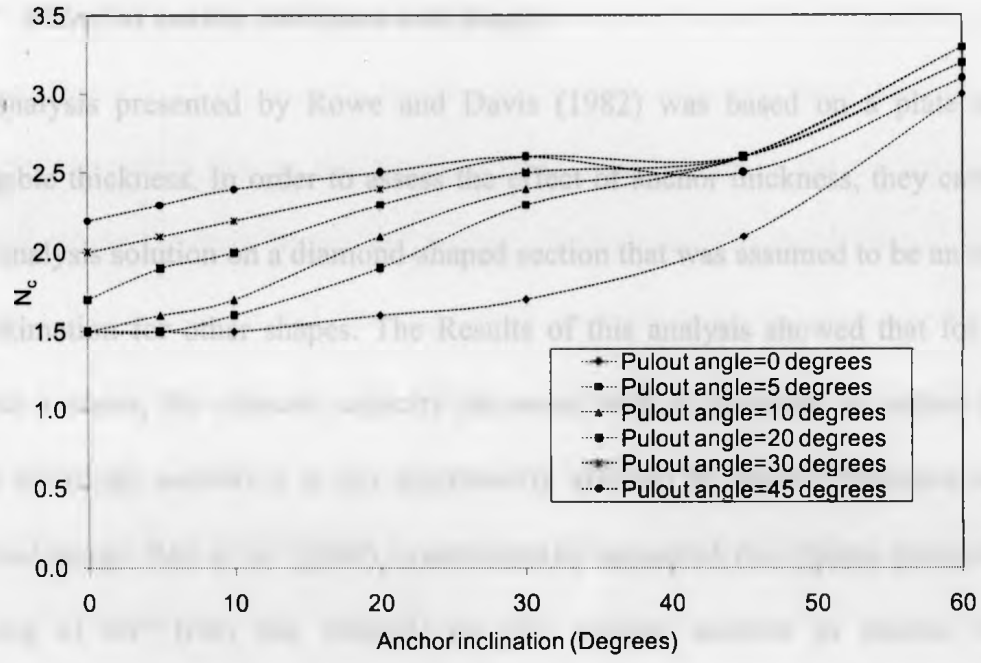

Figure 2. 9: Variation of N_c with anchor inclination at different pullout angles for D_g/B= 1 (Colwill 1996).

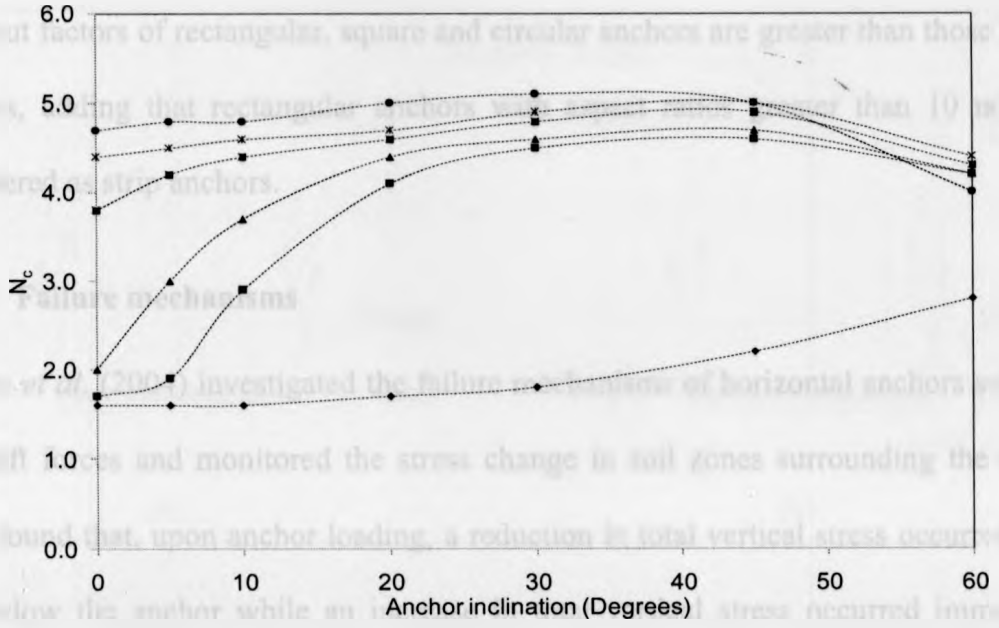

Figure 2. 10: Variation of N_c with anchor inclination at different pullout angles for D_g/B= 4 (Colwill 1996).

2.2.5 Effect of anchor thickness and shape

The analysis presented by Rowe and Davis (1982) was based on a plate anchor of negligible thickness. In order to assess the effect of anchor thickness, they carried out a limit analysis solution on a diamond-shaped section that was assumed to be an acceptable approximation for other shapes. The Results of this analysis showed that for perfectly smooth anchors, the ultimate capacity decreases with an increase in anchor thickness, while for rough anchors it is not significantly affected by anchor thickness within the practical range. Rao *et al.* (2006) experimentally measured the oblique pullout capacity (loading at 60° from the vertical) on pile suction anchors in marine clays. He demonstrated that the vertical pullout capacity of piles increased with increasing aspect ratio L/D, where L and D are the caisson length and diameter respectively.

Studies on different anchor shapes performed by Merifield *et al.* (2003) showed that the breakout factors of rectangular, square and circular anchors are greater than those of strip anchors, adding that rectangular anchors with aspect ratios greater than 10 might be considered as strip anchors.

2.2.6 Failure mechanisms

Thorne *et al.* (2004) investigated the failure mechanisms of horizontal anchors subjected to uplift forces and monitored the stress change in soil zones surrounding the anchor. They found that, upon anchor loading, a reduction in total vertical stress occurred in the soil below the anchor while an increase in total vertical stress occurred immediately above the anchor. They also reported that the soil above the anchor bulges during loading, causing the soil between the anchor and the ground surface to act as a beam.

This leads to a decrease in the horizontal stress, and hence the formation of tension stresses. Figure 2. 11 (a) shows a shallow anchor fully separated from the soil beneath it. Here failure occurs due to the tension cracks which form at the surface and to the shearing along the lines above the anchor. Shallow anchors fully bonded to the soil beneath fail as a result of soil shearing failure enclosed in the soil zone above the anchor as shown in Figure 2. 11 (b). For deeper conditions, shear failure is totally contained around the anchor without surface effects, and for fully bonded conditions, the soil self-weight had no significant effect on anchor failure load. Thorne *et al.* (2004) also compared the pullout of shallow anchors with both tension and breakaway and with breakaway but no tension. They found that tension failure above the anchor caused a reduction in uplift capacity, which ranged from 30% for $\gamma h/C_u = 1$ to less than 5% for $\gamma h/C_u = 6$.

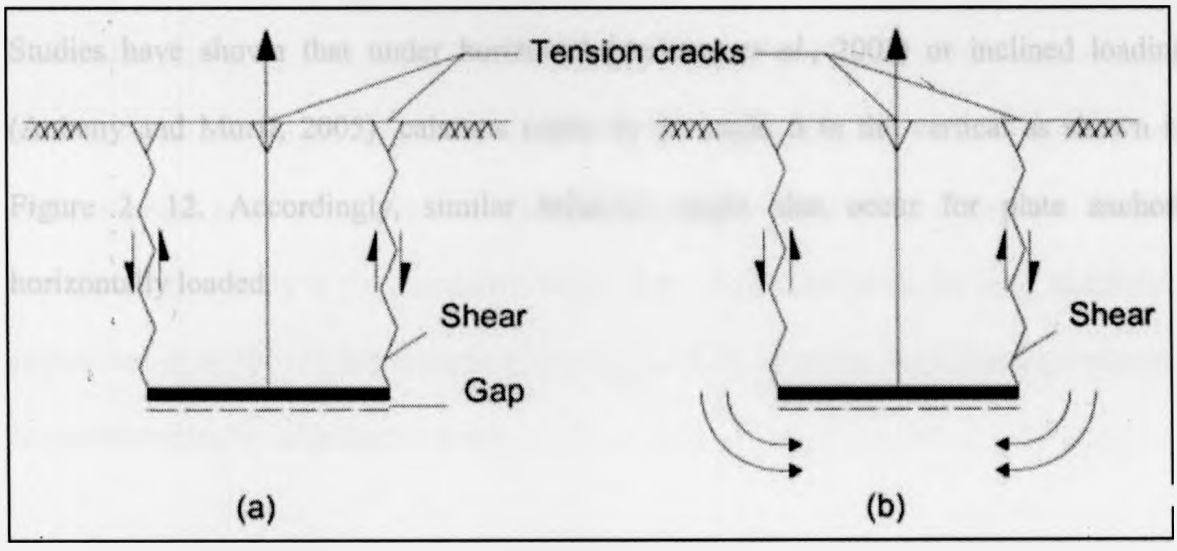

Figure 2. 11: Failure mechanisms for shallow anchor (a) full separation at bottom (b) fully bonded at bottom (Thorne *et al.*, 2004).

As part of their experimental analysis of plate anchors, Rowe and Davis (1982) reported that for anchors at *H/B* less than 2.5, tension cracks appeared even for relatively small displacements. However no signs of plastic flow around the anchor were noticed for shallow anchors.

Another application similar to plate anchors is suction caissons. Aubeny *et al.* (2001, 2003a, 2003b and 2005) have reported extensively on the performance of suction caissons under undrained conditions using the plastic limit approach. Aubeny *et al.* (2003a) showed that the horizontal capacity of caissons subjected to inclined loading up to 15° from the horizontal and embedded in linearly varying strength profiles was not markedly affected by the vertical load component.

Randolph and Houlsby (1984) used plasticity theory to calculate breakout factors for both perfectly smooth and rough horizontally loaded caissons of 9.14 and 11.94 respectively. Studies have shown that under horizontal (Aubeny *et al.*, 2001) or inclined loading (Aubeny and Murff, 2005), caissons rotate by an angle Δ to the vertical as shown in Figure 2. 12. Accordingly, similar behavior might also occur for plate anchors horizontally loaded.

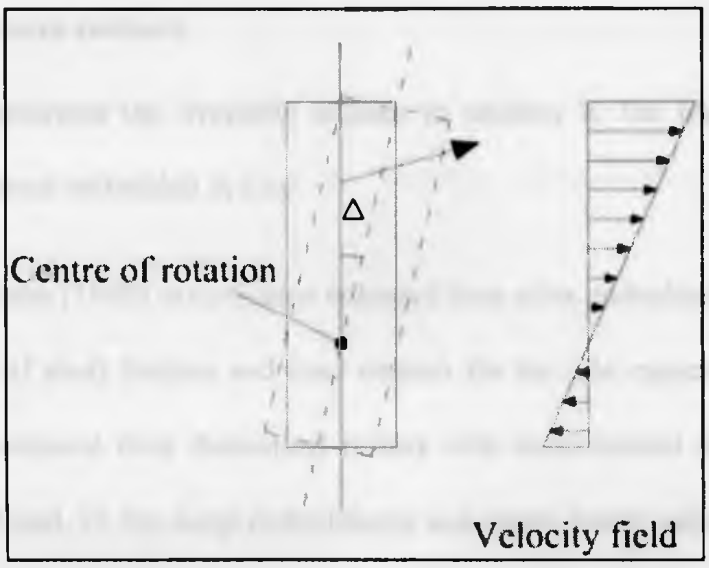

Figure 2. 12: Suction caissons rotation upon inclined loading (Aubeny *et al.* 2003a).

Plasticity analysis performed by Aubeny *et al.* (2001) for suction caissons under lateral loading demonstrated that the load attachment point has a great effect on caisson capacity. They showed that caisson capacity can decrease by a factor of five when the load attachment point is changed from its optimum location. The optimum location varies from mid-caisson height in uniform soil profiles to three-quarters of the height in soil with a strength profile that increases linearly from zero at the mudline. They also showed that the load capacity is very sensitive to the load attachment point for load inclination angles less than 30°. At larger inclination angles (45°), however, load capacity becomes less sensitive to line attachment depth.

2.3 Enlarged base anchors

This section summarizes the available studies in relation to the pullout behavior of enlarged base anchors embedded in clay.

Meyerhof and Adams (1968) investigated enlarged-base piles embedded in clay, ignoring the contributions of shaft friction and base tension for the pile capacity. Meyerhof and Adams (1968) compared their theoretical results with experimental data and found N_c values between 9 and 10 for deep embedments and much lower values. The origin of these values may be that their experimental tests were carried out at relatively shallow depths and in stiff fissured clay, and the mobilized strength was close to the residual value. Meyerhof and Adams (1968) also studied the effect of loading rate on the capacity of enlarged-base piles, and found that for soft clays, the capacity under long term loading was much higher than for short term loading, while for stiff clays, the opposite behavior occurred.

The behavior of grouted tieback and tiedown anchors can also be compared to that of inflatable anchors. Primarily used for tension loadings, tiebacks can be also be used to sustain compression loadings, particularly when installed in large diameter holes (Shnabel and Shnabel, 2002). Grouted anchors get their resistance from the skin friction mobilized along the grouted (bond) length as well as from the end bearing. Suction mobilized at the anchor tip is usually neglected in design to accommodate the long-term behavior of soil (Sabatini *et al.* 1999). Anchor capacity has been shown to increase with bond length up to about 9 to 12 m, beyond which it becomes independent of bond length (Sabatini *et al.* 1999).

Of the various types of tieback that have been considered, single underream tiebacks are most likely to show behavior similar to inflatable anchors. Weatherby (1982) proposed that the ultimate anchor capacity P for single underream tiebacks in cohesive soils could be calculated as

$$P = \alpha C_u L_s \pi D_s + \frac{\pi}{4}\left(D_u^2 - D_s^2\right) N_c C_u \qquad 2.14$$

where L_s and D_s are the anchor shaft length and diameter, D_u is the underreamed diameter and N_c is the breakout factor, which is usually taken to be equal to 9.

Inflatable anchors received much less attention in the literature compared to the other anchor shapes. Many parameters affecting their behavior need to be investigated to better understand their performance.

Cox and Reese (1976) performed tests to investigate the pullout capacity and the effect of lateral loading on grouted piles embedded in stiff clay. They found that lateral pile loading caused a significant reduction in the bond between the soil and the upper part of the grouted area. For the different examined piles, the length of top portion subjected to bond separation ranged from 5 to 9 feet.

Randolph *et al.* (2000) studied the behavior of both T-Bar and ball penetrometers in cohesive material. They provided upper and lower bound solutions supported by finite element simulations of spherical penetrometers penetrating a rigid-plastic material that obeyed a Trecsa or Von Mises failure mechanism. The assumed mechanism was based on solutions provided by Randolph and Houlsby (1984) for a T-bar penetrometer. Analysis

showed a breakout factor ranging from 11.8 for fully smooth to 15.54 for fully rough conditions, and gave excellent agreement with the finite element analysis. While theoretical solutions showed a difference in bearing resistance of 12 to 30% between spherical and cylindrical geometries, experimental results showed that the difference between net bearing resistances for the two geometries was at most 5% (Randolph *et al.*, 2000).

In their experimental studies, Newson *et al.* (2003b) tested a steel anchor with a lower rubber membrane embedded in an artificial clayey soil with an initial undrained shear strength of 1.5 to 2 kPa. During the tests, pressure was applied to inflate the lower membrane, then the anchor was pulled out. They studied the effects of the pullout rate and the anchor inflation, and investigated the improvement of anchor capacity with consolidation. They found an increase in the pullout capacity for stiffer clays as well as for increased membrane pressures. In addition, a further increase in capacity occurred with a waiting period between the anchor installation and the membrane inflation. In applications such as offshore ROVs, however, in which short term loading is required, such waiting periods are unlikely to be available. They also observed that a high mobilization distance is required for peak load to be achieved. The failure mechanism of the inflatable anchor system is still unknown and further investigation should be undertaken to allow better design of such systems.

Newson *et al.* (2003a) suggested that the equations calculating the pullout capacity of grouted nails/anchors/enlarged-base piles might be appropriately used with inflatable anchors. Accordingly, ignoring the effect of friction along the smooth steel part of the anchor, the membrane capacity when deflated (F_{uo}) and when inflated (F_{ui}) can be

estimated as follows:

$$F_{uo} = \alpha C_u A \qquad 2.15$$

$$F_{ui} = N_c C_u A' \qquad 2.16$$

where α is the adhesion factor, L is the membrane length, A is the membrane surface area for deflated condition and A' is the projected cross-sectional area of the inflated membrane.

Liang *et al.* (2008) numerically simulated the pullout behavior of vertical inflatable anchors embedded in very soft clay. Their results showed that local drainage around the anchor during installation and inflation significantly improved the clay undrained shear strength. Their analysis showed that the mobilized displacements at peak strength determined from their numerical analysis were found to be less than those measured experimentally by Newson *et al.* (2001).

2.4 Anchors with rectangular openings

The behavior of this proposed anchor system, being analyzed using a plane strain model, can be compared to the behavior of closely spaced anchors embedded in clay.

While many studies investigating the behavior of single plate anchors under different loading conditions are available (e.g. Merifield *et al.* 2001; Rowe and Davis 1982 and Das and Puri 1989), much less attention has been given to the interaction between closely spaced anchors. Furthermore, the few available studies are mainly concerned with anchors embedded in sand rather than clay.

Kouzer and Koumar (2009) studied the pullout behavior of two interfering horizontal plate anchors using an upper bound limit analysis. Their results showed that no interference occurred between anchors spaced at S greater than $2H\tan\varphi$, where φ is the soil angle of internal friction. They confirmed these results by monitoring the nodal velocities patterns around the anchors at various S/b values. They reported zero nodal velocities at the centerline between the anchors at S greater than $2H\tan\varphi$. For closer spaced anchors, the non-zero velocity nodes were contained in a wedge above the anchor plate, having rupture surfaces at both anchor ends making an angle φ with the vertical, and intersected by linear rupture surfaces. This soil wedge is believed to act as a rigid unit with an equal velocity to that of the anchor.

In their study, Kumar and Kouzer (2008) studied the same problem and also using an upper bound limit analysis. They studied the effect of spacing between rough anchors embedded in sand. They provided the following equations to calculate the failure load P_u of a group of closely spaced horizontal anchors:

- For two anchors at $S<2H\tan\varphi$

$$P_u = \gamma bH + 0.5\gamma H^2\tan\varphi + 0.5\gamma(\frac{S}{2})^2\cot\varphi + \gamma(\frac{S}{2})(H - \frac{S\cot\varphi}{2}) \qquad 2.17$$

$$F_\gamma = \frac{P_u}{\gamma bH} = 1 + 0.5\lambda\tan\varphi\frac{\alpha^2}{8\lambda\tan\varphi} + 0.5\alpha \qquad 2.18$$

- For multiple anchors at $S<2H\tan\varphi$

$$P_u = \gamma bH + 2[0.5\gamma(\frac{S}{2})^2 \cot\varphi + \gamma(\frac{S}{2})(H - \frac{S\cot\varphi}{2})] \quad 2.19$$

$$F_\gamma = 1 - \frac{\alpha^2}{4\lambda\tan\varphi} + \alpha \quad 2.20$$

where $\alpha = S/b$, λ is the embedment ratio, γ is the soil unit weight and F_γ is a non dimensional uplift capacity factor.

- For anchors at $S>2H\tan\varphi$

$$P_u = \gamma bH + 2(0.5\gamma H^2 \tan\varphi) \quad 2.21$$

$$F_\gamma = 1 + \lambda\tan\varphi \quad 2.22$$

Kumar and Bhoi (2009) experimentally studied the vertical pullout behavior of horizontal closely spaced strip anchors in sand. They investigated the effects of spacing, embedment depth as well as the sand angle of internal friction on the system capacity. Their results were presented in terms of an efficiency factor, defined as the ratio between the failure load of an intervening anchor and the failure load of a strip plate anchor having the same width. The results showed a significant efficiency reduction with the decrease of spacing between anchors. They also showed that the *S/b* value, after which each of the anchors behaves separately, increases with the increase of embedment ratio *H/b*. For example, at embedment ratios of 3, 5 and 7, the corresponding *S/b* values were 3, 5 and 7 respectively. While theory showed an efficiency decrease with the increase in sand angle of internal friction φ (e.g Kouzer and Koumar 2009), this behavior has not been clearly

shown in Kumar and Bhoi's experimental results.

Merifield and Smith (2010) numerically investigated the behavior of multiple vertically spaced horizontal plate anchors embedded in clay, and suggested a procedure to calculate their undrained capacity. The results showed that for anchors embedded in weightless soil, the effect of soil interaction on the shallowest anchor was insignificant. The results also showed that the capacity of the anchor below the shallowest one is not affected by the overall embedment ratio for *S/b* values less than 2. They suggested that the capacity of the anchors below the shallowest one, at *S/b* less than 3, could be conservatively calculated using the following equation, which they originally provided to calculate the breakout factor N_c of a single anchor, while assuming *H/b=S/b*.

$$N_c = 2.08 + 2.47Ln\left(\frac{H}{b}\right) \qquad 2.23$$

Merifield and Smith (2010) also studied multiple anchors embedded in soil with nonzero weight. The results showed that for closely spaced anchors both anchors will behave as a single unit, while above a critical spacing ratio $(S/b)_{cr}$, each anchor will behave independently. They suggested that the critical spacing ratio could be taken as $\left(\frac{2+3\pi}{\pi}\right)$.

The behavior of closely spaced footings can also be compared to that of the closely spaced anchors, especially at shallow depths. Griffiths *et al.* (2006) studied the behavior of two closely spaced strip footing resting on weightless soil having a randomly varying shear strength using a finite element technique. Their deterministic analysis showed that, for the studied range of spacings, the breakout capacities were nearly equal revealing the

insignificant interference effect of closely spaced footings resting on clay. For these analyses, the effect of the pore pressures generated by footings has not been taken into account (Griffiths *et al.* 2006). It is also worth mentioning that the used finite element mesh in their study was composed of square elements for simplicity; however a finer mesh specially near footing edges would give more accurate solutions (Griffiths *et al.* 2006). Their probabilistic studies also showed that, the interference effect is higher for footings supporting separate structures compared to those supporting a single structure.

Ghosh and Sharma (2010) numerically investigated the settlement pattern of two closely spaced strip footings resting on layered soils. The studied footings were resting on a strong top layer of thickness H_1 and of young's modulus E_1 underlying a weaker bottom layer of thickness H_2 and of young's modulus $E_2$and finally resting on a rigid base. They defined the settlement ratio as the ratio of the settlement of a single footing placed next to another one, to the settlement of an isolated footing. The results showed that the inference between footings causes a greater settlement in the bed compared to that caused by a single footing. For example, for footings subjected to a pressure of 0.25 MN/m resting on soils of E_2/E_1=0.25, a settlement ratio of more than 1.55 has been shown for $S/b = 0$. This value decreases with the increase of S/b reaching a value of approximately 1.1 at $S/b = 5$. They also found that the increase in S/b as well as E_2/E_1 decreases the settlement ratio (Gosh and Sharma 2010). The results also showed that variation of the applied load on footings significantly affected the settlement value; however the settlement ratio kept constant for the different studied S/b.

Kumar and Bhattachaya (2010) studied the capacity of multiple interfering strip footings using lower bound finite limit analysis. They considered footings with both rough and

smooth bases. For the different studied cases, an efficiency factor greater than 1 was found, for both smooth and rough bases. The results showed significantly higher efficiencies for rough based footings. For the range of studied cases, the results showed efficiency factors ranging between 1 and 10 for smooth bases, compared to 1 and 128 for rough bases. Their results also showed that for both rough and smooth bases, no interference occurred at *S/b* greater than 3 (Kumar and Bhattacharya 2010).

2.5 Summary

In this chapter, a literature survey on the behavior of soil anchors was presented. This survey highlights the developed solutions for anchors capacity, the effects of the different parameters on their pullout behavior and the suggested failure mechanisms.

This survey was divided into three sections, treating regular plate anchors, enlarged base anchors and anchors with rectangular openings.

Regarding regular plate anchors, a review of the available literature was performed. The effects of the different parameters on the anchor pullout capacity were presented. These parameters include the effects of embedment depth, overburden pressure, breakaway conditions, anchor thickness, clay strength increase with depth, soil anchor interface conditions, anchor rotation and load inclination. This survey showed the only loading condition considered in previous studies was of anchors subjected to normal loads applied through their centre of mass.

Regarding anchors with an enlarged base, anchors of similar shapes were not available in literature. Accordingly, a review of the similar applications was presented. These applications include enlarged based piles, inflatable anchors, tiebacks and underreamed

anchors, grouted piles, T-bars and ball penetrometers. It was shown from the results that the effects of many parameters still need further studies, especially for inflatable anchors since they are the most similar type to the studied enlarged base anchor shapes in this study.

Finally, for anchors with rectangular openings, the review covered the behavior of closely spaced footings and closely spaced plate anchors. This review showed that only few studies are available for interfering plate anchors in clay, while much more are available for sand. Many researchers suggested that no significant interaction occurs between vertically loaded footings resting on homogeneous clay.

2.6 References

Aubeny, C. P., and Murff, J. D. (2005). "Simplified limit solutions for the capacity of suction anchors under undrained conditions," *Ocean Engineering*, Vol.32, No.7, pp 864-877

Aubeny, C. P., Han, S., and Murff, J. D. (2003a). "Refined model for inclined load capacity of suction caissons," *Proceeding of 22nd International Conference of Offshore Mechanics and Arctic Engineering OMAE*, Vol.3, pp 883-887

Aubeny, C. P., Murff, J. D., and Moon, S. K. (2003b). "Inclined load capacity of suction caissons," *International Journal of Numerical and Analytical Methods in Geomechanics*, Vol.27, No.14, pp 1235-1254

Aubeny, C. P., Moon, S. K., and Murff, J. D (2001). "Lateral undrained resistance of suction caisson anchors," *International Journal of Offshore and Polar Engineering*, Vol.11, No.3, pp 211-219

Colwill, R. D. (1996). "Marine drag anchor behavior-a centrifuge modeling and theoretical investigation," Degree of doctor of philosophy thesis, The University of Manchester, Manchester, United kingdom

Cox, W. R. and Reese, L.C. (1976). "Pullout tests of grouted piles in stiff clay," *Offshore Technology Conference*, Dallas, Texas, pp 539-551

Das, B. M., and Singh, G. (1994). "Uplift capacity of rigid plate anchors in clay," *Proceedings of the fourth International Offshore and Polar Engineering Conference*, Japan, Vol.1, pp 436-442

Das, B. M., and Shin, E. C. (1993). "Uplift capacity of rigid vertical metal piles in clay under inclined pull," *International Journal of Offshore and Polar Engineering*, Vol.3, No.3, pp 231-235

Das, B. M., and Puri, V. K. (1989). "Holding capacity of inclined square plate anchors in clay," *Soils and Foundations Journal*, Vol.29, No.3, pp 138-144

El-Khatib, S., and Randolph, M. P. (2004). "Finite element modeling of drag-in plate anchor installation," *Proceedings of the 9th Symposium for Numerical Models in Geomechanics*, Ottawa, Canada, pp 541-547

El-Khatib, S., Lonnie, B. and Randolph, M. P. (2002). "Installation and pull-out capacities of drag-in plate anchors," *Proceedings of the 12th International Offshore and Polar Engineering Conference*, Japan, Vol.12, pp 648-654

Griffiths, D.V., Gordon, A., F.and Manoharan, N. (2006). "Undrained bearing capacity of two strip footings on spatially random soil," *International Journal of Geomechanics*, Vol.6, No.6, pp 421-427

Gunn, M., J. (1980). "Limit analysis of undrained stability problems using a very small computer," *Proc. Symp. on Computer Applications in Geotechnical Problems in Highway Engineering*, Cambridge University, Engineering Department, pp 5-30.

Jun, L., Li-ling, W. and Yu-xia, H. (2006). "Pullout capacity of circular plate anchors in NC clay," *Journal of Dalian University of Technology*, Vol.46 , No.5, pp 712-719

Liang, Y., Newson, T. A. and Hinchberger, S. (2008). "Numerical study of the mechanics

of inflatable anchors in clay," *Proceedings of the18th International Offshore and Polar Engineering Conference*, pp 546-551

MacKenzie, T. R. (1955). "Strength of deadman anchors in clay," Pilot tests, Degree of Master of Science thesis, Princeton University, The United States of America

Mandel, J. (1963). "Interference plastique de foundations superficielles, " *Proceeding of the International Conference on Soil Mechanics and Foundation Engineering*, Budapest, pp 267-280

Merifield, R. S., and Smith, C. C. (2010). "The ultimate uplift capacity of multi-plate strip anchors in undrained clay," *Computers and Geotechnics,* Vol.37, No.4, pp 504-514

Merifield, R. S., Lyamin, A. V., and Sloan, S. W. (2005). "Stability of inclined strip anchors in purely cohesive soil," *Journal of Geotechnical and Geoenvironmental Engineering*, Vol.131, No.6, pp 792-799

Merifield, R. S., Lyamin, A. V., Sloan, S. W., and Yu, H. S. (2003). "Three-dimensional lower bound solutions for stability of plate anchors in clay," *Journal of Geotechnical and Geoenvironmental Engineering*, Vol.129, No.3, pp 243-253

Merifield, R. S., Sloan, S. W., and Yu, H. S. (2001). "Stability of plate anchors in undrained clay," *Geotechnique* Vol.51, No.2, pp 141-153

Meyerhof, G. G. and Adams, J. (1968). "The ultimate uplift capacity of foundations," *Canadian Geotechnical Journal*, Vol.5, No.4, pp 225-244

Newson, T. A., Smith, F. W. and Brunning, P. (2003a). "An experimental study of inflatable offshore anchors in soft clay," *BGA International Conference on Foundations, Innovations, Observations, Design and Practice*, pp 695-704

Newson, T. A., Smith, F. W., Brunning, P. and Gallaher, S. (2003b). "An experimental study of inflatable offshore anchors," *Proceedings of the 13th International Offshore and Polar Engineering Conference, Design and Practice*, pp 1340-1345

O'Neill, M. P., Bransby, M. F. and Randolph, M. F (2003). "Drag anchor fluke-soil interaction in clays," *Canadian Geotechnical Journal*, Vol.40, No.1, pp 78-94

Plaxis Bv (2006). Plaxis 2D-Version 8 Manuals, Version 8

Randolph, M. F., and Houlsby, G. T. (1984). "The limiting pressure on a circular pile loaded laterally in cohesive soil," *Geotechnique*, Vol.34, No. 4, pp 613-623

Ranjan, G. and Arora, V. B. (1980). "Model studies on anchors under horizontal pull in clay," *Proceedings of the 3rd Aust., N.Z. Conf. Geomech.*, Wellington, N.Z. 1, pp. 65-70.

Rao, S. N., Latha, K. H., Pallavi, B., and Surendran, S. (2006). "Studies on pullout capacity of anchors in marine clays for mooring systems," *Applied Ocean Research*, Vol.28, No.2, pp 103-111

Rao, S. N., Ravi, R.. and Prasad, B. S. (1997). "Pullout behavior of suction anchors in soft marine clays," *Marine Geosources and Geotechnology*, Vol.15, No.2, pp 95-114

Rowe, R. K., and Davis, E. H. (1982). "The behavior of plate anchors in clay," *Geotechnique*, Vol32, No.1, pp 9-23

Rowe R. K. (1978). "Soil structure interaction analysis and its application to the prediction of anchor behavior," Degree of doctor of philosophy thesis, *The University of Sydney*, Australia.

Rowe, R. K., and Davis, E. H. (1977). "Application of the finite element method to the prediction of collapse loads," *The University of Sydney,* Australia, Research report No. R310

Sabatini, P. J, Pass, D. G. and Bachus, R.C. (1999). "Ground anchors and anchored systems report," *U.S department of Transportation-Federal Highway Administration*, Geotechnical Engineering circular No.4

Semple, R., and Rigden, W. J. (1984). "Shaft capacity of driven pipe in clay," *Proceedings of the American Society of Civil Engineers Symposium* "analysis and design of pile foundations" pp. 59-79

Shnabel, H. and Shnabel, H. W. (2002) "Tiebacks in foundation engineering and construction," Lisse [Netherlands]; Exton, PA : A.A. Balkema

Song, S., Hu, Y., and Randolph, M. F. (2008). "Numerical simulation of vertical pullout of plate anchors in clay," *Journal of Geotechnical and Geoenvironmental Engineering*, Vol.134, No.6, pp 866-875

Thorne, C. P., Wang, C. X., and Carter, J. P. (2004). "Uplift capacity of rapidly loaded strip anchors in uniform strength clay," *Geotechnique*, Vol.54, No.8, pp 507-517

Van Langen, H. and Vermeer, P.A. (1991). "Interface elements for singular plasticity points," *International Journal for Numerical and Analytical Methods in Geomechanics*, Vol.15, No.5, pp 301-315

Weatherby, D. E. (1982). "Tiebacks report, " *U.S department of Transportation-Federal Highway Administration*

Wilde, B., Treu, H. and Fulton, T. (2001). "Field testing of suction embedded plate anchors," *Proceedings of the 11th International Offshore and Polar Engineering Conference*, Stavanger, Norway, pp 544-551

Wood, D. M. (1990). "Strength of soils". *Soil behavior and critical state soil mechanics*, Cambridge University press, Cambridge

Yu, L., Liu, J., Kong, X., and Hu, Y. (2009). "Three dimensional numerical analysis of the keying of vertically installed plate anchors in clay," *Computers and Geotechnics*, Vol.36, No.4, pp 558-567

Chapter 3 Numerical Investigation of The Undrained Capacity of Plate Anchors Embedded in Clay

3.1 Introduction

Soil anchors are a common support system in geotechnical engineering to sustain tensile and uplift forces. Depending on the application, anchors can be subjected to a variety of loading conditions. For example, when used as foundations for transmission towers, the forces on the anchor are primarily uplift forces, whereas in shoring systems anchors are subjected to lateral loads (e.g. Merifield *et al.* 2003). The current trend in the offshore industry is for exploration in deeper waters (greater than 500m depth), rendering conventional piles, mat foundations and gravity structures generally uneconomical. Consequently, floating structures attached to the sea floor by means of mooring lines anchored to the seabed are becoming more widespread (Jun *et al.* 2006). The mooring line self weights, waves, wind, ice and currents can all apply significant lateral and inclined loads to embedded anchors.

Many theoretical and numerical techniques have been used to predict the ultimate pullout capacity of anchors and to understand their behavior under different loading conditions (e.g. Merifield *et al.* 2001; Gunn 1980; Rowe and Davis 1982; Das and Puri 1989). These include empirical solutions, upper and lower bound plasticity solutions, cavity expansion theory, and finite element solutions.

The majority of previous studies in this field have been concerned with embedded anchors subjected to loads applied through the centre of mass and perpendicular to the anchor as shown in Figure 3. 1. This assumes that the anchor is already in the optimal position for loading. Other loading cases have not received as much attention, despite

their potential importance. This study has therefore concentrated on situations where the anchor alignment and direction of the force are sub-optimal. The main objective of the present study is to numerically investigate the behavior of plane strain strip anchors subjected to these more complex loading conditions. Such conditions may arise particularly for deep offshore conditions (water depth greater than 500m) as a result of many factors, including the lower installation controllability and catenary effects for anchors connected by steel chains or steel wire ropes. To this end, a finite element parametric study was carried out to assess the behavior of anchors embedded in a cohesive soil under a range of loading conditions. Analyses were conducted to evaluate the effects of the different factors on the ultimate pullout capacity including: surface roughness, anchor thickness, load and anchor inclination, point of load application, clay strength increase with depth and soil disturbance following anchor installation. These results are compared to previously published work and conclusions drawn from the data.

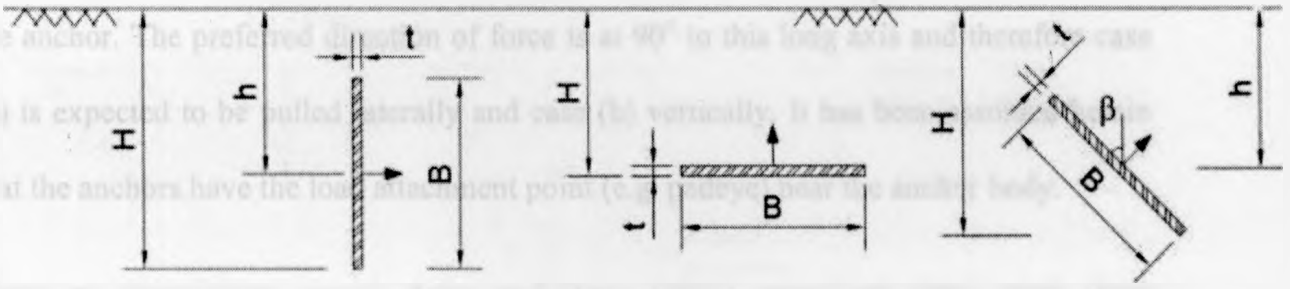

(a) Vertical anchor (b) Horizontal anchor (c) Inclined anchors

Figure 3. 1: Different configurations of embedded anchors studied in the literature and their geometric terminology.

3.2 Previous work

The ultimate capacity of plate anchors embedded in clay under a range of loading conditions and the effect of parameters such as embedment depth, overburden pressure, anchor inclination, anchor thickness and shape and surface roughness on their behavior have been studied using different techniques, including physical models, finite element models, upper and lower bound plasticity solutions and empirical equations.

Figure 3. 1 shows three embedded anchors and the terminology used within this study to describe their geometric conditions. Anchors typically have a high aspect ratio B/t, with the thickness t much less than the length B. In this study, a vertical anchor is that with the length B perpendicular to the ground surface as presented in Figure 3. 1 (a). A horizontal anchor is rotated by 90° and is shown in Figure 3. 1 (b), and an inclined anchor is rotated by an angle β to the vertical as shown in Figure 3. 1 (c). Anchors were studied at different embedment depths H, where H is the distance between ground surface to the bottom of the anchor. The preferred direction of force is at 90° to this long axis and therefore case (a) is expected to be pulled laterally and case (b) vertically. It has been assumed herein that the anchors have the load attachment point (e.g. padeye) near the anchor body.

Using an elasto-plastic model, Rowe and Davis (1982) carried out plane strain finite element analysis of both vertical and horizontal anchors, as shown in Figure 3. 1 (a) and (b) respectively. They considered two cases at the anchor-soil interface: the "immediate breakaway" condition, in which the interface cannot sustain any tension, and the "no breakaway" condition, in which a full bond between the anchor and soil was assumed. For intermediate interface strength, anchors will behave initially as though they are fully

bonded and then breakaway will occur during loading, and capacity will increase approximately linearly with overburden pressure between the limits of the immediate and no-breakaway conditions (Rowe and Davis, 1982).

They also classified anchors into shallow and deep depending on whether anchors are greatly affected by embedment and overburden pressure, and whether the plastic region extends to the ground surface as shown in Figure 3. 2 (a) and (b). Figure 3. 2 (c) illustrates the critical embedment depth H_c; at which the anchor behavior changes from shallow to deep. The capacity of deep anchors, is not noticeably affected by an increase in embedment or overburden pressure, and the localized zone of plastic deformation around a deep anchor is not influenced by the soil surface. This is a consequence of the undrained shear strength of clay being independent of the mean normal stress beyond a critical depth (Merifield *et al.*, 2003).

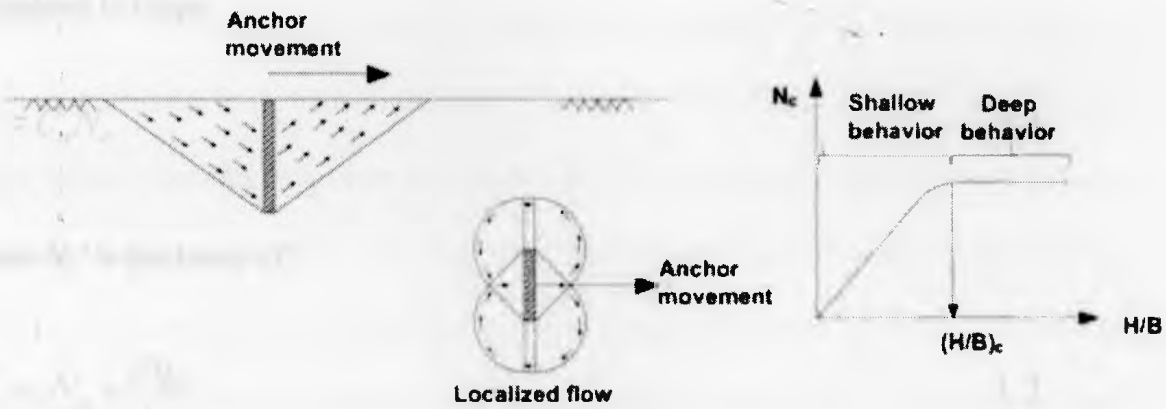

Figure 3. 2: Typical anchor failure mechanisms for horizontally loaded vertical anchors for (a) shallow and (b) deep conditions; (c) illustration of the critical embedment ratio $(H/B)_c$.

The value of the critical depth is influenced by many factors, including the inclination angle of the anchor and the load, overburden pressure, anchor surface roughness and the point of load application. Rowe and Davis (1982) showed that, for vertical anchors, deep anchor behavior occurs for embedment ratios *H/B* greater than 3, under both immediate breakaway conditions and no-breakaway conditions (Rowe and Davis 1982).

Their analysis also suggested that the overburden pressure value required to ensure a no-breakaway response in a homogeneous elasto-plastic material is in the range of $4C_u/K_o$ to $6C_u/K_o$ for vertical anchors, where K_o is the lateral earth pressure coefficient and C_u is the undrained shear strength.

Many analytical solutions have been proposed to calculate the ultimate capacity of plate anchors. Among these were the following equations [also provided by Rowe and Davis (1982)] to estimate the required applied pressure q_u causing undrained failure of anchors embedded in clays:

$$q_u = C_u N_c' \qquad 3.1$$

where N_c' is the lower of :

$$N_c' = \underline{N_c} + \frac{S q_h}{C_u} \qquad 3.2$$

and

$$N_c = N_c^*. \qquad 3.3$$

Here $\overline{N}_c$ is the breakout factor for the unbonded condition, N_c* is the breakout factor for a fully bonded condition, q_h is overburden pressure and S is the rate of increase of anchor capacity with overburden pressure.

Based on limit analysis using the finite element method, Merifield *et al.* (2001) also provided equations for N_c for vertical and horizontal anchors in homogeneous clay profiles, reflecting the influence of overburden pressure and embedment depth on anchor capacity. These results show that beyond a threshold value of overburden pressure, anchor behavior changes from shallow to deep condition. Accordingly, the dimensionless overburden pressure term $\gamma h/C_u$ was introduced to show this dependence, where h, as shown in Figure 3. 1, is the distance between ground surface to anchor centre of mass and γ is the soil unit weight.

Merifield *et al.* (2001) compared their results to the various laboratory and finite element solutions in the literature. Figure 3. 3 shows the variation of the breakout factor N_c (immediate breakaway) with embedment ratio H/B. This figure shows the upper and lower bound plasticity solutions after Rowe (1978), five-variable upper bound solution after Merifield *et al.* (2001), and the upper/lower bound solutions of Merifield *et al.* (2001) for a vertical anchor loaded horizontally through the centre of mass. The majority of these relationships are comparable up to embedment ratios H/B = 3, with a non-linear increase of N_c up to approximatley 4 for the Rowe (1978) results, while the other results show a continuing increase. For the highest embedment ratios, the solutions diverge, with N_c values ranging between 5 and 9 for deep embedments of H/B = 10. It should be noted that Merifield *et al.* reported that the five-variable upper bound solution was not capable

of defining the true collapse load for all of the studied embedment ratios and that beyond $H/B = 3$, values of breakout factors are over-estimated by 25 %.

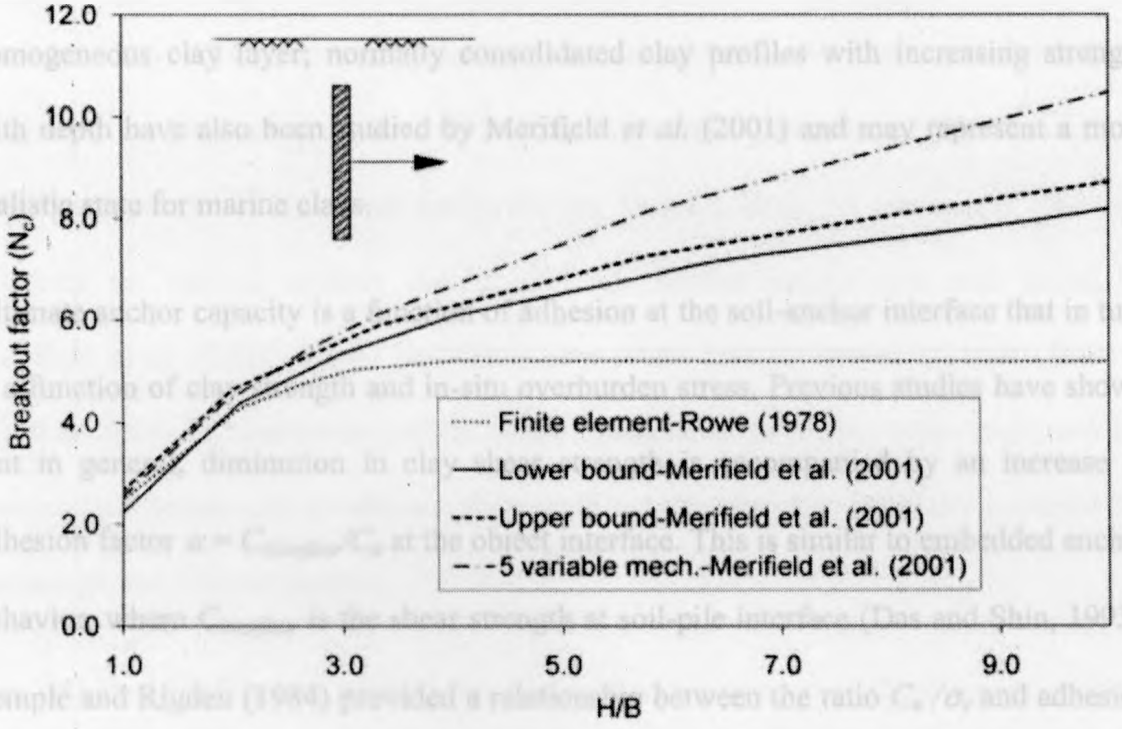

Figure 3. 3: Variation of breakout factor N_c with embedment ratio H/B for horizontally loaded vertical anchor through centre of mass (after Merifield *et al.* 2001).

The finite element analyses carried out by Merifield *et al.* (2001) for lower and upper bound plasticity solutions showed limiting values of the breakout factor N_c for a fully bonded case of 10.47 and 11.86, respectively, for vertical anchors. These are compatible with analytical solutions from Rowe (1978). Their analyses also showed that the increase in embedment depth increases the zone of plastic deformation to include an area above, below and behind the anchor.

Experimental results reported by Mackenzie (1955) and Ranjan and Arora (1980) on vertical strip anchors embedded in soft clay could not clearly define the breakaway

conditions, and adhesion or suction was not measured.

Most of the existing studies have concentrated on the behavior of anchors embedded in a homogeneous clay layer; normally consolidated clay profiles with increasing strength with depth have also been studied by Merifield *et al.* (2001) and may represent a more realistic state for marine clays.

Ultimate anchor capacity is a function of adhesion at the soil-anchor interface that in turn is a function of clay strength and in-situ overburden stress. Previous studies have shown that in general, diminution in clay shear strength is accompanied by an increase in adhesion factor $\alpha = C_{interface}/C_u$ at the object interface. This is similar to embedded anchor behavior, where $C_{interface}$ is the shear strength at soil-pile interface (Das and Shin, 1993). Semple and Rigden (1984) provided a relationship between the ratio C_u/σ_v and adhesion factor for clay, where σ_v is the effective overburden stress. They showed that for C_u/σ_v values less than or equal to 0.35, adhesion forces at a soil-pile interface might be assumed to be equal to clay shear strength, which could be applied for the case of soft and very soft clay.

Rowe and Davis (1982) suggested that anchor roughness has little effect on horizontal anchors (deep and shallow) and vertical anchors (deep only), since the development of significant shear stresses at the anchor surface is reduced due to the symmetry of the failure mechanism. On the other hand, they found that for shallow vertical anchors ($H/B<2$), the failure mechanism produced is asymmetric and high shear stresses might develop at the anchor interface. Hence any increase in anchor roughness will lead to an increase in ultimate capacity. Similar results were also found by Merifield *et al.* (2001

and 2003). However, these results are based only on numerical analyses, whereas no laboratory or field testing has been performed to date to validate them.

Rowe and Davis (1982) also suggested approximate solutions for inclined anchors. They suggested that for shallow anchors ($H/B<3$) at inclinations greater than 30° to the vertical, solutions reported for horizontal anchors might be used, while for angles less than 30°, solutions for vertical anchors should be used. Similar results were also found by Merifield *et al.* (2005). Rowe and Davis also found that for deeper anchors ($H/B>3$), solutions for both breakaway conditions are independent of anchor orientation, and for intermediate breakaway conditions, they modified the equation originally intended for horizontal and vertical anchors.

Das and Puri (1989) also studied the effect of inclination on shallow square anchors through laboratory test models. Based on their findings, they developed the following empirical equation for calculating inclined square anchor breakout factors:

$$N_c = N_{c(\psi=90^o)} + \left[N_{c(\psi=90^o)} - N_{c(\psi=0^o)}\right]\left(\frac{\psi}{90^o}\right)^2, \qquad 3.4$$

where ψ is the angle between the vertical plane and the pullout direction.

In their study for inclined strip anchors in clay, Merifield *et al.* (2005) used lower and upper bound theorems to investigate the effect of anchor inclination on the breakout factor N_c. They defined the inclination factor as the ratio of breakout factor for an inclined anchor to that of a vertical one for a weightless soil condition. As presented in Figure 3. 4, their results show that the inclination factor increases in a non-linear fashion

with increasing anchor inclination. These results are also consistent with the findings of the laboratory study carried out by Das and Puri (1989).

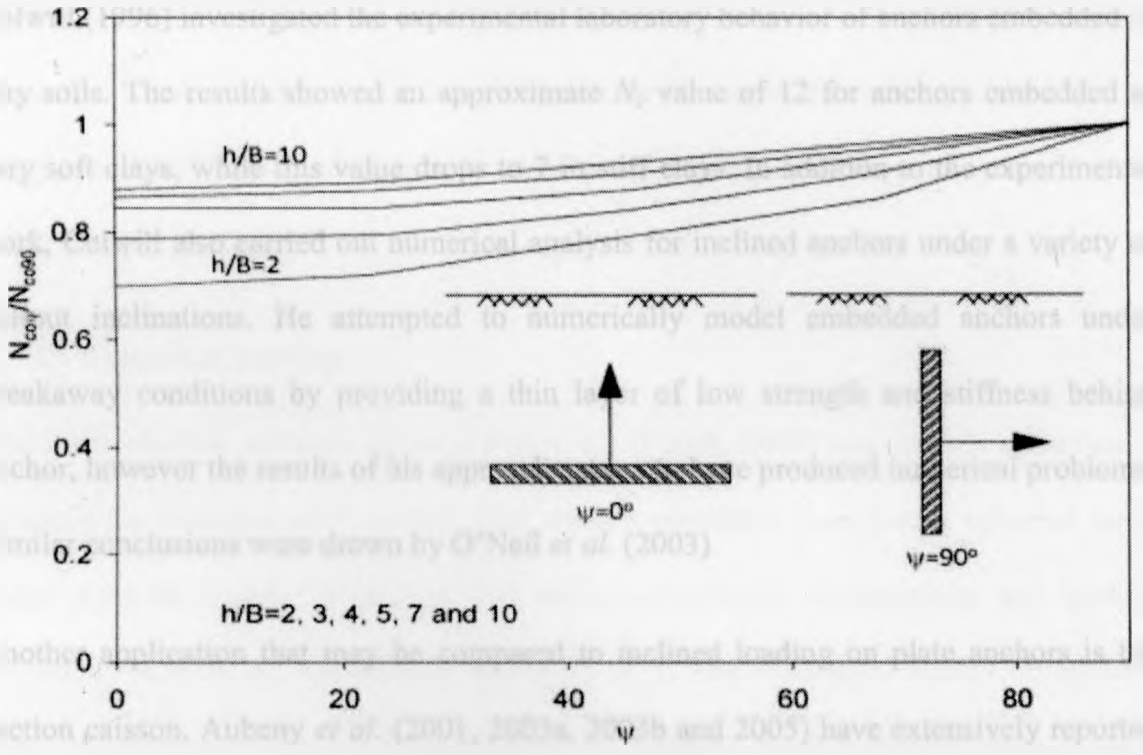

Figure 3. 4: Variation of inclination factor with anchor inclination (after Merifield *et al.* 2005).

Analyses presented by Rowe and Davis (1982) were based on a plate anchor of negligible thickness. To assess the anchor thickness effect, a limit analysis solution was performed on a diamond shaped section that is assumed to be an acceptable approximation for other shapes. Results of these analyses showed that for perfectly smooth anchors, the ultimate capacity decreases with an increase of anchor thickness, while in the case of rough anchors, ultimate capacity is not significantly affected by anchor thickness. Rao *et al.* (1997) experimentally tested the behavior of oblique pullout capacity (loading at 60° from the vertical) on pile suction anchors in marine clays. They demonstrated that the

vertical pullout capacity of piles increased with increasing aspect ratio L/D, where L and D are anchor length and diameter respectively.

Colwill (1996) investigated the experimental laboratory behavior of anchors embedded in clay soils. The results showed an approximate N_c value of 12 for anchors embedded in very soft clays, while this value drops to 7 in stiff clays. In addition to the experimental work, Colwill also carried out numerical analysis for inclined anchors under a variety of pullout inclinations. He attempted to numerically model embedded anchors under breakaway conditions by providing a thin layer of low strength and stiffness behind anchor, however the results of his approach appear to have produced numerical problems. Similar conclusions were drawn by O'Neil *et al.* (2003).

Another application that may be compared to inclined loading on plate anchors is the suction caisson. Aubeny *et al.* (2001, 2003a, 2003b and 2005) have extensively reported on the performance of suction caissons under undrained conditions mainly using upper bound plastic limit analysis. Aubeny *et al.* (2003) showed that for caissons subjected to inclined loading (orientation up to 15° from horizontal) and embedded in linearly varying strength profiles, the horizontal capacity was not markedly affected by the vertical component of load. At the optimum load attachment location, interaction between vertical and horizontal components is expected at load inclinations between 15° and 30°, where the optimum location varies from mid-caisson height in uniform soil profiles to three-quarters the height when the soil strength increases linearly with depth.

Plasticity analysis performed by Aubeny *et al.* (2001) on suction caissons under lateral loading demonstrated that the load attachment point has a great effect on caisson

capacity, and that a capacity change of up to a factor of five can result from changing the load attachment point from its optimum location. However, at larger inclination angles (45°), load capacity becomes less sensitive to load attachment depth.

A number of new anchor systems have also been developed recently (e.g. the SEPLA; Song *et al.* 2009), which are installed vertically and are required to rotate (i.e. key) before full loading is applied.

3.3 Numerical analysis

The finite element software package Plaxis 2D (Plaxis, 2006) was used to numerically simulate the behavior of a vertical steel anchor embedded in a purely cohesive layer under different loading conditions. The anchor dimensions, configuration and loading conditions studied are summarized in Figure 3. 5. The considered anchor dimensions were assumed based on the available data in literature for the different drag-in plate anchors types (i.e. Colwill 1996 and Wilde *et al.* 2001). It has been assumed that the anchor is loaded in a sub-optimal location or direction, and the following analyses have been designed to investigate the reduction in pullout capacity that occurs. In practice, some keying or rotation would be anticipated (dependent upon the location/direction of pull). This has been ignored in these analyses for the asymmetrically loaded cases; loss of embedment and distance could occur during this keying process and there may be serviceability constraints on the anchor. Hence a small strain approach was thought to be sufficient in the first instance. In the following sections, we will refer to the following specific cases:

- Case 1: Vertical load applied at the anchor top;

- Case 2: Inclined load applied at the anchor top;
- Case 3: Horizontal load applied at the anchor top;
- Case 4: Vertical load applied through the anchor centre of mass;
- Case 5: Inclined load applied through the anchor centre of mass;
- Case 6: Horizontal load applied through the anchor centre of mass.

Simulations for a 45° inclined anchor were also carried out. The following cases were modeled:

- Case 7: Inclined anchor subjected to loads parallel to the anchor axis applied at the anchor top;
- Case 8: Inclined anchor subjected to loads perpendicular to the anchor axis applied at the anchor top.

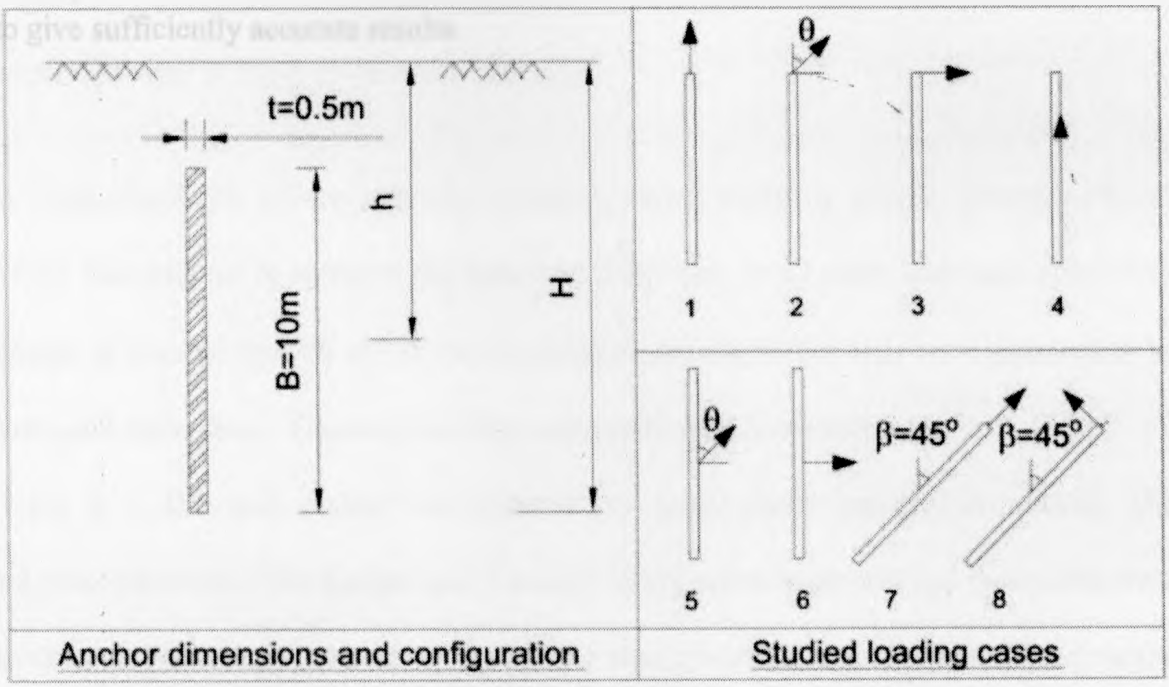

Figure 3. 5: The dimensions, configuration and loading geometries of the model anchors studied in the numerical analysis.

3.3.1 Discretization of the problem

The studied problem was discretized using 15-noded plane strain triangular elements. Mesh boundaries were extended to a distance $6B$ in X-direction on each side of the anchor centerline and a distance of $2B$ in Y-direction below anchor base. This mesh size was found to be necessary to ensure that the results were not affected by the domain boundaries. The mesh was generated automatically, based on a subroutine using a robust triangular principle searching for optimized triangles and resulted in an unstructured mesh. The vertical boundaries of the model were allowed to move in the Y-direction, while displacement in X-direction was restrained. For the lower boundary, displacement in both X and Y directions was restrained as shown in Figure 3. 6 (a), in which a typical mesh consisting of 4682 triangular elements is presented for the case of $H/B = 3$. Additional mesh refinement around the anchor, as shown in Figure 3. 6 (b), was required to give sufficiently accurate results.

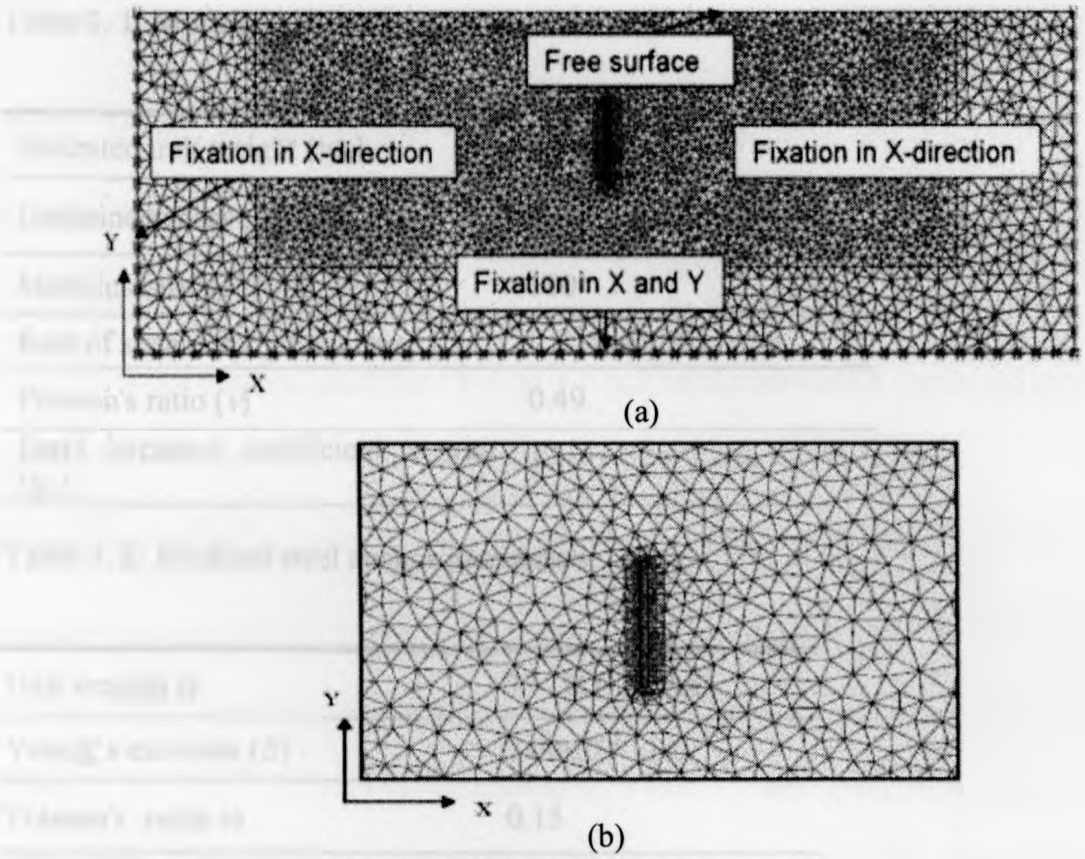

Figure 3. 6: (a) Example of discretized mesh of the model (width = 12B =120 m) and (b) expanded view of mesh close to the anchor.

A Mohr-Coulomb failure criterion modeling elastic-perfectly plastic behavior (Wood 1990) was adopted to simulate the behavior of the clay. In all cases undrained conditions (angle of internal friction $\varphi = 0^{o}$) were assumed and the model soils were assumed to be saturated throughout. The range of clay parameters used is presented in Table 3. 1. The steel anchor was modeled as a linear elastic non-porous material. The interface elements (Van Langen and Vermeer 1991) between the soil and the anchor were given a strength equal to a fraction α of the strength of the adjacent soil. The assumed anchor parameters are given in Table 3. 2.

Table 3. 1: Modeled clay parameters

Saturated unit weight (γ_{sat})	16 - 0.1[1] kN/m^3
Undrained shear strength (C_u)	20- 5[2] kPa
Modulus ratio (E/Cu)	100
Rate of shear strength increase (ρ) [2]	0, 1, 2 and 3 kPa/m
Poisson's ratio (ν)	0.49
Earth pressure coefficient at rest (K_o)	1

Table 3. 2: Modeled steel anchor parameters

Unit weight(γ)	77 - 0.1[1] kN/m^3
Young's modulus (E)	2.00x10^8 kPa
Poisson's ratio(ν)	0.15
Interface strength(α)	0.1, 0.4, 0.7 and 1

Preliminary analysis indicated that the plastic flow that occurred before failure could be quite significant, which is generally not acceptable for practical reasons due to the accompanying excessive displacements. Hence, the K4 criterion introduced by Rowe and Davis (1982) was adopted as a measure of the ultimate capacity of the anchor. The K4 failure load is defined as the load at which the stiffness of the material has declined to one quarter of its initial elastic stiffness. To determine this quantity, prescribed displacements were applied to the model anchors and load-displacement curves were produced at predefined nodes. A similar approach was taken by Song *et al.* (2008) for horizontal anchor pullout analyses, where they adopted initial small strain analyses and

[1] Value used in case of immediate breakaway conditions
[2] Value used in case of increasing clay shear strength profiles

capacities were assumed to be at displacement values of 20% of the anchor diameter.

3.3.2 Results and discussion

Effects of embedment depth and overburden pressure

The finite element models were used to calculate the pullout capacity of the vertical anchors under loading conditions 1-6, as a function of embedment depth and overburden pressure. The results for fully bonded anchors ($\alpha = 1$) are shown in Figure 3. 7, which is a plot of the breakout factor N_c (normalized pullout capacity = $\frac{P}{BC_u}$) as a function of the embedment ratio *H/B*. The capacity was found to increase with embedment depth, approaching a constant value for deep embedment. This increase was found to be in the order of 60%, 230% and 180% for cases 1, 2 and 3 respectively, when changing *H/B* value from 1 to 5. Similar values were found for cases 4, 5 and 6. The depth at which the anchor capacity becomes constant depends on the load inclination angle θ, being highest for horizontally loaded anchors ($\theta = 90°$) and smallest for vertical loading ($\theta = 0°$). For horizontal loading (cases 3 and 6), the transition to deep behavior occurred for *H/B* between 3 and 4, with the behavior for top loading and loading through the centre of mass being essentially identical, while vertically loaded anchors showed deep behavior for *H/B*>2 in the case of top loading (case 1) and for *H/B*>1.7 for loading through the centre of mass (case 4). As shown in Figure 3. 7, these results are comparable to those determined by Rowe and Davis (1982) from the actual anchors collapse loads. They stated that their numerical calculated collapse loads would lie within 5% of the actual collapse loads for intermediate embedments. Comparison with the current analysis shows consistent results at shallow and deep embedments, but more conservative pullout

capacities were assumed to be at displacement values of 20% of the anchor diameter.

3.3.2 Results and discussion

Effects of embedment depth and overburden pressure

The finite element models were used to calculate the pullout capacity of the vertical anchors under loading conditions 1-6, as a function of embedment depth and overburden pressure. The results for fully bonded anchors ($\alpha = 1$) are shown in Figure 3. 7, which is a plot of the breakout factor N_c (normalized pullout capacity = $\frac{P}{BC_u}$) as a function of the embedment ratio *H/B*. The capacity was found to increase with embedment depth, approaching a constant value for deep embedment. This increase was found to be in the order of 60%, 230% and 180% for cases 1, 2 and 3 respectively, when changing *H/B* value from 1 to 5. Similar values were found for cases 4, 5 and 6. The depth at which the anchor capacity becomes constant depends on the load inclination angle θ, being highest for horizontally loaded anchors ($\theta = 90°$) and smallest for vertical loading ($\theta = 0°$). For horizontal loading (cases 3 and 6), the transition to deep behavior occurred for *H/B* between 3 and 4, with the behavior for top loading and loading through the centre of mass being essentially identical, while vertically loaded anchors showed deep behavior for *H/B*>2 in the case of top loading (case 1) and for *H/B*>1.7 for loading through the centre of mass (case 4). As shown in Figure 3. 7, these results are comparable to those determined by Rowe and Davis (1982) from the actual anchors collapse loads. They stated that their numerical calculated collapse loads would lie within 5% of the actual collapse loads for intermediate embedments. Comparison with the current analysis shows consistent results at shallow and deep embedments, but more conservative pullout

capacities at intermediate embedments.

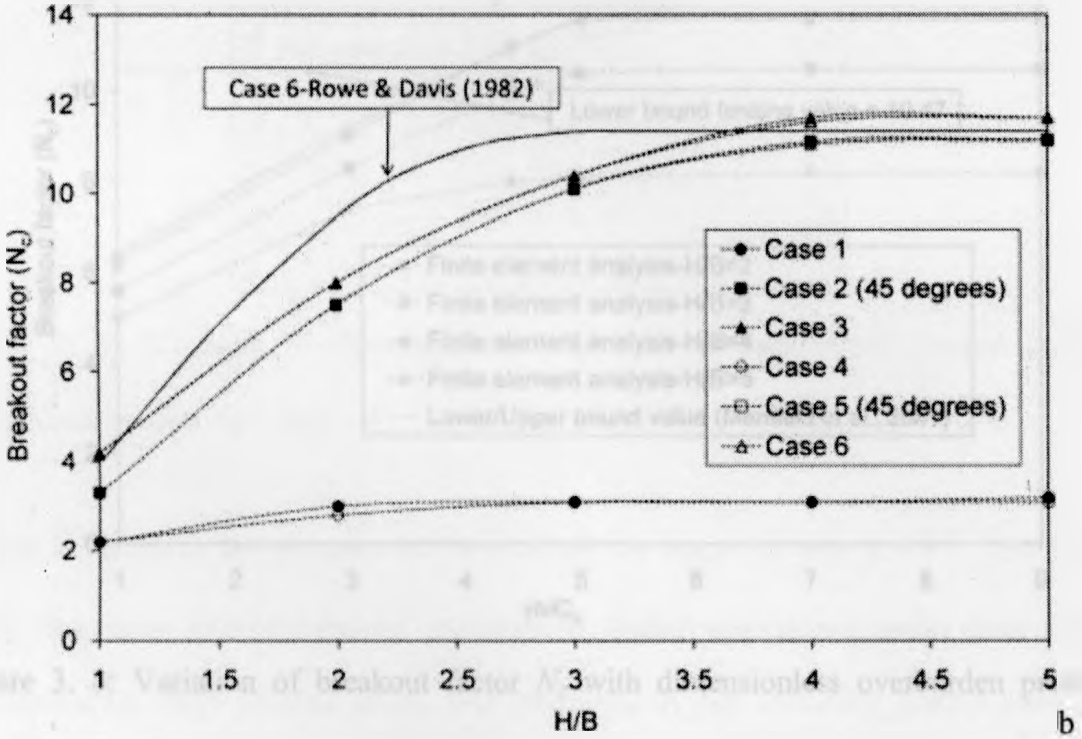

Figure 3. 7: Variation of breakout factor N_c with embedment ratio H/B for different cases (fully bonded).

Merifield *et al.* (2001) demonstrated that deep behavior can be obtained at constant embedment depth by increasing the dimensionless overburden pressure $\gamma h/C_u$. Figure 3. 8 shows the results for the variation of N_c with $\gamma h/C_u$ for a vertical anchor (case 6) at four different embedment ratios (H/B = 2, 3, 4 and 5). The upper and lower bounds for N_c reported by Merifield *et al.* (2001) are also shown. The calculations show deep behavior for $\gamma h/C_u$ >5, with a limiting breakout factor of 11.6. This is approximately equal to the value of 11.86 obtained from the upper bound analysis of Merifield *et al.* (2001) for deep vertical anchors.

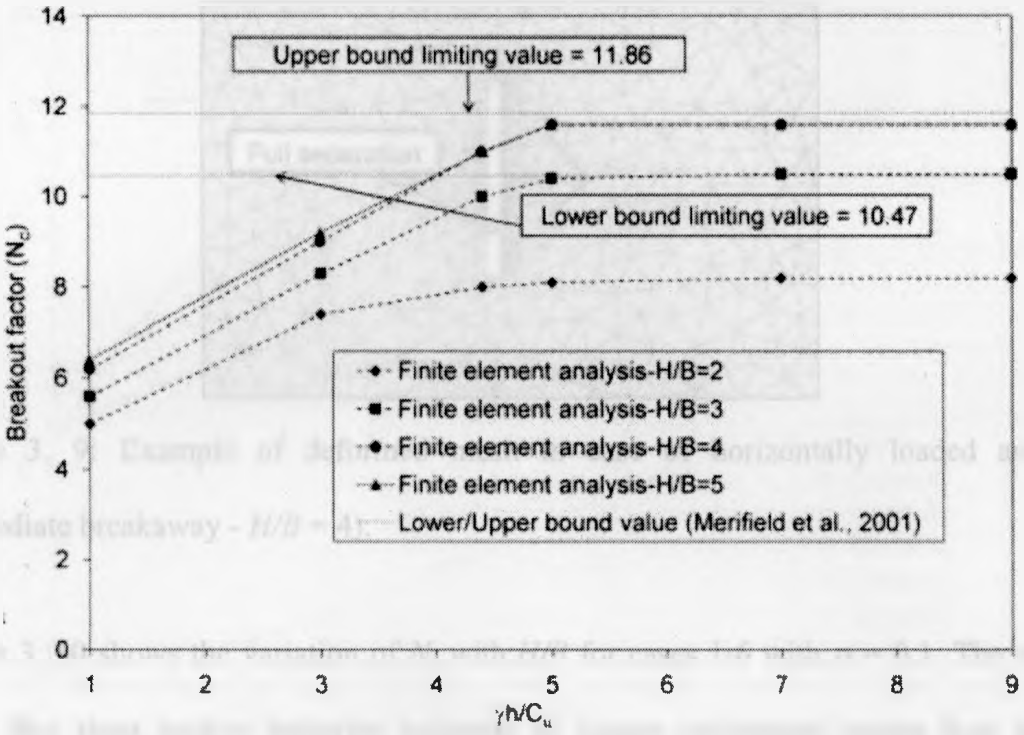

Figure 3. 8: Variation of breakout factor N_c with dimensionless overburden pressure $\gamma h/C_u$ (case 6).

The immediate breakaway case was also studied, in which the interface between the anchor and soil cannot sustain tension and full separation is assumed to occur when load is applied. Figure 3. 9 shows an example of the separation that developed behind the anchor in a simulation of case 6 with $H/B = 4$ and $\alpha = 0.1$.

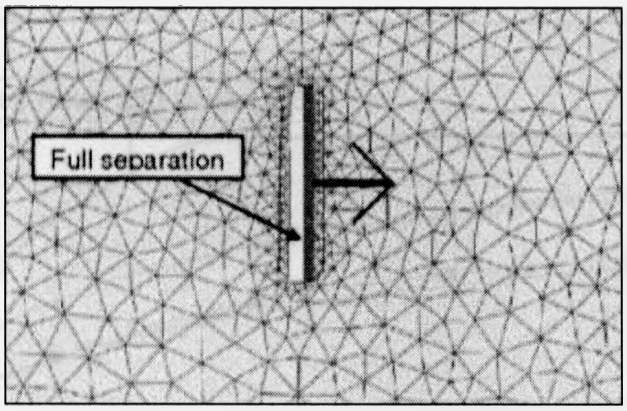

Figure 3. 9: Example of deformed mesh in case of horizontally loaded anchors (immediate breakaway - $H/B = 4$).

Figure 3. 10 shows the variation of N_c with H/B for cases 1-6 with $\alpha = 0.1$. The results show that deep anchor behavior occurred at higher embedment ratios than in the corresponding fully bonded cases. For example, in the vertically loaded case, the transition to deep anchor behavior occurred around $H/B = 3.5$ under immediate breakaway conditions, compared to $H/B = 2$ under fully bonded conditions. In the horizontally loaded cases, deep behavior has not been reached at $H/B = 5$, the maximum embedment ratio studied. A plot of the values reported by Rowe and Davis (1982) for case 6 is also presented in Figure 3. 10. Comparison of their results with the current analysis shows consistent values at shallow and deep embedments with a maximum difference of 10%, however a greater difference is apparent at intermediate depths.

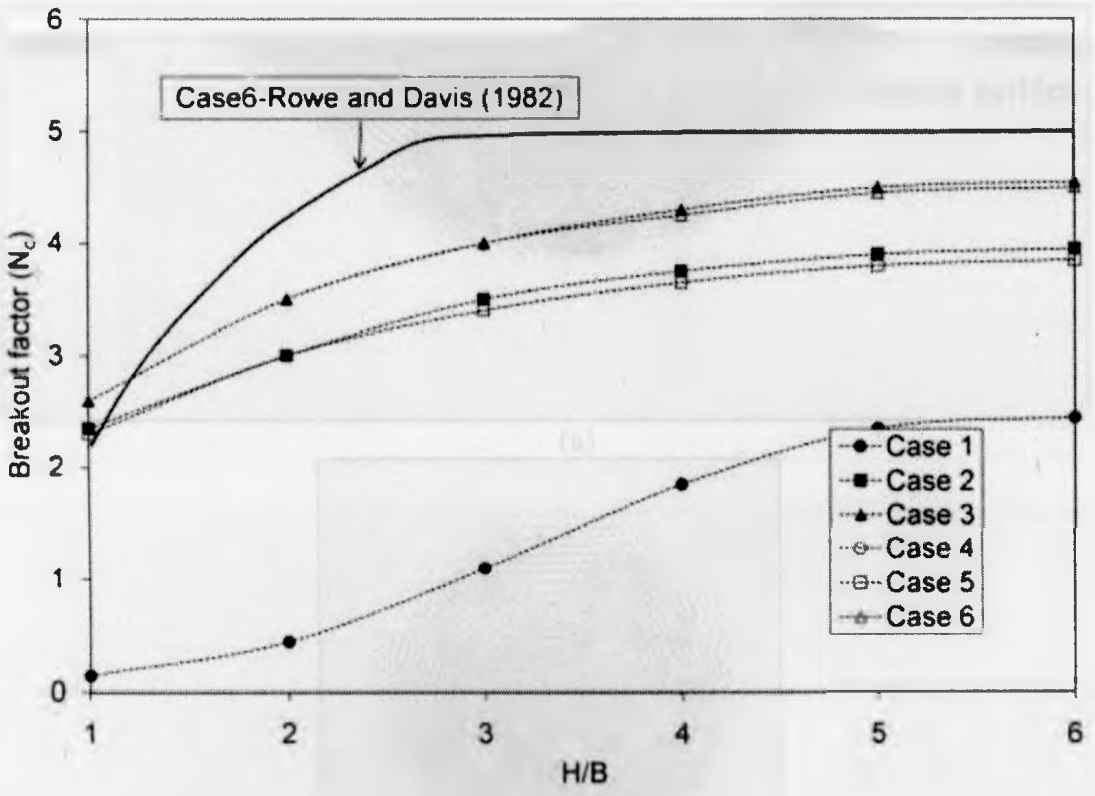

Figure 3. 10: Variation of breakout factor N_c with embedment ratio *H/B* for vertical anchor (immediate breakaway).

Effect of point of load application

To assess the effect of the point of load application, the load has been applied at the top of the anchor and through the centre of mass as shown in Figure 3. 7 and Figure 3. 10. The results showed that at the same embedment ratio *(H/B)* the anchor capacities were equivalent, regardless of the point of load application.

Figure 3. 11 (a) and (b) show the total displacement increments diagrams for shallow (*H/B* = 1) and deep (*H/B* = 5) horizontally loaded anchors (case 6) respectively, under fully bonded conditions.

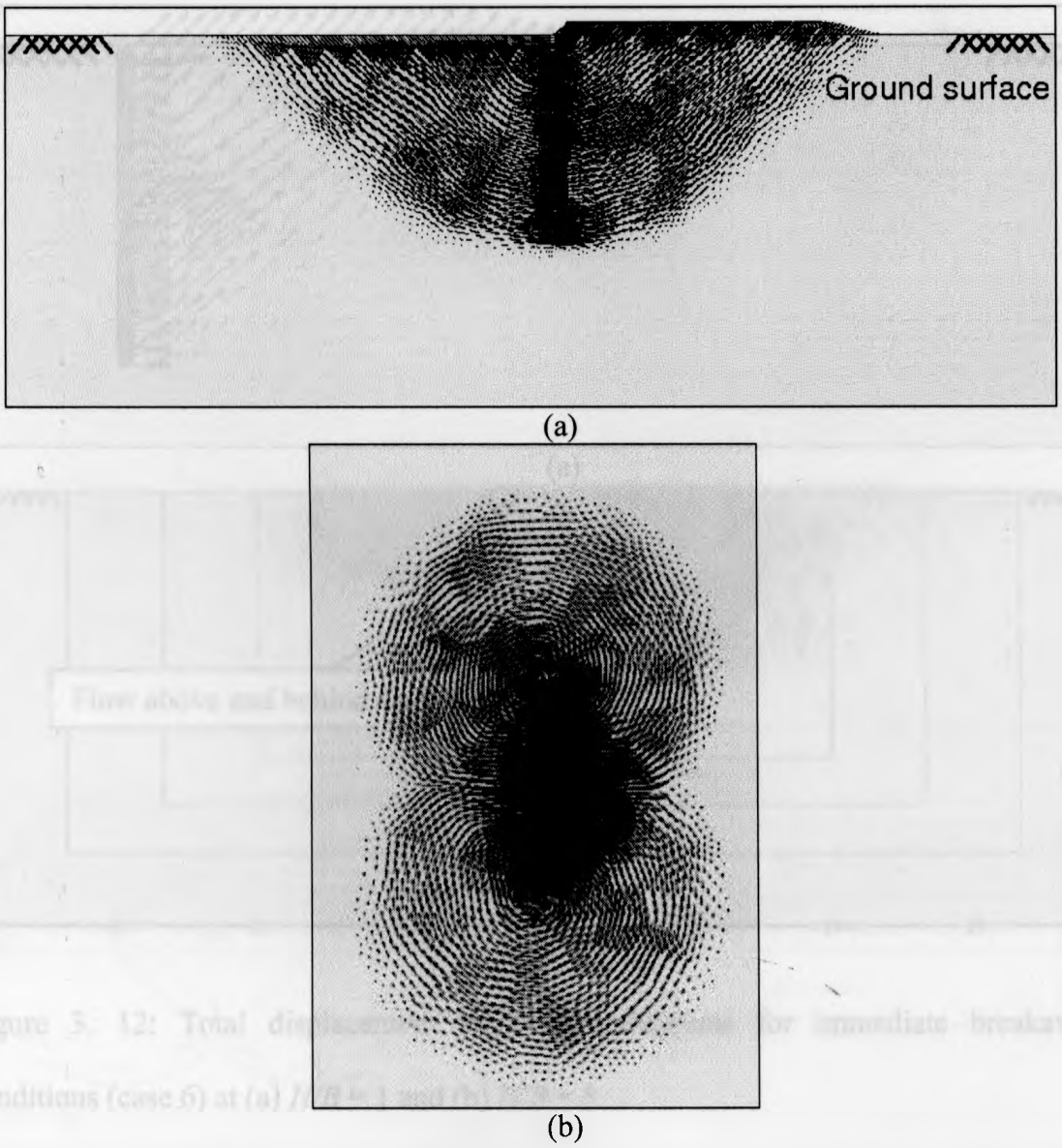

Figure 3. 11: Total displacement increments diagrams for fully bonded conditions (case 6) at (a) $H/B = 1$ and (b) $H/B = 5$.

Figure 3. 12 (a) and (b) shows the total displacement increments diagrams corresponding to the same loads and geometry in Figure 3. 11 but for immediate breakaway conditions. In the latter case, the soil immediately behind the anchor is not affected by the anchor loading because of the full separation that has taken place, although some soil flow is observed above and behind the anchor in the deep case.

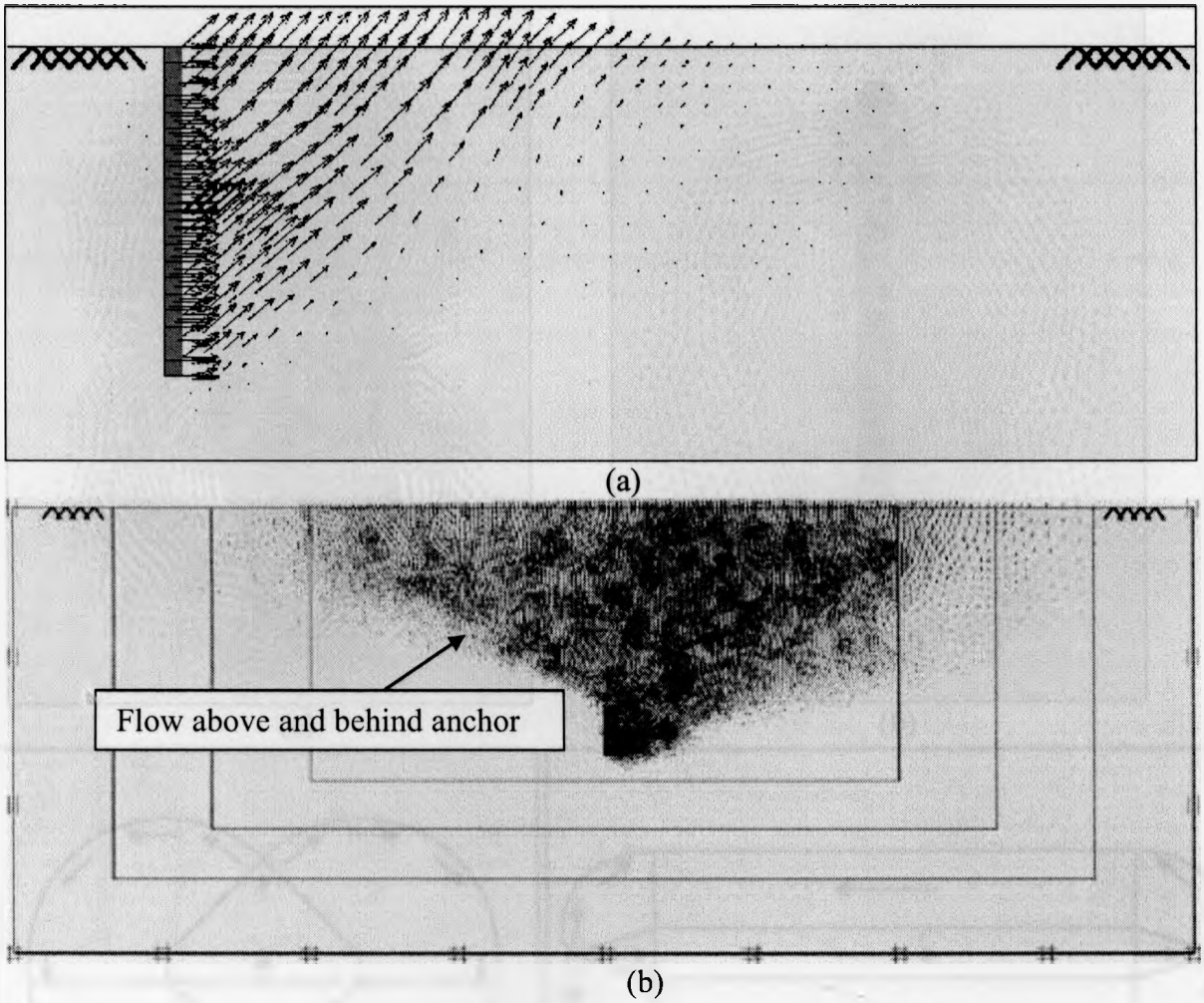

Figure 3. 12: Total displacement increments diagrams for immediate breakaway conditions (case 6) at (a) $H/B = 1$ and (b) $H/B = 5$.

The total displacement increments diagrams for the deep anchor loaded horizontally and vertically through the centre of mass are presented in Figure 3. 13 (a) and (b) respectively. These show good agreement with those reported by O'Neil *et al.* (2003) and illustrated in Figure 3. 13 (c), who investigated the behavior of deeply embedded rectangular drag anchors under vertical and horizontal loadings using upper bound mechanisms.

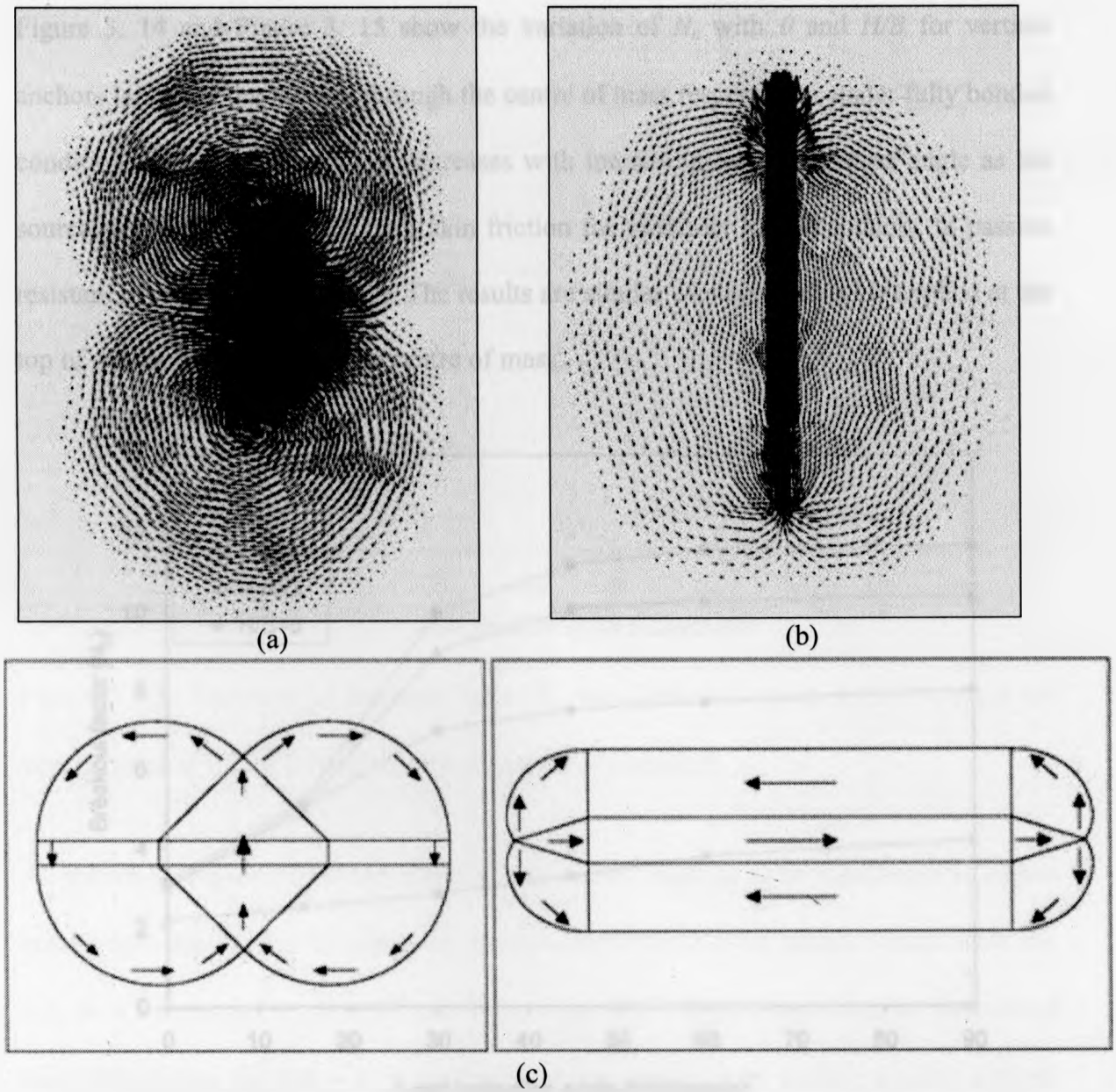

Figure 3. 13: Total displacement increments diagrams for deep anchors from current numerical analysis for (a) Case 6, (b) Case 4, compared to the (c) Upper bound mechanisms of O'Neil *et al.(* 2003).

Effect load inclination angle

The dependence of anchor capacity on the load inclination angle θ was also studied. Loads were applied at angles between 0° and 90° from the vertical at increments of 15°.

Figure 3. 14 and Figure 3. 15 show the variation of N_c with θ and H/B for vertical anchors loaded at the top and through the centre of mass respectively, under fully bonded conditions. The anchor capacity increases with increasing load inclination angle as the source of resistance changes from skin friction for vertically loaded anchors, to passive resistance for horizontal loading. The results are similar whether the load is applied at the top of the anchor or through the centre of mass.

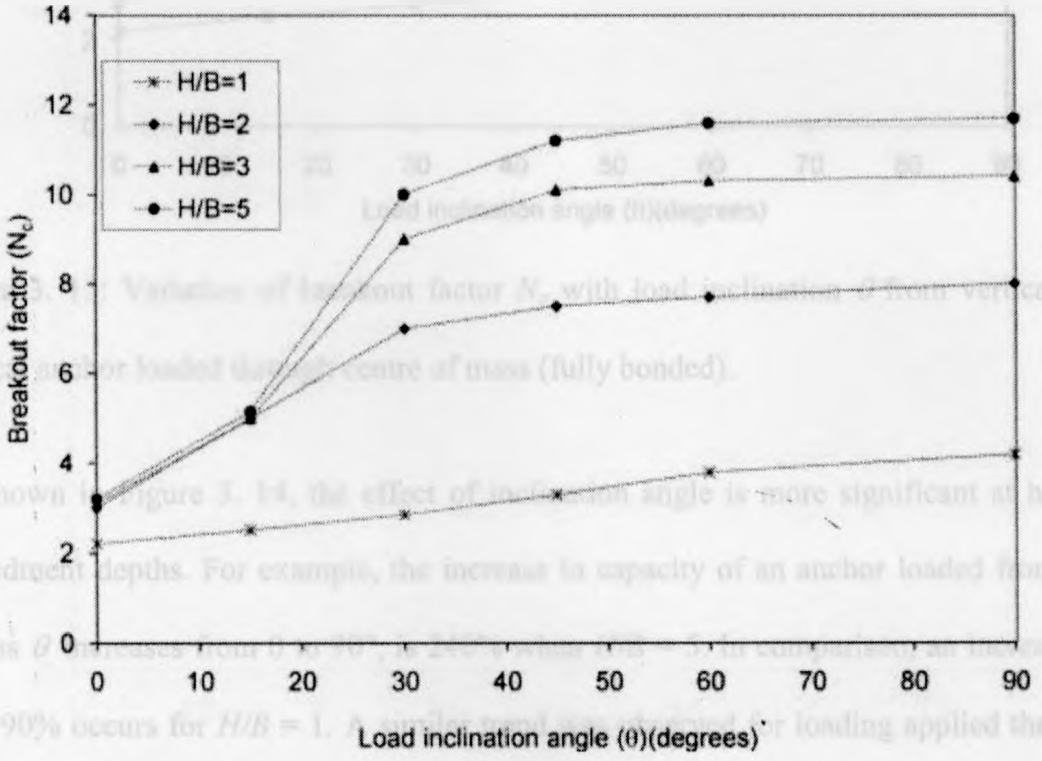

Figure 3. 14: Variation of breakout factor N_c with load inclination from vertical θ for vertical anchor loaded at top (fully bonded).

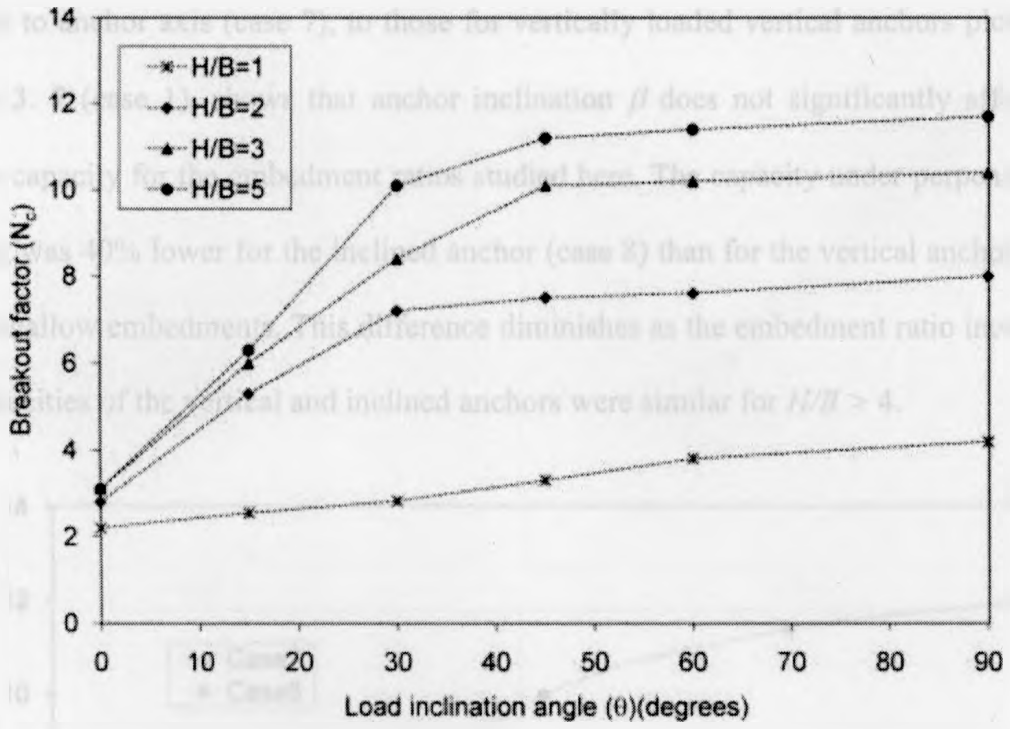

Figure 3. 15: Variation of breakout factor N_c with load inclination θ from vertical for vertical anchor loaded through centre of mass (fully bonded).

As shown in Figure 3. 14, the effect of inclination angle is more significant at higher embedment depths. For example, the increase in capacity of an anchor loaded from the top, as θ increases from 0 to 90°, is 240% when H/B = 5. In comparison, an increase of only 90% occurs for H/B = 1. A similar trend was observed for loading applied through the centre of mass.

Effect of anchor rotation

Fully bonded anchors inclined at an angle β = 45° to the vertical and subjected to loads parallel and perpendicular to the anchor axis (cases 7 and 8 respectively), were also studied. The breakout factors calculated for these cases are plotted against embedment ratio H/B in Figure 3. 16. Comparing the results obtained for inclined anchors with loads

parallel to anchor axis (case 7), to those for vertically loaded vertical anchors plotted in Figure 3. 7 (case 1), shows that anchor inclination β does not significantly affect the anchor capacity for the embedment ratios studied here. The capacity under perpendicular loading was 40% lower for the inclined anchor (case 8) than for the vertical anchor (case 3) for shallow embedments. This difference diminishes as the embedment ratio increases; the capacities of the vertical and inclined anchors were similar for $H/B > 4$.

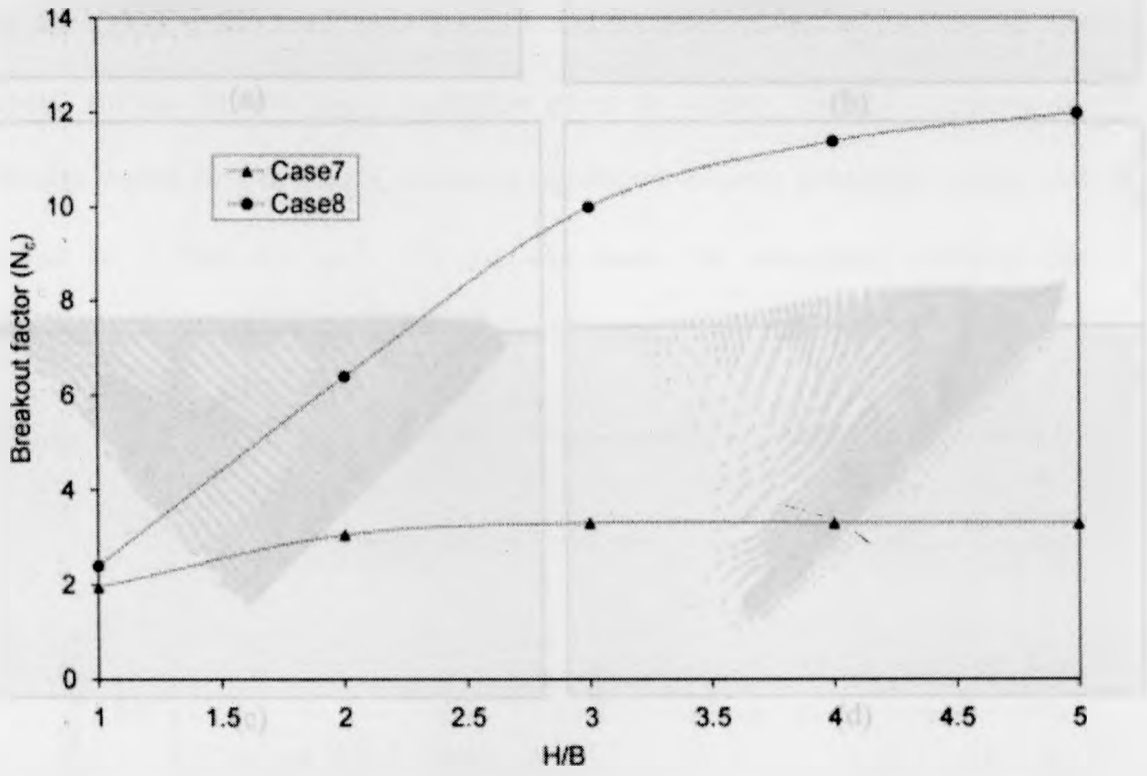

Figure 3. 16: Variation of breakout factor N_c with embedment ratio H/B for 45° inclined anchors loaded at top (fully bonded).

The total displacement increments diagrams for inclined embedded anchors (cases 7 and 8) are shown in Figure 3. 17 (a) and (b) for deep conditions, and (c) and (d) for shallow conditions. These show similar trends to those shown for vertical anchors for loading cases 4 and 6, presented in Figure 3. 13.

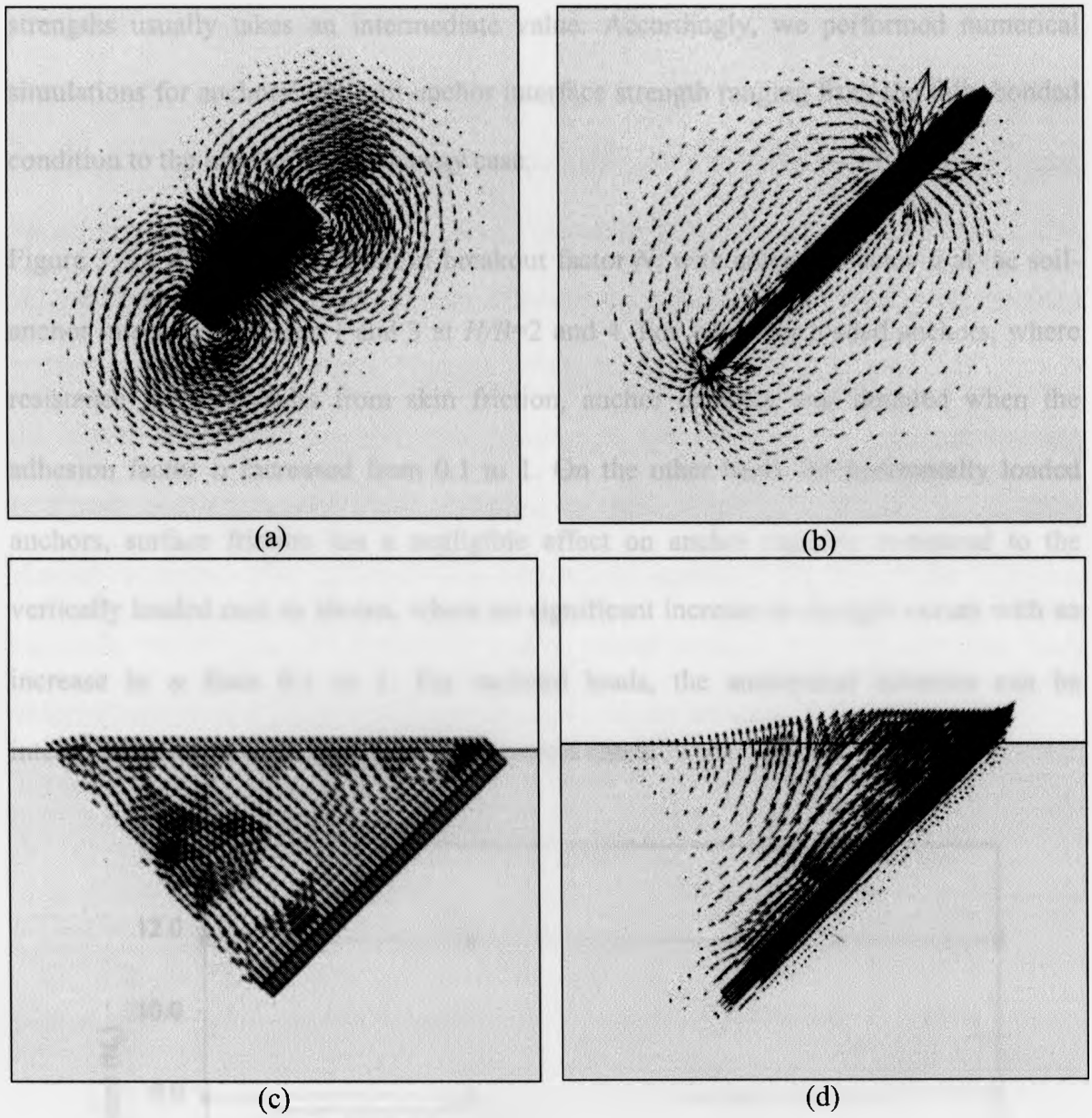

Figure 3. 17: Total displacement increments diagrams for inclined anchors (a) Case (8)-*H/B* = 5, (b) Case (7)-*H/B* = 5, (c) Case (8)-*H/B* = 1 and (d) Case (7)-*H/B* = 1.

Effect of soil-anchor interface strength

As previously mentioned, for anchors embedded in soft clays, the anchor-soil interface strength could be assumed equal to the clay strength. However, neither fully bonded nor fully separated conditions are likely to occur in practice, and soil-anchor interface

strengths usually takes an intermediate value. Accordingly, we performed numerical simulations for anchors with soil-anchor interface strength ranging from the fully bonded condition to the immediate breakaway case.

Figure 3. 18 shows the variation of breakout factor N_c with adhesion factor α at the soil-anchor interface for cases 1 and 3 at H/B=2 and 4. For vertically loaded anchors, where resistance mainly results from skin friction, anchor capacity was doubled when the adhesion factor α increased from 0.1 to 1. On the other hand, for horizontally loaded anchors, surface friction has a negligible effect on anchor capacity compared to the vertically loaded case as shown, where no significant increase in strength occurs with an increase in α from 0.1 to 1. For inclined loads, the anticipated behavior can be interpolated between the horizontal and vertical cases.

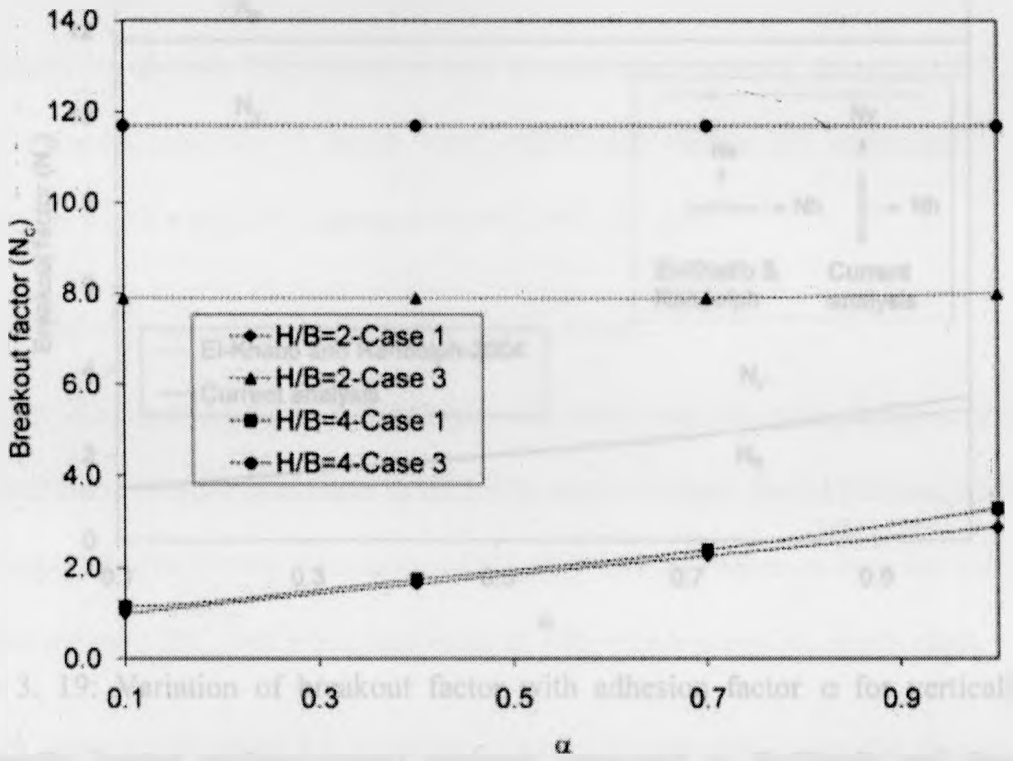

Figure 3. 18: Variation of breakout factor N_c with adhesion factor α.

El-Khatib and Randolph (2004) modeled a deep horizontal plate anchor subjected to loads parallel and perpendicular to its length. Due to the invariance of the pullout capacity of the deep case to anchor inclination, this study provides a good approximation for comparison to the results of the deep vertical embedded anchors studied herein. The vertical load component has a similar effect to the horizontal load component on deep vertical anchors and vice versa. Figure 3. 19 illustrates the variation of breakout factors in the vertical direction N_v and horizontal direction N_h with friction coefficient α reported in El-Khatib and Randolph, (2004) compared to those obtained from the current finite element analyses. The plot shows a reasonable agreement between both analyses, especially for the case of horizontally loaded vertical anchors, while for the other case, values obtained from the current finite element analyses are slightly higher.

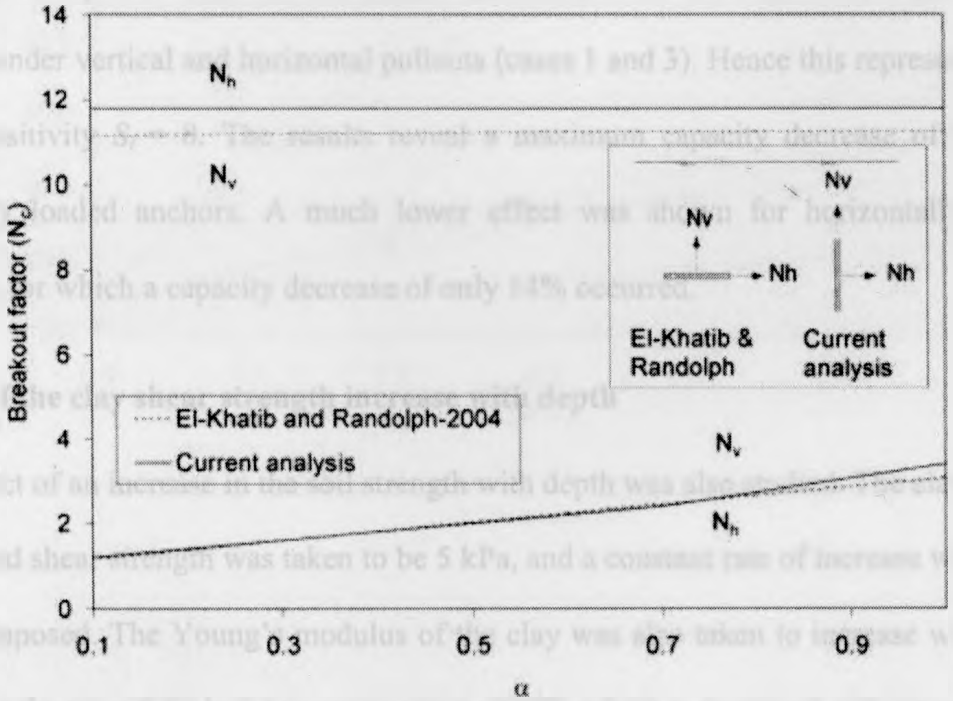

Figure 3. 19: Variation of breakout factor with adhesion factor α for vertically and horizontally loaded anchors-current analyses compared to El-Khatib and Randolph (2004).

Effect of clay disturbance following the anchor embedment

Considerable reduction in strength may occur due to the induced excess pore pressures and remolding following anchor embedment in sensitive cohesive soils. Although a recovery of strength would occur after dissipation of these excess water pressures and thixotropy, this process might take many months. For this reason, a series of models to study this phenomenon was also performed. These considered the width of disturbed soil next to the anchor to be comparable with the disturbed area around driven piles, which is equal to 2 times the anchor/pile diameter.

A surface anchor (H/B = 1) was modeled for which the undrained shear strength of the surrounding soil increased gradually from 2.5 kPa at anchor interface up to the in-situ value (20 kPa) at 1 m (twice the anchor diameter) from the anchor. The anchor was studied under vertical and horizontal pullouts (cases 1 and 3). Hence this represents a soil with sensitivity S_t = 8. The results reveal a maximum capacity decrease of 72% for vertically loaded anchors. A much lower effect was shown for horizontally loaded anchors, for which a capacity decrease of only 14% occurred.

Effect of the clay shear strength increase with depth

The effect of an increase in the soil strength with depth was also studied. The clay surface undrained shear strength was taken to be 5 kPa, and a constant rate of increase with depth ρ was imposed. The Young's modulus of the clay was also taken to increase with depth such that the ratio E/C_u had a constant value of 100, which is typical of soft clays.

Figure 3. 20 is a plot of the inhomogeneous breakout factor $N_{co\rho}$ as a function of $\rho B/C_u$ for vertically, horizontally and 45° top-loaded anchors at embedment ratios of 2 and 4

under fully bonded conditions. The results show that the ultimate anchor capacity increases at a decreasing rate as $\rho B/C_u$, increases. The effect of embedment depth on the ultimate capacity is minimal for $\rho B/C_u = 0$, while for greater $\rho B/C_u$ values, changing H/B from 2 to 4 increased the ultimate capacity by approximately 1.5 times. The breakout factors calculated from our model are about 10% lower than those obtained by Merifield *et al.* (2001) from a numerical bounding analysis of inhomogeneous soils, as shown in Figure 3. 21.

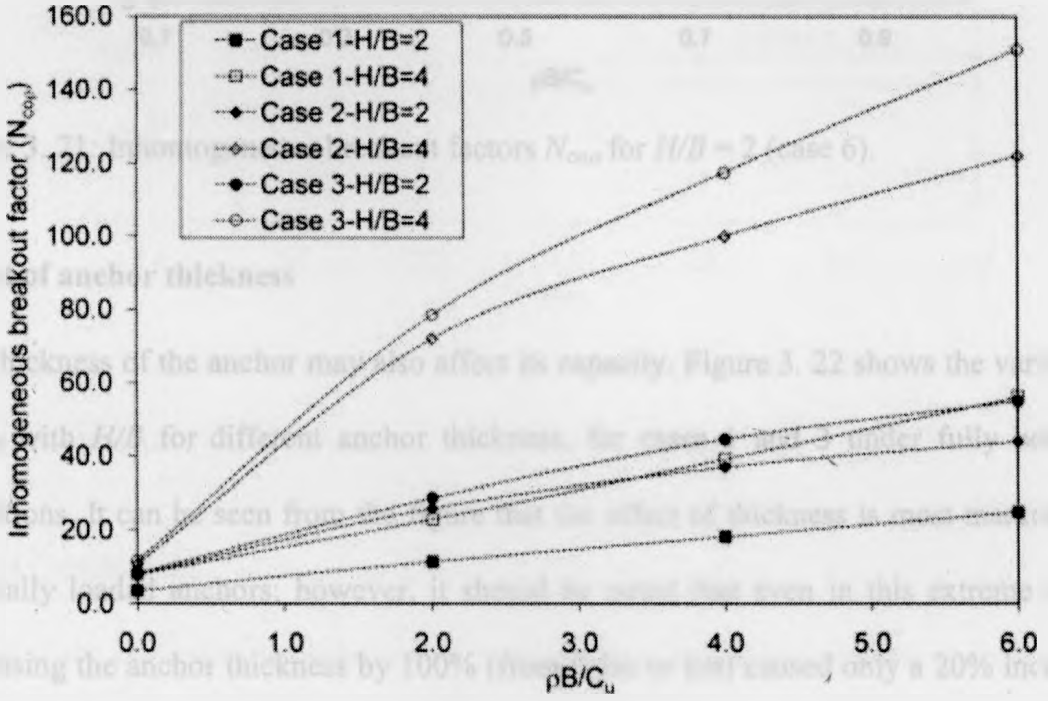

Figure 3. 20: Variation of breakout factors N_c with rate of increase of strength $\rho B/C_u$ (fully bonded).

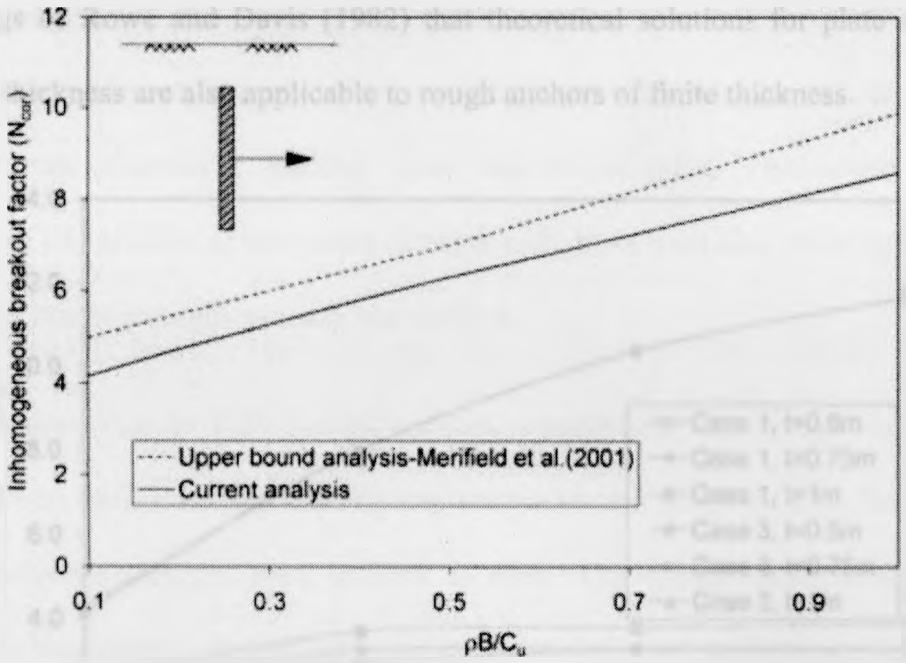

Figure 3. 21: Inhomogeneous breakout factors $N_{co\rho}$ for $H/B = 2$ (case 6).

Effect of anchor thickness

The thickness of the anchor may also affect its capacity. Figure 3. 22 shows the variation of N_c with H/B for different anchor thickness, for cases 1 and 3 under fully bonded conditions. It can be seen from the figure that the effect of thickness is most marked for vertically loaded anchors; however, it should be noted that even in this extreme case, increasing the anchor thickness by 100% (from 0.5m to 1m) caused only a 20% increase in breakout factor. For horizontally loaded anchors, the increase in anchor capacity with thickness was negligible, as found by Rowe and Davis (1982). This is due to the horizontal pullout resistance resulting mainly from the developed passive wedge in front of the anchor. The size of this soil wedge appears not to be influenced by the anchor thickness. In comparison, the surface friction and top/bottom bearing/suction have less significant contributions compared to the passive wedge resistance. These results confirm

the findings of Rowe and Davis (1982) that theoretical solutions for plate anchors of negligible thickness are also applicable to rough anchors of finite thickness.

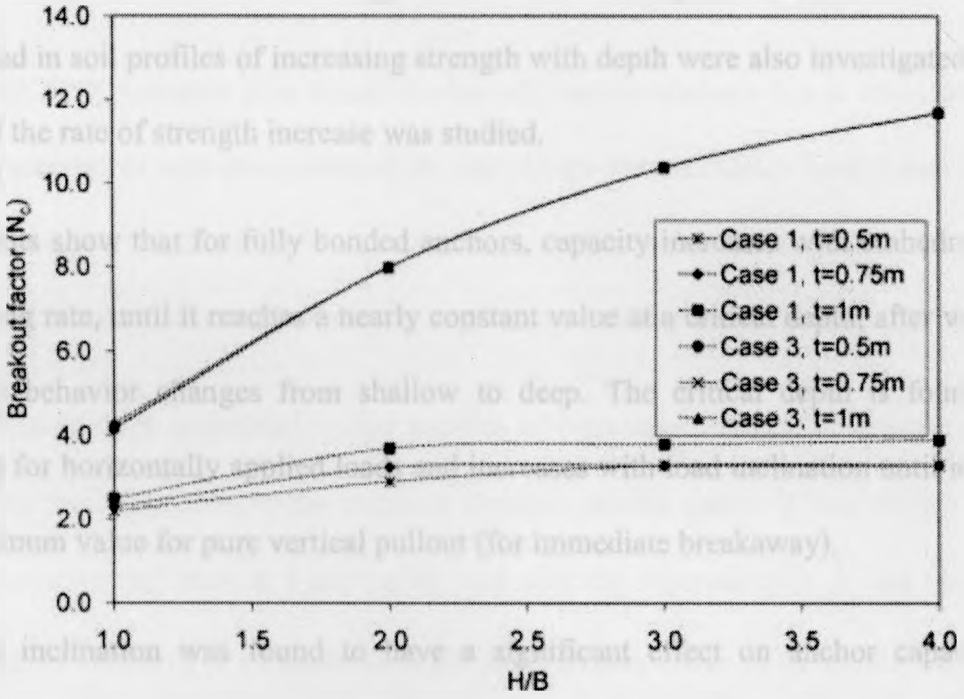

Figure 3. 22: Variation of breakout factor N_c with embedment ratio H/B for different anchor thicknesses t (fully bonded).

3.4 Conclusions

In this study, the undrained behavior of vertical steel anchors embedded in soft clay was examined.

A plane strain finite element model of the problem was created using the software Plaxis 2D (Plaxis 2006)and the ultimate capacity was defined using the K4 criterion defined by Rowe and Davis (1982).

An extensive parametric study was carried out and the effect of the different parameters on anchor capacity was assessed separately. The studied parameters included embedment

depth, overburden pressure, point of load application, load and anchor inclination and the soil-anchor interface condition. In addition, disturbance of the adjacent soil due to anchor embedment for short-term loading cases was investigated. Furthermore, anchors embedded in soil profiles of increasing strength with depth were also investigated and the effect of the rate of strength increase was studied.

The results show that for fully bonded anchors, capacity increases with embedment at a decreasing rate, until it reaches a nearly constant value at a critical depth, after which the anchor's behavior changes from shallow to deep. The critical depth is found to be minimal for horizontally applied loads and increases with load inclination until it reaches its maximum value for pure vertical pullout (for immediate breakaway).

Loading inclination was found to have a significant effect on anchor capacity. For vertical loading, anchor capacity is minimal as it is mainly attributed to skin friction along the anchor sides. As the loading inclination further increases, capacity increases, until it reaches its maximum value for horizontal loads, where it is mainly developed from passive resistance. This increase was shown to be greater at higher embedment depths.

Simulation of different soil-anchor interface strengths showed that their effect is more apparent for the case of vertically loaded anchors. This effect decreases with an increase in the loading angle from the vertical, reaching a minimum value for horizontal loading.
In this study, loads have been applied to both the anchor top and through the centre of mass, and it was shown that changing the load application point has only a minor effect on the anchor's capacity with small strain analysis.

Anchor thickness was shown to have a small effect for vertically loaded anchors and a negligible effect for horizontally loaded ones, as the capacity is mainly developed from passive resistance.

The effect of disturbance of a sensitive clay adjacent to anchors due to remolding upon anchor embedment was also assessed. It was shown that vertically loaded cases are the most affected by the disturbance, as capacity is mainly dependent on side friction, while lesser effects are anticipated for loading angles approaching the horizontal.

Analysis of anchors embedded in clay profiles of increasing strength with depth was also performed and compared to the constant strength profile cases. It was shown that the anchor capacity increases at a decreasing rate with the increase of ρ. It was also shown that at higher values of ρ, embedment depth has a greater effect on the anchor capacity.

3.5 References

Aubeny, C. P., and Murff, J. D. (2005). "Simplified limit solutions for the capacity of suction anchors under undrained conditions," *Ocean Engineering*, Vol.32, No.7, pp 864-877

Aubeny, C. P., Han, S., and Murff, J. D. (2003a). "Refined model for inclined load capacity of suction caissons," *Proceedings of 22nd International Conference of Offshore Mechanics and Arctic Engineering OMAE*, Vol.3, pp 883-887

Aubeny, C. P., Murff, J. D., and Moon, S. K. (2003b). "Inclined load capacity of suction caissons," *International Journal for Numerical and Analytical Methods in Geomechanics*, Vol.27, No.14, pp 1235-1254

Aubeny, C. P., Moon, S. K., and Murff, J. D (2001). "Lateral undrained resistance of suction caisson anchors," *International journal of Offshore and Polar Engineering*, Vol.11, No.3, pp 211-219

Das, B. M., and Shin, E. C. (1993). "Uplift capacity of rigid vertical metal piles in clay under inclined pull," *International Journal of Offshore and Polar Engineering*, Vol.3, No.3, pp 231-235

Das, B. M., and Puri, V. K. (1989). "Holding capacity of inclined square plate anchors in clay," *Soils and Foundations Journal*, Vol.29, No.3, pp 138-144

Colwill, R. D. (1996). "Marine drag anchor behavior-a centrifuge modeling and theoretical investigation," Degree of doctor of philosophy thesis, The University of Manchester, Manchester, United Kingdom

El-Khatib, S., and Randolph, M. P. (2004). "Finite element modeling of drag-in plate anchor installation," *Proceedings of the 9th Symposium on Numerical Models in Geomechanics*, Ottawa, Canada, pp 541-547

Gunn, M., J. (1980). "Limit analysis of undrained stability problems using a very small computer," *Proc. Symp. on Computer Applications in Geotechnical Problems in Highway Engineering*, Cambridge University, Engineering Department, pp 5-30.

Jun, L., Li-ling, W. and Yu-xia, H. (2006). "Pullout capacity of circular plate anchors in NC clay," *Journal of Dalian University of Technology*, Vol.46, No.5, pp 712-719

MacKenzie, T. R. (1955). "Strength of deadman anchors in clay," Pilot tests, Degree of Master of Science thesis, Princeton University, The United States of America

Merifield, R. S., Lyamin, A. V., and Sloan, S. W. (2005). "Stability of inclined strip anchors in purely cohesive soil," *Journal of Geotechnical and Geoenvironmental Engineering*, Vol.131, No.6, pp 792-799

Merifield, R. S., Lyamin, A.V., Sloan, S. W., and Yu, H. S. (2003). "Three-dimensional lower bound solutions for stability of plate anchors in clay," *Journal of Geotechnical and Geoenvironmental Engineering*, Vol.129, No.3, pp 243-253

Merifield, R. S., Sloan, S. W., and Yu, H. S. (2001). "Stability of plate anchors in

undrained clay," *Geotechnique,* Vol.51, No.2, pp 141-153

Plaxis Bv (2006). Plaxis 2D-Version 8 Manuals, Version 8

Ranjan, G. and Arora, V. B. (1980). "Model studies on anchors under horizontal pull in clay," *Proceedings of the 3rd Aust., N.Z. Conf. Geomech.*, Wellington, N.Z. 1, pp. 65-70.

Rao, S. N., Latha, K. H., Pallavi, B., and Surendran, S. (2006). "Studies on pullout capacity of anchors in marine clays for mooring systems," *Applied Ocean Research*, Vol.28, No.2, pp 103-111

Rao, S. N., Ravi, R.. and Prasad, B. S. (1997). "Pullout behavior of suction anchors in soft marine clays," *Marine Geosources and Geotechnology*, Vol.15, No.2, pp 95-114

Rowe, R. K., and Davis, E. H. (1982). "The behavior of plate anchors in clay," *Geotechnique,* Vol32, No.1, pp 9-23

Rowe, R. K. (1978). "Soil structure interaction analysis and its application to the prediction of anchor behavior," Degree of doctor of philosophy thesis, University of Sydney, Australia.

Semple, R., and Rigden, W. J. (1984). "Shaft capacity of driven pipe in clay," *Proceedings of the American. Society of Civil engineers symposium "analysis and design of pile foundations*" pp. 59-79

Song, Z., Hu, Y., O'Loughlin, C. and Randolph, M. F. (2009). "Loss in anchor embedment during plate anchor keying in clay," *Journal of Geotechnical and Geoenvironmental Engineering*,Vol.135, No.10, pp 1475-1485.

Song, S., Hu, Y., and Randolph, M. F. (2008). "Numerical simulation of vertical pullout of plate anchors in clay," *Journal of Geotechnical and Geoenvironmental Engineering*, Vol.134, No.6, pp 866-875

O'Neill, M. P., Bransby, M. F. and Randolph, M. F (2003). "Drag anchor fluke-soil interaction in clays," *Canadian Geotechnical Journal*, Vol.40, No.1, pp 78-94

Van Langen, H. and Vermeer, P. A. (1991). "Interface elements for singular plasticity points," *International Journal for Numerical and Analytical Methods in Geomechanics*, Vol.15, No.5, pp 301-315

Wilde, B., Treu, H. and Fulton, T. (2001). "Field testing of suction embedded plate anchors," *Proceedings of the 11th International Offshore and Polar Engineering Conference*, Stavanger, Norway, pp 544-551

Wood, D. M. (1990). "Strength of soils". *Soil behavior and critical state soil mechanics,* Cambridge University press, Cambridge

Chapter 4 Numerical Investigation of The Undrained Capacity of Enlarged Based Anchors Embedded in Clay

4.1 Introduction

Offshore ships and structures are often required to use anchoring systems to ensure temporary or permanent stability. Remotely operating vehicles and other seabed-based working platforms are also commonly used tools for many offshore applications, including site investigation, cable and pipeline maintenance, and other uses related to offshore hydrocarbon extraction. To ensure full control of these working platforms, these also require a reaction force to provide stability during operation.

Regular strip plate anchors are typically used for this purpose and the shortcomings of this form of anchor has been discussed previously (e.g. Liang *et al.* 2008). To address the issue of effectiveness of the anchor in terms of weight and pullout capacity, this study has been designed to investigate the effect of the shape on the pullout performance of anchors

In particular, the present work is intended to provide a better understanding of the pullout behavior of anchors with an irregular basal shape compared to the simpler strip anchor. A detailed parametric study was carried out using finite element analysis to investigate the effect of embedment depth, load and anchor inclination and basal shape and size.

4.2 Previous work

The operation of many offshore structures/facilities, such as barges and semi-submersible platforms involves special anchoring constraints, including high tension capacities and limited tolerated operational movements (Poulos 1988).

While many anchor types, mainly made of steel, have been developed for offshore use including fluke anchors, pile anchors and gravity anchors, two anchor concepts produce high capacities: suction anchors and direct embedment anchors (Poulos 1988). While suction anchors are installed by suction, embedment anchors could be installed using many alternatives including vibration, free-fall and propellant actuation. Embedment anchors are initially installed in a vertical position, then the applied force might rotate them up to a horizontal position (Poulos 1988).

While a wide range of marine anchors of different shapes are commercially available (Puech *et al.*1978), it is common to idealize the different anchor shapes to a horizontally or vertically oriented plate anchor, with high aspect ratio for the simplicity of the analysis (e.g. Merifield *et al.* 2001; Das and Puri 1989 and Rowe and Davis 1982). Researchers have used many theoretical and numerical techniques to predict the ultimate pullout capacity of plate anchors, and to understand their behavior under different loading conditions.

Rowe and Davis (1982) carried out plane strain finite element analysis of normally loaded vertical and horizontal plate anchors. They considered two cases at the anchor-soil interface: the "immediate breakaway" condition, in which the interface cannot sustain any tension, and the "no-breakaway" condition, in which a full bond between the anchor and soil was assumed. They also classified anchors into shallow and deep depending on whether anchors are greatly affected by embedment and overburden pressure, and whether the plastic region extends to the ground surface. Rowe and Davis (1982) showed that, for vertical anchors, deep anchor behavior occurs at H/B greater than 3, under both breakaway conditions, where H is the depth of the lowest point of the anchor from the

ground surface and B is the total anchor length. They also suggested that the overburden pressure required to ensure a no breakaway response in a homogeneous elasto-plastic material is in the range of $4C_u/K_o$ to $6C_u/K_o$ for vertical anchors, where K_o is the lateral earth pressure coefficient and C_u is the undrained shear strength. Rowe and Davis (1982) also suggested that for $H/B<3$, the capacity of plate anchors inclined at less than 30° to the vertical could be calculated using the solutions reported for vertical anchors, while at greater inclinations, solutions for horizontal anchors might be used. For deeper anchors ($H/B>3$), they found that solutions for both breakaway conditions are independent of anchor orientation.

Using finite element analyses, Merifield *et al.* (2001) suggested limiting breakout factors N_c for fully bonded vertical anchors of 10.47 and 11.86 using lower and upper bound plasticity solutions respectively. They also studied the behavior of plate anchors in normally consolidated clay profiles having a strength that increased with depth, representing a more realistic state for marine clays.

Fahmy *et al.* (2010) performed a detailed parametric study of regular plate anchors embedded in clay. Their results showed that the anchor capacity depended significantly on the loading inclination angle θ, with the capacity being minimum for vertically-loaded anchors ($\theta = 0$), and increasing as θ approaches 90°. They also found that the effect of soil-anchor interface strength was most apparent for vertically loaded anchors and decreased as θ increased. The effect of embedment depth on anchor capacity was found to be more significant in clays whose shear strength increased with depth. Fahmy *et al.* (2010) also modeled the effect on pullout capacity of the disturbance of the soil following anchor insertion in sensitive clays and found a decrease in pullout capacity of up to 70%

for vertically-loaded anchors. This effect was found to be much smaller in horizontally-loaded anchors. Fahmy *et al.* (2010) also found that some parameters, such as the point of load application and the anchor thickness, had little effect on anchor capacity.

Meyerhof and Adams (1968) investigated enlarged-base piles embedded in clay, ignoring the contributions of shaft friction and base tension for the pile capacity. Meyerhof and Adams (1968) compared their theoretical results with experimental data and found N_c values between 9 and 10 for deep embedments and much lower values for shallow embedments. The origin of these values may be that their experimental tests were carried out at relatively shallow depths and in stiff fissured clay, and the mobilized strength was close to the residual value. Meyerhof and Adams (1968) also studied the effect of loading rate on the capacity of enlarged-base piles, and found that for soft clays, the capacity under long term loading was much higher than for short term loading, while for stiff clays, the opposite behavior occurred.

The behavior of grouted tieback and tiedown anchors can also be compared to that of enlarged base anchors. Primarily used for tension loadings, tiebacks can also be used to sustain compression loadings, particularly when installed in large diameter holes (Shnabel and Shnabel, 2002). Grouted anchors achieve their resistance from the skin friction mobilized along the grouted (bonded) length as well as from end bearing. Suction mobilized at the anchor tip is usually neglected in design to accommodate for the long-term behavior of the soil (Sabatini *et al.* 1999). Anchor capacity has been shown to increase with bond length up to about 9 to 12 m, beyond which it becomes independent of bond length (Sabatini *et al.* 1999).

Of the various types of tieback that have been considered, single underream tiebacks are most likely to show behavior similar to enlarged base anchors. Weatherby (1982) proposed that the ultimate anchor capacity P for single underream tiebacks in cohesive soils could be calculated as

$$P = \alpha C_u L_s \pi D_s + \frac{\pi}{4}\left(D_u^2 - D_s^2\right) N_c C_u \qquad 4.1$$

where L_s and D_s are the anchor shaft length and diameter, D_u is the underreamed diameter and N_c is the breakout factor, which is usually taken to be equal to 9.

Cox and Reese (1976) performed tests to investigate the pullout capacity and the effect of lateral loading on grouted piles embedded in stiff clay. They found that lateral pile loading caused a significant reduction in the bond between the soil and the upper part of the grouted area. For the different examined piles, the length of top portion subjected to bond separation ranged from 5 to 9 feet.

Randolph *et al.* (2000) studied the behavior of static vertical T-Bar and ball penetrometers in cohesive materials and provided upper and lower bound solutions, supported by finite element analyses, for penetrometers in a rigid-plastic material obeying a Tresca or Von Mises failure mechanism. They assumed a mechanism based on solutions provided by Randolph and Houlsby (1984) for a laterally-loaded deep pile. They found breakout factors ranging from 11.8 for fully smooth to 15.54 for fully rough conditions, with excellent agreement between their analytical and finite element analyses. While the theoretical solutions showed a difference of 12 to 30% in bearing resistance between spherical and cylindrical geometries, experimental results for the two geometries

differed by only 5% (Randolph *et al.* 2000). For practical application, the authors suggested the values of 10.5 for penetrometers in deep states.

In their experimental studies, Newson *et al.* (2003b) tested a steel anchor with an inflatable lower rubber membrane embedded in an artificial clayey soil of initial undrained shear strength C_u of 1.5 to 2 kPa. Pressure was applied to inflate the lower membrane, after which the anchor was pulled out vertically. They investigated the effect of the pullout rate and anchor inflation, and studied the improvement of anchor capacity with consolidation. They found an increase in pullout capacity for stiffer clays and for increased membrane pressures. In addition, a further increase in capacity was observed following a waiting period between anchor installation and membrane inflation. In practical applications such as anchoring offshore ROVs where short term loading is required, such waiting periods are, however, unlikely to be available. Newson *et al.* (2003b) also observed that high mobilization distances were required for peak loads to be achieved.

Newson *et al.* (2003a) also suggested that the equations used for calculating the pullout capacity of grouted nails or anchors and enlarged-base piles might be appropriate for use with inflatable anchors. Accordingly, if the effect of friction along the smooth steel part of the anchor is ignored, Newson *et al.* (2003a) suggested that the capacity can be estimated as

$$F_{uo} = \alpha C_u A L \qquad 4.2$$

when the membrane is deflated, and

$$F_{ui} = N_c C_u A' \qquad 4.3$$

when it is inflated. Here α is the adhesion factor, L the membrane length, N_c the breakout factor, and A and A' are the membrane surface area when deflated and inflated, respectively.

Liang *et al.* (2008) simulated the pullout of vertical inflatable anchors embedded in very soft clay. Their results showed that local drainage around the anchor during installation and inflation leads to a significant improvement in the undrained shear strength of the clay surrounding the anchor. Their analysis showed that, increasing the membrane inflation pressure significantly increases the peak pullout loads, reduces the mobilization distance and minimizes the reduction in residual strengths.

Gaudin *et al.* (2010) experimentally investigated the behavior of a plate anchors with a keying flap when embedded in clay. The main advantage of introducing this flap was to reduce the vertical displacement accompanying the anchor keying. Their results showed lower pullout capacities for this innovative system compared to a regular anchor of same width. However, these anchors follows a trajectory with a significant horizontal movement, which they believe will help reduce the post peak capacity reduction.

4.3 Numerical analyses

The finite element software package Plaxis 2D (Plaxis 2006) was used to numerically simulate the behavior of a steel anchor with irregular shapes embedded in a purely cohesive soil under different loading conditions. This study has investigated the behavior

of vertical anchors of configurations # 0 - 12 subjected to vertical and horizontal loads as shown in Figure 4. 1, where W and L are the base width and length, t the thickness of the steel rod, h the distance from the ground surface to the anchor's centre of mass. An illustration of the studied anchor dimensions and configurations are presented in Figure 4. 2. Due to the similarity of a number of the capacities, only data for configurations # 0-4 are shown herein.

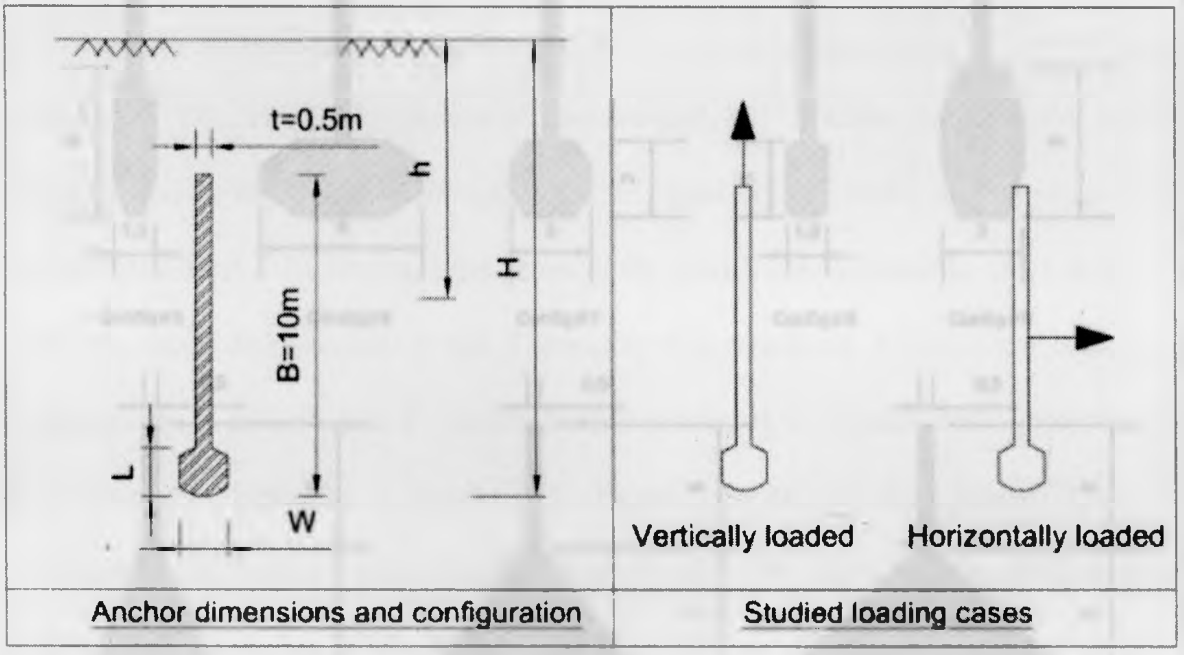

Figure 4. 1: Terminology and loading cases for the enlarged base anchors studied in the numerical analysis.

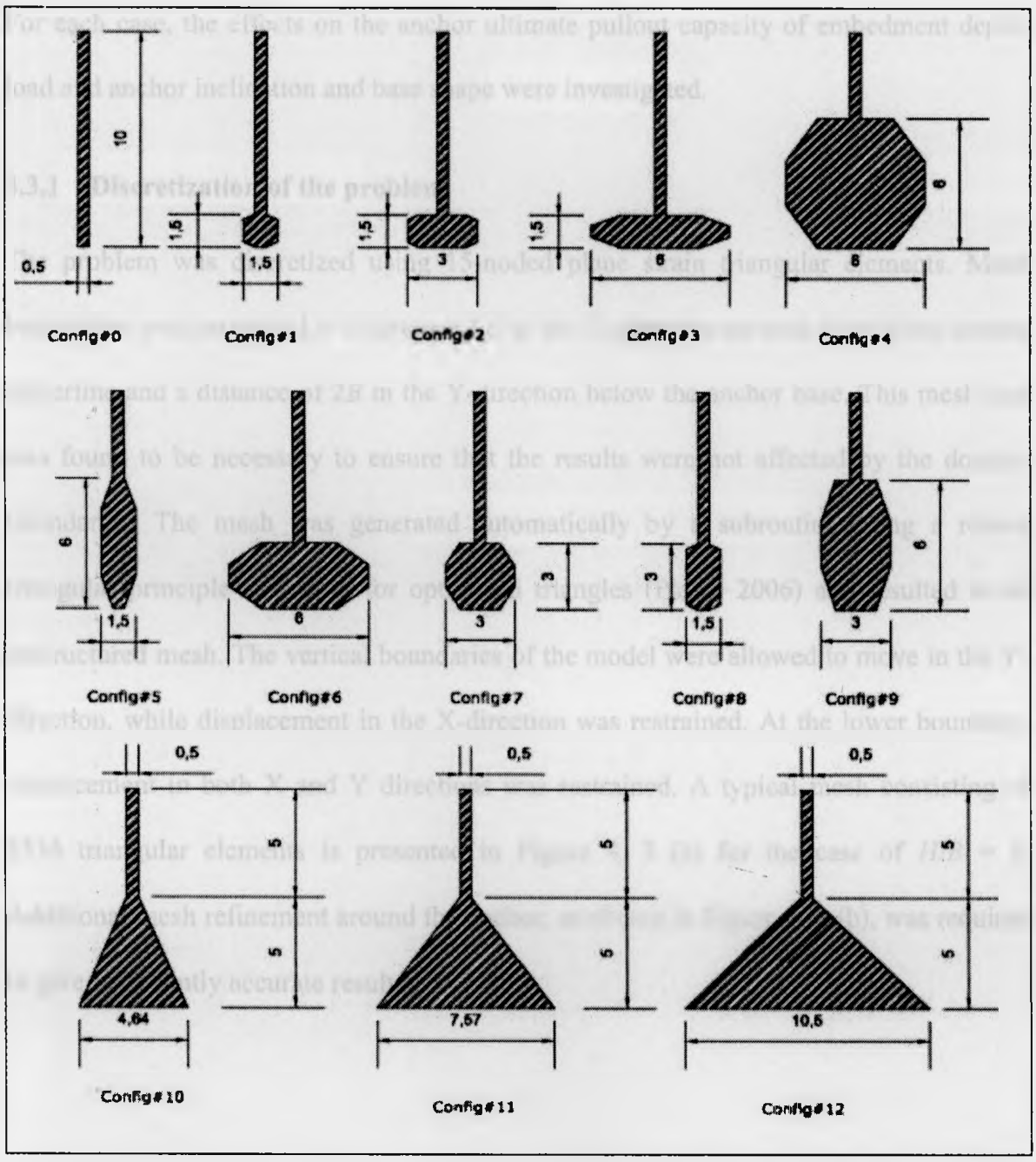

Figure 4. 2: Dimensions of the different studied anchor shapes (all dimensions in m).

As well as the vertical anchor cases, simulations for anchors inclined at $\beta = 45^{\circ}$ were also carried out. Two loading cases were modeled: parallel and normal to the anchor orientation.

For each case, the effects on the anchor ultimate pullout capacity of embedment depth, load and anchor inclination and base shape were investigated.

4.3.1 Discretization of the problem

The problem was discretized using 15-noded plane strain triangular elements. Mesh boundaries were extended to a distance $6B$ in the X-direction on each side of the anchor centerline and a distance of $2B$ in the Y-direction below the anchor base. This mesh size was found to be necessary to ensure that the results were not affected by the domain boundaries. The mesh was generated automatically by a subroutine using a robust triangular principle searching for optimized triangles (Plaxis 2006) and resulted in an unstructured mesh. The vertical boundaries of the model were allowed to move in the Y-direction, while displacement in the X-direction was restrained. At the lower boundary, displacement in both X and Y directions was restrained. A typical mesh consisting of 5334 triangular elements is presented in Figure 4. 3 (a) for the case of H/B = 4. Additional mesh refinement around the anchor, as shown in Figure 4. 3 (b), was required to give sufficiently accurate results.

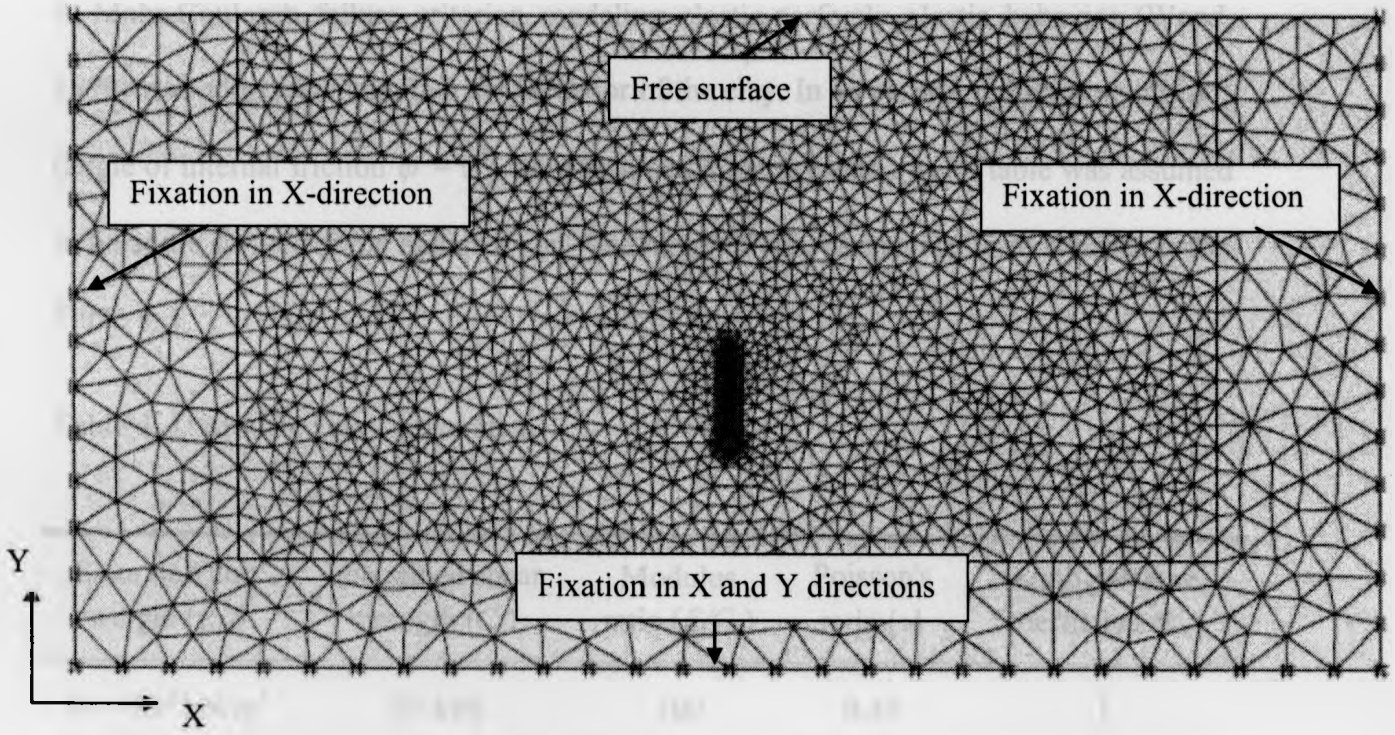

(a)

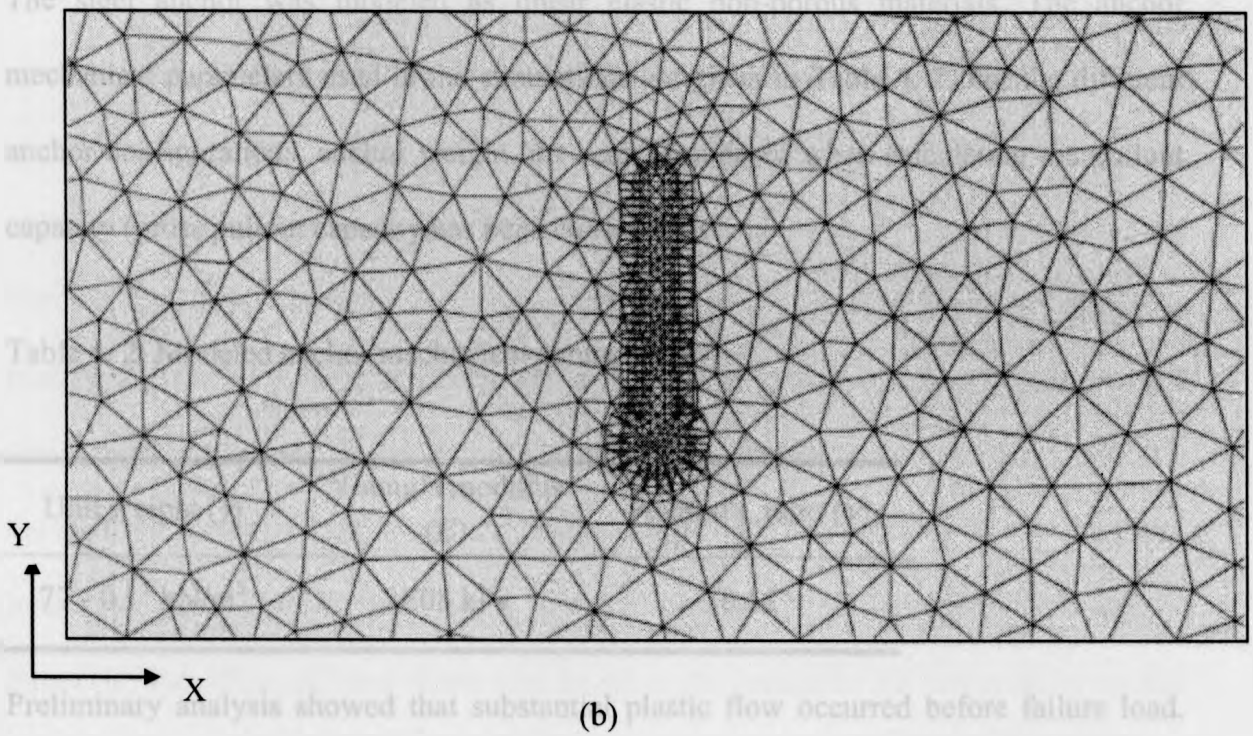

(b)

Figure 4. 3: (a) Example of discretized mesh of the model for configuration # 1 (width = 12B = 120 m) and (b) expanded view of mesh close to the anchor ($H/B = 4$).

A Mohr-Coulomb failure criterion modeling elastic-perfectly plastic behavior (Wood, 1990) was adopted to simulate the behavior of the clay. In all cases, undrained conditions (angle of internal friction $\varphi = 0^0$) were assumed and the ground water table was assumed to lie at the surface of the modeled soil. The range of clay parameters used is presented in Table 4. 1.

Table 4. 1: Modeled clay parameters

Saturated unit weight (γ_{sat})	Undrained shear strength (C_u)	Modulus ratio (E/C_u)	Poisson's ratio (ν)	Earth pressure coefficient (K_o)
16 - 0.1[3] kN/m^3	20 kPa	100	0.49	1

The steel anchor was modeled as linear elastic non-porous materials. The anchor mechanical parameters used in the simulations are given in Table 4. 2. For the different anchor configurations, anchor weight has been considered when calculating the pullout capacity (gross pullout capacity has been considered).

Table 4. 2: Modeled anchor mechanical parameters

Unit weight (γ)	Young's modulus (E)	Poisson's ratio (ν)
77 - 0.1[1] kN/m^3	2E08 kPa	0.15

Preliminary analysis showed that substantial plastic flow occurred before failure load. This is generally not acceptable for practical reasons due to the accompanying excessive

[3] Value used in case of immediate breakaway conditions

displacement. Accordingly, the K4 criterion introduced by Rowe and Davis (1982) was adopted as a measure of the ultimate capacity of the anchor. The K4 failure load is defined as the load at which the stiffness of the material has declined to one-quarter of its elastic stiffness. To determine this quantity, prescribed displacements were applied to the model anchors and load-displacement curves were produced at predefined nodes. Song *et al.* (2008) used a similar approach for the analysis of horizontal anchor pullout.

4.3.2 Results and discussion

The finite element models were used to calculate the pullout capacity of vertically oriented anchors under vertical and horizontal loading conditions as a function of embedment depth. In Figure 4. 4, the results for fully bonded anchors in configurations # 0 - 4 are shown ($\alpha = 1$). The pullout capacity non-linearly increases at a decreasing rate until reaching a constant value at a threshold depth referred to as the critical depth, beyond which it acts as a deep anchor. The results show that deep behavior occurred at a value of *H/B* between 2 and 3 for vertically loaded anchors and at *H/B* greater than 3 for horizontally loaded anchors. This shows that the value of critical depth is higher for horizontally loaded anchors and decreases with load inclination, reaching its lowest value when vertically loaded. The results show that the base shape had a significant effect in the case of vertically loaded anchors. For example, the difference in N_c for vertically loaded anchors is more than 190% between anchors of configurations # 0 and 4. However, the effect of base shape was found to be negligible for horizontally loaded anchors. The variation of N_c with *H/B* for fully bonded anchors of configuration # 1 is also presented in Figure A. 2 in appendix A for different loading cases.

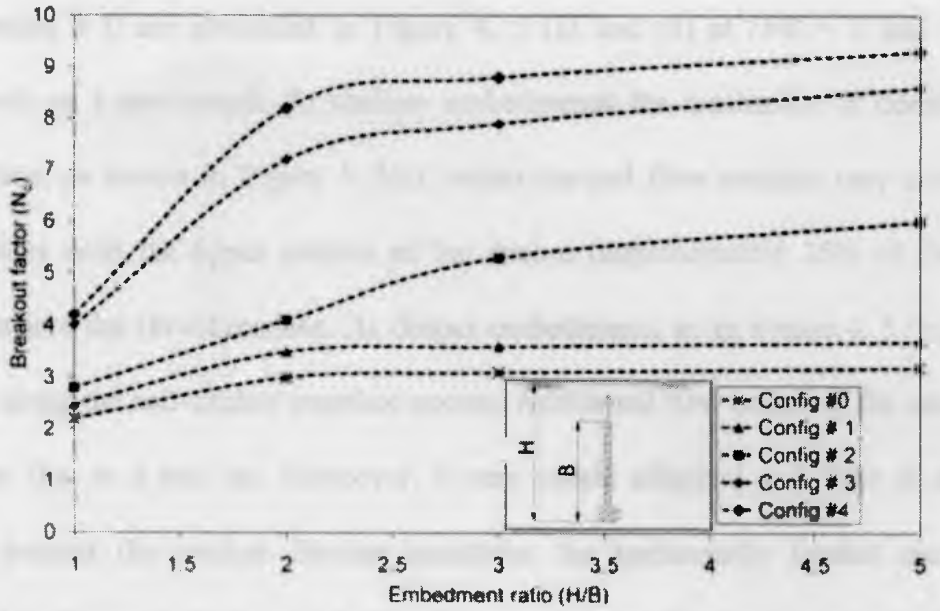

(a)

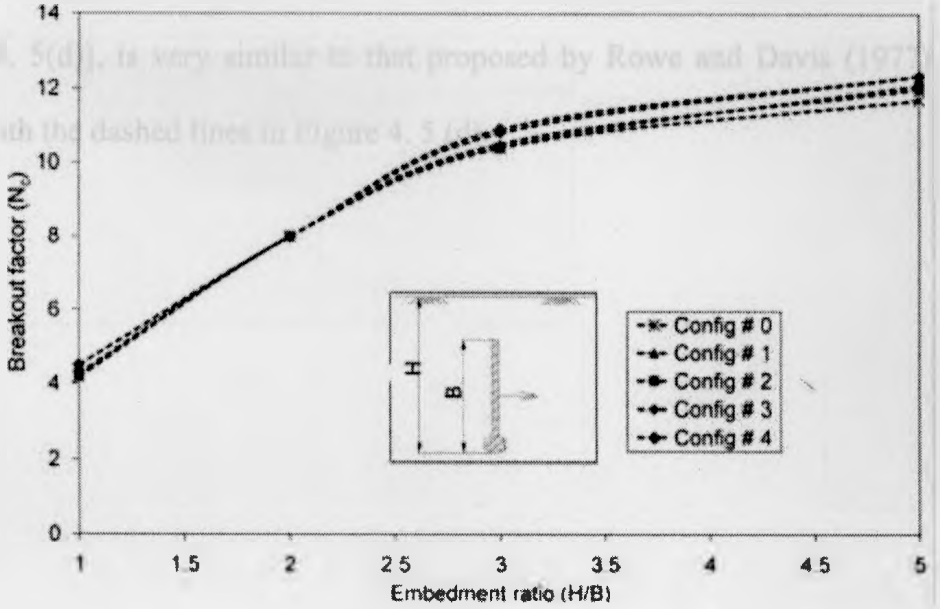

(b)

Figure 4. 4: Variation of breakout factor N_c with embedment ratio *H/B* for anchors with configurations # 1, 2, 3 and 4 compared to results for a regular plate anchor (configuration # 0) for (a) vertical loading and (b) horizontal loading (fully bonded case).

The total displacement increments diagrams for vertically loaded fully bonded anchors of

configuration # 0 are presented in Figure 4. 5 (a) and (b) at H/B = 1 and H/B = 4 respectively as a benchmark. At shallow embedments, the mechanism is dominated by skin friction, as shown in Figure 4. 5(a), where the soil flow remains very close to the anchor sides until the upper portion of the anchor (approximately 25% of the anchor height), where the flow broadens. At deeper embedments, as in Figure 4. 5 (b), intense shearing along the soil-anchor interface occurs. Additional flow occurs at the anchor end, similar to that at a pile tip. Moreover, a very subtle elliptical soil flow is shown to develop around the anchor. Similar quantities for horizontally loaded anchors are presented in Figure 4. 5(c) and (d). The flow mechanism for deeply embedded anchors [Figure 4. 5(d)], is very similar to that proposed by Rowe and Davis (1977) which is shown with the dashed lines in Figure 4. 5 (d).

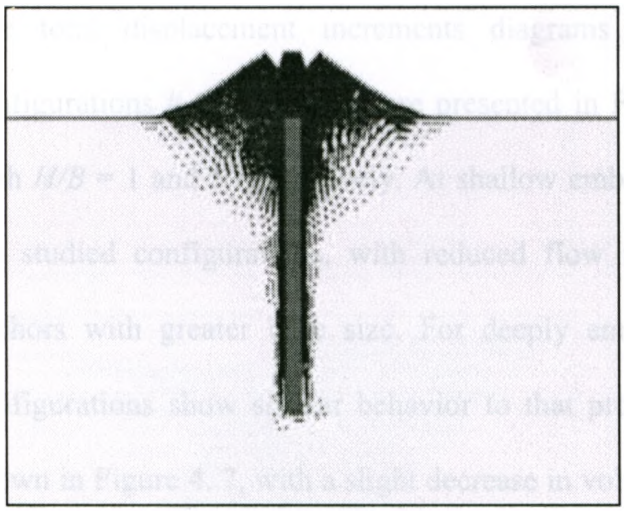

(a)

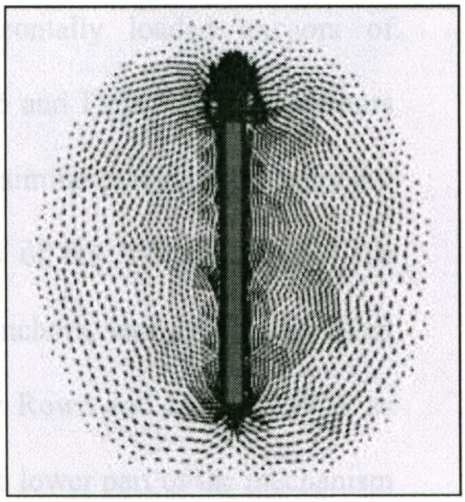

(b)

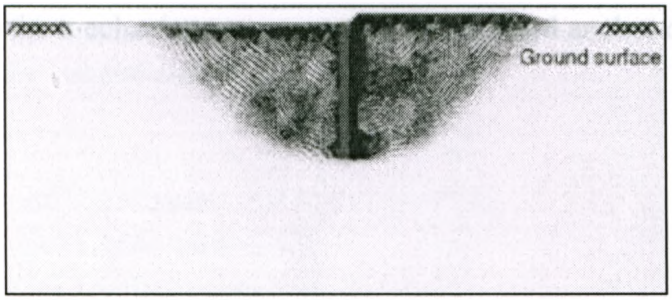

(c)

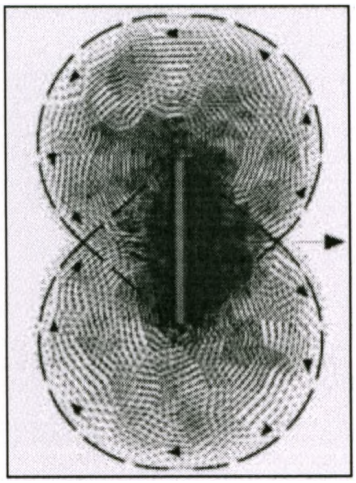

(d)

Figure 4. 5: Total displacement increments diagrams for fully bonded anchor configuration # 0 (regular anchor) for:

a) Vertically loaded – $H/B = 1$;

b) Vertically loaded – $H/B = 4$ (deep condition);

c) Horizontally loaded – $H/B = 1$;

d) Horizontally loaded – $H/B = 4$ (deep condition) and also showing the mechanism proposed by Rowe and Davis (1977) with dashed lines.

The total displacement increments diagrams for horizontally loaded anchors of configurations # 1, 2, 3 and 4 are presented in Figure 4. 6 and Figure 4. 7 for anchors with H/B = 1 and 5 respectively. At shallow embedments, similar mechanisms occur for the studied configurations, with reduced flow intensities of the trailing portions for anchors with greater base size. For deeply embedded anchors, the different studied configurations show similar behavior to that proposed by Rowe and Davis (1977), as shown in Figure 4. 7, with a slight decrease in volume in the lower part of the mechanism compared to the upper, for anchors of greater base size, as shown in (c) and (d). Interestingly, for horizontally loaded anchors, there appears to be relatively little change in the mechanisms compared to the standard anchor configuration # 0.

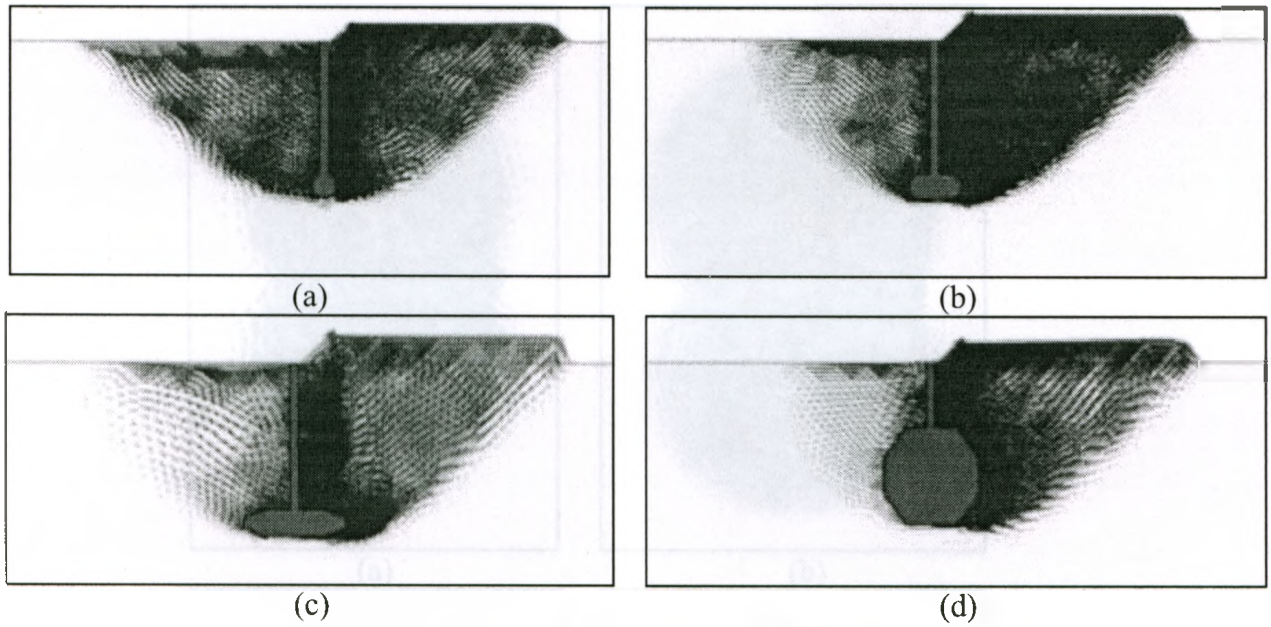

Figure 4. 6: Total displacement increments diagrams at H/B =1 for horizontally loaded fully bonded anchors of:

(a) Configuration # 1;
(b) Configuration # 2;
(c) Configuration # 3;
(d) Configuration # 4.

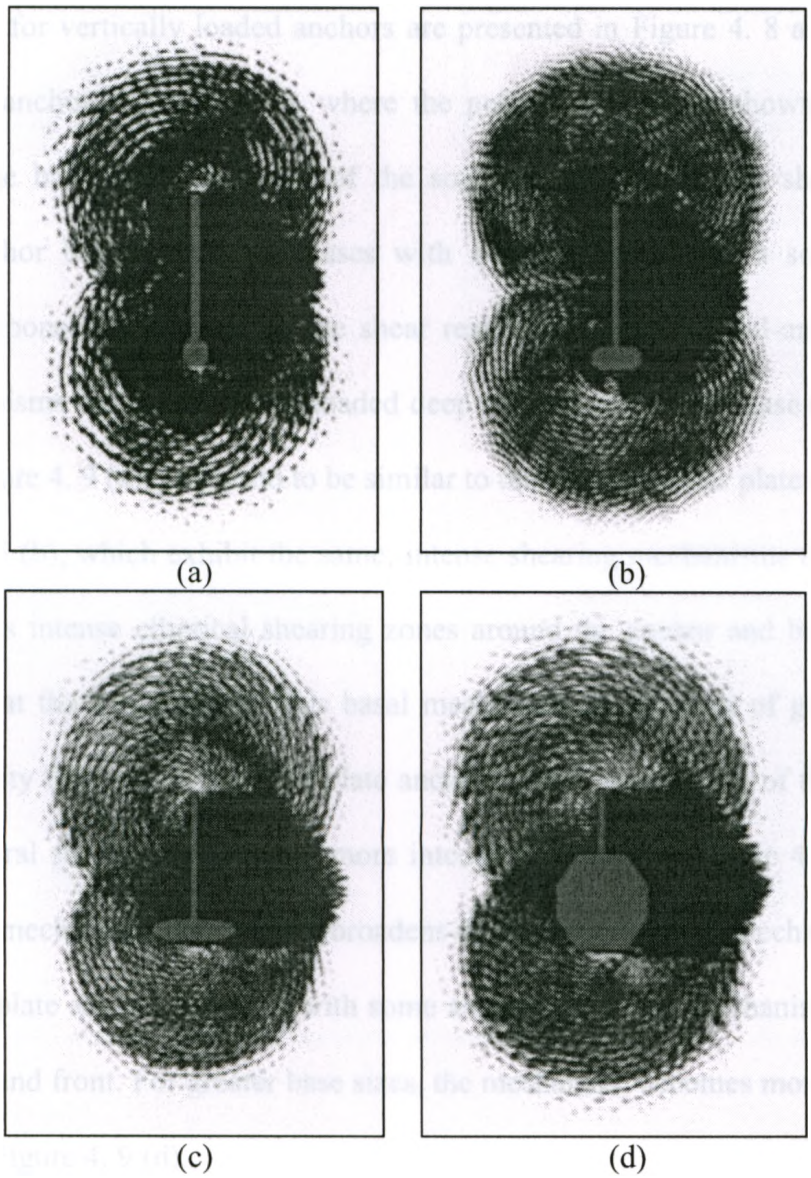

Figure 4. 7: Total displacement increments diagrams at H/B =5 for horizontally loaded fully bonded anchors of:

(a) Configuration # 1;
(b) Configuration # 2;
(c) Configuration # 3;
(d) Configuration # 4.

Similar plots for vertically loaded anchors are presented in Figure 4. 8 and Figure 4. 9. For shallow anchors (Figure 4. 8), where the pullout capacity is shown to double by increasing the base size, the width of the soil flow extends to the shoulders of the enlarged anchor base, which, for cases with a larger base, adds a soil own-weight capacity component in addition to the shear resistance along the soil-anchor interface. Flow mechanisms around vertically loaded deep anchors with small base dimensions, as shown in Figure 4. 9 (a), are found to be similar to that of the regular plate anchors shown in Figure 4. 5 (b), which exhibit the same; intense shearing mechanisms along the sides, but much less intense elliptical shearing zones around the anchor and bearing capacity mechanisms at the anchor ends. This basal mechanism is, however of greater area and higher intensity than it is for regular plate anchors. With the increase of the anchor base size, the central shear zone becomes more intense, as shown in Figure 4. 9 (b) and (c), and the flow mechanism significantly broadens developing a similar mechanism to that of a horizontal plate anchor, however with some asymmetry in the mechanism between the anchor back and front. For greater base sizes, the mechanism becomes more symmetrical, as shown in Figure 4. 9 (d).

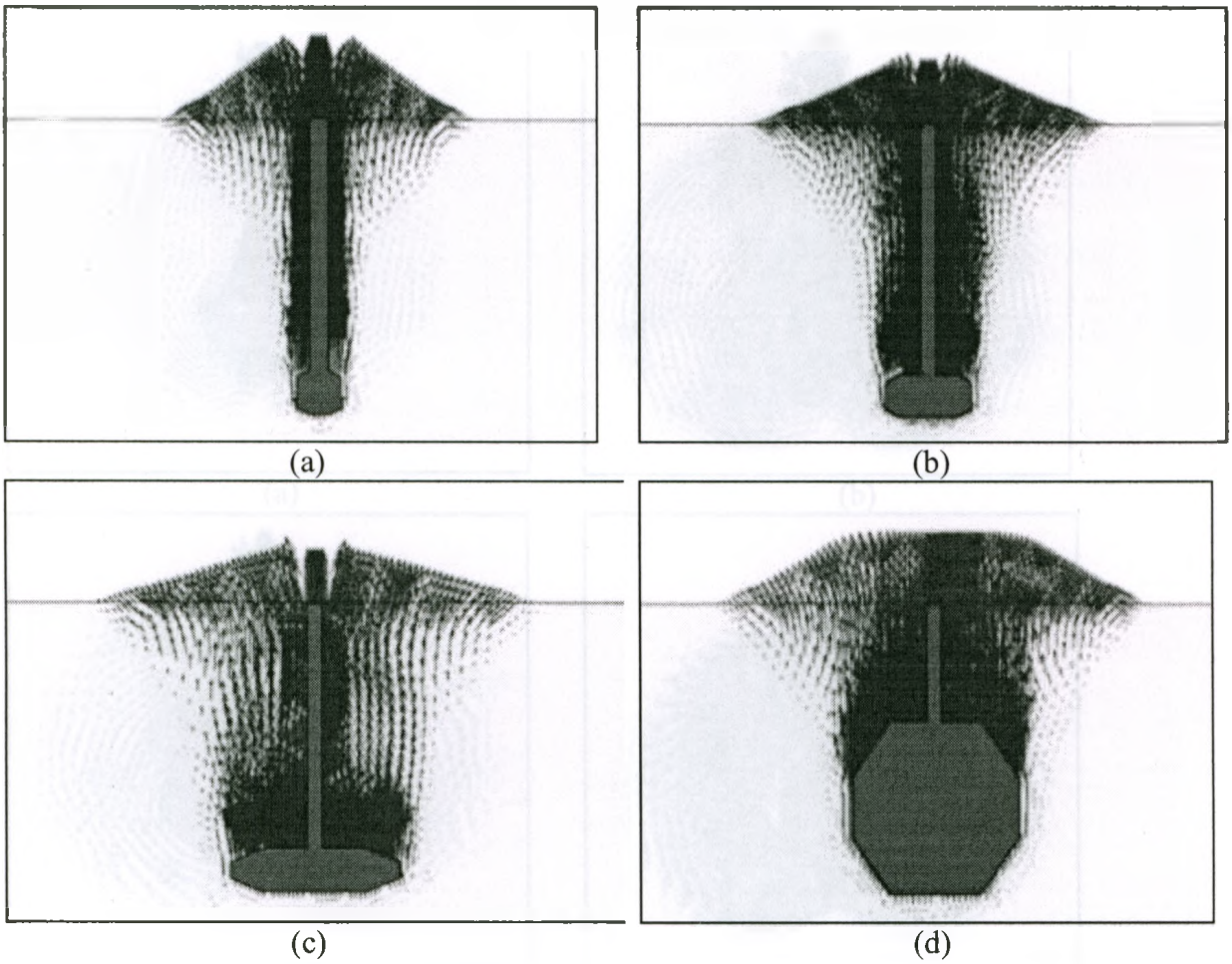

Figure 4. 8: Total displacement increments diagrams at H/B =1 for vertically loaded fully bonded anchors of :

(a) Configuration # 1;
(b) Configuration # 2;
(c) Configuration # 3;
(d) Configuration # 4.

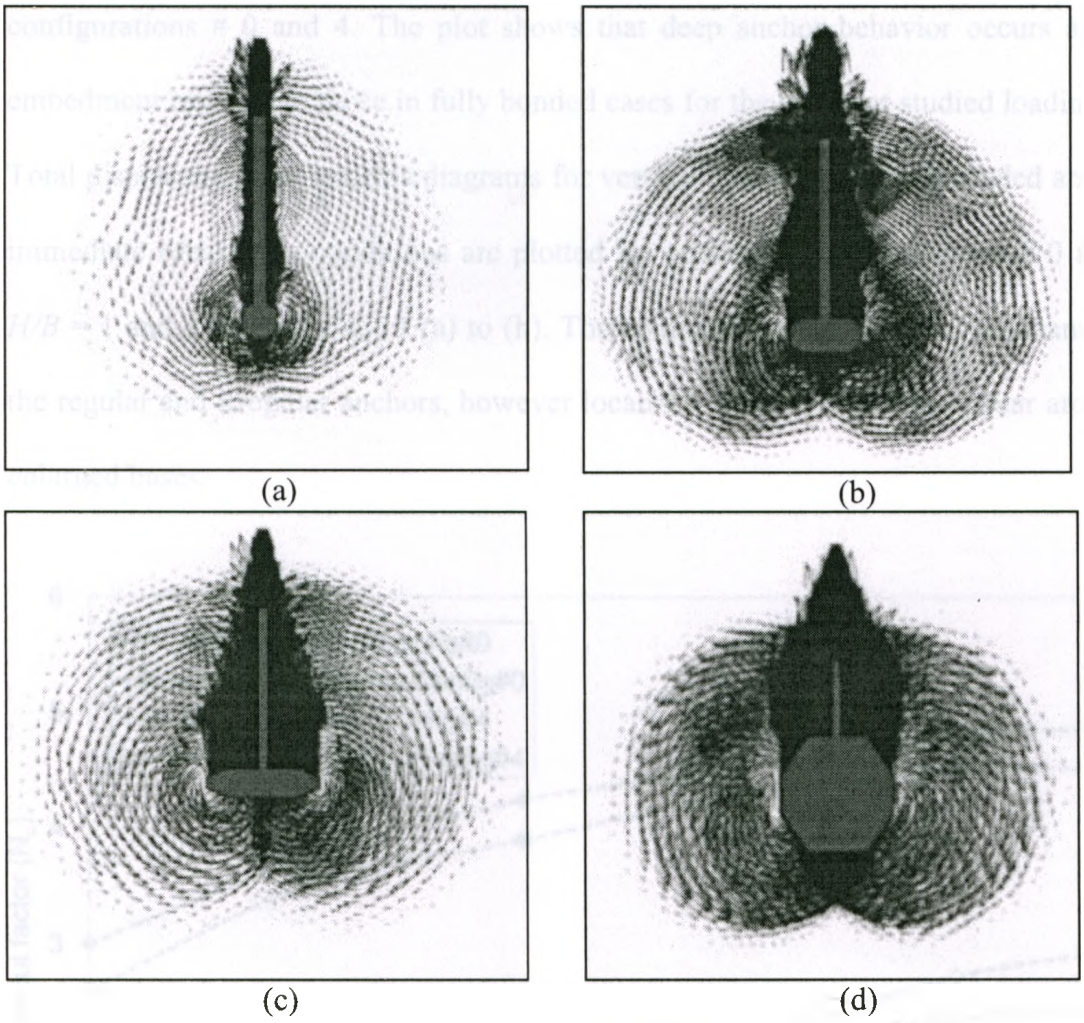

Figure 4. 9: Total displacement increments diagrams at H/B =5 for vertically loaded anchors of :

(a) Configuration # 1;
(b) Configuration # 2;
(c) Configuration # 3;
(d) Configuration # 4.

Immediate breakaway conditions were also considered, in which the interface between the anchor and soil cannot sustain tension and full separation is assumed to occur upon loading. The variation of N_c with H/B for the vertical and horizontal loading for immediate breakaway conditions is presented in Figure 4. 10 for anchors of

configurations # 0 and 4. The plot shows that deep anchor behavior occurs at higher embedment ratios than those in fully bonded cases for the different studied loading cases. Total displacement increments diagrams for vertically and horizontally loaded anchors at immediate breakaway conditions are plotted for anchors of configurations # 0 and 4 at H/B = 1 and 4 in Figure 4. 11 (a) to (h). The comparison shows similar mechanisms for the regular and irregular anchors, however localized flow mechanisms appear around the enlarged bases.

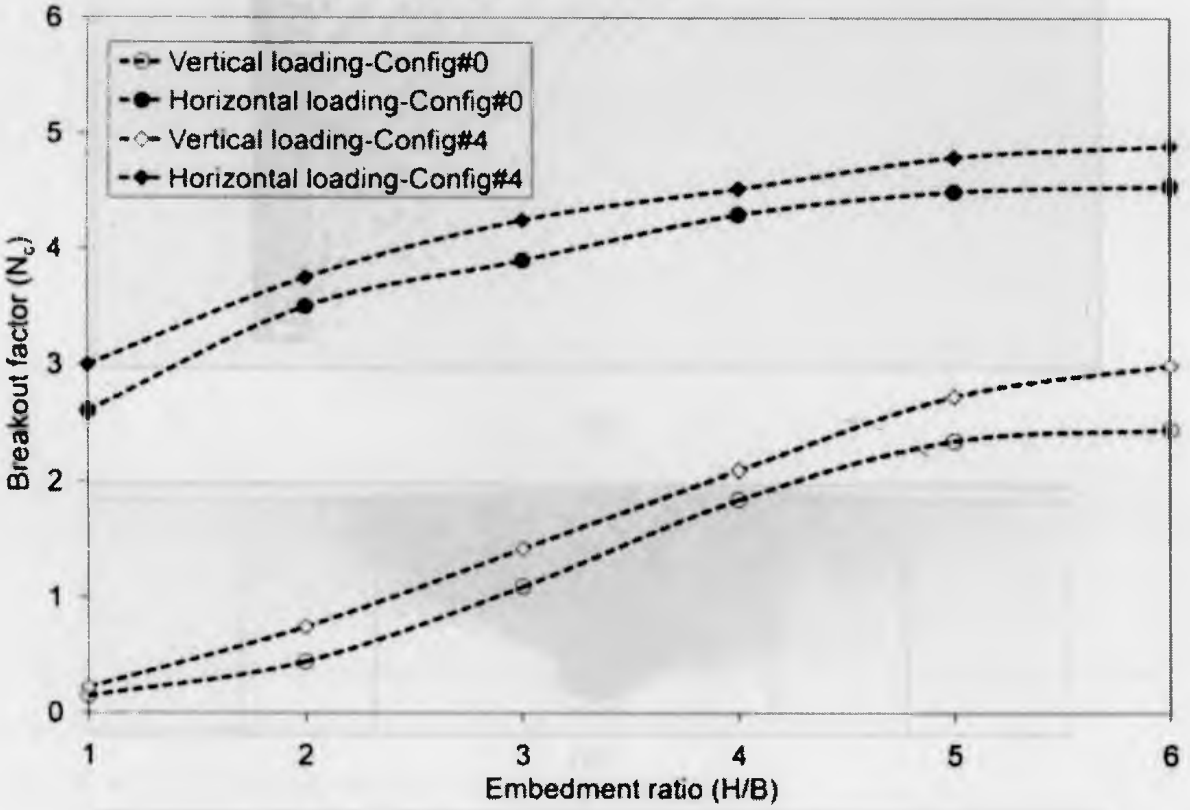

Figure 4. 10: Variation of breakout factor N_c with embedment ratio H/B for vertical anchor of configurations # 0 and # 4 subjected to vertical and horizontal loadings (immediate breakaway).

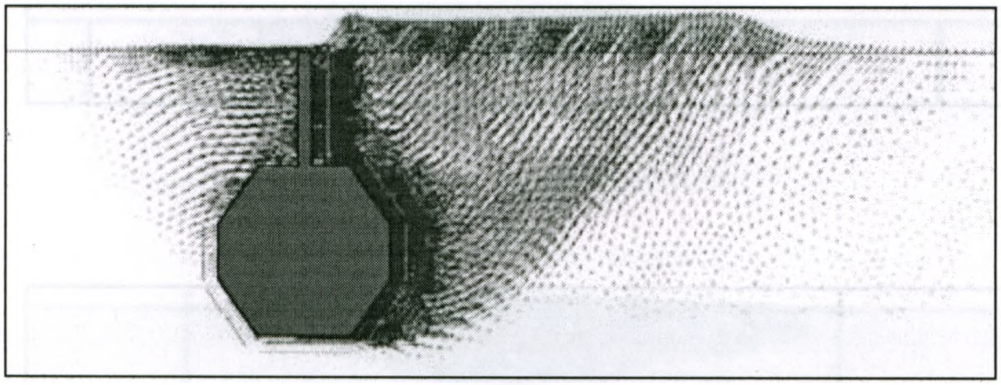

(a)

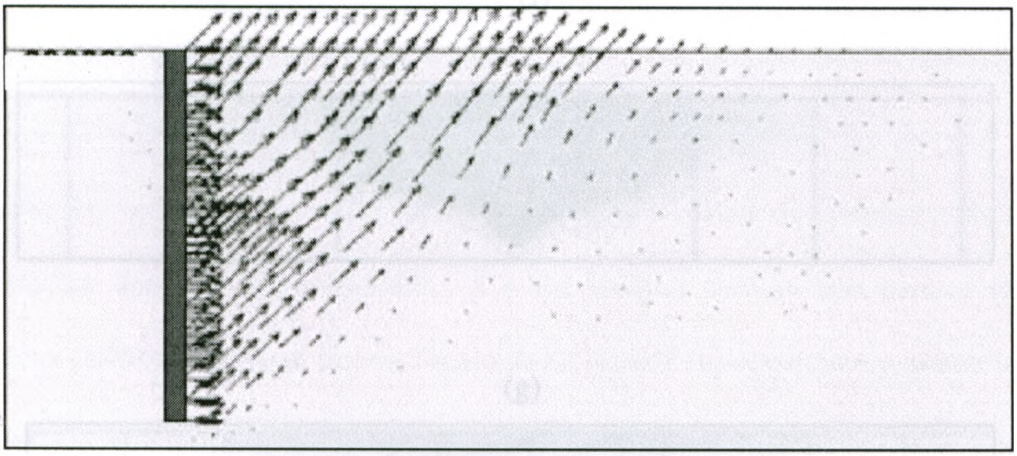

(b)

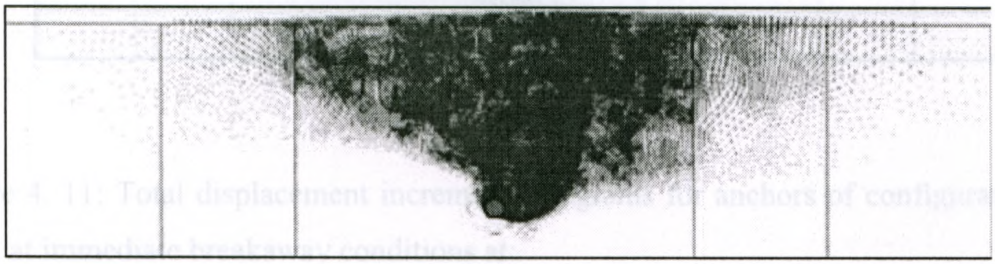

(c)

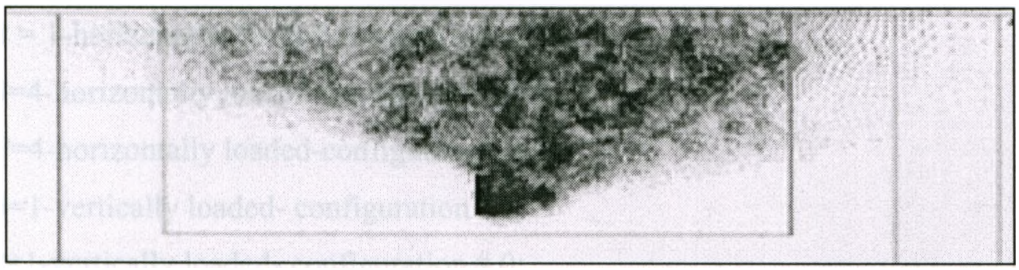

(d)

(e)

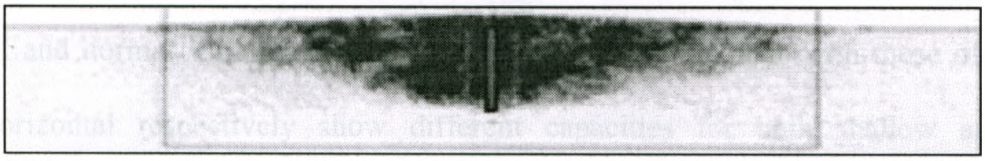

(f)

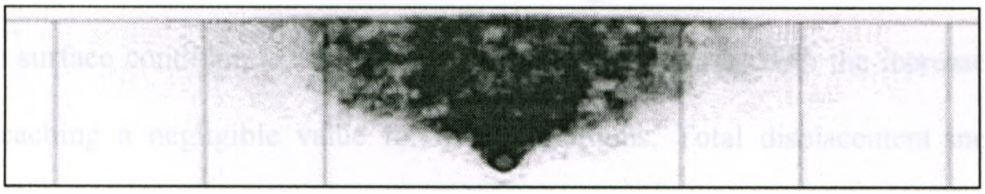

(g)

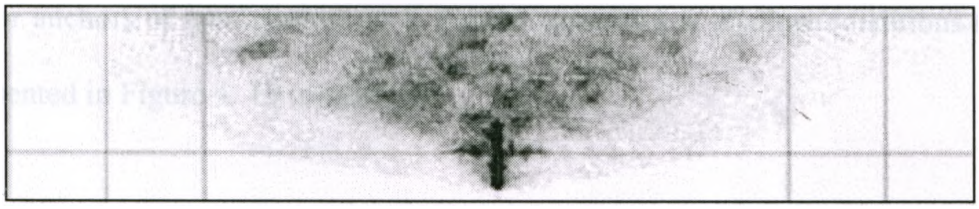

(h)

Figure 4. 11: Total displacement increments diagrams for anchors of configurations # 0 and 4 at immediate breakaway conditions at:

a) *H/B* = 1-horizontally loaded-configuration # 4;

b) *H/B* = 1-horizontally loaded-configuration # 0;

c) *H/B*=4-horizontally loaded-configuration # 4;

d) *H/B*=4-horizontally loaded-configuration # 0;

e) *H/B*=1-vertically loaded- configuration #4;

f) *H/B*=1-vertically loaded- configuration # 0;

g) *H/B*=4-vertically loaded- configuration # 4;

h) *H/B*=4-vertically loaded- configuration # 0.

Fully bonded anchors inclined at an angle $\beta = 45^{\circ}$ from the vertical have also been modeled. Anchors subjected to loads parallel and normal to the anchor axis applied at the centre of mass were studied. The variation of the resulting N_c with *H/B* is plotted in Figure 4. 12 for anchors of configurations # 0 and 4 for loading cases horizontal, vertical, parallel and normal. Comparison of parallel and normal loadings with those of vertical and horizontal respectively show different capacities for both shallow and deep conditions. The breakout factors for horizontal and vertical loading cases have shown to be greater than those for normal and parallel loading cases respectively by approximately 25% at surface condition (*H/B* = 1). This difference decreases with the increase of *H/B* until reaching a negligible value for deep conditions. Total displacement increments diagrams for anchors of configuration # 4 for loading parallel and normal for deep conditions (*H/B*=5) are presented in Figure 4. 13 (a) and (b) respectively, plotted against those for anchors of configuration # 0. Similar quantities at shallow conditions (*H/B*=1) are presented in Figure 4. 13 (c) and (d).

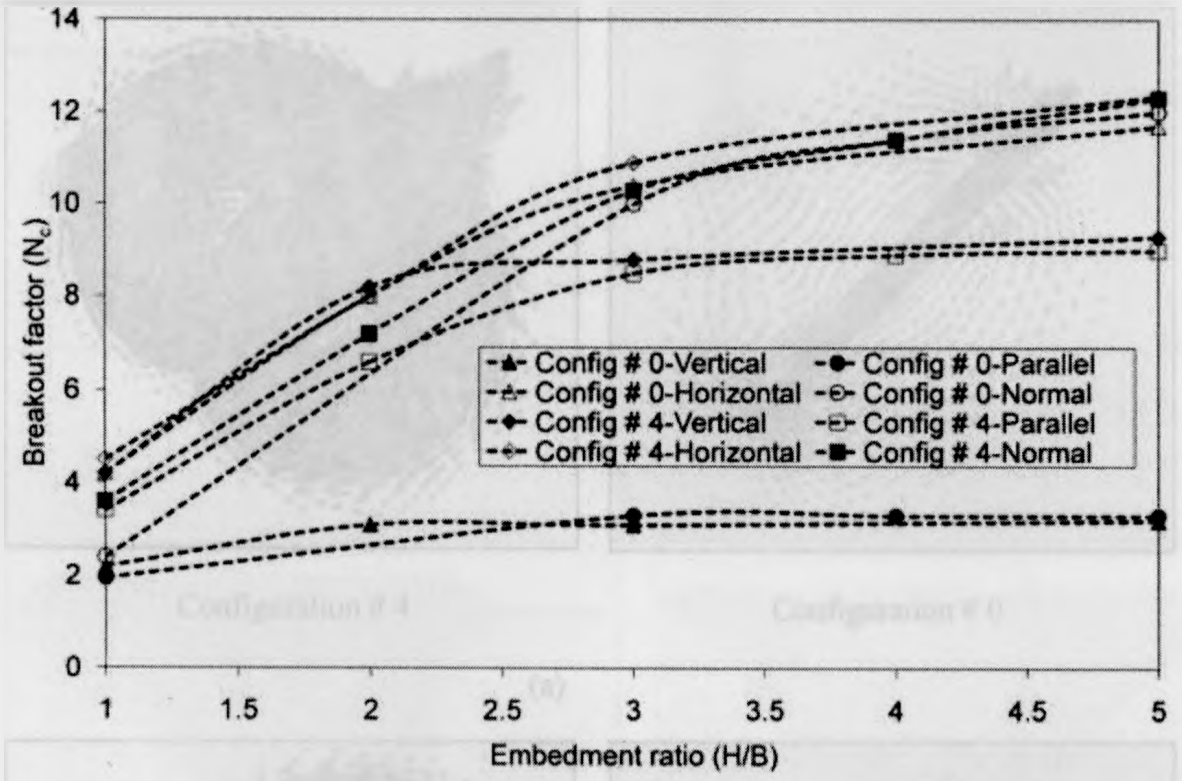

Figure 4. 12: Variation of breakout factor N_c with embedment ratio H/B for anchors of configurations # 0 and 4 for 45° inclinations and parallel/normal loading plotted against vertical and horizontally loaded vertical anchors cases.

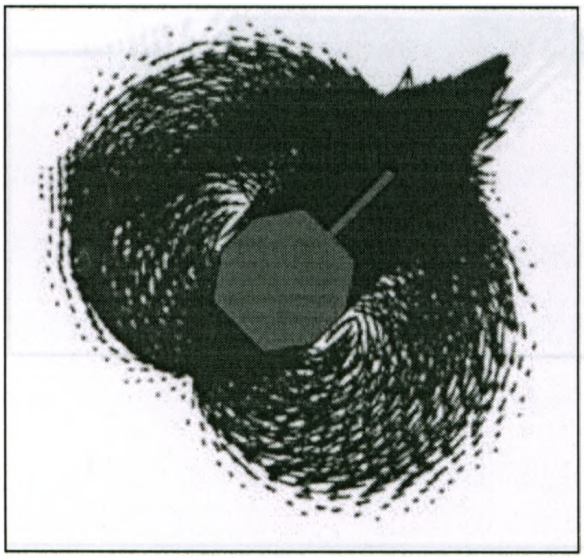

Configuration # 4

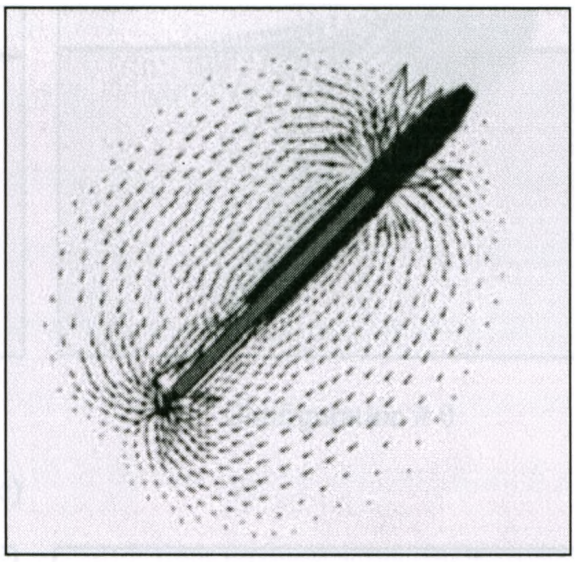

Configuration # 0

(a)

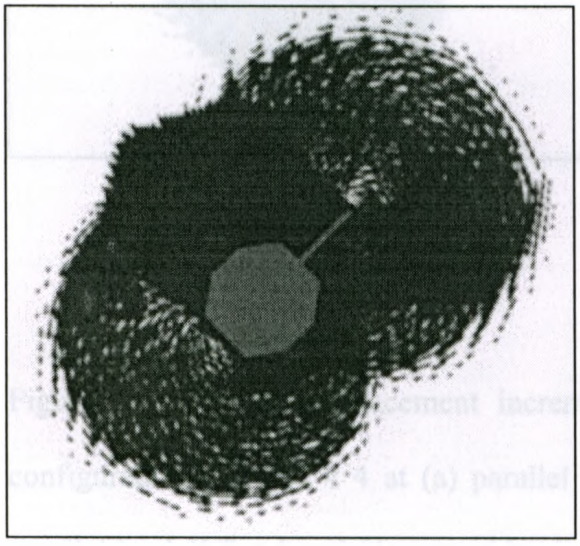

Configuration # 4

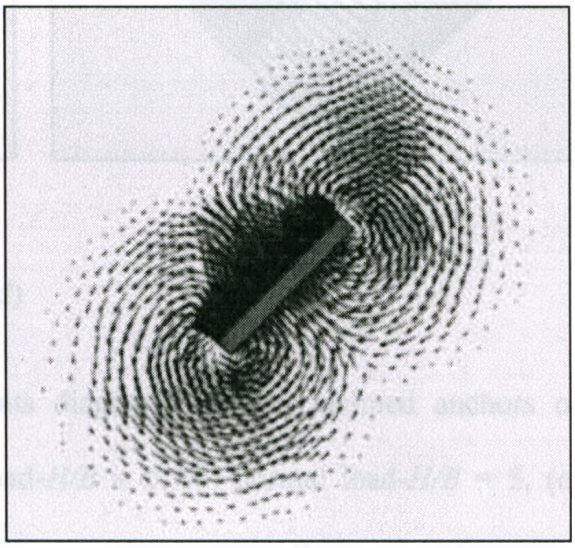

Configuration # 0

(b)

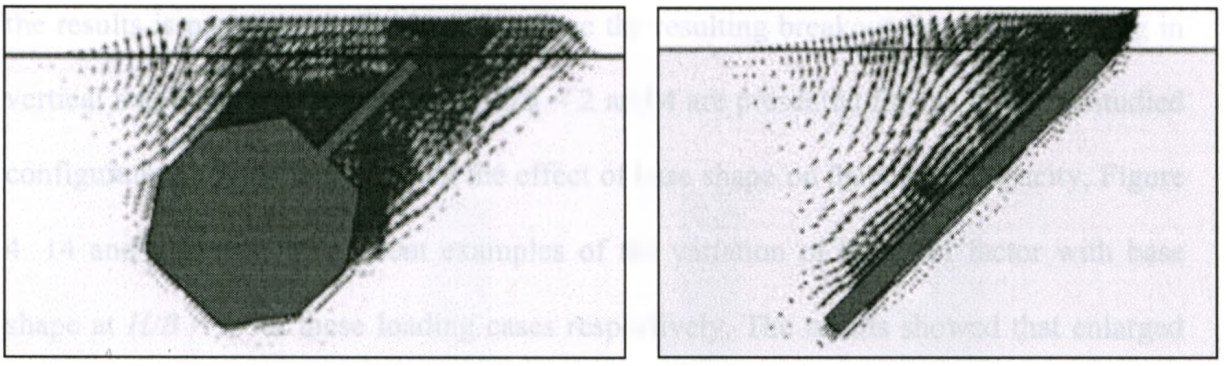

Configuration # 4 Configuration # 0

(c)

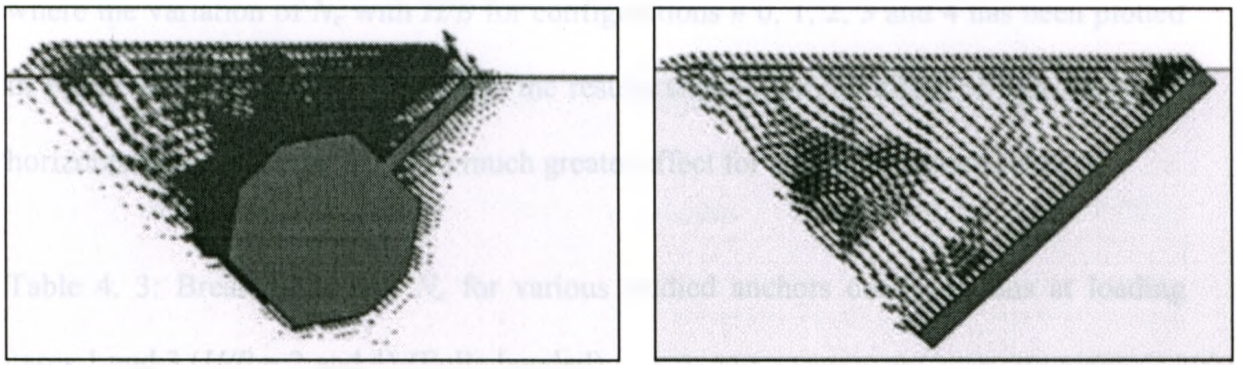

Configuration # 4 Configuration # 0

(d)

Figure 4. 13: Total displacement increments diagrams for 45° inclined anchors of configuration # 0 and # 4 at (a) parallel load-*H/B* = 5, (b) normal load-*H/B* = 5, (c) parallel load-*H/B* = 1 and (d) normal load-*H/B* = 1, plotted against those of configuration # 0.

Further investigation of the effect of base shape on the pullout capacity was conducted. Fully bonded anchors with the different base configurations, as illustrated in Figure 4. 2, were numerically simulated under different loading conditions. The results have show that the effect of base size and shape varies depending on load inclination. A summary of

the results is presented in Table 4. 3, where the resulting breakout factors for loading in vertical and horizontal directions at H/B = 2 and 4 are presented for the different studied configurations. To better illustrate the effect of base shape on the anchor capacity, Figure 4. 14 and Figure 4. 15 present examples of the variation of breakout factor with base shape at H/B = 4 for these loading cases respectively. The results showed that enlarged base width (W) has a greater effect on anchor capacity, while the effect of enlarged base height (L) is negligible. Another example is given in the previously presented Figure 4. 4, where the variation of N_c with H/B for configurations # 0, 1, 2, 3 and 4 has been plotted in Figure 4. 4 (a) and (b). Generally, the results show a limited effect of base shape on horizontally loaded anchors, but a much greater effect for vertically loaded anchors.

Table 4. 3: Breakout factors N_c for various studied anchors configurations at loading cases 1 and 3 (H/B = 2 and 4)-(Fully bonded)

Configuration	W (m)	Enlarged base area (m^2)	L (m)	Vl load H/B = 2	Vl load H/B = 4	Hzl load H/B = 2	Hzl load H/B = 4
1	1.5	1.99	1.5	3.5	3.6	8.0	11.6
2	1.5	4.25	3.0	3.6	3.7	8.0	11.6
3	3.0	7.69	1.5	4.1	5.1	8.0	11.6
4	6.0	30.50	1.5	7.2	7.9	8.0	11.8
5	1.5	7.50	6.0	3.7	3.7	8.0	11.6
6	6.0	15.25	3.0	7.5	8.0	8.0	12.0
7	3.0	7.75	3.0	5.0	5.1	8.0	11.9
8	6.0	4.25	6.0	8.2	9.0	8.0	12.0
9	3.0	15.50	6.0	5.0	5.2	8.0	11.9

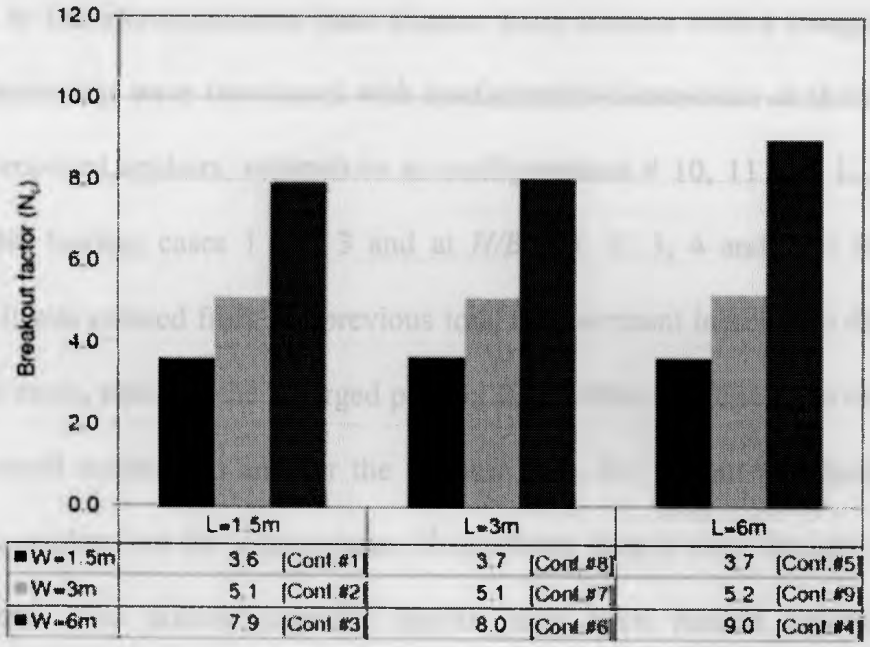

Figure 4. 14: Variation of N_c with different base shapes – vertically loaded-H/B = 4 (fully bonded).

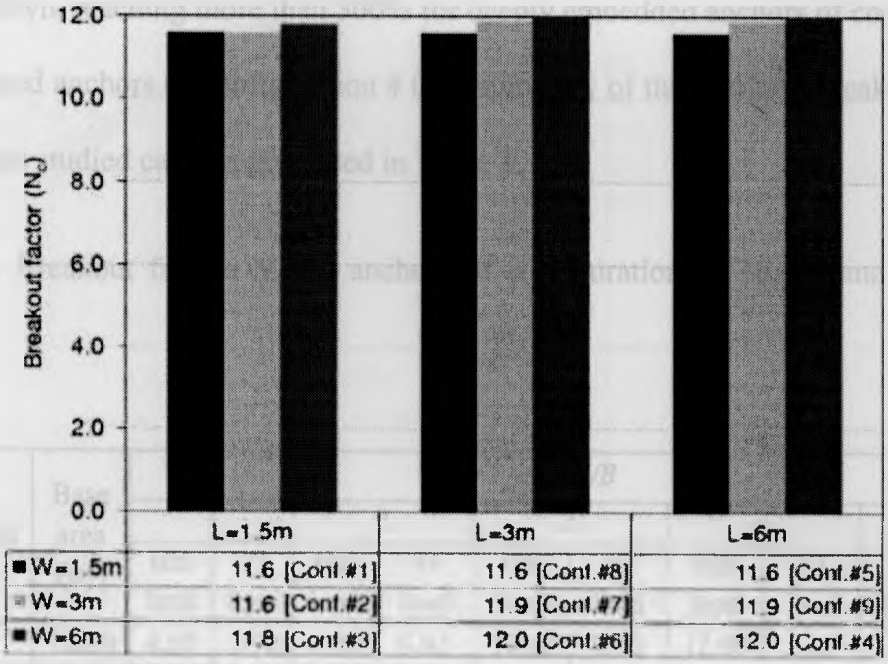

Figure 4. 15: Variation of N_c with the different base shapes – horizontally loaded-H/B = 4 (fully bonded).

In addition to the aforementioned base shapes, three anchors with a triangular base of different dimensions were introduced with configuration/dimensions as shown in Figure 4. 2. The proposed anchors, referred to as configurations # 10, 11 and 12, have been studied under loading cases 1 and 3 and at H/B = 1, 2, 3, 4 and 5 at fully bonded conditions. It was noticed from the previous total displacement increments diagrams that for the deep cases, much of the enlarged portion falls within the false-head of material in the flow around mechanism and for the shallow case, the pullout is a function of the width of the anchor, not the volume/area. Hence these shapes were thought to optimize these features. The pullout capacity results have been plotted against those of configuration # 0 and 4 as shown in Figure 4. 16. The results show the limited effect of the proposed shapes for laterally loaded anchors, with the percentage increase in N_c being always less than 20%. However, for vertically loaded anchors, a significant increase in N_c has been shown, reaching more than 300% for deeply embedded anchors of configuration # 12 compared anchors of configuration # 0. A summary of the resulting breakout factors of the various studied cases is presented in Table 4. 4.

Table 4. 4: Breakout factors N_c for anchors of configurations # 10, 11 and 12 (Fully bonded)

Configuration	Base area (m^2)	*H/B*									
		1		2		3		4		5	
		Hzl load	Vl load	Hzl load	Vl load	Hzl load	Vl load	Hzl load	Vl load	Hzl load	Vl load
10	12.86	4.60	3.90	8.00	6.65	10.40	7.40	12.00	7.45	12.70	7.45
11	20.18	4.80	4.86	8.00	8.50	10.45	10.15	12.00	10.20	13.00	10.50
12	27.50	4.94	5.50	8.20	11.15	10.50	13.40	12.10	13.50	13.30	13.70

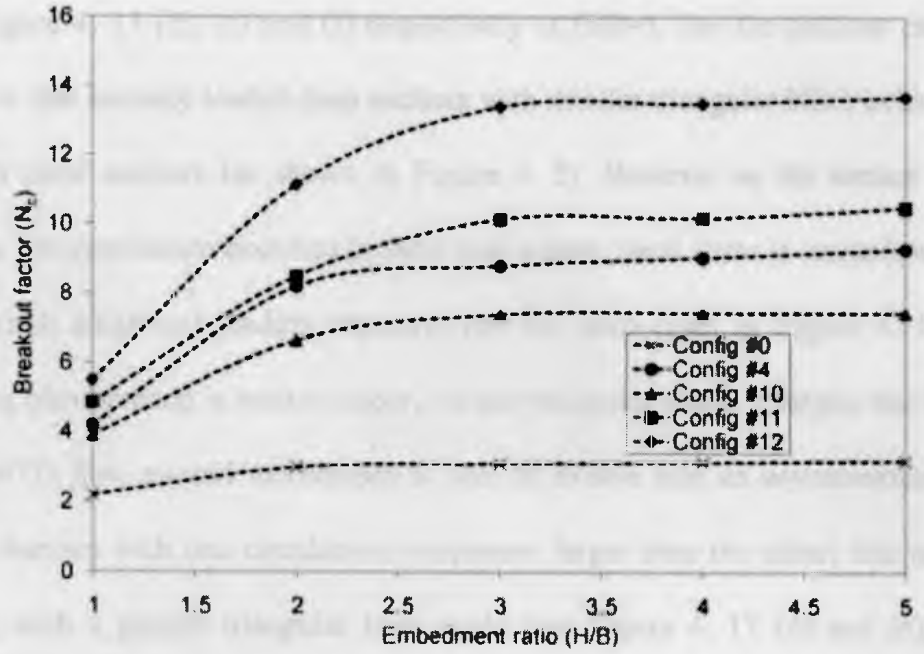

(a)

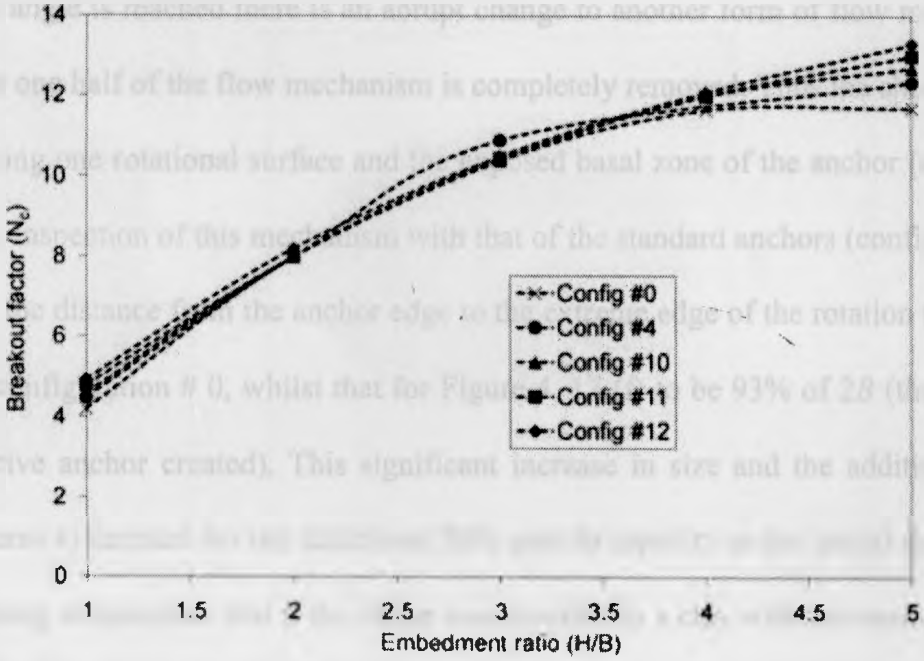

(b)

Figure 4. 16: Variation of N_c with *H/B* for fully bonded anchors of configurations # 0, 4, 10, 11 and 12 subjected to (a) vertical loads and (b) horizontal loads.

The total displacement increments diagrams for anchors of configurations # 10, 11 and 12 for horizontal loading are shown in Figure 4. 17 (a), (b) and (c) respectively at *H/B*=1,

and in Figure 4. 17 (d), (e) and (f) respectively at H/B=5. For the shallow cases, these plots show that laterally loaded deep anchors with smaller triangular bases behave similar to regular plate anchors (as shown in Figure 4. 5). However as the anchor base size increases, the mechanism becomes broader and greater basal shear is created, accounting for the small additional loading capacity. For the deep cases in Figure 4. 17, a very interesting phenomenon is seen to occur. As the triangular shape enlarges, the Rowe and Davis (1977) flow around mechanism is seen to evolve into an asymmetrical form of flow mechanism with one circulation component larger than the other; this asymmetry increases with a greater triangular base angle [see Figure 4. 17 (d) and (e)]. Once a threshold angle is reached there is an abrupt change to another form of flow mechanism, where the one half of the flow mechanism is completely removed. Thus the shearing only occurs along one rotational surface and the exposed basal zone of the anchor [see Figure 4. 17 (f)]. Inspection of this mechanism with that of the standard anchors (configuration # 0) shows the distance from the anchor edge to the extreme edge of the rotation to be 83% of B for configuration # 0, whilst that for Figure 4. 17 (f) to be 93% of $2B$ (the width of the effective anchor created). This significant increase in size and the additional basal shear, seems to account for the additional 20% gain in capacity in the lateral direction. It is interesting to speculate that if the shape was inverted in a clay with increasing strength with depth, that more significant capacity would occur.

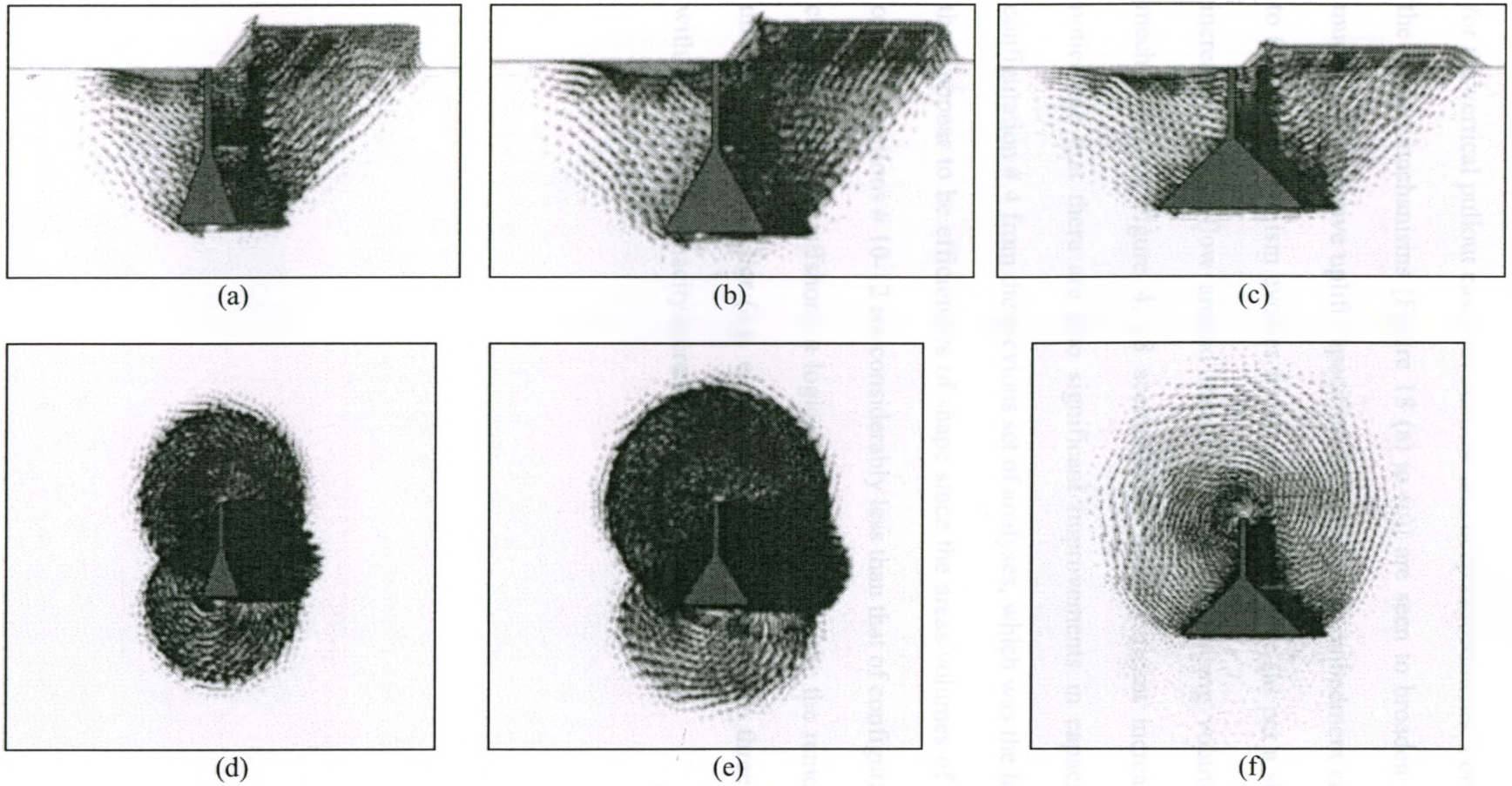

Figure 4. 17: Total displacement increments diagrams of fully bonded anchors for horizontal loading:

(a) Configuration # 10 - *H/B*=1;
(b) Configuration # 11 - *H/B*=1;
(c) Configuration # 12 - *H/B*=1;
(d) Configuration # 10 - *H/B*=5;
(e) Configuration # 11 - *H/B*=5;
(f) Configuration # 12 - *H/B*=5.

Figure 4. 18 (a) to (f) shows the corresponding total displacement increments diagrams for the vertical pullout cases for shallow and deep embedments. For shallow embedments the wedge mechanisms [Figure 18 (a) to (c)] are seen to broaden significantly creating much higher relative uplift capacities. For the deeper embedment cases [Figure 4. 18 (d) to (f)], the mechanism evolves from a skin friction case (as per a standard anchor) to an increasing width flow around mechanism. The increasing volume of these modified mechanisms in Figure 4. 18 accounts for the significant increase in capacity. It is noticeable that there are also significant improvements in capacity in comparison to configuration # 4 from the previous set of analyses, which was the largest anchor. Indeed, there appear to be efficiencies of shape since the areas/volumes of the enlarged sections of configurations # 10-12 are considerably less than that of configuration # 4. Given fixed cranage capacities offshore, a logical extension would be the removal of steel from the underside of the anchor (e.g. configuration # 12) creating a three pointed star anchor, with considerable capacity increase but reduced weight.

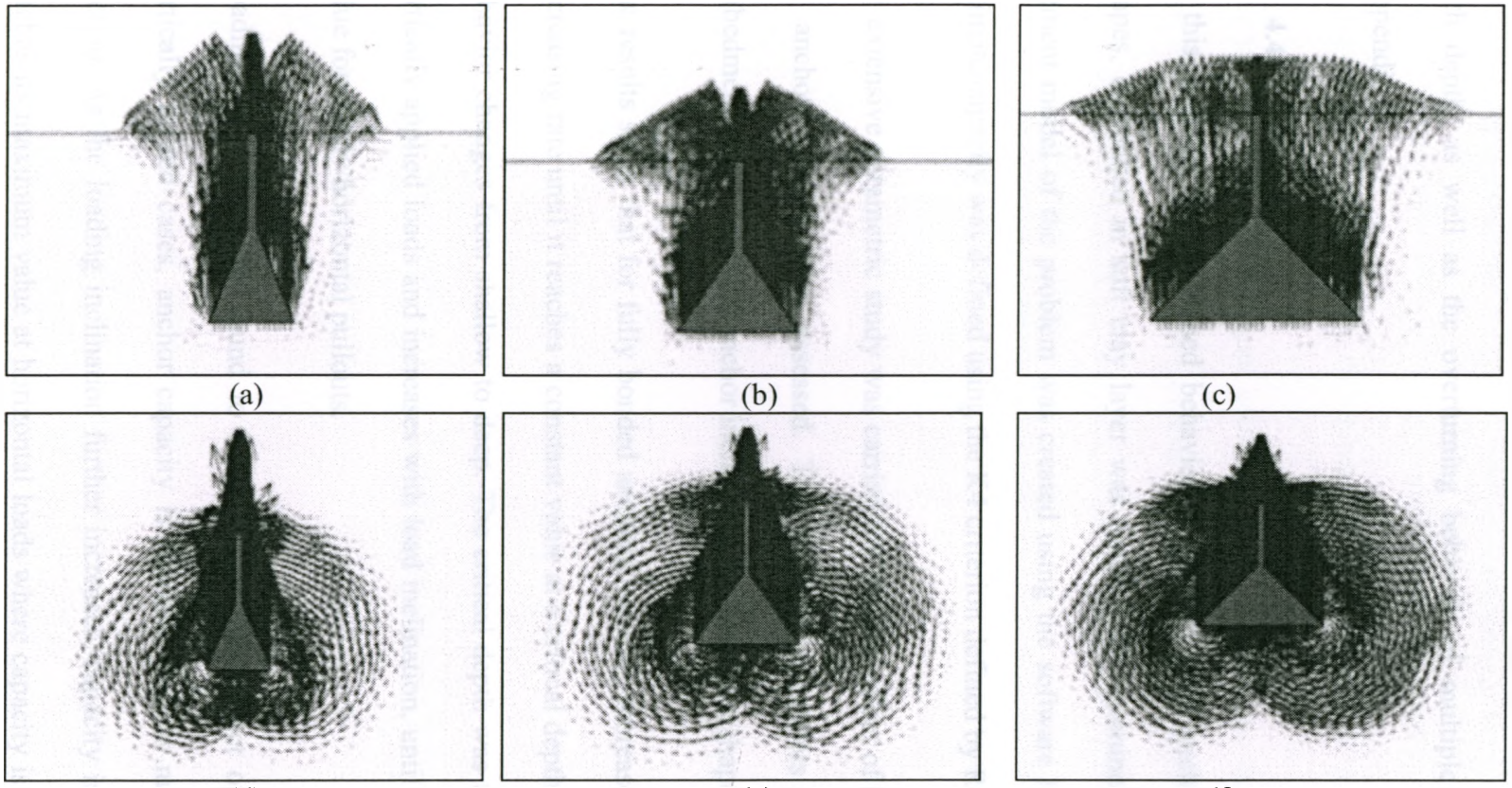

Figure 4. 18: Total displacement increments diagrams of fully bonded anchors for vertical pullout:

(a) Configuration # 10 - *H/B*=1;
(b) Configuration # 11 - *H/B*=1;
(c) Configuration # 12 - *H/B*=1;
(d) Configuration # 10 - *H/B*=5;
(e) Configuration # 11 - *H/B*=5;
(f) Configuration # 12 - *H/B*=5.

Additional analyses for the effects on the anchor pullout behavior of point of load application, overburden pressure, soil-anchor interface strength, point of load application, soil disturbance following anchor installation, and rate of clays hear strength increase with depth, as well as the overturning behavior of multiple anchors are shown in Appendix A.

4.4 Conclusions

In this chapter, the undrained behavior of vertical steel anchors with irregular base shapes, embedded in soft clay layer was numerically examined. A plane strain finite element model of the problem was created using the software Plaxis 2D V8.5. and the ultimate capacity was defined using the K4 criterion defined by Rowe and Davis (1982).

An extensive parametric study was carried out and the effect of the different parameters on anchor capacity was assessed. The studied parameters include the effect of embedment depth, load and anchor inclination and base size/shape.

The results show that for fully bonded anchors, capacity increases with embedment at a decreasing rate until it reaches a constant value at a critical depth, after which the anchor behavior changes from shallow to deep. The critical depth was found to be minimal for vertically applied loads and increases with load inclination, until it reaches its maximum value for purely horizontal pullouts.

Loading inclination was found to have a significant effect on anchor capacity. For vertically loaded cases, anchor capacity is minimal as it is mainly attributed to skin friction. As the loading inclination further increases, capacity increases as well until it reaches its maximum value at horizontal loads where capacity is mainly developed from

passive resistance. This increase was shown to be greater at higher embedment depths.

The effect of base size/shape on anchor pullout capacity was also studied. The results show that base shape has a limited effect on horizontally loaded anchors, while a much greater effect is shown for vertically loaded cases. The results also show that the anchor base width has a greater effect on anchor pullout capacity than base height.

Among the studied base shapes, anchors with triangular base shapes showed the highest vertical pullout capacity. This increase in capacity reached more than three times that of the regular plate anchors in some cases. Less increase was shown for horizontal loading, but this configuration seems to be the most effective in terms of steel area, compared to pullout capacity.

4.5 References

Cox, W. R. and Reese, L. C. (1976). "Pullout tests of grouted piles in stiff clay," *Offshore Technology Conference*, Dallas, Texas, pp 539-551

Das, B. M., and Puri, V. K. (1989). "Holding capacity of inclined square plate anchors in clay," *Soils and Foundations Journal*, Vol.29, No.3, pp 138-144

El-Khatib, S, and Randolph, M. P. (2004). "Finite element modeling of drag-in plate anchor installation," *Proceedings of the 9th Symposium on Numerical Models in Geomechanics*, Ottawa, Canada, pp 541-547

El-Khatib, S., Lonnie, B. and Randolph, M. P. (2002). "Installation and pull-out capacities of drag-in plate anchors," *Proceedings of the 12th International Offshore and Polar Engineering Conference*, Japan, Vol.12 , pp 648-654

Fahmy, A. M., de Bruyn, J. R. and Newson, T. A. (Submitted 2010). "Numerical investigation of the inclined pullout behavior of vertical anchors embedded in clay," *International Journal of Geomechanics*

Gaudin, C., Simkin, M., White, D., J. and O'Loughlin, C. D. (2010). "Experimental investigation into the influence of a keying flap on the keying behavior of plate anchors," *Proceedings of the20th International Offshore and Polar Engineering Conference*, pp 533-540

Liang, Y., Newson, T. A. and Hinchberger, S. (2008). "Numerical study of the mechanics of inflatable anchors in clay," *Proceedings of the18th International Offshore and Polar Engineering Conference*, pp 546-551

Merifield, R. S., Sloan, S. W., and Yu, H. S.(2001). "Stability of plate anchors in undrained clay," *Geotechnique,* Vol.51, No.2, pp 141-153

Meyerhof, G. G. and Adams, J. (1968). "The ultimate uplift capacity of foundations," *Canadian Geotechnical Journal*, Vol.5, No.4, pp 225-244

Newson, T. A., Smith, F. W. and Brunning, P. (2003a). "An experimental study of inflatable offshore anchors in soft clay," *BGA International Conference on Foundations, Innovations, Observations, Design and Practice*, pp 695-704

Newson, T. A., Smith, F. W., Brunning, P. and Gallaher, S. (2003b). "An experimental study of inflatible offshore anchors," *Proceedings of the 13th International Offshore and Polar Engineering Conference, Design and Practice*, pp 1340-1345

Plaxis Bv (2006). Plaxis 2D-Version 8 Manuals, Version 8

Poulos, H. G. (1943). "Marine Geotechnics," Unwin Hyman, London

Puech, A., Meunier. J., Pallard, M. (1978). "Behavior of anchors in different soil conditions," *Proceedings of the 10th annual OTC*, Houston.

Randolph, M. F., Martin, C. M. and Hu, Y. (2000). "Limiting resistance of a spherical penetrometer in cohesive material," Geotechnique, Vol.50, No.5, pp 573-582

Randolph, M. F. and Houlsby, G. T. (1984) "The limiting pressure on a circular pile loaded laterally in cohesive soil," *Geotechnique*, Vol.34, No.4, pp 613-623

Rowe, R. K., and Davis, E. H. (1982). "The behavior of plates in clay," *Geotechnique,* Vol.32, No.1, pp 9-23

Rowe, R. K., and Davis, E. H. (1977). "Application of the finite element method to the prediction of collapse loads," *The University of Sydney,* Australia, Research report No. R310

Sabatini, P. J., Pass, D. G. and Bachus, R. C. (1999). "Ground anchors and anchored systems report," *U.S department of Transportation-Federal Highway Administration*, Geotechnical Engineering circular No.4

Shnabel, H. and Shnabel, H. W. (2002) "Tiebacks in foundation engineering and construction," Lisse [Netherlands]; Exton, PA : A.A. Balkema

Song, S., Hu, Y., and Randolph, M. F. (2008). "Numerical simulation of vertical pullout of plate anchors in clay," *Journal of Geotechnical and Geoenvironmental Engineering*, Vol.134, No.6, pp 866-875

Weatherby, D. E. (1982). "Tiebacks report," *U.S department of Transportation-Federal Highway Administration*

Chapter 5 Numerical Investigation of The Undrained Capacity of Anchors with Rectangular Openings Embedded in Clay

5.1 Introduction

Plate anchors used in practice are mostly made from steel with densities typically ranging between 7.75 and 8 g/cm^3. The resulting anchors can be quite heavy and may require specialized lifting equipment for onshore or offshore deployment. The creation of reduced weight anchors allows larger anchors to be utilized and potentially greater forces to be sustained. One option is to create anchors with slots or regular shaped cutouts, reducing the effective weight of the anchor. Grillage of this form have been suggested for use previously as mudmats (Martin and Hazzel 2005). An open anchor structure will also have an advantage during deployment due to reduce forces when travelling through the wave zone.

Hence, the main objective of this study was to investigate alternative slotted forms of anchor that provide similar pullout capacity. A plate anchor system with intermediate rectangular slots or openings is shown in Figure 5. 1. A simple form of anchor is that with a single opening, as shown in Figure 5. 2.

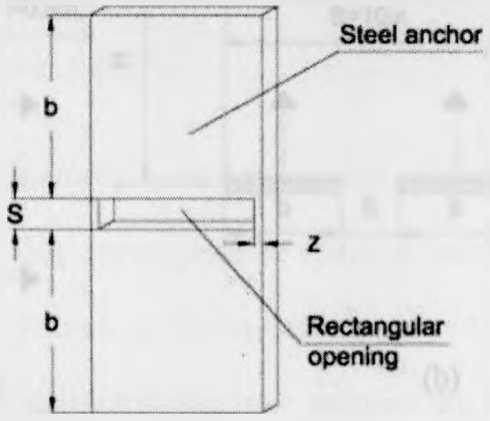

Figure 5. 1: Configuration of the proposed anchor with intermediate openings

The study uses finite element modeling to understand the pullout performance of this form of anchor embedded in clay soils. Thus the results can be applied to strip anchor with a single opening or two parallel strip anchors moving together. A plane strain model was developed to represent the proposed system. The two plate anchors of width *b* separated by a distance *S* have been subjected to coupled normal loads applied through their centre of mass. Anchors with a vertical and horizontal orientation have been studied, as shown in Figure 5. 2 (a) and (b) respectively, where *B* is the total distance between both anchor ends, *t* is the anchor thickness, *b* is the width of each anchor, *S* is the spacing between anchors. The parameter *H* is the distance between the ground surface and the lower anchor tip for vertically oriented anchors, while for horizontally oriented anchors, *H* is the distance between the ground surface and the anchor centerline. For the current study, it was decided to ignore the bending stresses in the steel connection between the two modeled plates, since the main objective is to understand the general behavior of the system and to identify the effect of the anchor openings. In practice this additional step would be taken and with multiple openings, may provide additional mass due to the stiffening elements.

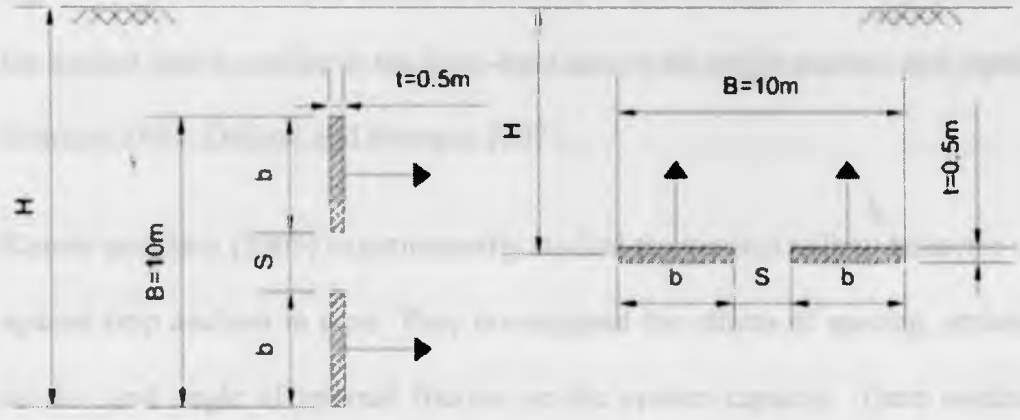

Figure 5. 2: Dimensions and configuration of the anchors studied. (a) vertical anchor and (b) horizontal anchor

5.2 Previous work

While many studies investigating the behavior of single plate anchors under different loading conditions are available (e.g. Merifield *et al.* 2001; Rowe and Davis 1982 and Das and Puri 1989), much less attention has been given to the interaction between closely spaced anchors. Furthermore, the few available studies are mainly concerned with anchors embedded in sands rather than clay.

Kouzer and Koumar (2009) and Kumar and Kouzer (2008) studied the pullout behavior of two interfering horizontal plate anchors using an upper bound plasticity limit analysis. Their results showed that no interference occurred between anchors spaced at S greater than $2H\tan\varphi$, where φ is the soil angle of internal friction. They confirmed these results by monitoring the nodal velocities around the anchors at various S/b values. They reported zero nodal velocities at the centerline between the anchors at S greater than $2H\tan\varphi$. For more closely spaced anchors, the non-zero velocity nodes were contained in a wedge above the anchor plate, having rupture surfaces at both anchor ends making an angle φ with the vertical, and intersected by linear rupture surfaces. This soil wedge is believed to act as a rigid unit with an equal velocity to that of the anchor and is similar to the false-head seen with single anchors and pipelines (Randolph and Houlsby 1984; Deljoui and Newson 2007).

Kumar and Bhoi (2009) experimentally studied the vertical pullout behavior of horizontal closely spaced strip anchors in sand. They investigated the effects of spacing, embedment depth as well as the sand angle of internal friction on the system capacity. Their results were presented in terms of an efficiency factor, defined as the ratio between the failure load of an intervening anchor and the failure load of a strip plate anchor having the same width. The results showed a

significant efficiency reduction with the decrease of spacing between anchors. They also showed that the *S/b* value, after which each of the anchors behaves separately, increases with the increase of embedment ratio *H/b*. For example, at embedment ratios of 3, 5 and 7, the corresponding *S/b* values were 3, 5 and 7 respectively. While theory showed an efficiency decrease with increase in angle of internal friction φ (e.g Kouzer and Koumar 2009), this behavior has not been clearly shown in Kumar and Bhoi's experimental results.

Meyerhof and Adams (1968) developed a general theory of the uplift resistance of footings based on the testing results reported by Adams and Hayes (1967). In their study, Meyerhof and Adams defined the efficiency of a group of footings as the ratio of the uplift capacity of the group to the sum of capacities of single footings. The results of testing of footings in soft clay showed an efficiency increase with the increase in spacing as well as with the decrease of embedment depth. A decrease in efficiency was also observed with the increase of number of footings in the group. The theoretically calculated efficiencies were found to be greater than those observed during the tests. The authors suggested that such behavior might be due to many factors including the overlapped shearing zones preventing the full mobilization of the clay shear strength.

Merifield and Smith (2010) numerically investigated the behavior of multiple vertically spaced horizontal plate anchors embedded in clay, and suggested a procedure to calculate their undrained capacity. The results showed that for anchors embedded in weightless soil, the effect of soil interaction on the shallowest anchor was insignificant. The results also showed that the capacity of the anchor below the shallowest one is not affected by the overall embedment ratio for *S/b* values less than 2. They suggested that the capacity of the anchors below the shallowest one, at *S/b* less than 3, could be conservatively calculated using the following equation, which they originally provided to calculate the breakout factor N_c of a single anchor, while assuming

H/b=S/b.

$$N_c = 2.08 + 2.47Ln\left(\frac{H}{b}\right) \qquad 5.1$$

Merifield and Smith (2010) also studied multiple anchors embedded in soil with nonzero weight. The results showed that for closely spaced anchors both anchors will behave as a single unit, while above a critical spacing ratio $(S/b)_{cr}$, each anchor will behave independently. They suggested that the critical spacing ratio could be taken as $\left(\frac{2+3\pi}{\pi}\right)$.

The behavior of closely spaced footings on clay can also be compared to that of the closely spaced anchors, especially at shallow depths. In particular the interaction between footings causing arching and squeezing failures have been addressed, along with the efficiency of the footings working together. Griffiths *et al.* (2006) used the finite element technique to study the behavior of two closely spaced strip footings resting on weightless soil having a randomly varying shear strength. Their deterministic analysis showed that the breakout capacities did not change significantly over the studied range of spacings, suggesting that interference effects were insignificant for closely spaced footings resting on clay. This supports the earlier findings of Mandel 1963, although Martin and Hazell (2005) found positive interaction effects for both uniform soils and soils with strength that increased linearly with depth at low *S/b* ratios.

Ghosh and Sharma (2010) numerically investigated the settlement pattern of two closely spaced strip footings resting on layered soils. The results showed that interference between footings causes a greater settlement in the bed than that caused by a single footing. They also found that increases in *S/b* and the ratio of elastic moduli for the layers decreased the settlement ratio

(Ghosh and Sharma 2010). The results also showed that variation of the applied load on the footings significantly affected the settlement value; however the settlement ratio independent of *S/b*.

Kumar and Bhattacharya (2010) studied the capacity of multiple interfering strip footings on cohesionless soil using a lower bound finite limit analysis. They considered footings with rough and smooth bases. They found an efficiency factor greater than 1, with significantly higher efficiencies for rough-based footings. Their results showed efficiency factors ranging between 1 and 10 for smooth bases, and between 1 and 128 for rough bases. Their results also showed that for both rough and smooth bases, no interference occurred at *S/b* greater than 3 (Kumar and Bhattacharya 2010).

Gourvenec and Steinepreis (2007) investigated the undrained limit state capacity of two rigidly connected footings under general loading conditions involving moment, vertical and horizontal loads. The modeled footings were assumed to rest on soil of uniform undrained shear strength, following the Drucker-Prager failure mechanism. Their results showed that for purely vertical loads, footings with *S/b* less than 1 have a higher bearing capacity than a single footing, with a maximum increase of 5%. At greater *S/b* values, no interaction is believed to occur. The results showed also that the horizontal capacity of the two-footing system is equal to that of a single footing with similar base area. Unlike the vertical and horizontal capacities, a significant increase in the moment capacity was observed due to the interaction between the two footings. For *S/b* less than 3, the moment capacity was found to be proportional to S^2 with a single scoop flow mechanism comprising both footings. For *S/b* greater than 5, the moment capacity was found to be linearly proportional to *S*, with a general shear failure mechanism for each of the footings. Gourvenec and Steinepreis (2007) provided failure envelopes for the studied system at various

S/b values and various load combinations. The results showed that the interaction between footings was only a function of the applied vertical load, with independent mechanisms at greater applied vertical loads.

5.3 Numerical analysis

The finite element software package Plaxis 2D (Plaxis. 2006) was used to numerically simulate the behavior of normally loaded vertical and horizontal-oriented steel anchors with intermediate rectangular openings of width *S* as shown in Figure 5. 2, embedded in a clay soil. Anchors with *S/b* = 0.1, 0.2, 0.4, 1 and 2 were considered at a range of embedment ratios *H/B*.

5.3.1 Discretization of the problem

The problem was discretized using 15-noded plane strain triangular elements. The mesh was extended a distance of 7.5*B* in the X-direction on each side of the anchor centerline and a distance of 2*B* in the Y-direction below the base of the anchors. This mesh configuration was found to be necessary to ensure that the domain boundaries did not affect the results. The mesh was automatically generated based on a subroutine using a robust triangular principle searching for optimized triangles (Plaxis 2006) resulting in an unstructured mesh. The vertical model boundaries were fixed in the X-direction, while the lower boundary was fixed in both X and Y directions as shown in Figure 5. 3(a), where a typical mesh consisting of 2548 triangular elements is presented for the case of *S/b = 2*. Additional mesh refinement around the anchor, as shown in Figure 5. 3 (b), was required to give sufficiently accurate results.

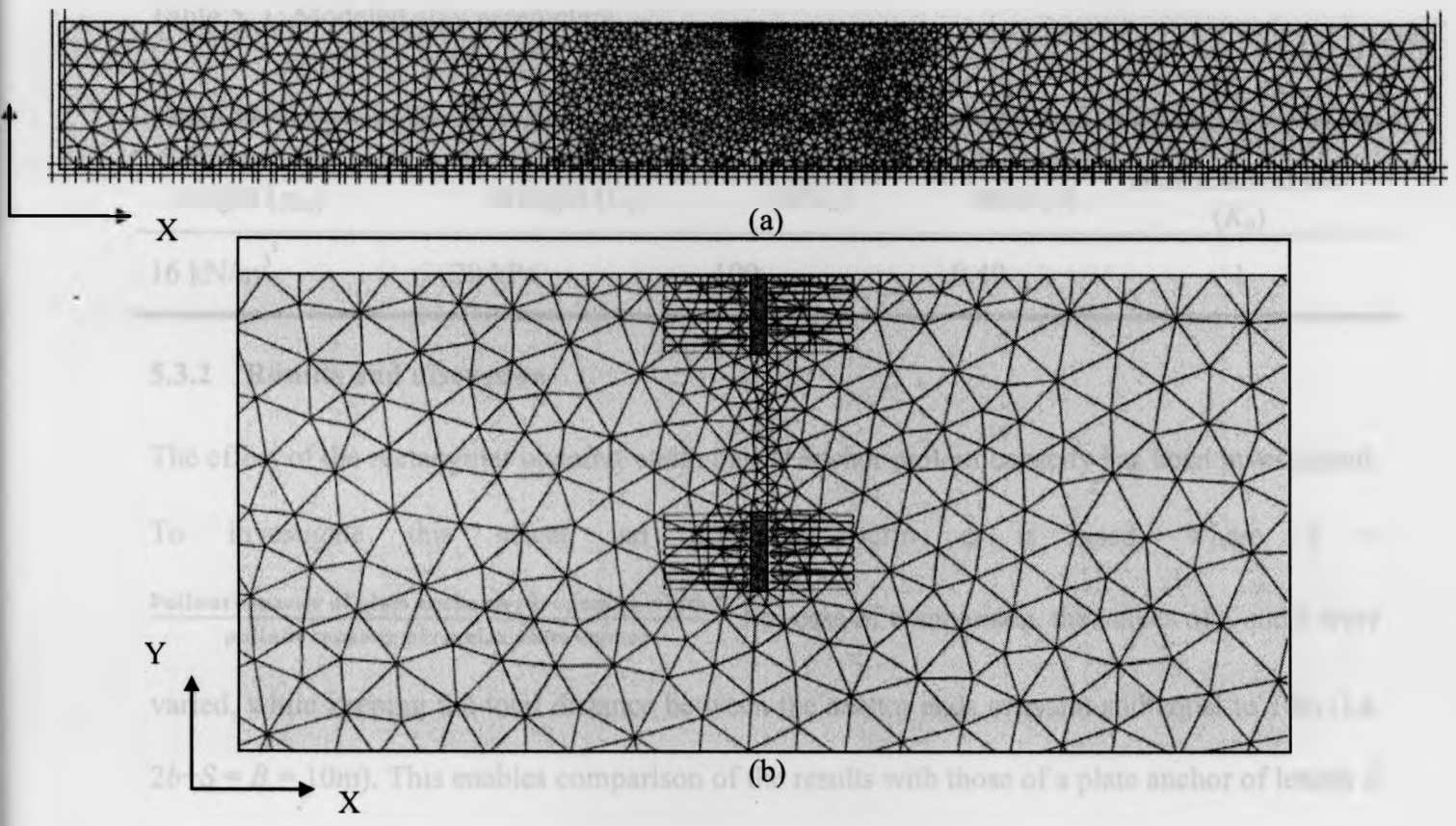

Figure 5. 3: Example of discretized mesh of the model (width = 15*B* = 150 m) and (b) expanded view of mesh close to the anchor at *S*/*b*=2. The insets on the left of the figures show the X and Y-directions

The clay used in the analysis was simulated using Mohr-Coulomb failure criterion modeling elastic-perfectly plastic behavior (Wood, 1990), assuming undrained conditions (angle of internal friction $\varphi = 0^{o}$). The ground water table was assumed to lie at the surface of the modeled soil. The clay parameters are presented in Table 5. 1.

Table 5. 1: Modeled clay parameters

Saturated unit weight (γ_{sat})	Undrained shear strength (C_u)	Modulus ratio (E/C_u)	Poisson's ratio (ν)	Earth pressure coefficient at rest (K_o)
16 kN/m^3	20 kPa	100	0.49	1

5.3.2 Results and discussion

The effect of the rectangular opening width on the anchor pullout capacity has been investigated. To investigate this effect, an efficiency term ξ is used, where $\xi = \frac{\text{Pullout capacity of plate anchor with opening width } S}{\text{pullout capacity of regular plate anchor}}$. For ease of comparison, the values of S and b were varied, while keeping the total distance between the anchor ends constant and equal to 10m (i.e. $2b+S = B = 10$m). This enables comparison of the results with those of a plate anchor of length B without intermediate openings.

We first present results assuming a full bond at the anchor-soil interface. Figure 5. 4 (a) and (b) shows the variation of ξ with S/b for vertical and horizontal fully bonded anchors respectively at H/B = 1, 2, 3 and 5. The results show that for vertical anchors with openings of $S/b < 0.4$, the decrease in efficiency is less than 10%. At higher S/b values, the increase is greater. Similar results were found for the horizontal anchors, as shown in Figure 5. 4 (b).

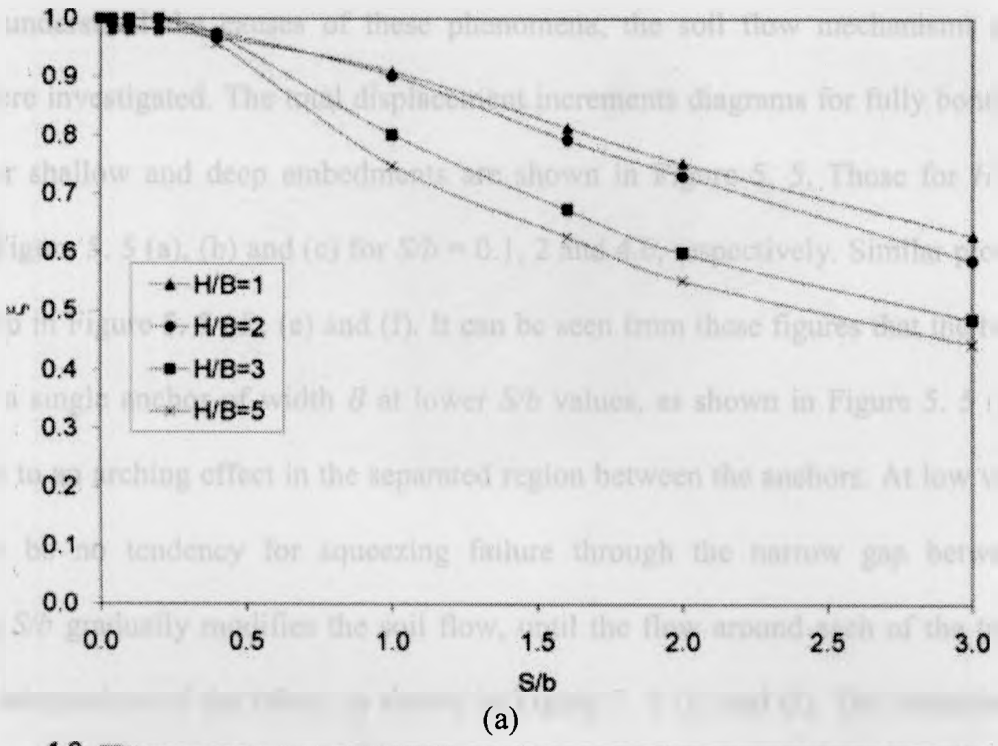

(a)

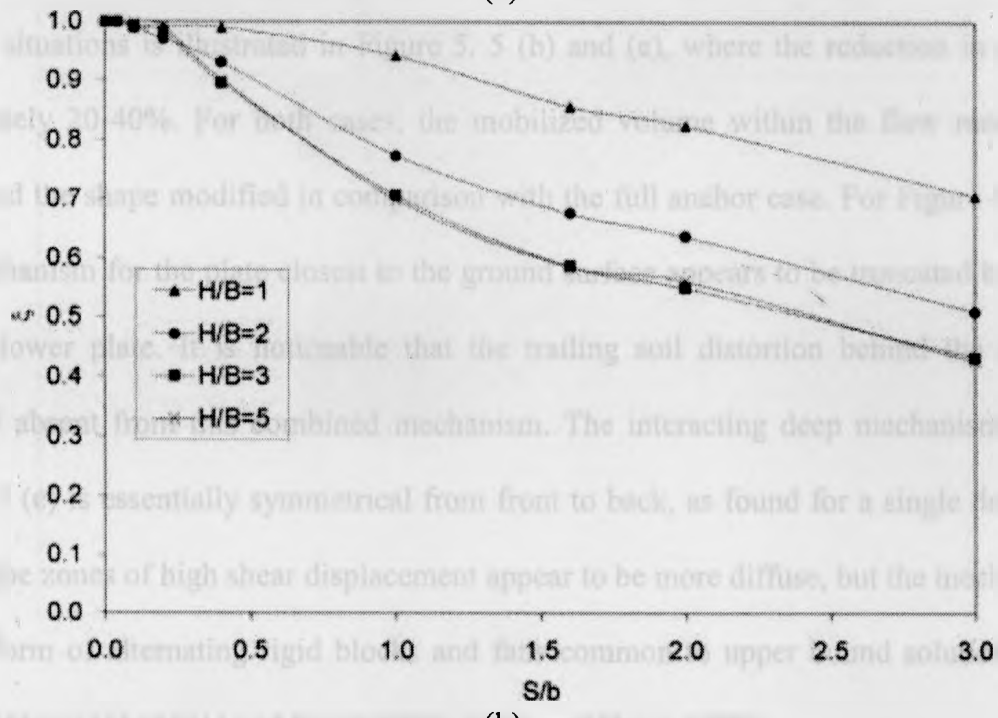

(b)

Figure 5. 4: Variation of efficiency ξ with *S/b* for (a) vertical anchors and (b) horizontal anchors (Fully bonded)

To better understand the causes of these phenomena, the soil flow mechanisms around the anchors were investigated. The total displacement increments diagrams for fully bonded vertical anchors for shallow and deep embedments are shown in Figure 5. 5. Those for H/B = 1 are shown in Figure 5. 5 (a), (b) and (c) for S/b = 0.1, 2 and 4.6, respectively. Similar plots at H/B = 5 are shown in Figure 5. 5 (d), (e) and (f). It can be seen from these figures that the two anchors behave as a single anchor of width B at lower S/b values, as shown in Figure 5. 5 (a) and (d). This is due to an arching effect in the separated region between the anchors. At low values there appears to be no tendency for squeezing failure through the narrow gap between plates. Increasing S/b gradually modifies the soil flow, until the flow around each of the two anchors becomes independent of the other, as shown in Figure 5. 5 (c) and (f). The transition between these two situations is illustrated in Figure 5. 5 (b) and (e), where the reduction in capacity is approximately 20-40%. For both cases, the mobilized volume within the flow mechanism is reduced and the shape modified in comparison with the full anchor case. For Figure 5. 5 (b) the upper mechanism for the plate closest to the ground surface appears to be truncated by soil flow from the lower plate. It is noticeable that the trailing soil distortion behind the anchors is essentially absent from this combined mechanism. The interacting deep mechanism shown in Figure 5. 5 (e) is essentially symmetrical from front to back, as found for a single deep anchor. However the zones of high shear displacement appear to be more diffuse, but the mechanism still have the form of alternating rigid blocks and fans common to upper bound solutions of other anchor problems (Merifield and Smith 2010; Rowe and Davis 1977).

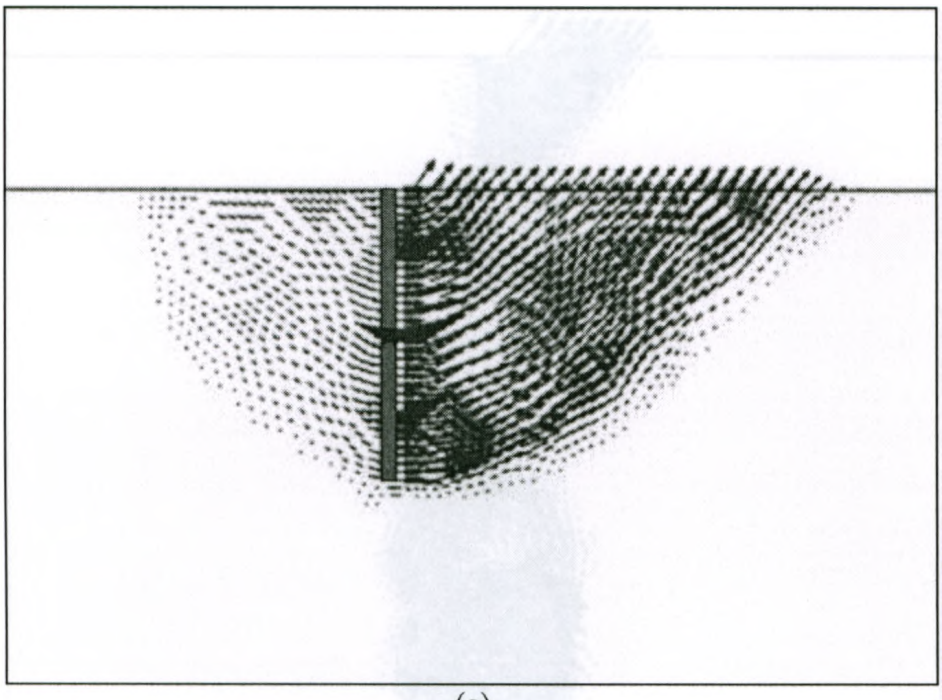

(a)

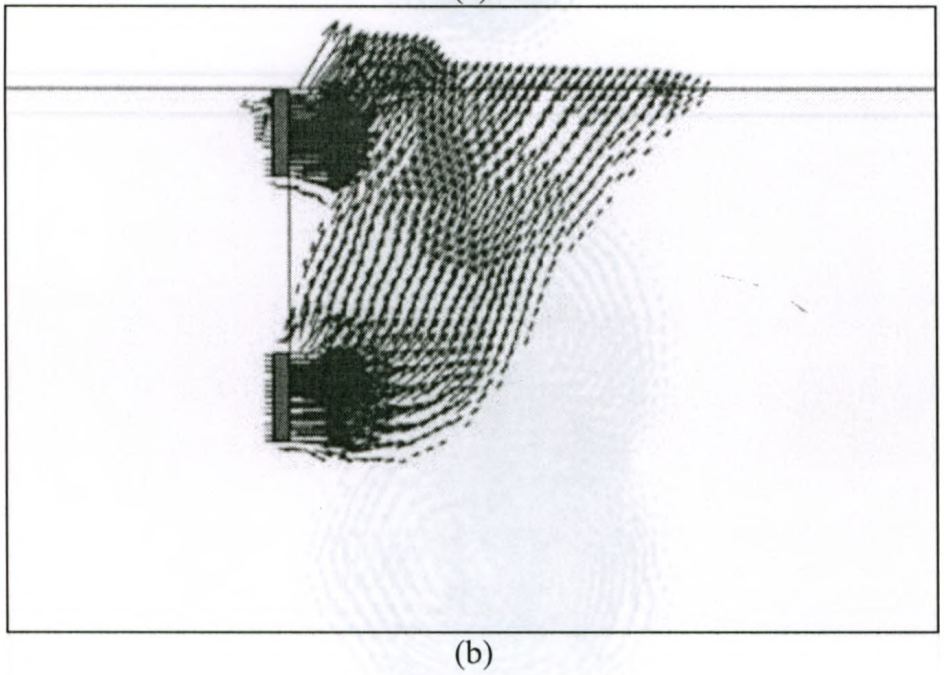

(b)

(c)

(d)

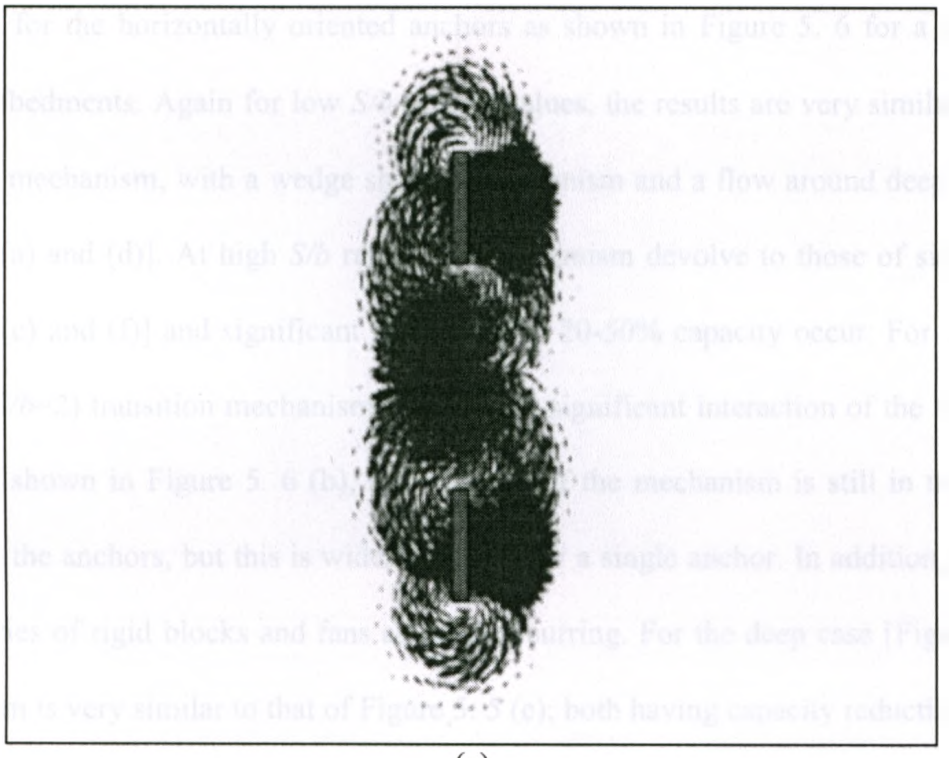

(e)

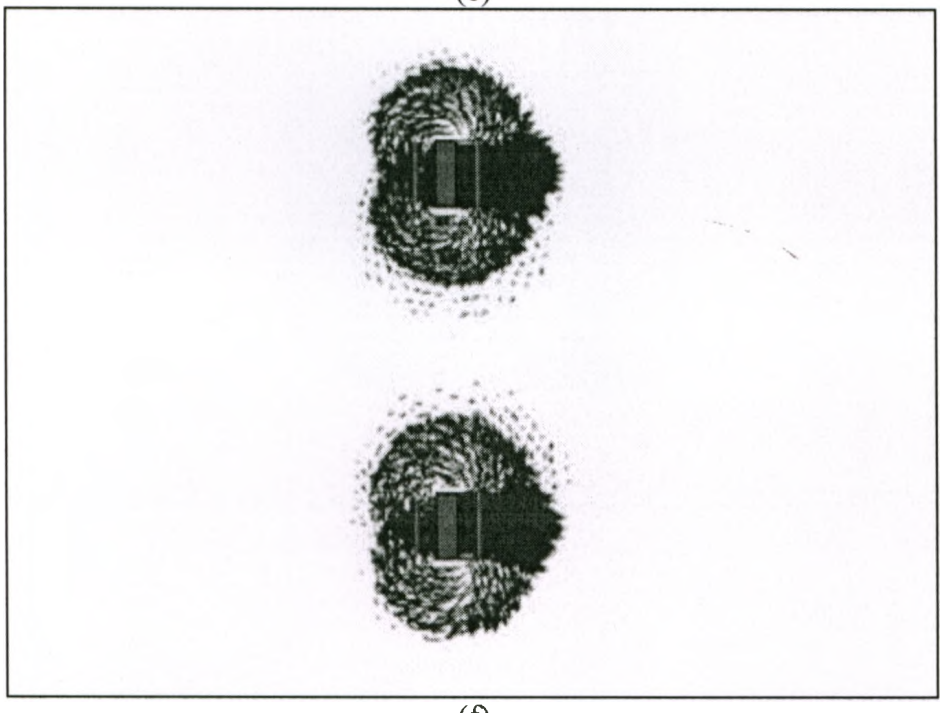

(f)

Figure 5. 5: Total displacement increments diagram for fully bonded vertical anchors at (a) H/B = 1, S/b = 0.1; (b) H/B = 1, S/b = 2; (c) H/B = 1, S/b = 4; (d) H/B=5, S/b = 0.1; (e) H/B = 5, S/b = 2 and (f) H/B = 5, S/b = 4.2

Similar plots for the horizontally oriented anchors as shown in Figure 5. 6 for a range of *S/b* ratios and embedments. Again for low *S/b* (≤ 0.5) values, the results are very similar to a single anchor uplift mechanism, with a wedge shallow mechanism and a flow around deep mechanism [Figure 5. 6 (a) and (d)]. At high *S/b* ratios, the mechanism devolve to those of single anchors [Figure 5. 6 (c) and (f)] and significant reductions of 20-50% capacity occur. For intermediate *S/b* ratios ($\approx S/b=2$) transition mechanisms occur with significant interaction of the flow. For the shallow case shown in Figure 5. 6 (b), the majority of the mechanism is still in the form of a wedge above the anchors, but this is wider than that for a single anchor. In addition, close to the anchors a series of rigid blocks and fans are also occurring. For the deep case [Figure 5. 6 (e)], the mechanism is very similar to that of Figure 5. 5 (e); both having capacity reduction of 50%.

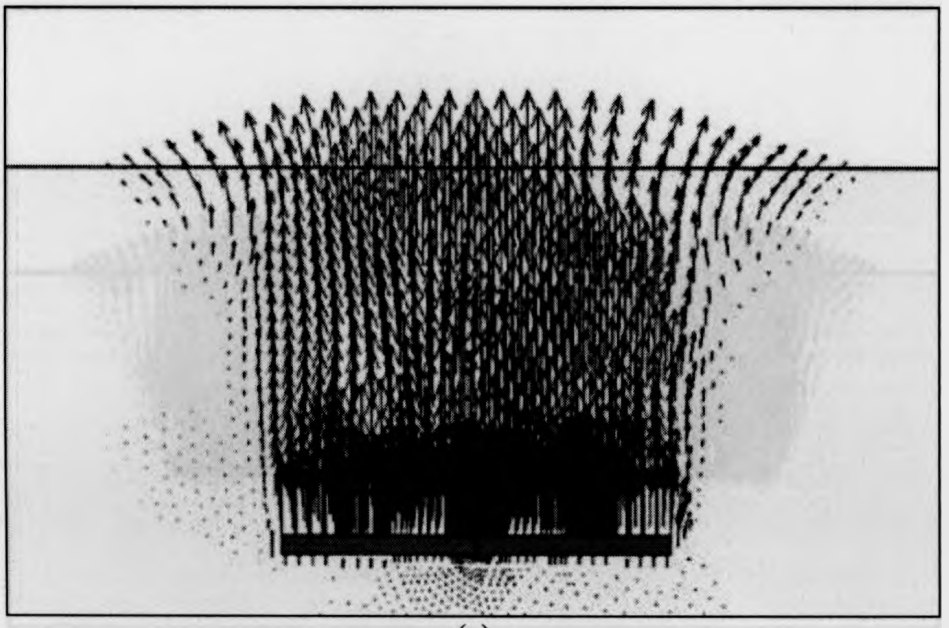

(a)

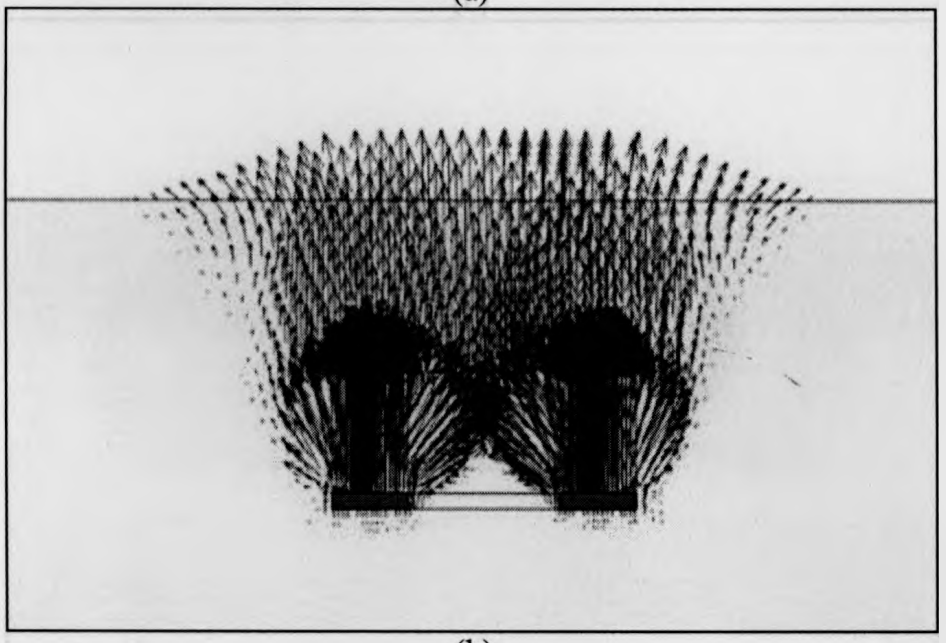

(b)

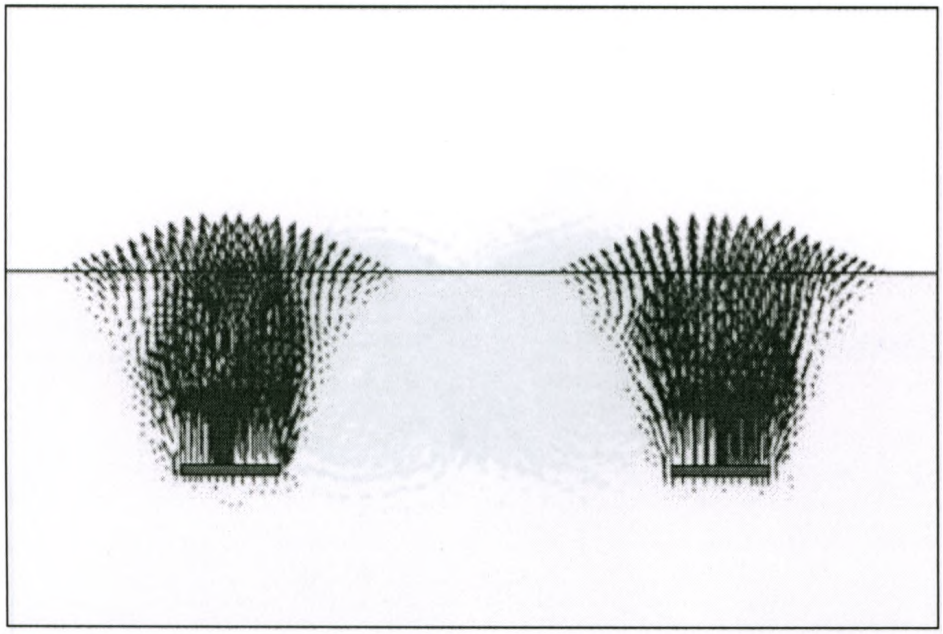

(c)

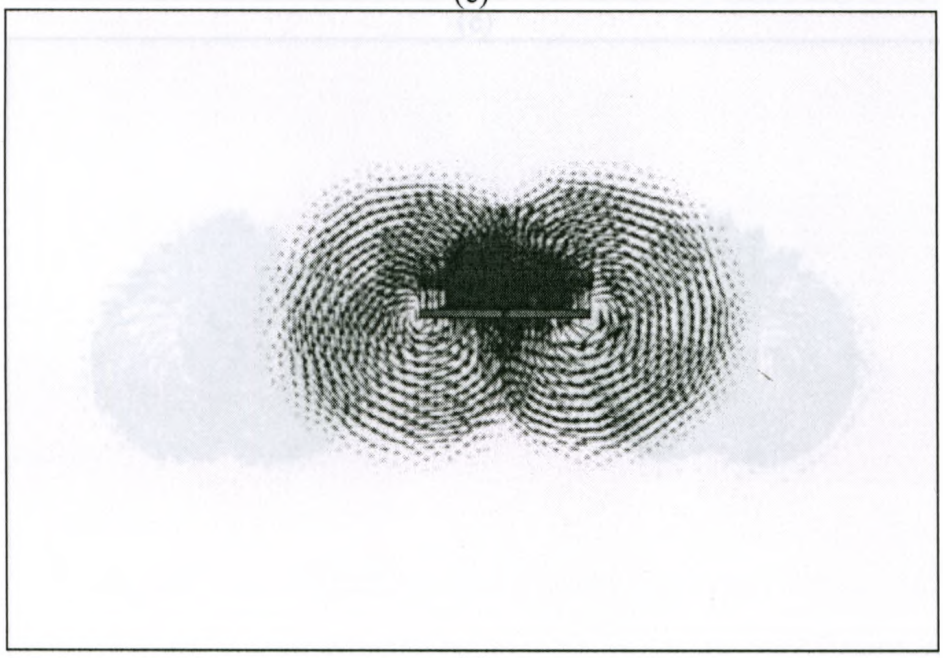

(d)

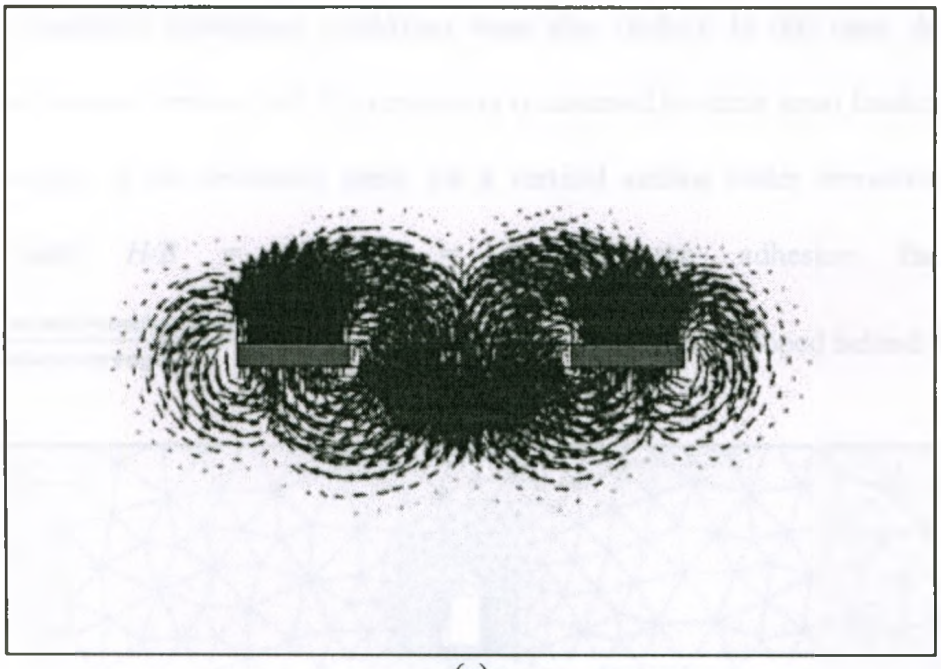

(e)

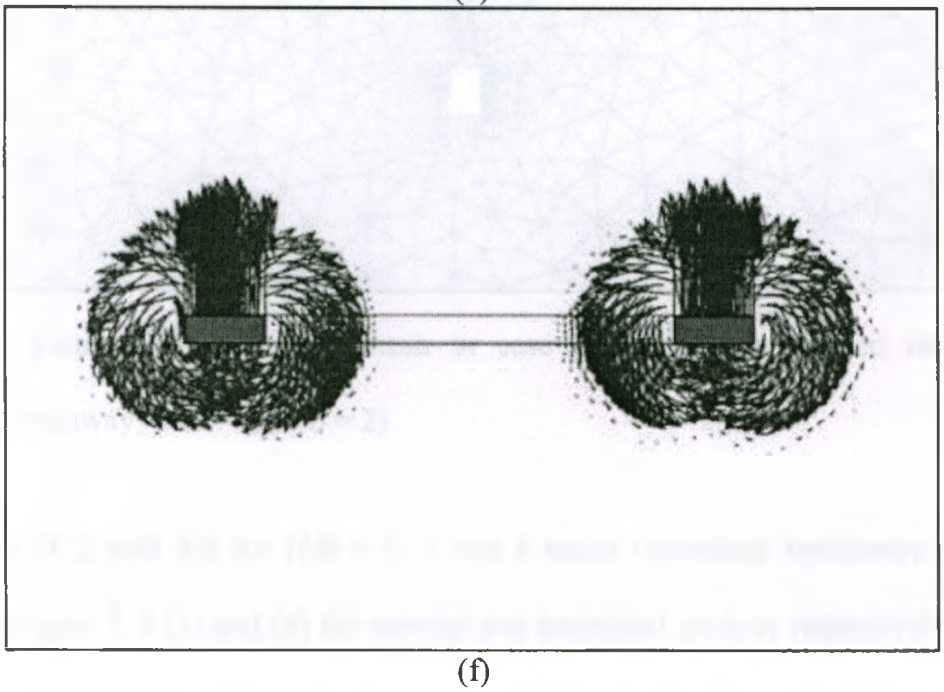

(f)

Figure 5. 6: Total displacement increments diagram for fully bonded horizontal anchors at (a) H/B = 1-S/b = 0.1, (b) H/B = 1-S/b = 2, (c) H/B = 1-S/b = 4, (d) H/B = 5-S/b = 0.1, (e) H/B = 5-S/b = 2 and (f) H/B = 5-S/b = 5

Anchors for immediate breakaway conditions were also studied. In this case, the soil-anchor interface cannot sustain tension and full separation is assumed to occur upon loading. Figure 5. 7 shows an example of the deformed mesh for a vertical anchor under immediate breakaway conditions, with H/B = 3, S/b = 2 and the adhesion factor $\alpha = \frac{shear\ strength\ at\ soil-anchor\ interface}{clay\ shear\ strength} = 0.1$. A clear separation has developed behind the anchor.

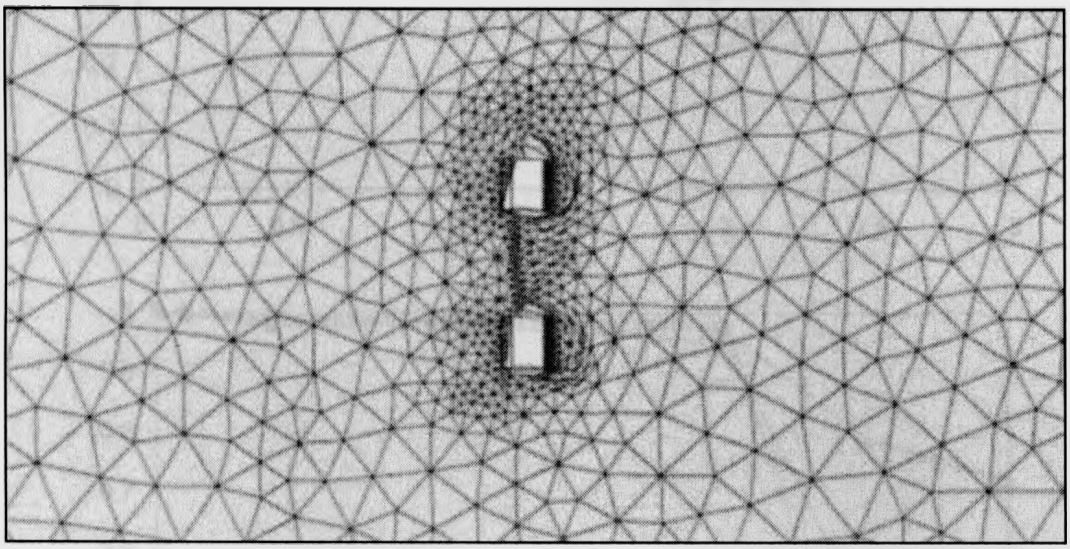

Figure 5. 7: Example of deformed mesh in case of horizontally loaded vertical anchor (immediate breakaway - $H/B = 3$, $S/b = 2$)

The variation of ξ with S/b for H/B = 1, 3 and 5 under immediate breakaway conditions is presented in Figure 5. 8 (a) and (b) for vertical and horizontal anchors respectively. The results for vertical anchors show a negligible decrease in efficiency for $S/b < 0.4$, followed by a higher decrease at a nearly constant rate. For horizontal anchors, the efficiency decrease was found to be negligible for $S/b<2$, followed by a sudden drop in efficiency. The results show a less embedment susceptibility on the rate of efficiency decrease than for fully-bonded anchors, especially for vertical anchors.

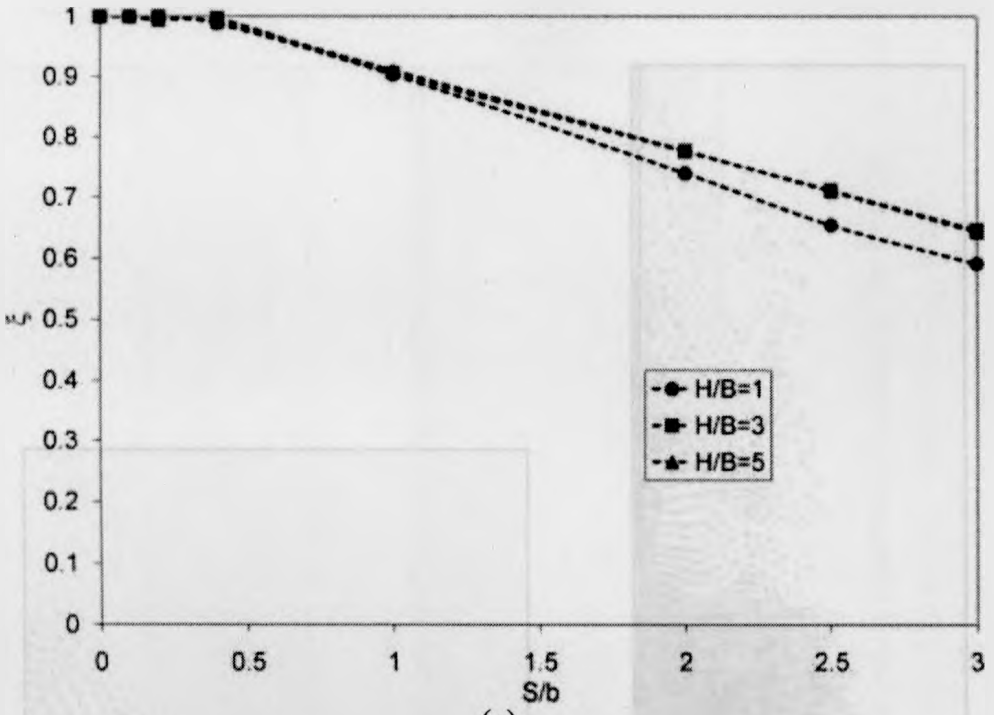

(a)

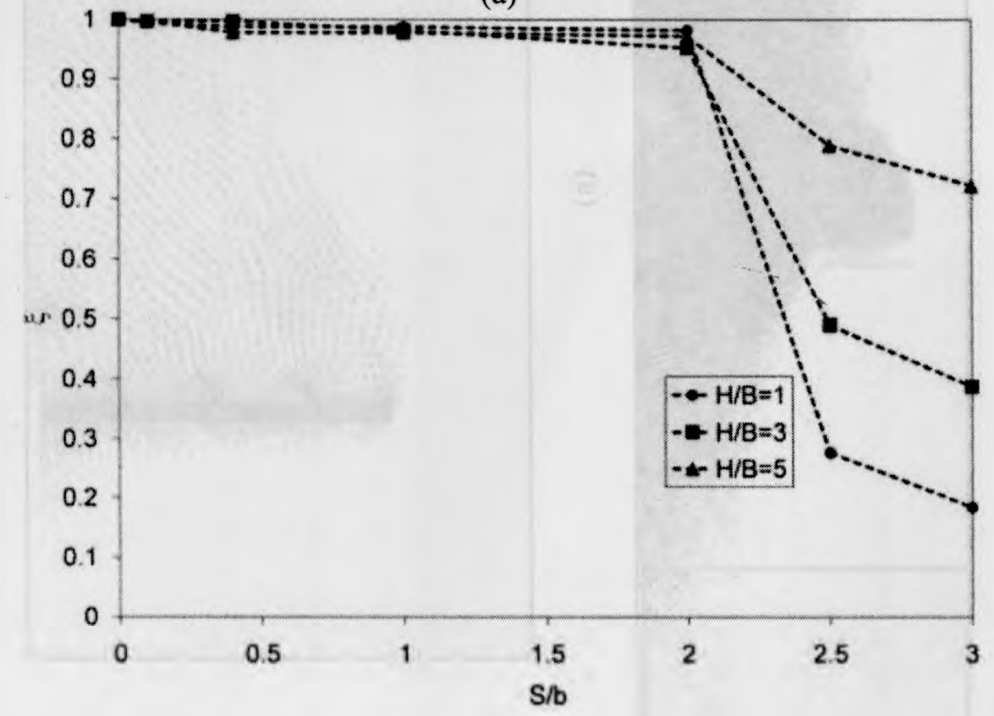

(b)

Figure 5. 8: Variation of efficiency ξ with *S/b* for (a) vertical anchors and (b) horizontal anchors– (Immediate breakaway)

Figure 5. 9 shows the total displacement increments diagrams for vertical anchors at immediate breakaway conditions for (a) H/B = 1-S/b = 0.1, (b) H/B = 3-S/b = 0.1, (c) H/B = 1-S/b = 2 and (d) H/B = 3- S/b = 2. Similar plots for horizontal anchors are shown in Figure 5. 10. In general, these mechanisms are mobilizing greater volumes of soil

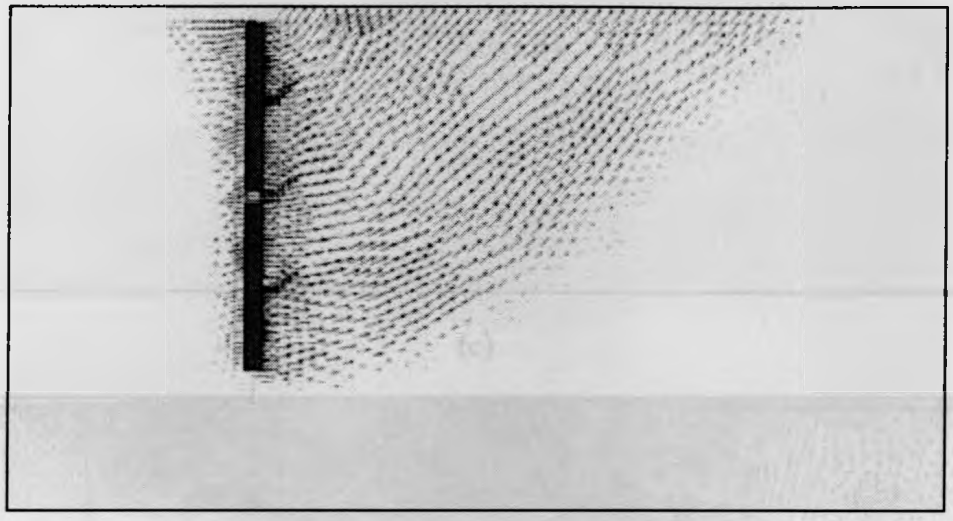

(a)

(b)

154

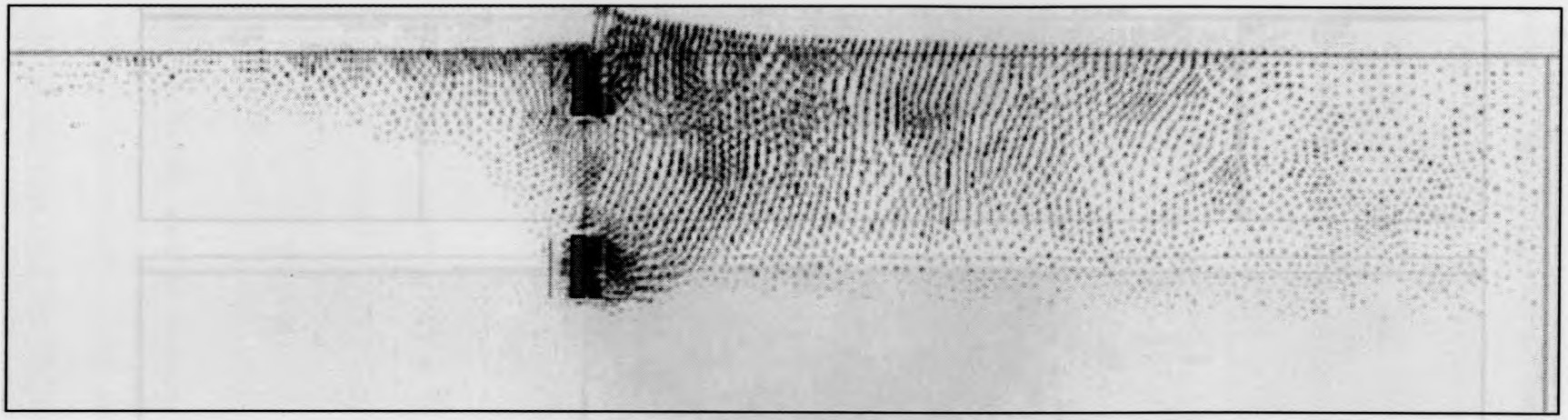

(c)

(d)

Figure 5. 9: Total displacement increments diagrams for vertical anchors at immediate breakaway conditions for (a) $H/B = 1$, $S/b = 0.1$; (b) $H/B = 3$, $S/b = 0.1$; (c) $H/B = 1$, $S/b = 2$ and (d) $H/B = 3$, $S/b = 2$

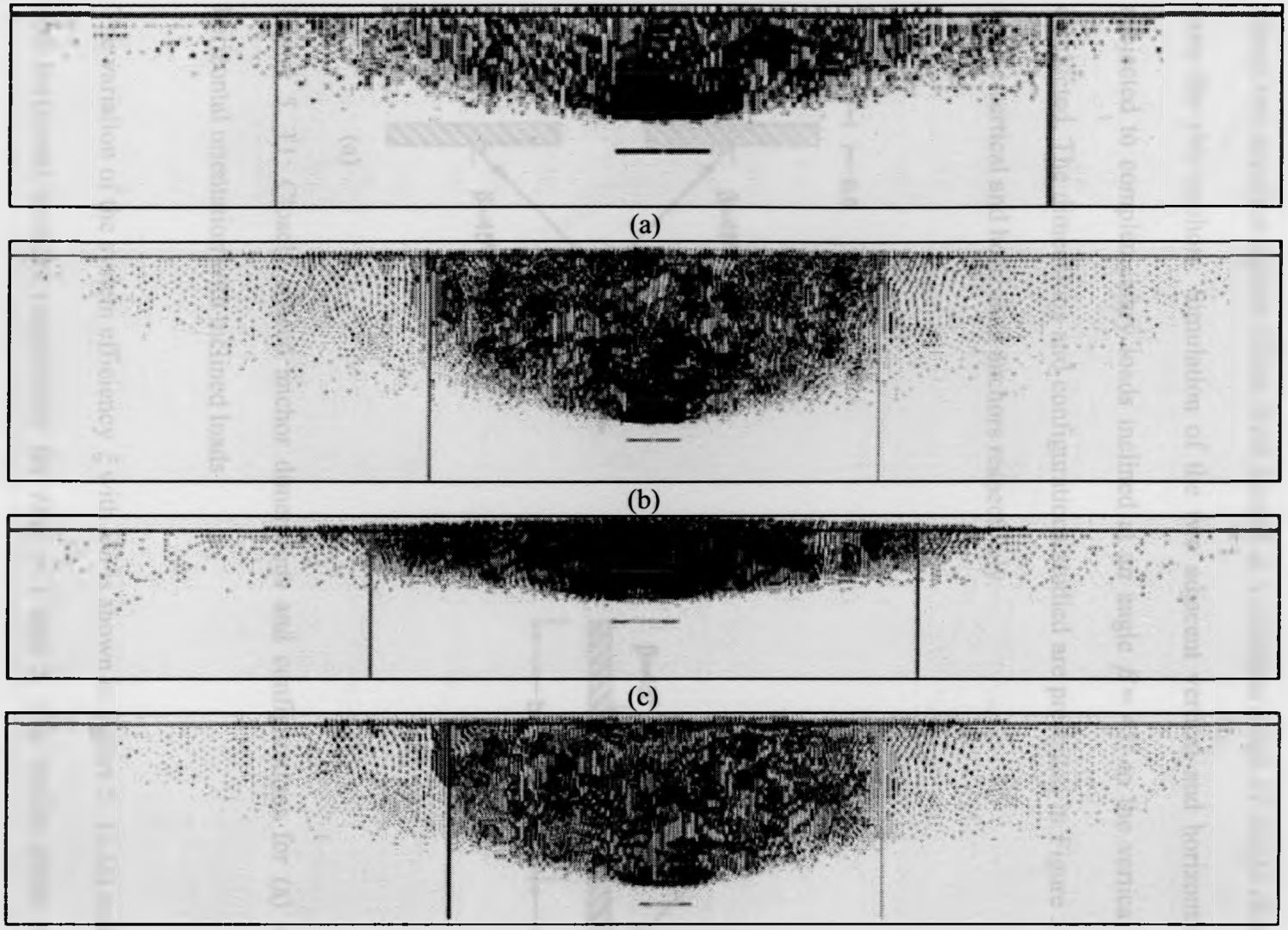

Figure 5. 10: Total displacement increments diagrams for horizontal anchors at immediate breakaway conditions for (a) *H/B*=1, *S/b* = 0.1; (b) H/B = 3, *S/b* = 0.1; (c) *H/B* = 1, S/b = 2 and (d) *H/B* = 3, *S/b* = 2

In addition to the proposed slotted anchor system presented, two closely spaced individual plate anchors, subjected to inclined loadings were also studied. This was assumed to represent the case where two separate anchor plates were joined at a common point of single chain at a distance from the two anchors. Simulation of the two adjacent vertical and horizontal plate anchors subjected to complementary loads inclined at an angle $\beta = 45^{\circ}$ to the vertical were therefore conducted. The dimensions and configurations studied are presented in Figure 5. 11 (a) and (b) for the vertical and horizontal anchors respectively.

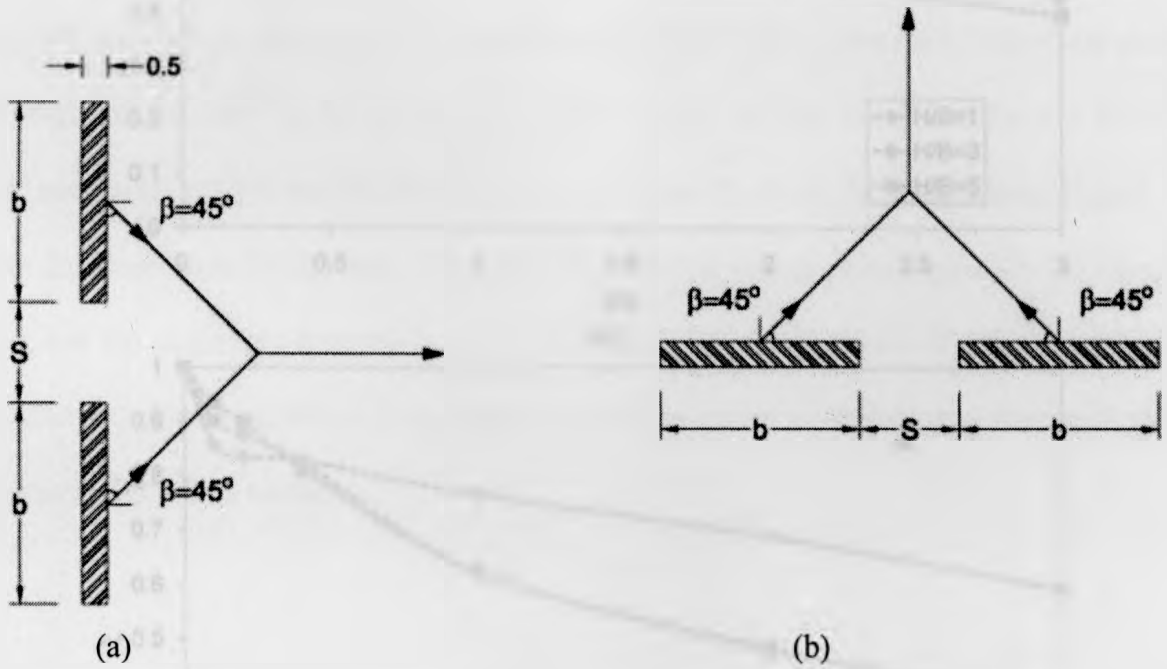

Figure 5. 11: Closely spaced anchor dimensions and configurations for (a) vertical and (b) horizontal orientation with inclined loads

The variation of the system efficiency ξ with *S/b* is shown in Figure 5. 12 (a) and (b) for vertical and horizontal anchors respectively for *H/B* = 1 and 5. The results show that, for deeply embedded anchors, the system efficiency decreases at a nearly-constant rate with an increase in *S/b*. On the other hand, the shallow anchor efficiency drops significantly when *S/b* changes from

0 to 0.1. This initial decrease was approximately 25% and 14% for vertical and horizontal anchors, respectively. As *S/b* is increased further, the efficiency continues to decrease, but at a lower rate than that found for the case of deeply embedded anchors.

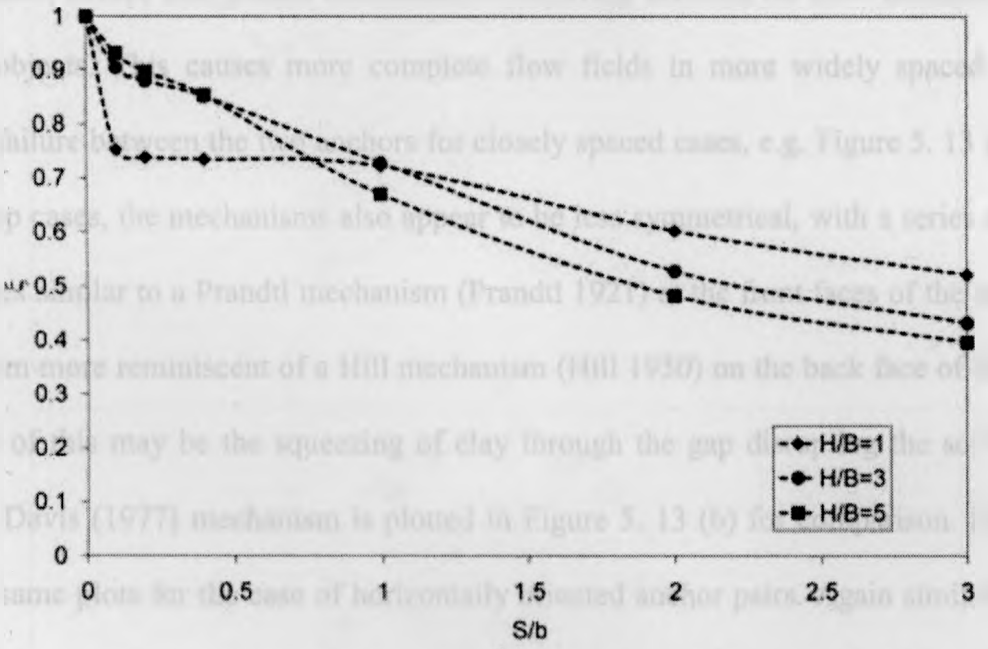

(a)

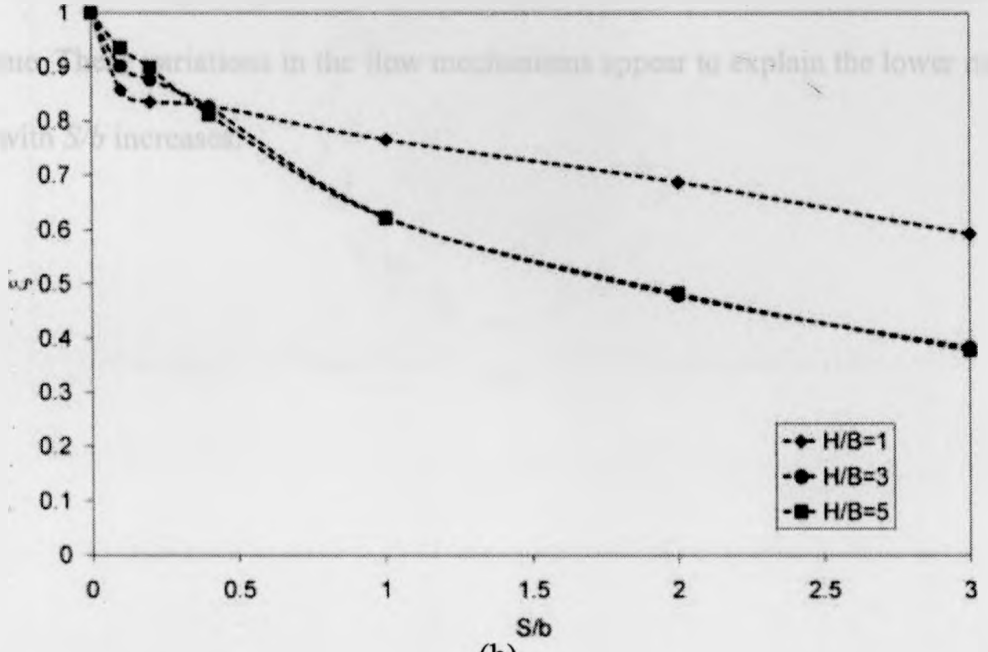

(b)

Figure 5. 12: Variation of efficiency ξ with *S/b* for (a) vertically and (b) horizontally oriented closely spaced anchors

Figure 5. 13 shows the total displacement increments diagrams for fully bonded horizontal anchors for (a) H/B = 1-S/b = 0.1, (b) H/B = 5-S/b = 0.1, (c) H/B = 1-S/b = 2 and (d) H/B = 5- S/b = 2. The mechanisms for the vertically oriented anchors are generally similar to those of the previous cases, except that greater interaction is occurring between the flow mechanisms of the separated objects. This causes more complete flow fields in more widely spaced cases and squeezing failure between the two anchors for closely spaced cases, e.g. Figure 5. 13 (a) and (b). For the deep cases, the mechanisms also appear to be less symmetrical, with a series of fans and rigid wedges similar to a Prandtl mechanism (Prandtl 1921) at the front faces of the anchors and a mechanism more reminiscent of a Hill mechanism (Hill 1950) on the back face of the anchors. The origin of this may be the squeezing of clay through the gap disrupting the soil flow. The Rowe and Davis (1977) mechanism is plotted in Figure 5. 13 (b) for comparison. Figure 5. 14 shows the same plots for the case of horizontally oriented anchor pairs. Again similar trends are found, but the squeezing component is more evident and modifications of the mechanisms are more extreme. These variations in the flow mechanisms appear to explain the lower reductions in efficiency with S/b increases.

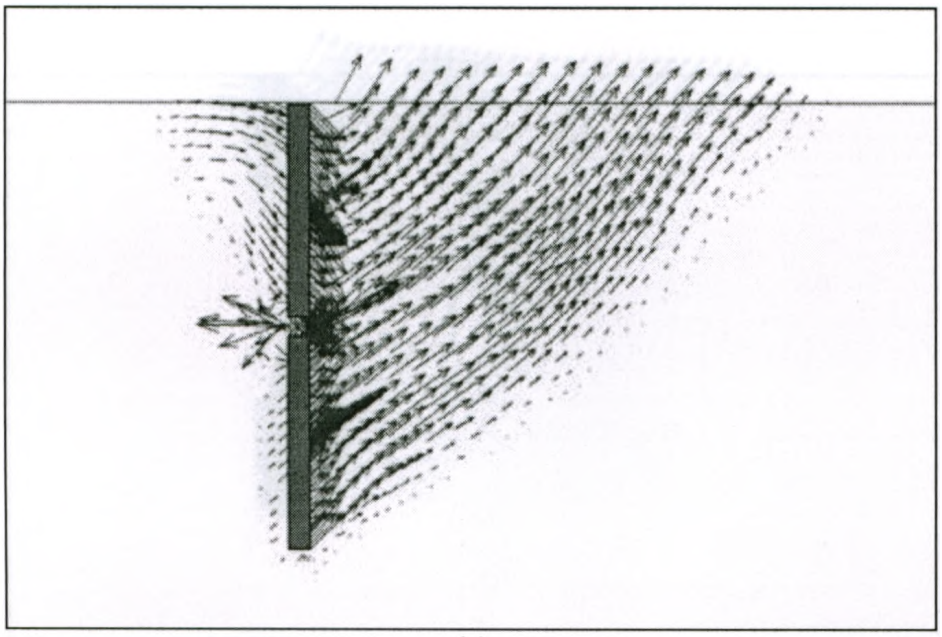

(a)

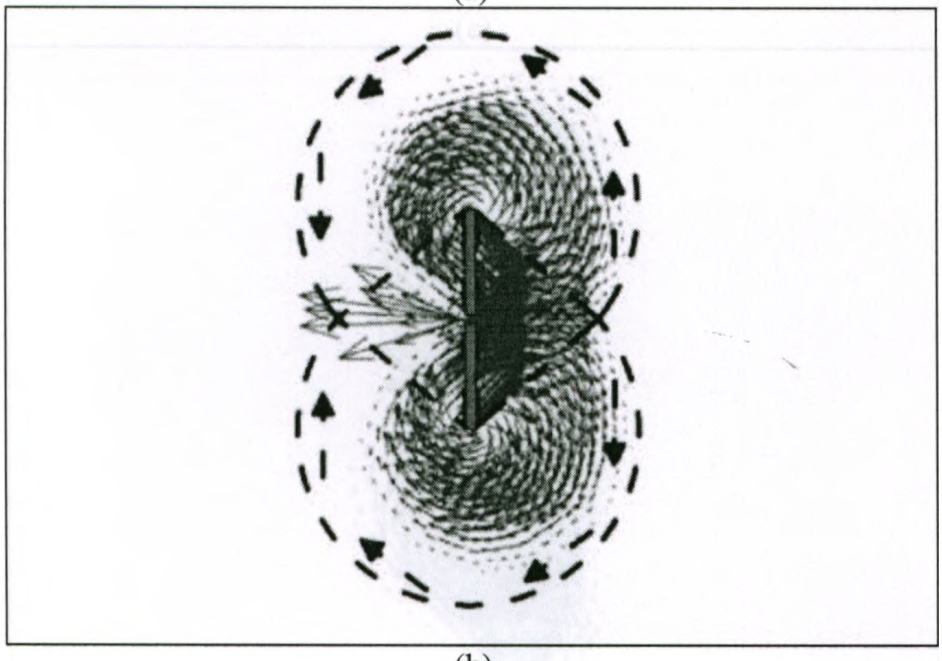

(b)

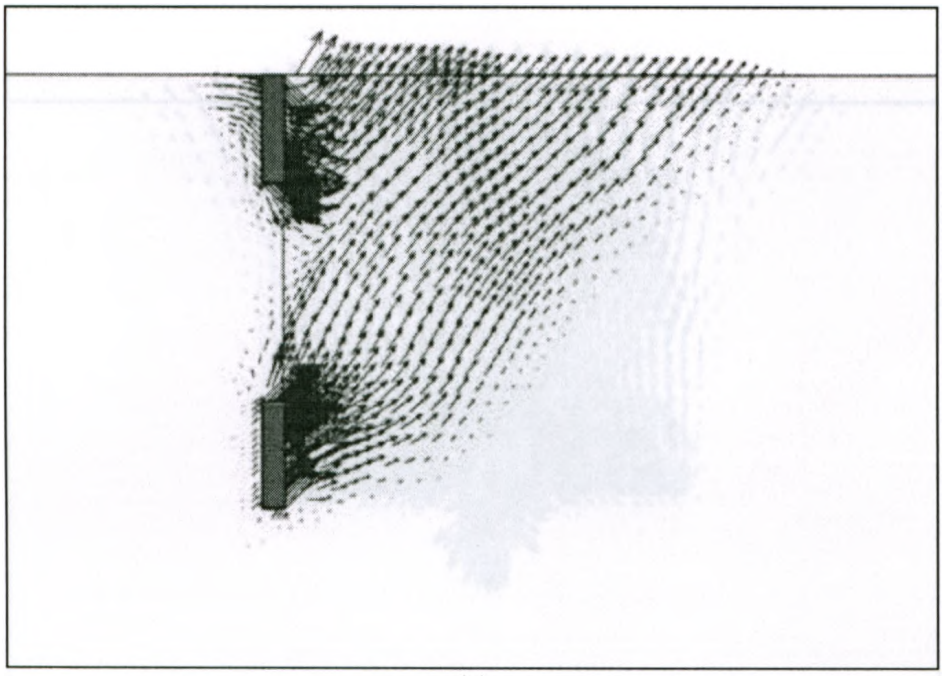

(c)

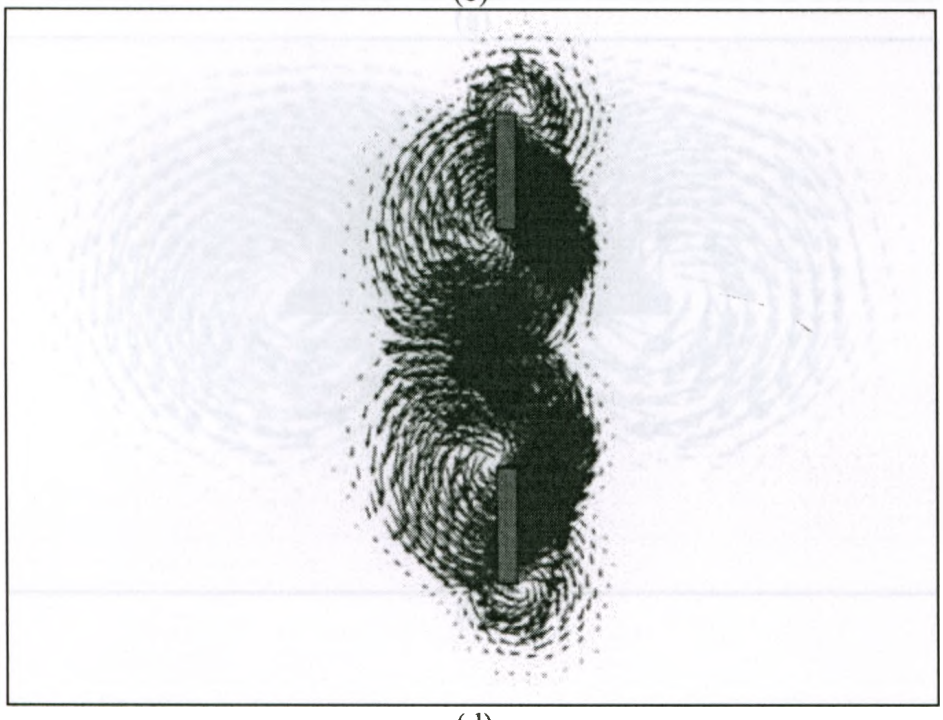

(d)

Figure 5. 13: Total displacement increments diagrams for fully bonded vertical anchors subjected to 45° inclined loads for (a) $H/B = 1$, $S/b = 0.1$; (b) $H/B = 5$, $S/b = 0.1$. The mechanism proposed by Rowe and Davis (1977) is plotted as dashed lines for comparison. (c) $H/B = 1$, $S/b = 2$ and (d) $H/B = 5$, $S/b = 2$

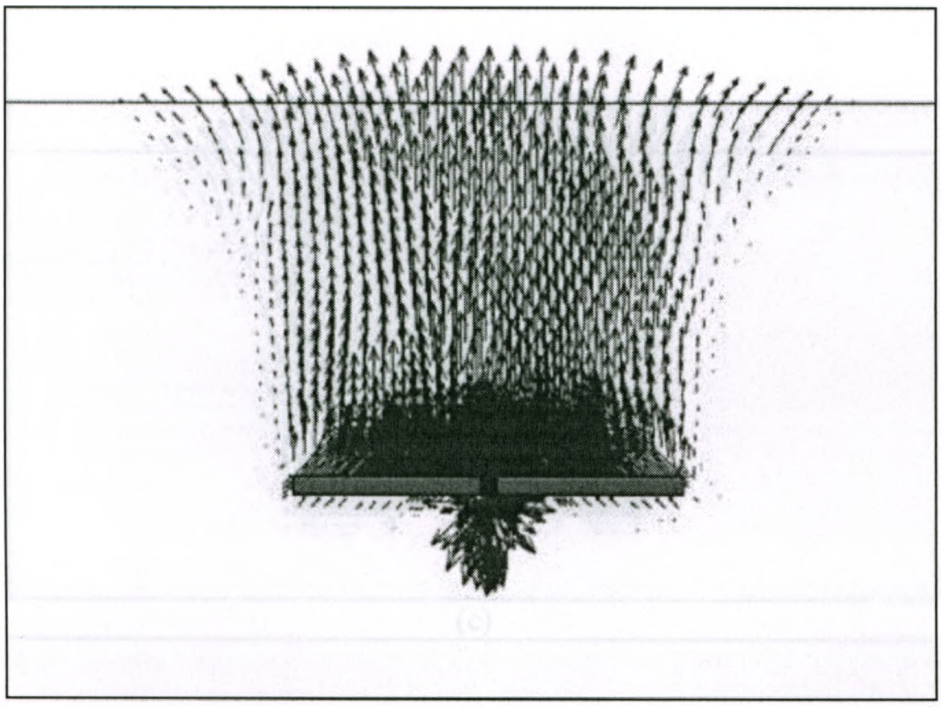

(a)

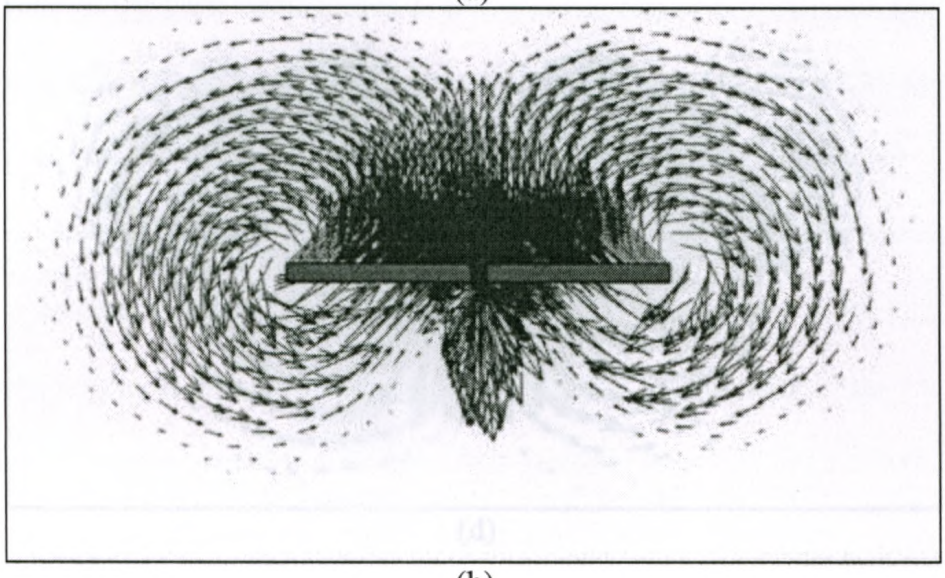

(b)

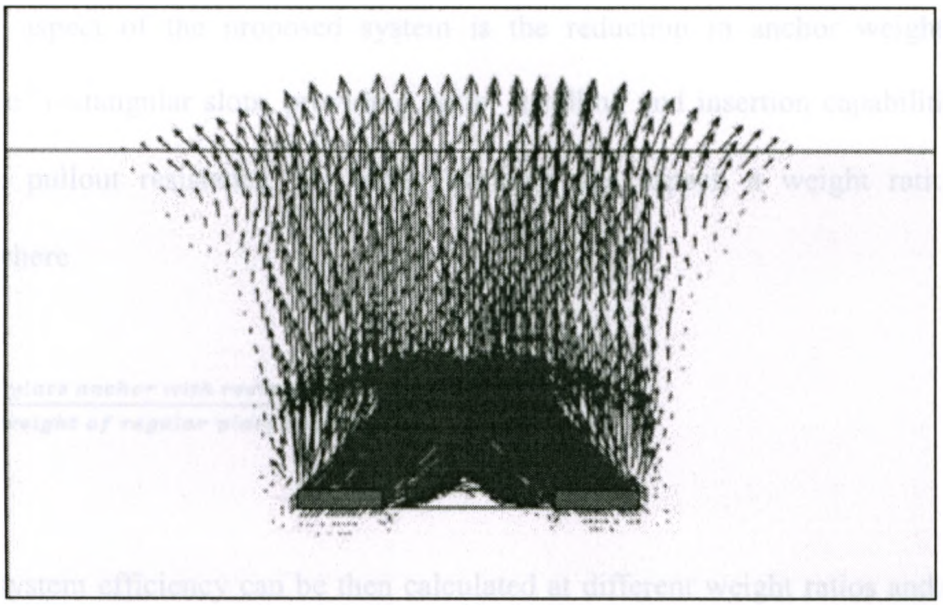

(c)

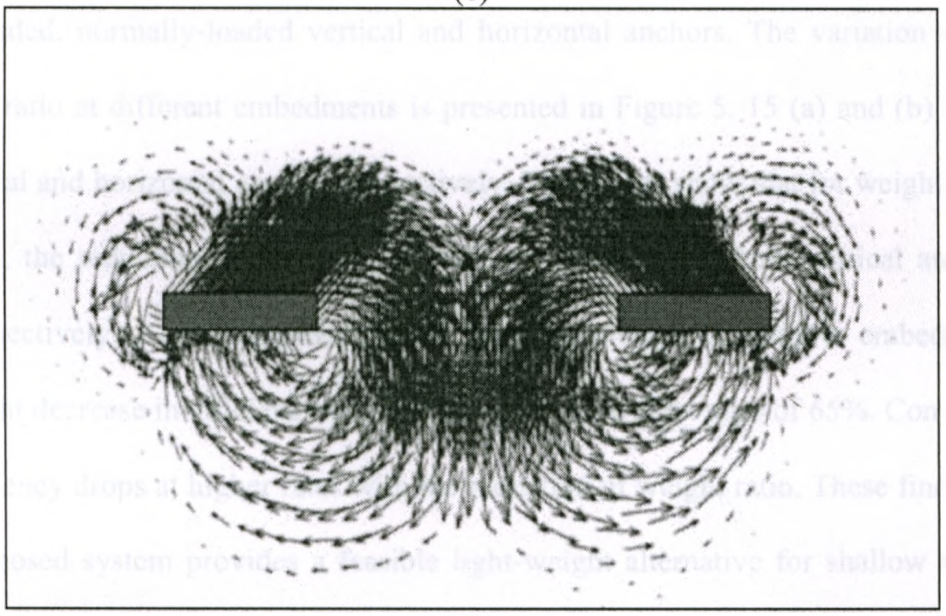

(d)

Figure 5. 14: Total displacement increments diagrams for fully bonded horizontal anchors subjected to 45° inclined loads for (a) $H/B = 1$, $S/b = 0.1$; (b) $H/B = 5$, $S/b = 0.1$; (c) $H/B = 1$, $S/b = 2$ and (d) $H/B = 5$, $S/b = 2$

Further shear strain contour shadings and principle stress direction diagrams for the various cases in Figure 5. 5, Figure 5. 6, Figure 5. 13 and Figure 5. 14 are shown in Appendix B.

A beneficial aspect of the proposed system is the reduction in anchor weight due to the introduction of rectangular slots, providing easier handling and insertion capabilities while not affecting the pullout resistance. To better evaluate this aspect, a weight ratio term ω is introduced, where

$$\omega = \frac{weight\ of\ plate\ anchor\ with\ rectangular\ openings}{weight\ of\ regular\ plate\ anchor} \qquad 5.2$$

The anchor system efficiency can be then calculated at different weight ratios and embedments for fully-bonded, normally-loaded vertical and horizontal anchors. The variation of efficiency with weight ratio at different embedments is presented in Figure 5. 15 (a) and (b) for normally loaded vertical and horizontal anchors respectively. The results show that for weight ratios above 85 and 90%, the reduction in anchor efficiency is negligible for both vertical and horizontal anchors respectively. A further reduction of the weight ratio of shallow embedded anchors causes a slight decrease in efficiency of less than 10% at a weight ratio of 65%. Conversely, deep anchor efficiency drops at higher rates with the reduction of weight ratio. These findings suggest that the proposed system provides a feasible light-weight alternative for shallow embedments, but may not provide much benefit for large embedments.

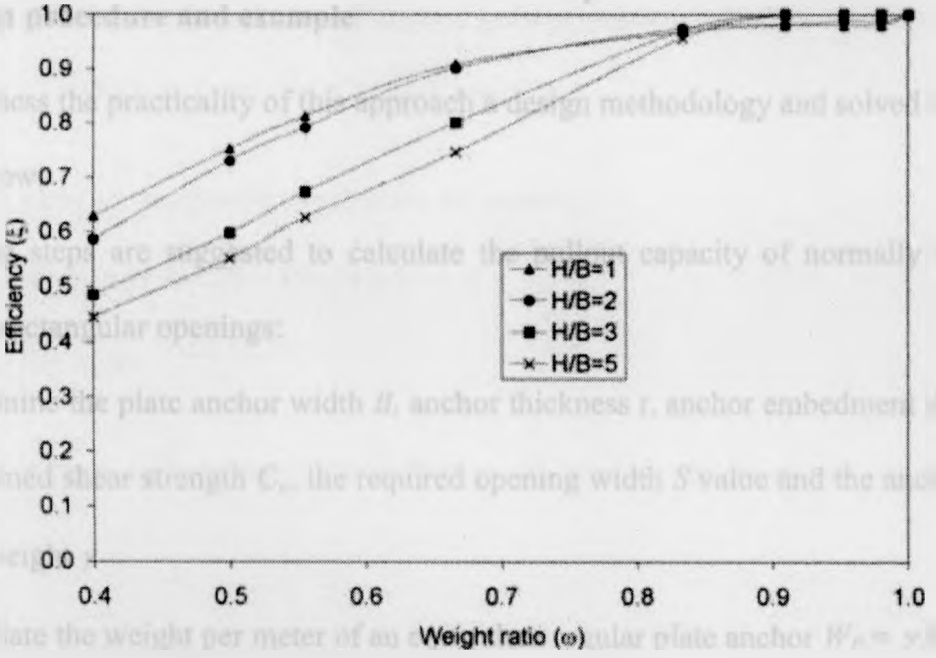

(a)

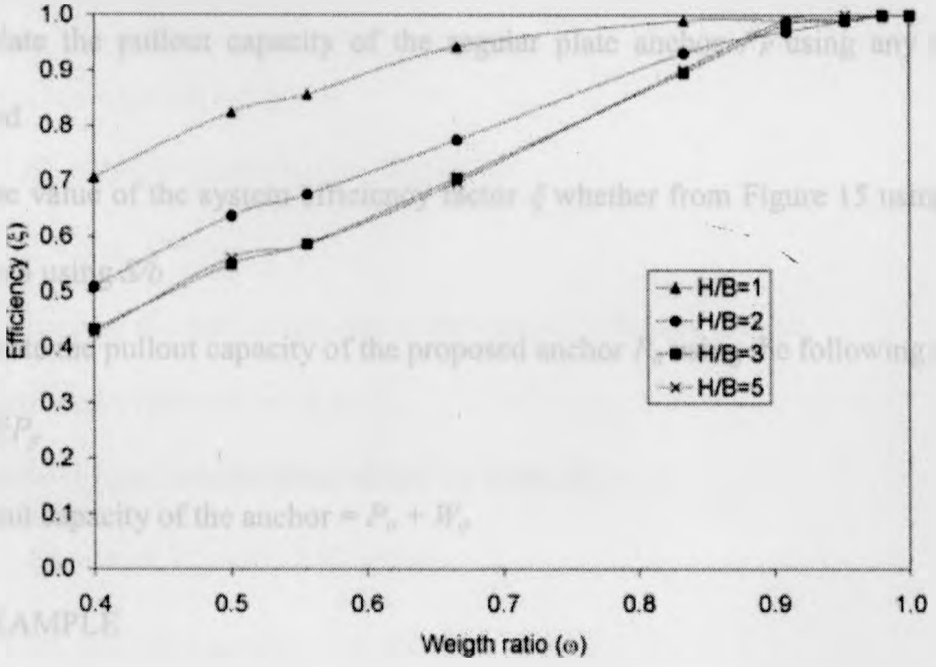

(b)

Figure 5. 15: Variation of efficiency ξ with weight ratio ω at different embedments for normally loaded (a) vertical anchors and (b) horizontal anchors

5.4 Design procedure and example

In order to assess the practicality of this approach a design methodology and solved examples are presented below.

The following steps are suggested to calculate the pullout capacity of normally loaded plate anchors with rectangular openings:

1. Determine the plate anchor width B, anchor thickness t, anchor embedment depth H, clay undrained shear strength C_u, the required opening width S value and the anchors material unit weight γ
2. Calculate the weight per meter of an equivalent regular plate anchor $W_F = \gamma Bt$
3. Calculate the weight per meter of the anchor with openings $W_o = 2\gamma bt$
4. Calculate the pullout capacity of the regular plate anchor P_F using any conventional method
5. Get the value of the system efficiency factor ξ whether from Figure 15 using ω, or from Figure 4 using S/b
6. Calculate the pullout capacity of the proposed anchor P_o using the following equation:

$$P_o = \xi P_F$$

The full pullout capacity of the anchor = $P_o + W_o$

SOLVED EXAMPLE

Since the aim is to maximize the pullout capacity (which includes weight) of the anchor with a fixed cranage ability (lifting capacity), we will assume a vertical anchor of thickness t = 0.5 m, S/b = 0.4 unit weight γ = 80 kN/m^3 and embedded in clay of undrained shear strength C_u=30 kPa as our benchmark case.

Next, we will determine the maximum anchor pullout capacity given a maximum allowable anchor weight of 400 kN/m (equivalent to 40 T crane).

The following steps are suggested to calculate its capacity:

$$W_F = \gamma Bt = 400 = 80\text{x}B\text{x}0.5$$

$$B = 10\ m$$

If we assume a deep embedment ($H/B \geq 5$) then we can use the proposed solution of Rowe (1978)

$$P_F = (2+3\pi)BC_u = 3427.4 \text{ kN/m}$$

Thus the total pullout capacity of a whole anchor $P_{FT} = P_F + W_F = 3427.4 + 400 = 3827.4$ kN/m

For a slotted anchor with $S/b = 0.4$

$$W_o = 2\gamma bt = 2\text{x}80\text{x}b\text{x}0.5 = 400 \text{ kN/m}$$

$$b = 5\ m,\ S = 2\ m$$

Hence we can increase the anchor size due to the reduced effective weight.

The new anchor total width = $B' = 12$ m

The capacity of a regular (whole) plate anchor of width $B' =$

$$(2+3\pi)B'C_u = 4112.92 \text{ kN/m}$$

From Figure 4 (a), the corresponding ξ at $S/b = 0.4$ is 0.96

Therefore

$$P_o = 0.96\text{x}4112.92 = 3948.4 \text{ kN/m}$$

Thus the full capacity of an enlarged slotted anchor is

$P_{Fo} = P_o + W_o = 3948.4 + 400 = 4348.4$ kN/m

Hence we can see that the addition of the slots for a fixed lifting capacity allows a greater overall pullout capacity for this case.

The variation of the full anchor capacity for a range of anchor weights and *S/b* values (at different embedments) are also presented in Figure 5. 16 (a) and (b) for vertical and horizontal anchors respectively, for a fixed crane capacities of 25 T, 40 T and 100 T. It can be seen that the gains in efficiency of these slotted anchors increases with weight and shallow embedments. It should be also noted that for larger slot sizes, the controllability of the anchor through the wave zone will be improved since the anchor will experience less drag. It is suggested that further analyses are conducted for anchors with higher numbers of individual slots and multiple separate anchor systems.

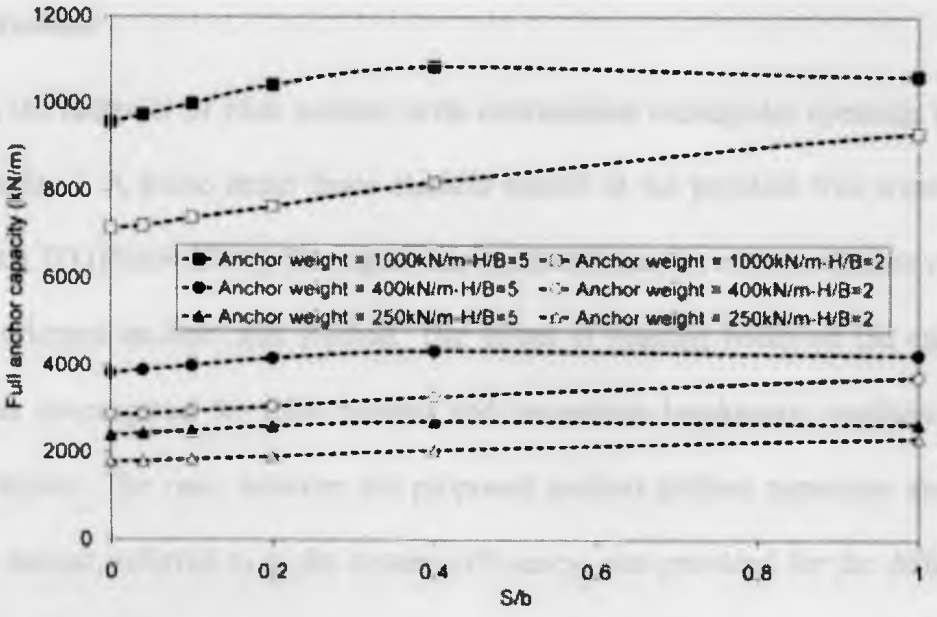

(a)

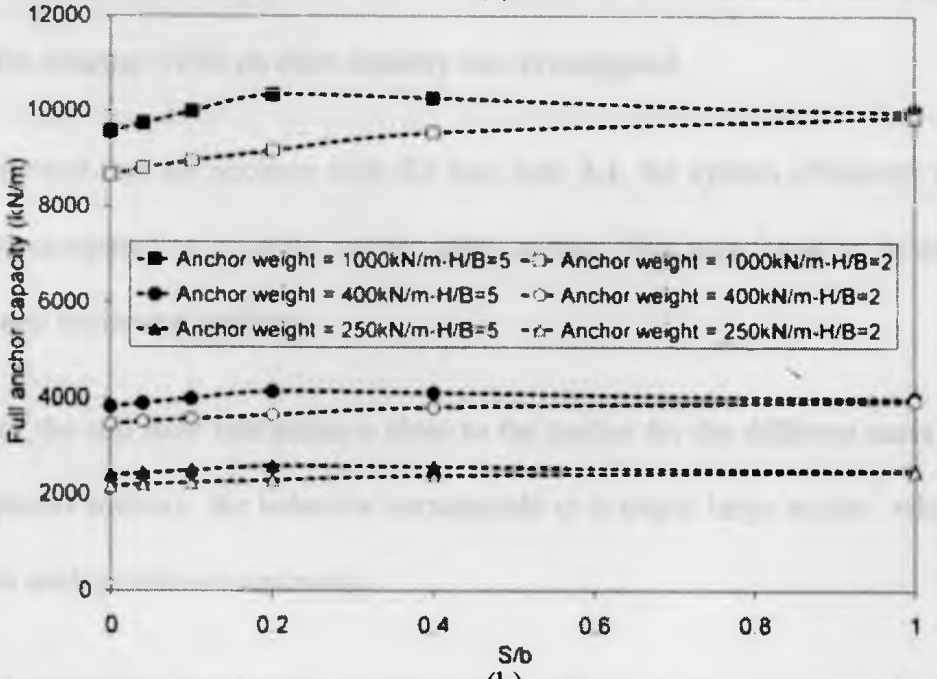

(b)

Figure 5. 16: Variation of full anchor capacity with *S/b* for a range of anchor weights for normally loaded (a)vertical anchors and (b) horizontal anchors for *H/B* = 2 and *H/B* = 5

5.5 Conclusions

In this study, the behavior of plate anchors with intermediate rectangular openings embedded in clay was examined. A plane strain finite element model of the problem was created using the software Plaxis 2D (Plaxis 2006). The equivalent pullout behavior of two adjacent vertically and horizontally oriented anchors was studied. The effect of spacing width on the anchor pullout capacities was investigated for fully bonded and immediate breakaway conditions at various embedment depths. The ratio between the proposed anchors pullout capacities and those of a regular plate anchor, referred to as the system efficiency, was provided for the different studied opening widths. Finally, closely spaced anchors subjected to inclined loads were also studied and the effect of the spacing width on their capacity was investigated.

The results showed that for anchors with S/b less than 0.4, the system efficiency decreases by less than 10% compared to a single regular plate anchor. This was found to be applicable for both vertical and horizontal anchors.

Observation of the soil flow mechanisms close to the anchor for the different cases showed that for closely spaced anchors, the behavior corresponds to a single large anchor, while at greater spacings, both anchors behave separately.

The effect of immediate breakaway on the anchor efficiency in comparison to regular plate anchors was also studied. Vertical anchor efficiency decreased by a negligible value for $S/b <$ 0.4, then starts to decrease by a constant rate at greater spacings. On the other hand, efficiency of a horizontal anchor for immediate breakaway conditions was not significantly affected for $S/b<2$, then a sudden efficiency drop occurred.

For closely spaced anchors subjected to inclined pullouts, the results showed that for deeply

embedded anchors, the system efficiency decreases at a nearly-constant rate with an increase of plate spacing. For shallow anchors, the system efficiency significantly drops by changing *S/b* from 0 to 1. This is followed by a nearly constant efficiency. This decrease rate is believed to be lower than that of the deeply embedded anchors.

The variation of the system efficiency with the anchor weight ratio at the different embedment depths was investigation. The results showed that for a weight ratio reduction of up to 10% and 15% for vertical and horizontal anchors respectively, the reduction in the system efficiency was negligible. Beyond these values, further reduction of the weight ratio caused more noticeable efficiency decrease, and at a greater rate of decrease for deep anchors.

The results of this study suggest the feasibility of using the proposed system as an alternative to existing regular plate anchors, especially for shallow embedments, when limitations on lifting capacity offshore exist.

5.6 References

Adams, J. I., and Hayes, D. C. (1967). "The uplift capacity of shallow foundations," *Ontario Hydro Research Quarterly*, Vol.19, No.1, pp 1-13

Das, B. M., and Puri, V. K. (1989). "Holding capacity of inclined square plate anchors in clay," *Soils and Foundations Journal*, Vol.29,No.3, pp 138-144

Deljoui, P. and Newson, T. A. (2007). "Numerical modeling of buried pipeline pullout through layered soil," *Proceedings of the Canadian Geotechnical Conference*, OttawaGeo2007: The Diamond Jubilee Conference,

Ghosh, P., and Sharma, A. (2010). "Interference effect of two nearby strip footings on layered soil: Theory of elasticity approach," *Acta Geotechnica*, Vol.5, No.3, pp 189-198

Gourvenec, S., and Steinepreis, M. (2007). "Undrained limit states of shallow foundations acting in consort," *International Journal of Geomechanics*, Vol.7, No.3, pp 194-205

Griffiths, D. V., Fenton, G. A., and Manoharan, N. (2006). "Undrained bearing capacity of two strip footings on spatially random soil," *International Journal of Geomechanics*, Vol.6, No.6, pp 421-427

Hill, R. (1950). "The mathematical theory of plasticity," Clarendton press, Oxford

Kouzer, K. M., and Kumar, J. (2009). "Vertical uplift capacity of two interfering horizontal anchors in sand using an upper bound limit analysis," *Computers and Geotechnics*, Vol.36, No.6, pp 1084-1089

Kumar, J., and Bhattacharya, P. (2010). "Bearing capacity of interfering multiple strip footings by

using lower bound finite element limit analysis," *Computers and Geotechnics*, Vol.37, No.5, pp 731-736

Kumar, J., and Bhoi, M. K. (2009). "Vertical uplift capacity of equally spaced multiple strip anchors in sand," *Geotechnical and Geological Engineering*, Vol.27, No.3, pp 461-472

Kumar, J., and Kouzer, K. M. (2008). "Vertical uplift capacity of a group of shallow horizontal anchors in sand," *Geotechnique*, Vol.58, No.10, pp 821-823

Mandel, J. (1963). " Plastic interference between surface strip foundations," *Proceeding of The International Conference of Soil Mechanics and Foundation Engineering*, Rotterdam, pp 267-279.

Martin, C. M. & Hazell, E.C.J. (2005). "Bearing capacity of parallel strip footings on non-homogeneous clay," *Proceedings of the International Symp. on Frontiers in Offshore Geotechnics*, Perth, pp 427-433.

Merifield, R. S., and Smith, C. C.(2010). "The ultimate uplift capacity of multi-plate strip anchors in undrained clay," *Computers and Geotechnics,* Vol.37, No.4, pp 504-514

Merifield, R. S., Sloan, S. W., and Yu, H. S.(2001). "Stability of plate anchors in undrained clay," *Geotechnique,* Vol.51, No.2, pp 141-153

Randolph, M. F and Houlsby, G. T. (1984) "The limiting pressure on a circular pile loaded laterally in cohesive soil," *Géotechnique*, Vol.34, No.4, pp 613 –623

Plaxis Bv (2006). Plaxis 2D-Version 8 Manuals, Version 8

Prandtl, L. (1921). "Über die Eindringungsfestigkeit (Härte) plastischer Baustoffe und die

Festigkeit von Schneiden, " Zeit. angew. Math. Mech. 1,pp 15-20.

Rowe, R. K., and Davis, E. H. (1982). "The behavior of plate anchors in clay,"*Geotechnique,* Vol2, No.1, pp 9-23

Rowe R. K. (1978). "Soil structure interaction analysis and its application to the prediction of anchor behavior," Degree of doctor of philosophy thesis, University of Sydney, Australia

Rowe, R. K., and Davis, E. H. (1977). "Application of the finite element method to the prediction of collapse loads," *The University of Sydney,* Australia, Research report No.R310

Terzaghi, K. 1943. "*Theoretical soil mechanics,*" John Wiley, New York

Chapter 6 Summary, Conclusions and Recommendations for Future Study

6.1 Introduction

The use of different anchoring systems is required for many onshore and offshore applications. These include tower foundations, ships and offshore structures requiring the anchoring systems to ensure temporary or permanent stability. Remotely operating vehicles and other seabed-based working platforms are also commonly used tools for many offshore applications, including site investigation, cable and pipeline maintenance, and other uses related to offshore hydrocarbon extraction. To ensure full control of these working platforms, these also require a reaction force to provide stability during operation.

Regular strip plate anchors are typically used for this purpose. A review of the existing literature showed that the majority of available studies concerning the application of plate anchors has mainly concentrated on the behavior of a single anchor subjected to normal loads applied through the anchor centre of mass. Meanwhile, other loading conditions and shapes have not received much attention, despite their importance in other applications, especially offshore application. The literature review has also shown that the standard anchor type has many shortcomings (e.g. Liang *et al.* 2008).

Accordingly, this study was carried out to first numerically investigate the behavior of regular plate anchors embedded in clay when subjected to complex loading conditions, primarily due to offshore environmental conditions such as wave and current forces. More specifically, loading conditions where inclination of mooring lines and hence pullout force direction is not perpendicular to the anchor were studied.

The second goal was to numerically investigate the behavior of anchors with irregular base shapes embedded in clay and to study the effect of the different parameters affecting their pullout capacity. From the results we determined the most effective anchor shape and assessed the parameters governing its design.

Finally, a plate anchor system with rectangular openings was proposed and its behavior under various loading conditions was investigated. The results were then compared to those of regular plate anchors to assess the feasibility of this newly proposed system.

For these three sections, plane strain finite element models were developed using the software Plaxis 2D (Plaxis 2006).

In this chapter, a summary of the numerical analysis results is presented, followed by a list of suggested recommendations for future study.

6.2 Numerical analysis results

6.2.1 Regular anchors

Numerical analysis revealed that, for fully bonded anchors, capacity increases with embedment at a decreasing rate until it reaches a nearly constant value at a critical depth after which the anchors behavior changes from shallow to deep. The deep behavior occurred at H/B value between 3 and 4 at horizontally applied loads and this value decreases and reaches a minimal value of 1.7 at pure vertically applied loads.

It was also shown that at the same embedment depth, anchor behavior changes from shallow to deep by changing the overburden pressure. The results showed that deep behavior occurred at $\gamma h/C_u$ of 5.

The results showed a greater load inclination effect on anchors pullout capacity at greater embedment depths.

Studying the immediate breakaway anchor condition proved that, for the different studied loading conditions, deep behavior occurred at higher embedments compared to the fully bonded condition.

Soil-anchor interface strength effect was found to be more apparent in case of vertically loaded anchors and this effect decreases with the increase in the loading angle from vertical.

The analysis also showed that the location of the anchors point of load application has a minor effect on its capacity.

The effect of the anchor thickness was found to be small for vertically loaded anchors. For example, changing the anchor thickness by 100% increases the pullout capacity by 20% only . Smaller effect was found for horizontally loaded anchors.

Simulation of the clay disturbance following anchor insertion have been studied. The results showed that the vertically loaded cases are the most affected by the disturbance with maximum pullout resistance decrease of 72%. Less effect has been shown for loading angles approaching horizontal.

Anchors embedded in normally consolidated clays have been studied. The results showed that, the anchors pullout capacity increases at a decreasing rate with the increase of ρ. It was also shown that at higher values of ρ, embedment depth has a greater effect on anchor capacity.

6.2.2 Irregular anchors shapes

The results of this section show that, similar to regular plate anchors, fully bonded anchors, capacity increases at a decreasing rate with embedment until it reaches a constant value at a critical depth, after which the anchor behavior changes from shallow to deep. The critical depth was found to be minimal for vertically applied loads and increases with the increase of load inclination from the vertical.

The results show a significant loading inclination effect on the anchor capacity. Vertically loaded anchors capacity was found to be minimal as it is mainly attributed to skin friction. As the loading inclination further increases, capacity increases as well until it reaches its maximum value at horizontal loads where capacity is mainly developed from passive resistance. This increase was shown to be greater at higher embedment depths.

The effect of base size/shape on anchor pullout capacity was investigated. The results show that, although the base shape has a limited effect on horizontally loaded anchors, a much greater effect is shown for vertically loaded cases. The results also show that the anchor base width has a greater effect on anchor pullout capacity than base height.

While different base shapes have been studied, anchors with triangular base shapes showed the highest vertical pullout capacity, with an increase in capacity reaching more than three times that of the regular plate anchors in some cases. Less increase was shown for horizontal loading, however this configuration was found to be the most effective in terms of steel area and pullout capacity.

The effect of the soil-anchor interface strengths was found to be more apparent for vertically loaded anchors and decreases with the increase in the loading angle from vertical reaching a

minimum value for horizontally loaded anchors.

Soil disturbance following anchor driving was also assessed. The results showed that vertically loaded cases are the most affected by the disturbance as capacity is mainly dependent on side friction, with a maximum pullout resistance decrease of 48%. This value is less than that found for regular plate anchors. Less effect is anticipated for pullout inclinations approaching horizontal.

Analysis of anchors embedded in normally consolidated clay profiles of linearly increasing strength with depth was carried out. The results were drawn and compared to those of anchors embedded in a constant strength profile. Anchor capacity has shown to increase at a decreasing rate with the increase of ρ with a greater effect at greater embedments.

The results also showed that the point of load application has a negligible effect on the anchor pullout capacity.

Finally, simulation of two adjacent anchors subjected to moment loading was carried out. The results reflects the significant decrease of moment capacity of closely spaced anchors due to the interaction between them.

6.2.3 Plate anchors with intermediate rectangular openings

The results of this section were presented in terms of the ratio between the proposed anchor pullout capacities and that of a regular plate anchor, referred to as the system efficiency.

The results showed that, for both vertical and horizontal anchors, *S/b* less than 0.4, the system efficiency decreases by less than 10%. This was found to be applicable for both vertical and horizontal anchors. These results were also confirmed by the observation of the soil flow

mechanisms close to the anchor showing for the different cases that for closely spaced anchors, the behavior corresponds to a single regular plate anchor.

The effect of immediate breakaway on the anchor efficiency was assessed. The results shows that for vertical anchors, the efficiency decreased by a negligible value for $S/b < 0.4$, then starts to decrease by a constant rate at greater spacings. On the other hand, efficiency of a horizontal anchor for immediate breakaway conditions was not significantly affected for $S/b<2$, then a sudden efficiency drop occurred.

Simulation of closely spaced anchors subjected to inclined pullouts was also performed. The results showed that for deeply embedded anchors, the system efficiency decreases at a nearly-constant rate with the increase in spacing. For shallow anchors, the system efficiency significantly drops by changing S/b from 0 to 1. This is followed by a nearly constant efficiency. This decrease rate is believed to be lower than that of the deeply embedded anchors.

The variation of the system efficiency with the anchor weight ratio at the different embedment depths was investigation. The results showed that for a weight ratio reduction of up to 10% and 15% for vertical and horizontal anchors respectively, the reduction in the system efficiency was negligible. Beyond these values, further reduction of the weight ratio caused more noticeable efficiency decrease, and at a greater rate of decrease for deep anchors.

The results of this chapter suggest the feasibility of using the proposed system as an alternative to existing regular plate anchors, especially for shallow embedments, when limitations on lifting capacity offshore exist.

6.3 Recommendations for future study

Based on the results of this study, the following is a list of suggested ideas for future studies:

- Experimental modeling at natural and enhanced gravity of irregular shaped anchors embedded in soft clay profiles to further validate the available numerical analysis results. This should include a series of tests covering the different parameters provided in the numerical analysis as presented in Chapter 4.
- Numerical and experimental modeling of regular and irregular shaped anchors embedded in a dense sand layer overlaying clay layer, presenting a typical offshore soil profile in many cases.
- Developing upper and lower bound plasticity solutions for triangular bases anchor to provide simple design equation for this anchor shape and verify the current results.
- Experimental and three dimensional numerical modelling of the proposed anchors with rectangular openings are required to validate the numerical analysis results provided in this study.
- Experimental and three dimensional modelling of multiple anchors subjected to moment and lateral loads to evaluate the interaction effect on their capacity.
- Experimental modelling of enlarged based anchors and anchors with rectangular openings embedded in clay with increasing shear strength with depth to assess the feasibility of using these anchor types in normally consolidated clay profiles.

Appendix A

In addition to the parameters studied in chapter 4 regarding the application of enlarged base anchors, additional parameters and loading conditions were investigated. Results of these analyses are presented in this Appendix. The loading cases studied are referred to as cases 1 to 8 and illustrated in Figure A. 1.

The effect of the overburden pressure on the anchor's pullout capacity was investigated. The results showed that, at constant embedment depth, the anchor's behavior changes from shallow to deep when the overburden pressure is increased. Figure A. 3 (a) shows the variation of N_c with $\gamma h/C_u$ for a vertical anchor (Case 2) of configuration # 1 at four different embedment ratios (H/B = 2, 3, 4 and 5) compared to the lower and upper bound limiting values found by Merifield *et al.* (2001) for regular plate anchors subjected to the same conditions. Our calculations showed deep behavior at $\gamma h/C_u > 5$, with a limiting breakout factor of 12. Similar plots for anchors of configurations # 3 and 4 at H/B = 2 and 5 are shown in Figure A. 3 (b).

The dependence of anchor capacity on pullout inclination was studied. Loads were applied at angles θ from the vertical ranging from 0° to 90° at increments of 15°. Figure A. 4 and Figure A. 5 illustrate the variation of N_c with θ for fully bonded anchors, loaded at the top and through the centre of mass respectively for several embedment ratios (H/B = 1, 2, 3, 4 and 5) for an anchor of configuration # 1. The plots showed that anchor capacity increases with load inclination as the resistance changes from pure skin friction at vertical loadings, to passive resistance at horizontal loadings. This effect is more significant at higher embedment depths. For example, a change in load inclination from vertical to horizontal increased the pullout capacity by 65% at H/B = 1, while at H/B = 5 similar change caused a 225% increase. These changes are consistent with those found for regular plate anchors by Fahmy *et al.* (2010).

In the previous sections, anchors were studied under no-breakaway and immediate breakaway conditions. However, these extreme cases are unlikely to occur in practice. Accordingly, different adhesion factor values were proposed in this study in order to identify the effect of soil-anchor interface strength on the anchor pullout capacity. The variation of N_c with adhesion factor "α" at soil-anchor interface for anchors of configurations # 0 and 1 loaded at cases 1 and 2 at H/B = 2 and 4 are presented in Figure A. 6. These two embedment ratios were chosen to represent both shallow (H/B = 2) and deep (H/B = 4) conditions. The results showed that, for anchors loaded at case 1, where resistance mainly results from skin friction, anchor capacity increased by 50% when the adhesion factor α increased from 0.1 to 1. On the other hand, for anchors loaded at case 2, surface friction has a diminishing effect on anchor capacity compared to the vertically loaded case as shown in Figure A. 6, where no significant increase in strength (less than 10%) occurs with the increase in α from 0.1 until the fully bonded case is reached (α = 1). For inclined loads, anticipated behavior could be interpolated between horizontal and vertical cases.

To assess the effect of point of load application, the load has been applied at the top of the anchor and through its centre of mass. The results showed that, at the same H/B value, and for the different studied load inclinations, anchor capacities were nearly equal regardless of the point of load application assuring that the point of load application has negligible effect on anchor ultimate capacity.

Considerable reduction in strength may occur due to the induced excess pore pressures and remolding following anchor embedment in sensitive clay. Although a regain of strength would occur after dissipation of these excess water pressures, this process might take many months.

Accordingly, modeling this phenomenon has been performed. The considered width of disturbed soil adjacent to the anchor was found to be comparable with that around driven piles, which is equal to 2 times anchor/pile diameter. A surface anchor of configuration # 1 (H/B = 1) was considered where the undrained shear strength of the surrounding soil increased gradually from 2.5kPa at anchor interface up to the initial value of 20kPa at 1m from anchor (twice the anchor diameter), hence representing clay of sensitivity S_t = 8. The results reveal a maximum capacity decrease of 48% for vertically loaded anchors (case 1) while a much lower effect was shown for horizontally loaded anchors (case 2), where a capacity decrease of only 14% occurred. Comparison with results of the regular plate anchors (configuration # 0) showed comparable results with lower decrease for case 1 (48% compared to 72%).

In addition to the constant strength soil profile, simulation of vertical anchors embedded in normally consolidated clay, with linearly increasing strength with depth was carried out. Three different rates of shear strength increase ρ (1, 2 and 3 kPa/m) were considered as well as a constant strength profile (ρ = 0). For all cases, the initial clay shear strength was 5 kPa and a constant E/C_u value of 100 was maintained along the profile representing soft clays. Figure A. 7 shows the variation of the inhomogeneous breakout factor $N_{co\rho}$ with $\rho B/C_u$ for anchor of configuration # 1 at loading cases 1, 2 and 3 at H/B of 2 and 4 under a fully bonded condition. The results showed that the rate of increase in ultimate anchor capacity decreases with the increase of $\rho B/C_u$. It was also noticed that the effect of embedment depth increases with the increase in the value of $\rho B/C_u$. For example, for loading case 1, changing H/B from 2 to 4 had no significant effect on the anchor's capacity at $\rho B/C_u$ = 0, while at $\rho B/C_u$ = 6, the same change induced a pullout capacity increase of more than 1.2 times.

The previous sections of this chapter dealt mainly with the pullout behavior of anchors. However, occasionally other loading conditions, such as lateral and moment loadings, govern the design. This would particularly be the case for enlarged base anchors (or inflatable versions) attached to an ROV. Accordingly, two adjacent fully bonded anchors of configuration # 1, subjected to moment loads have been modeled. The spacing S between anchors was varied in order to investigate the interaction between the adjacent anchors and its effect on the anchors moment capacity. Figure A. 8 shows the resulting variation of the anchors moment capacity with S/B at H/B = 1, 2 and 4. The results show that interaction between closely spaced anchors significantly affects their moment capacity. On the other hand, for relatively distant anchors, the results show that each anchor behaves separately. This is also demonstrated in Figure A. 9, where the total displacement increments diagrams for anchors at S/B = 0.5 for H/B = 1 and 4 are presented in (a) and (b) respectively. The plotted soil flow mechanisms show that both anchors behave as one single anchor. On the other hand, at higher S/B values, each anchor behaves separately and no interaction occurs between the soil flows around each anchor. This is shown in Figure A. 9 (c) and (d), where the total displacement increments diagrams for anchors at S/B = 1 for H/B = 1 and 4 are plotted respectively.

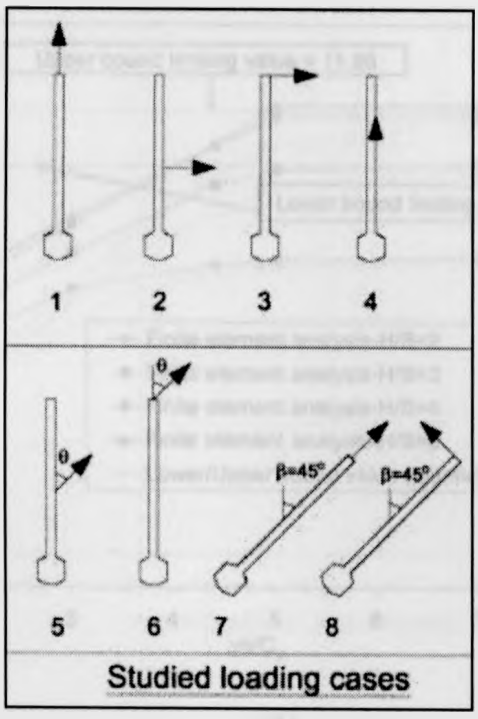

Figure A. 1: Different studied loading cases.

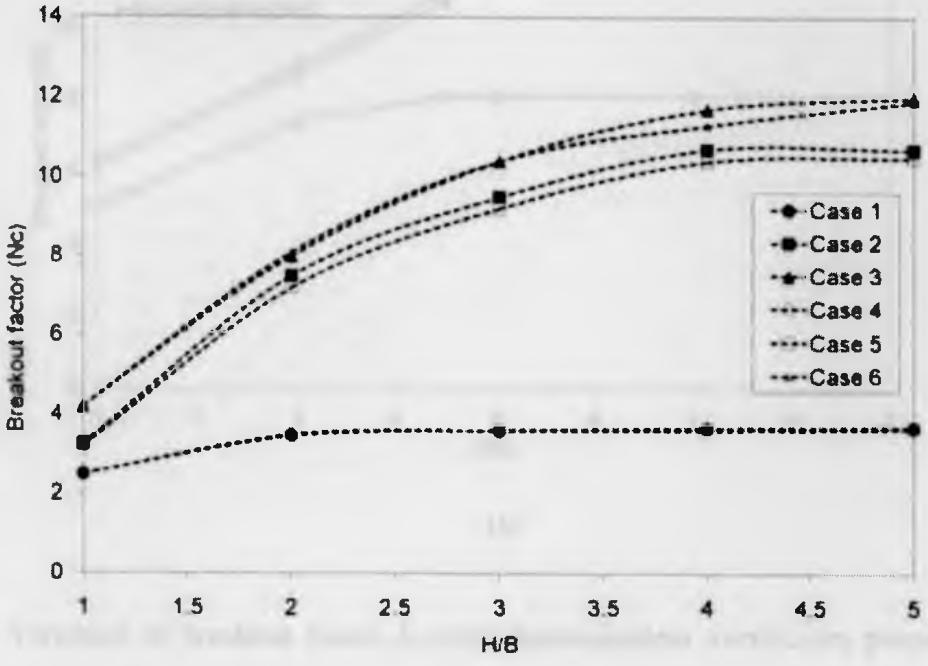

Figure A. 2: Variation of breakout factor N_c with embedment ratio H/B for anchors of configuration # 1 at different cases (fully bonded).

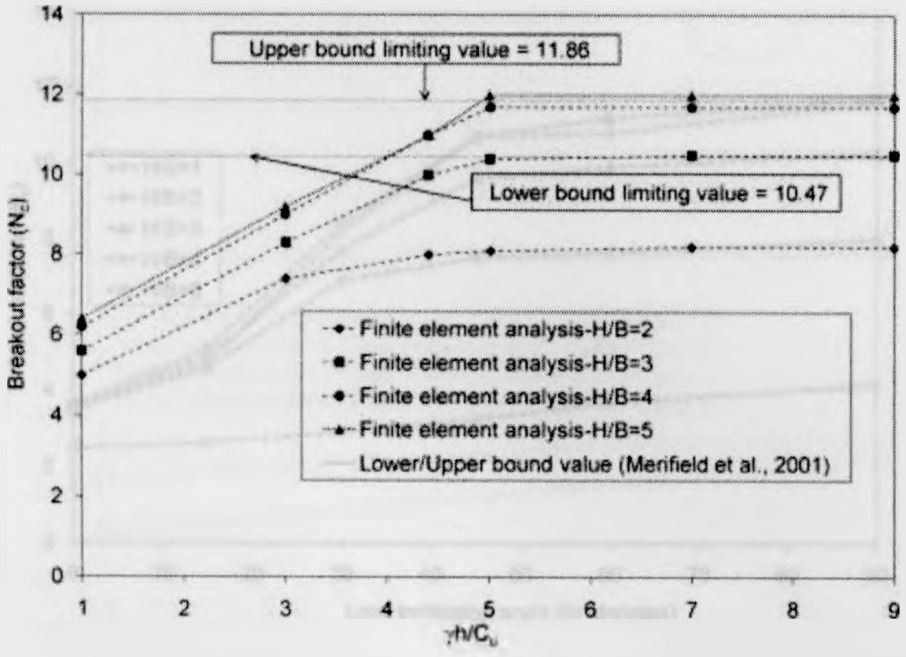

(a)

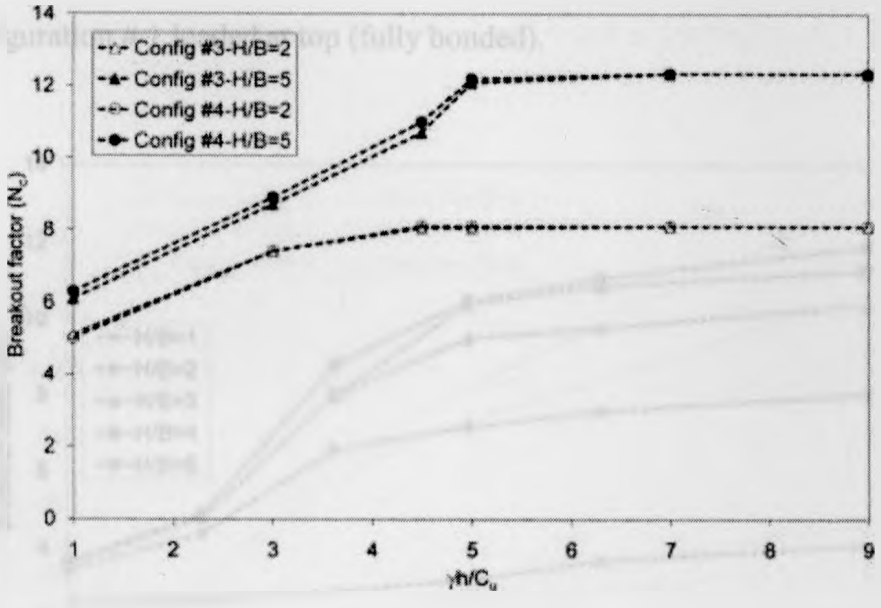

(b)

Figure A. 3: Variation of breakout factor N_c with dimensionless overburden pressure $\gamma h/C_u$ for horizontally loaded (Case 2) anchors of (a) configuration # 1 and (b) configurations # 3 and 4 .

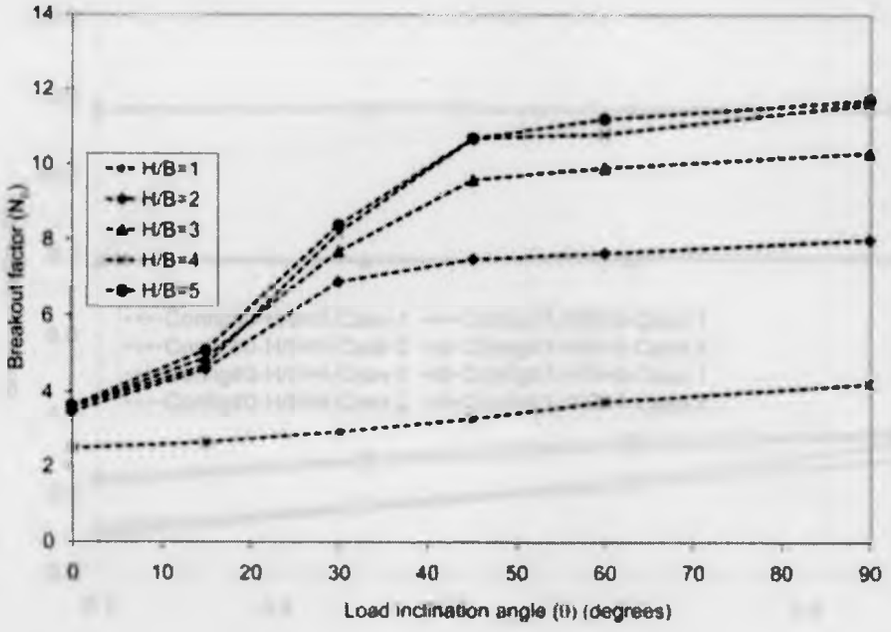

Figure A. 4: Variation of breakout factor N_c with load inclination from vertical (θ) for vertical anchor of configuration # 1 loaded at top (fully bonded).

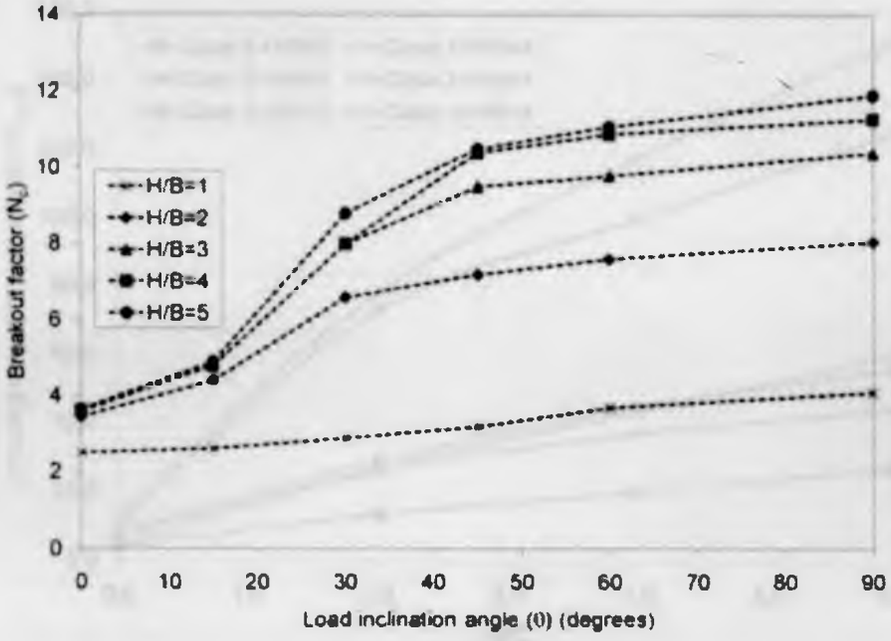

Figure A. 5: Variation of breakout factor N_c with load inclination (θ) from vertical for vertical anchor of configuration # 1 loaded through centre of mass (fully bonded).

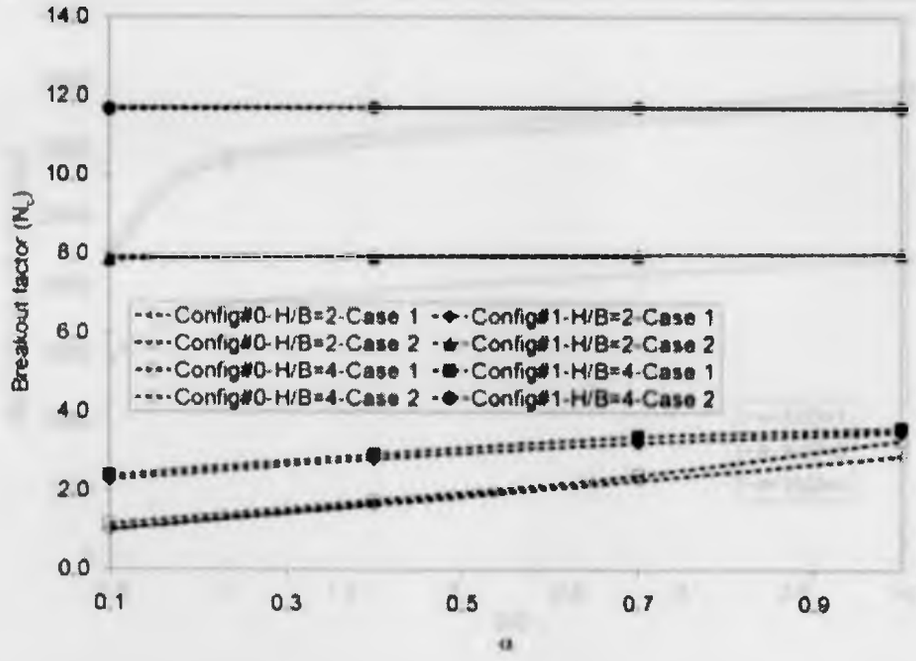

Figure A. 6: Variation of breakout factor N_c with adhesion factor (α) for anchors of configuration # 1compared to those of configuration#0 at $H/B = 2$ and 4 and at loading cases 1 and 2.

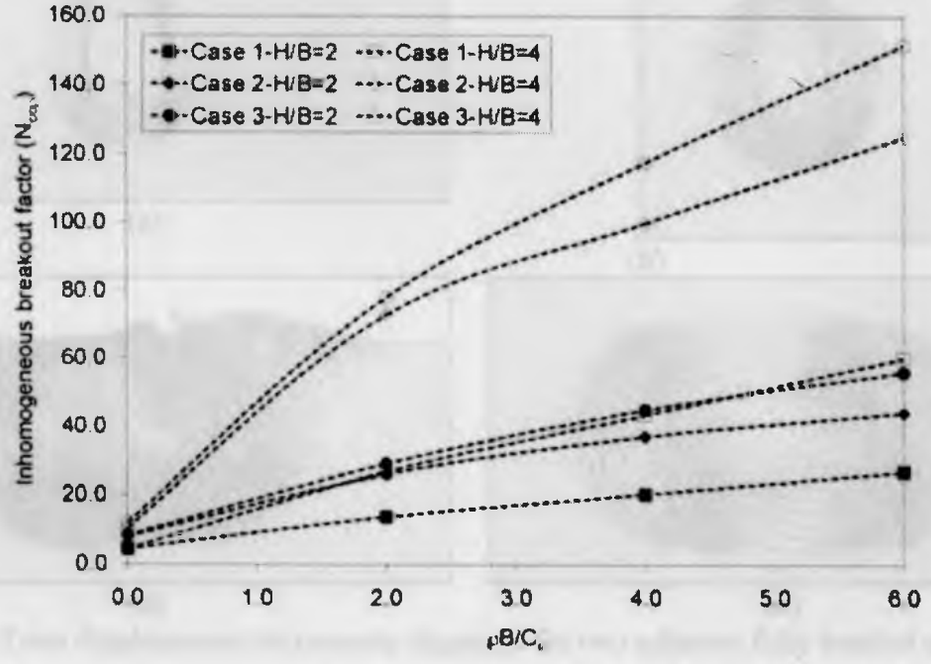

Figure A. 7: Variation of inhomogeneous breakout factors $N_{co\rho}$ with rate of increase of strength $\rho B/C_u$ for anchors of configuration # 1 (fully bonded).

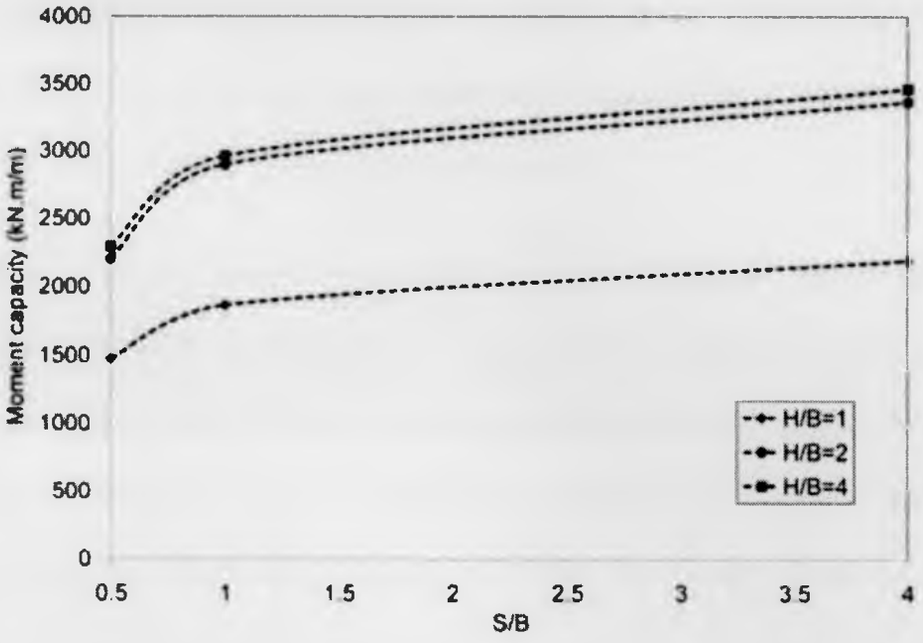

Figure A. 8: Variation of anchors moment capacity with *S/B* at *H/B* = 1, 2 and 4 for anchors of configuration # 1.

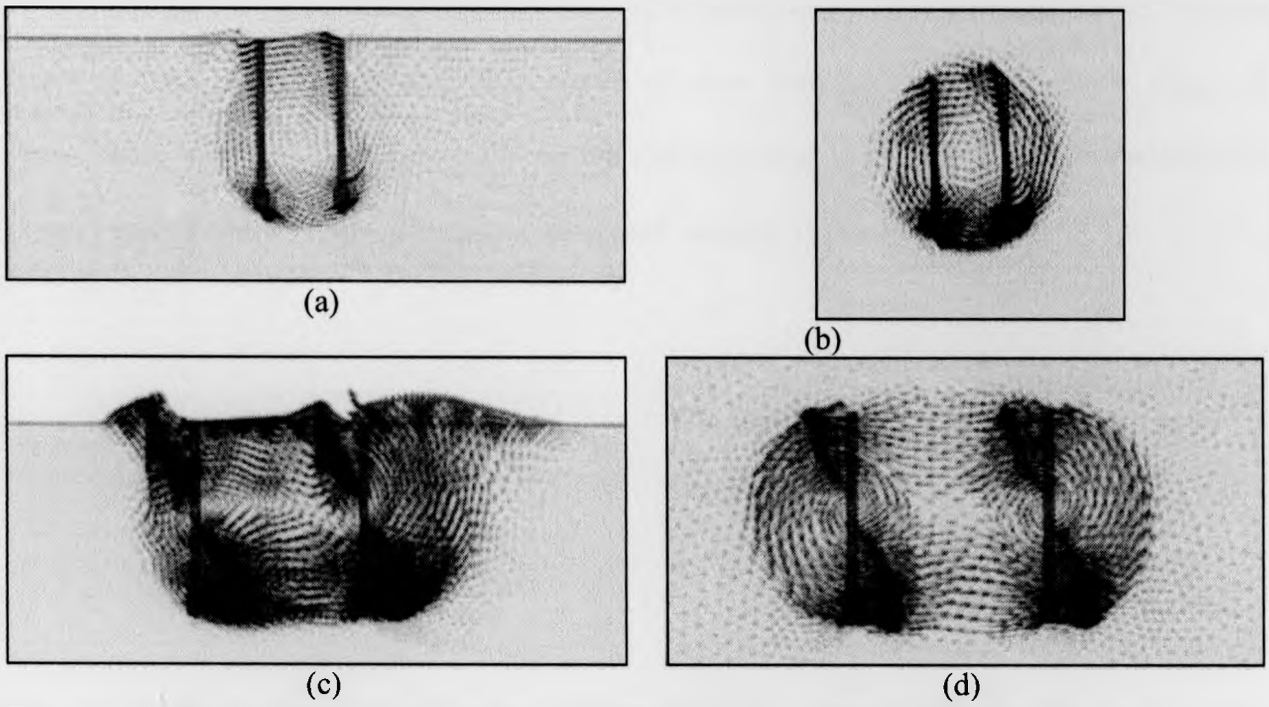

Figure A. 9: Total displacement increments diagrams for two adjacent fully bonded anchors of configuration 1 subjected to moment loads at (a) *H/B* = 1-*S/B* = 0.5, (b) *H/B* = 4-*S/B* = 0.5, (c) *H/B* = 1-*S/B* = 1 and (d) *H/B* = 4-*S/B* = 1.

Appendix B

To further understand the behavior of slotted anchors under the different loading conditions presented in Chapter 5, Incremental strain diagrams by means of shear shadings and principal stress directions are plotted and presented in this Appendix.

Principal stress directions diagrams are plotted for normally loaded vertical and horizontal slotted anchors in Figure B. 1 and Figure B. 2 respectively under fully bonded conditions. In addition, incremental strains of the same loading cases are also plotted in Figure B. 3 and Figure B. 4 by means of shadings. The plots shows the development of two separate mechanisms for widely spaced anchors, unlike closely spaced ones where both anchors behave a an equivalent single one.

Similarly, incremental strain plots are presented by means of principal stress directions in Figure B. 5 and Figure B. 6 for horizontal and vertical anchors respectively subjected to 45° inclined loads. Similar quantities are plotted by means of shear shadings are plotted also in Figure B. 7and Figure B. 6 B. 8. The figures shows the soil squeezing in the gap in-between anchors for closely spaced cases while it disappears for greater spacing values.

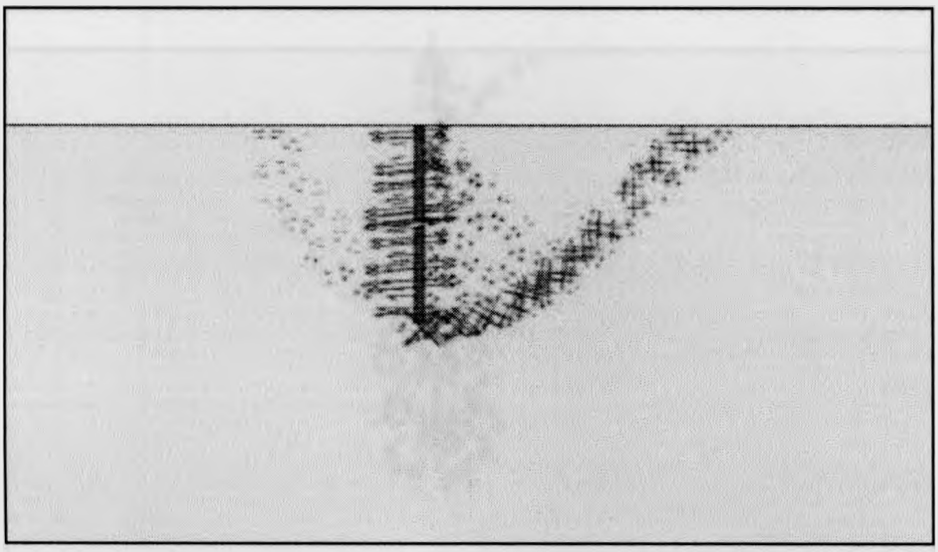

(a)

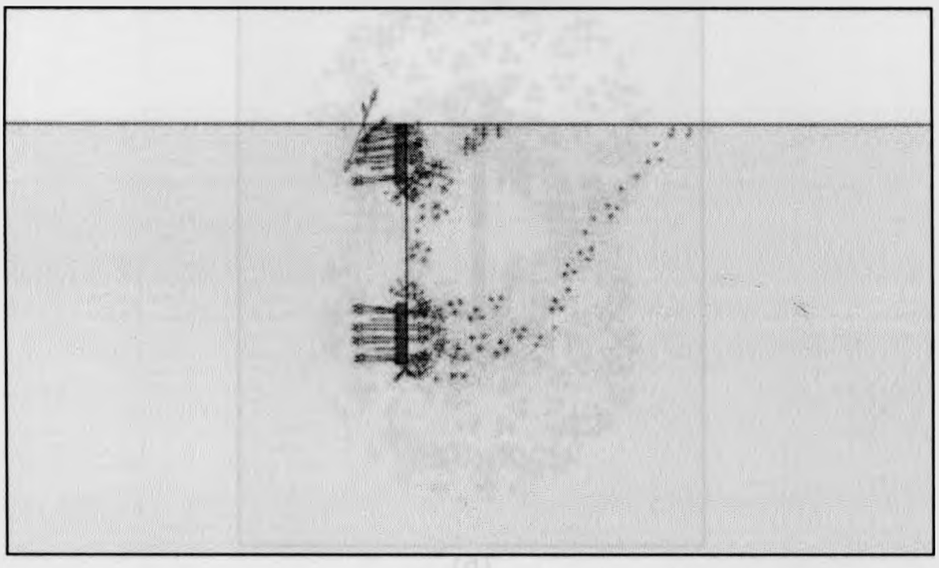

(b)

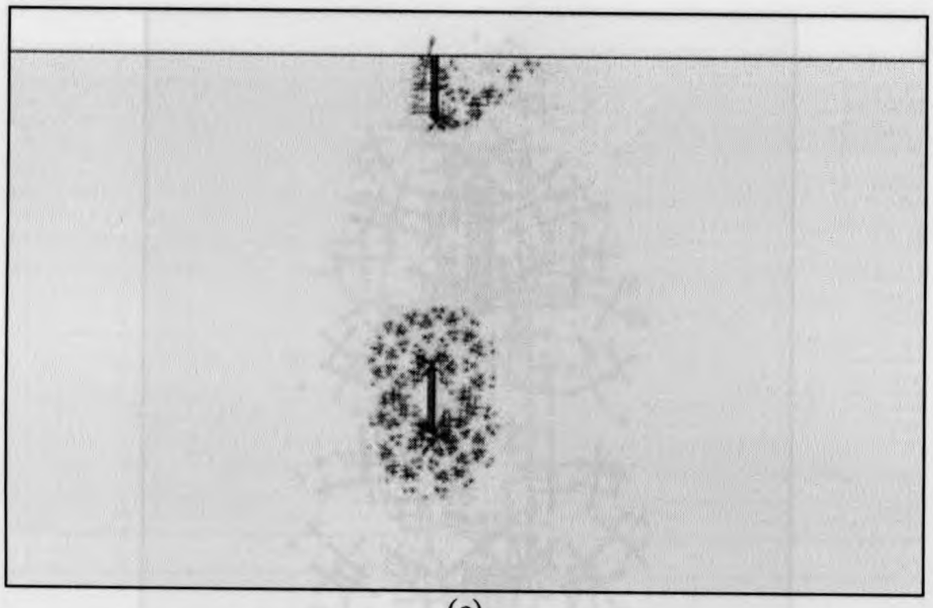

(c)

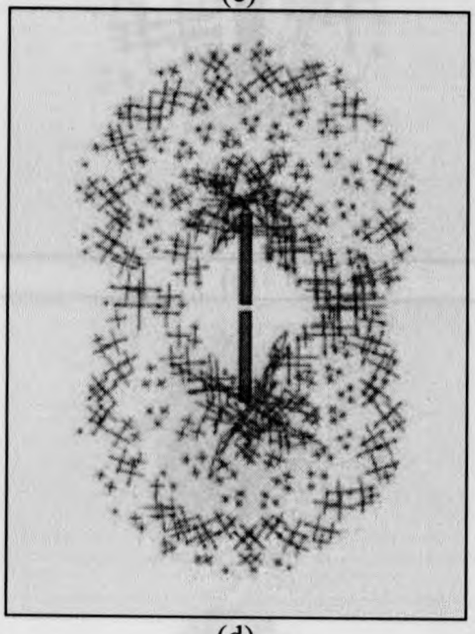

(d)

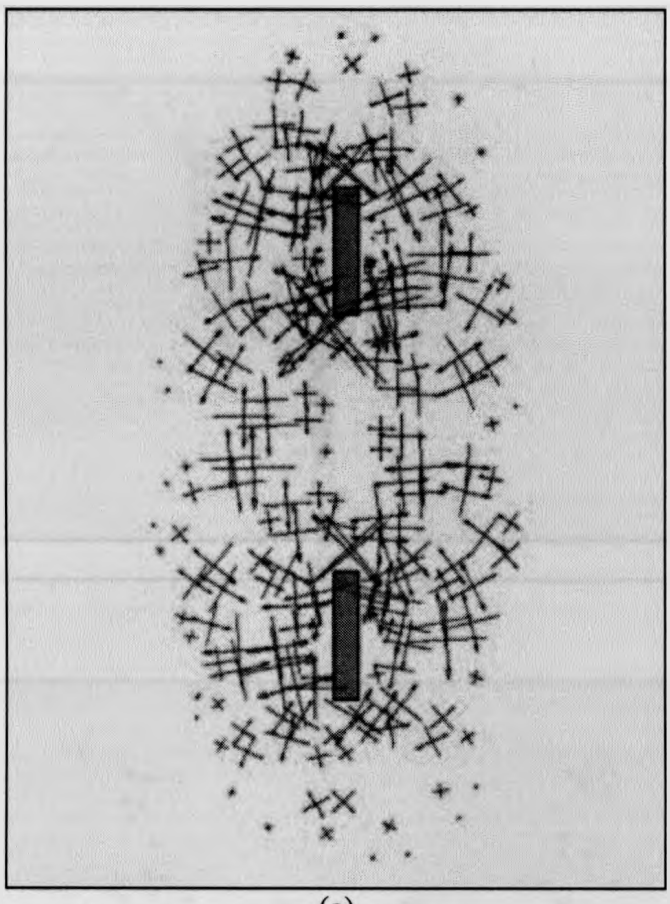

(e)

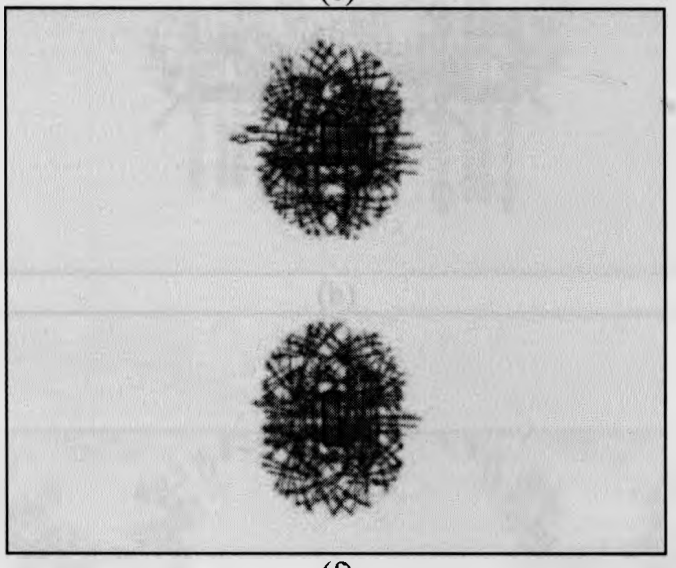

(f)

Figure B. 1: Incremental strain-principal stresses directions diagrams for fully bonded normally-loaded vertical anchors at (a) $H/B = 1$, $S/b = 0.1$; (b) $H/B = 1$, $S/b = 2$; (c) $H/B = 1$, $S/b = 4$; (d) $H/B=5$, $S/b = 0.1$; (e) $H/B = 5$, $S/b = 2$ and (f) $H/B = 5$, $S/b = 4.2$

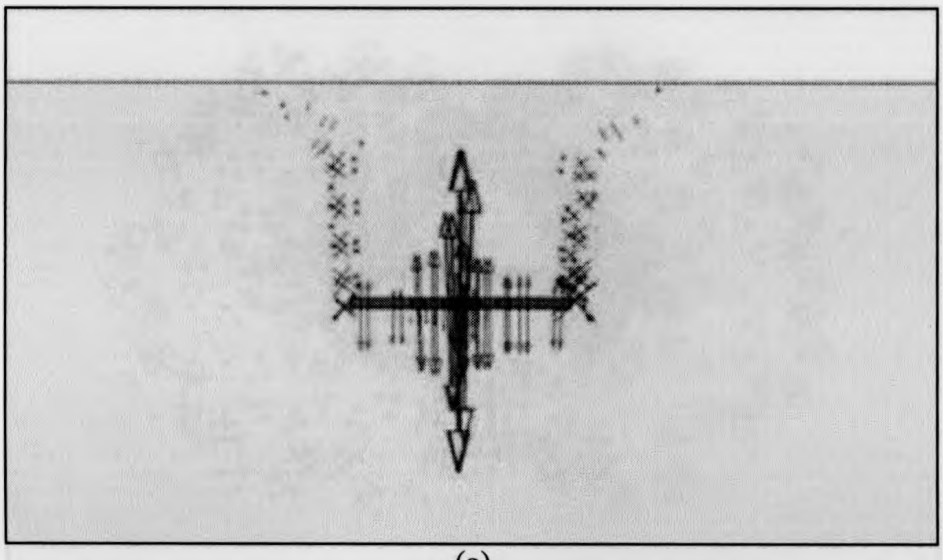

(a)

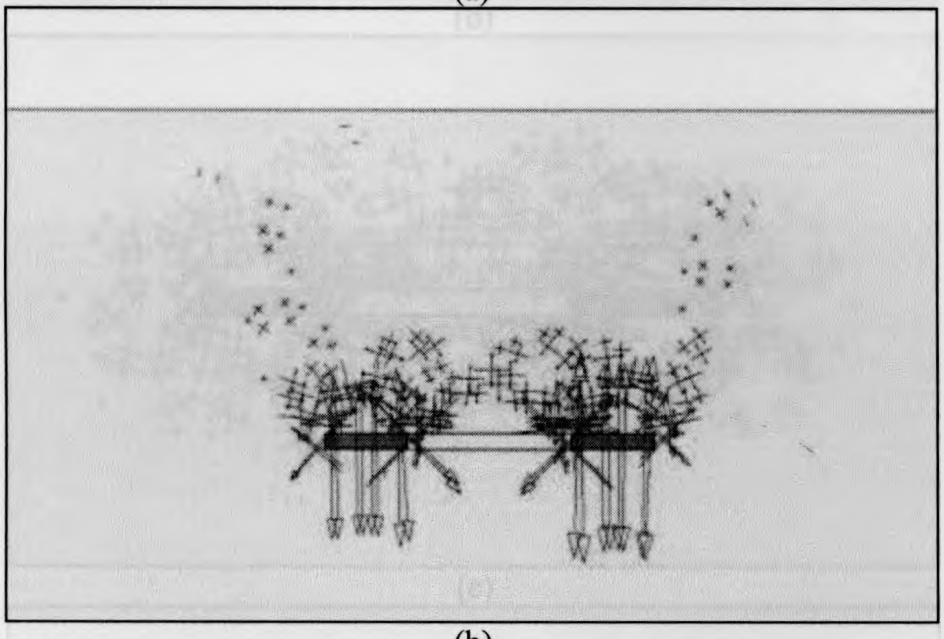

(b)

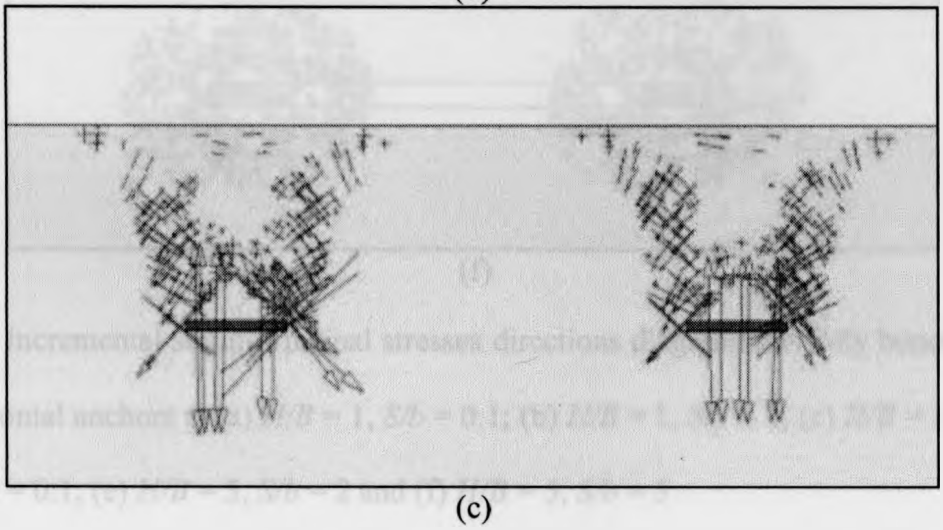

(c)

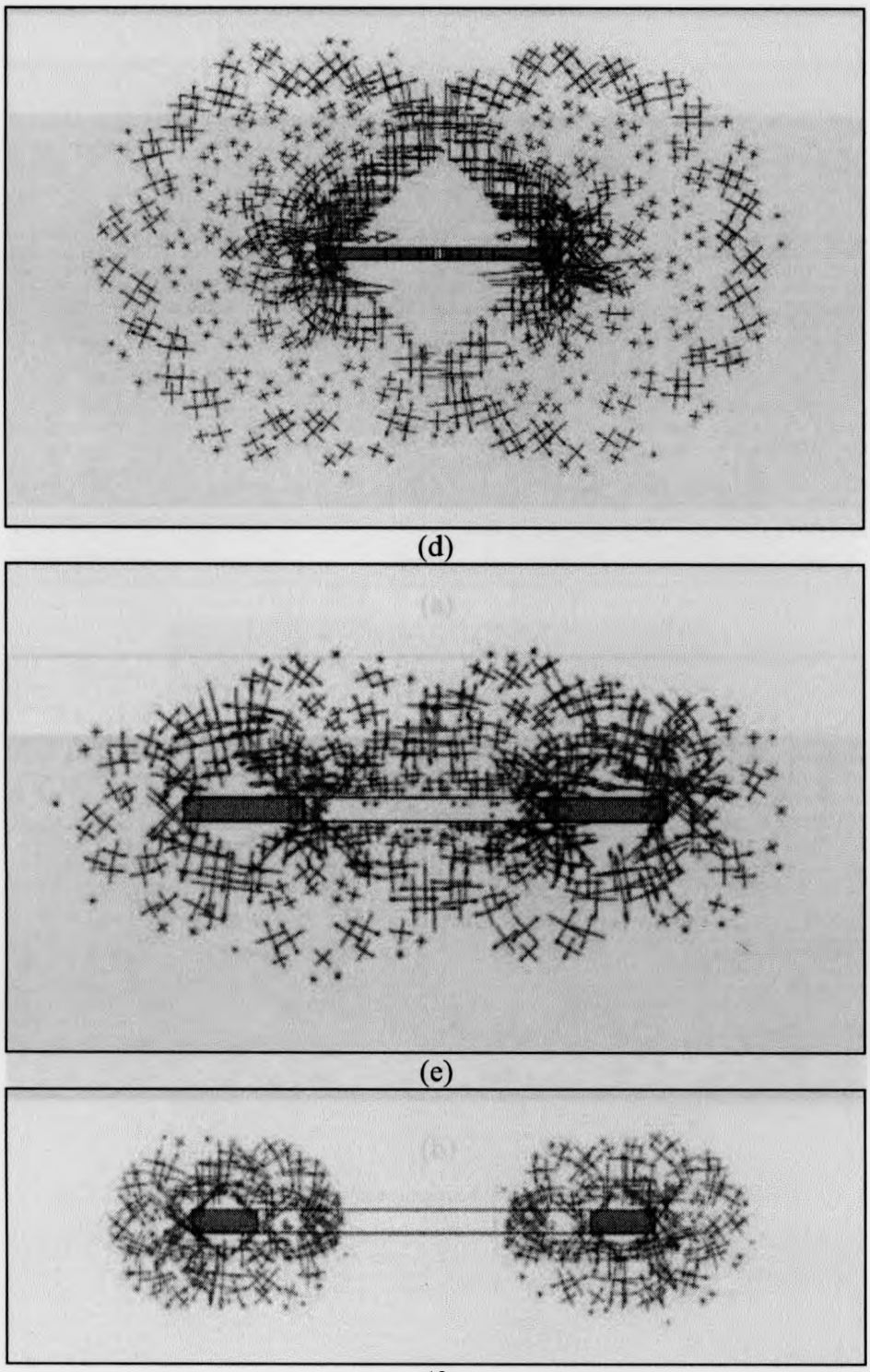

Figure B. 2: Incremental strain-principal stresses directions diagrams for fully bonded normally-loaded horizontal anchors at (a) $H/B = 1$, $S/b = 0.1$; (b) $H/B = 1$, $S/b = 2$; (c) $H/B = 1$, $S/b = 4$; (d) $H/B = 5$, $S/b = 0.1$; (e) $H/B = 5$, $S/b = 2$ and (f) $H/B = 5$, $S/b = 5$

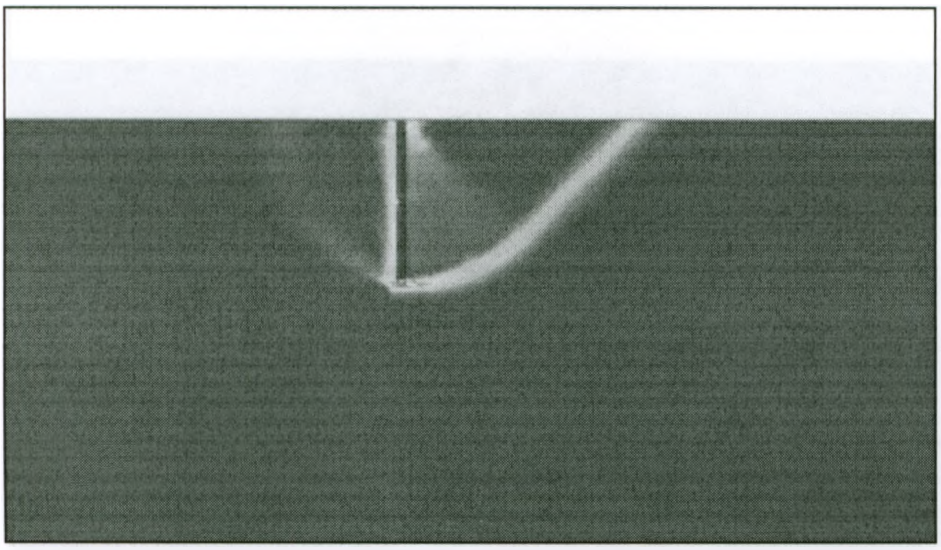

(a)

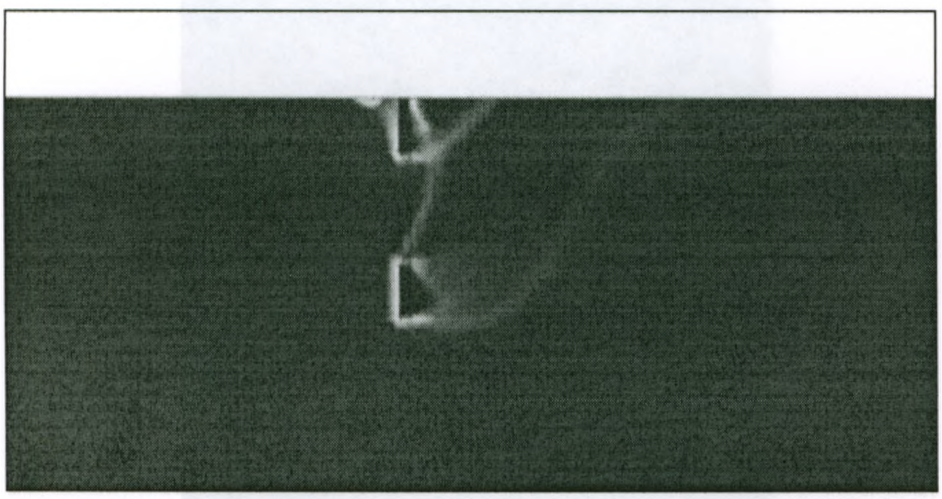

(b)

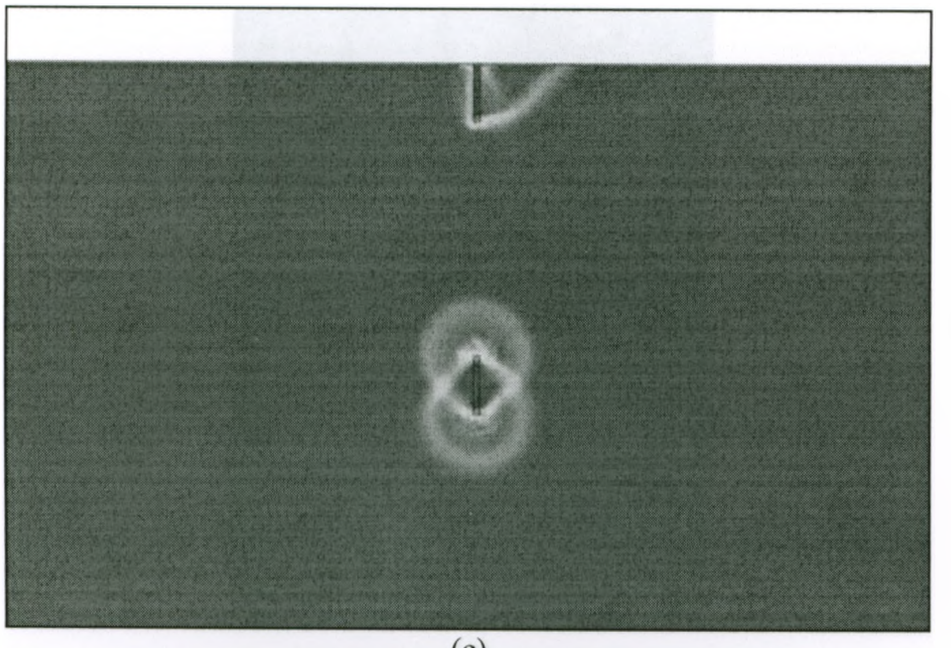

(c)

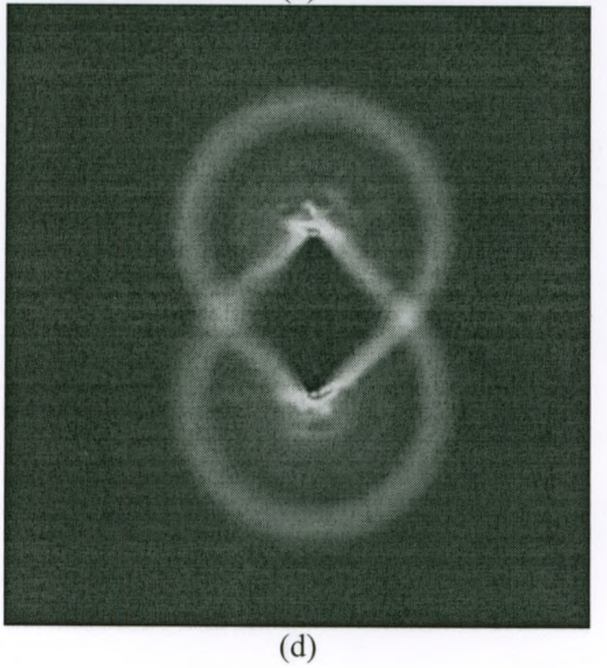

(d)

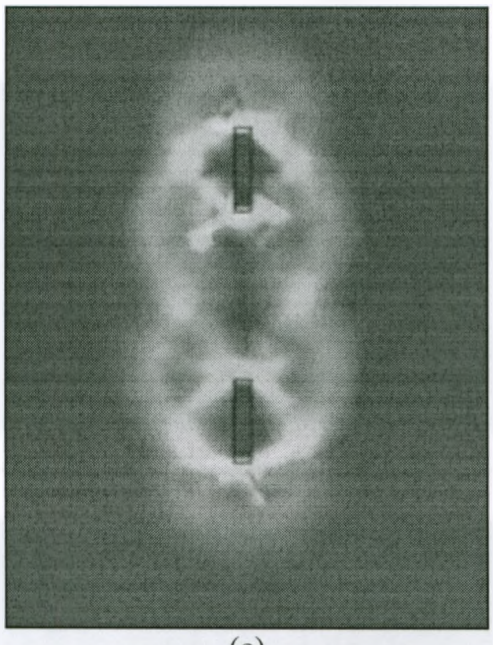

(e)

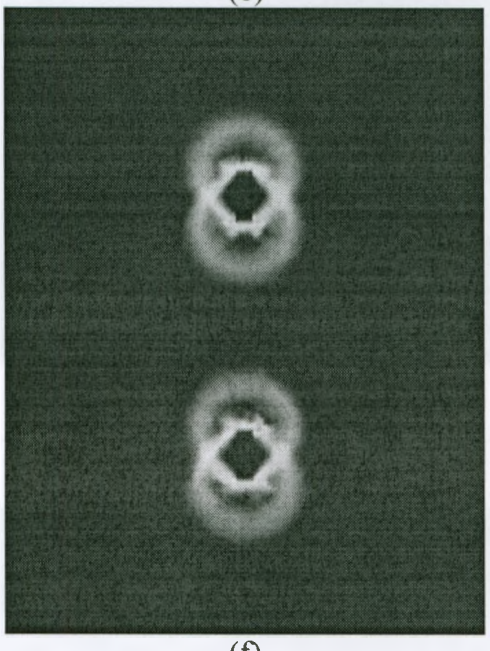

(f)

Figure B. 3: Incremental strain-shear shading diagrams for fully bonded normally-loaded vertical anchors at (a) $H/B = 1$, $S/b = 0.1$; (b) $H/B = 1$, $S/b = 2$; (c) $H/B = 1$, $S/b = 4$; (d) $H/B=5$, $S/b = 0.1$; (e) $H/B = 5$, $S/b = 2$ and (f) $H/B = 5$, $S/b = 4.2$

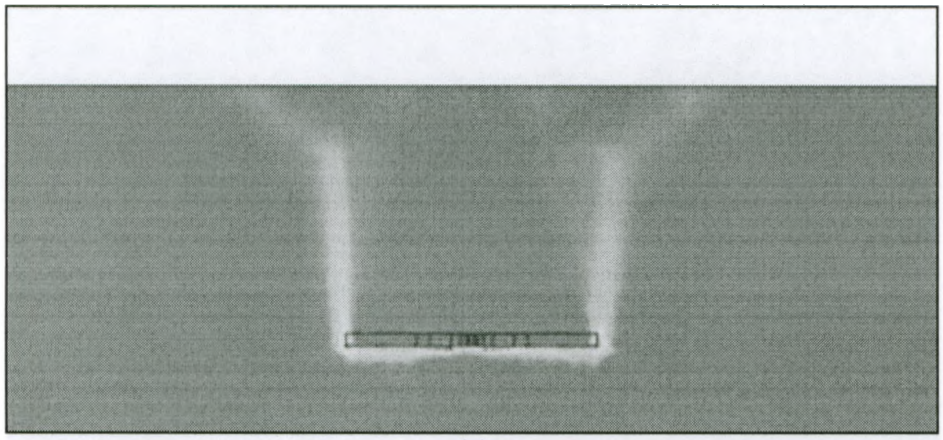

(a)

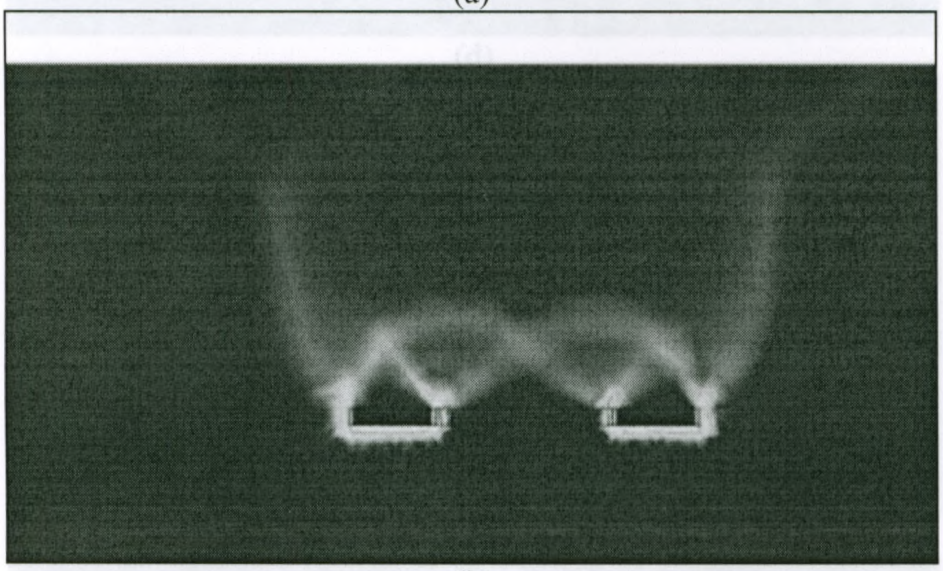

(b)

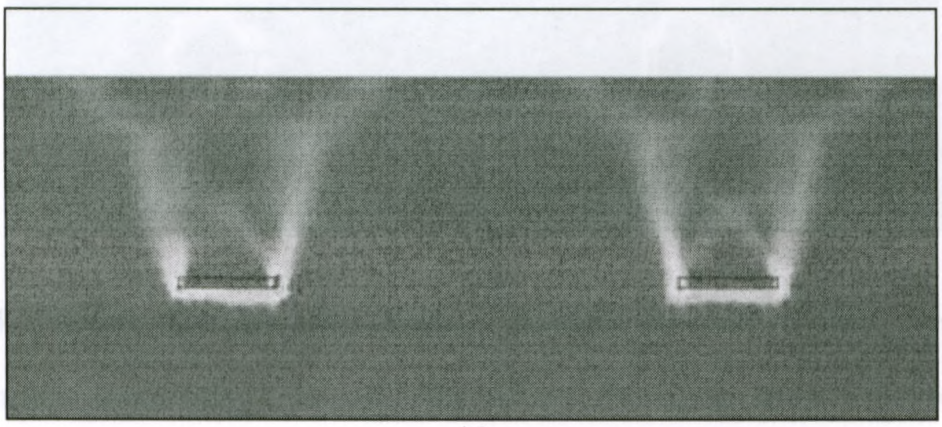

(c)

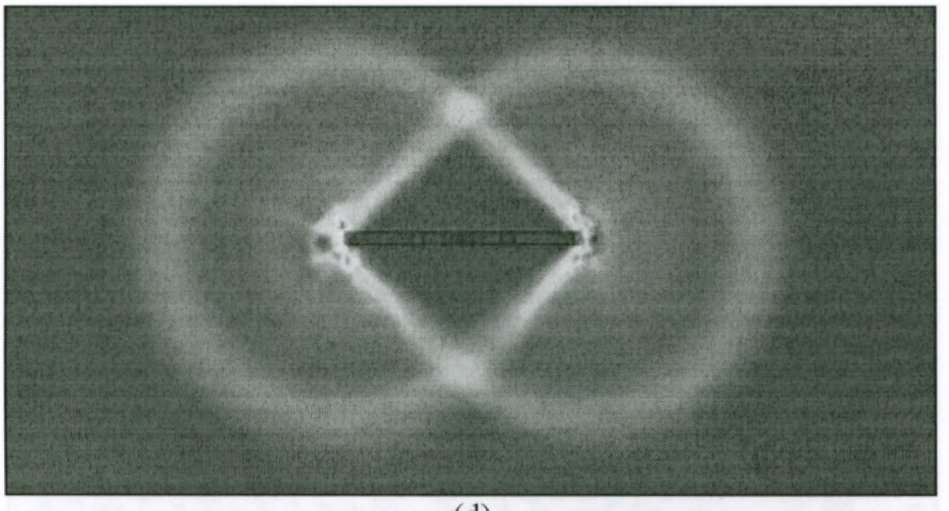

(d)

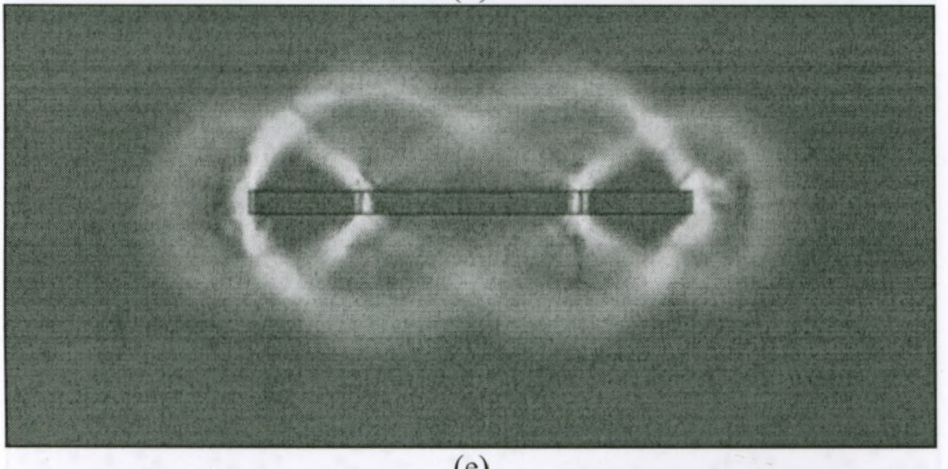

(e)

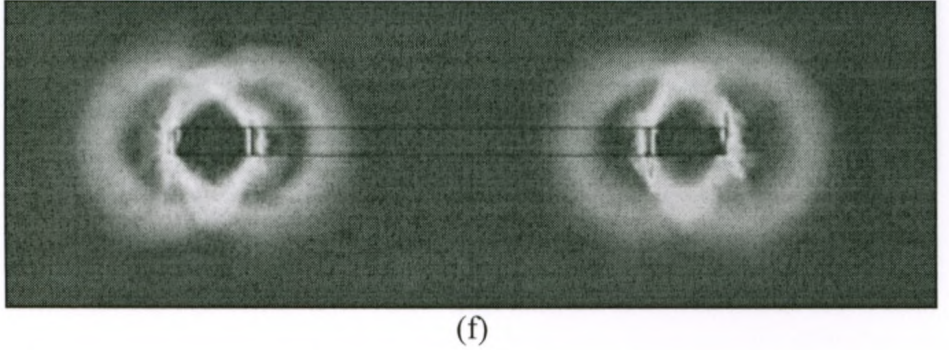

(f)

Figure B. 4: Incremental strain-shear shading diagrams for fully bonded normally-loaded horizontal anchors at (a) $H/B = 1$, $S/b = 0.1$, (b) $H/B = 1$, $S/b = 2$; (c) $H/B = 1$, $S/b = 4$; (d) $H/B = 5$, $S/b = 0.1$; (e) $H/B = 5$, $S/b = 2$ and (f) $H/B = 5$, $S/b = 5$

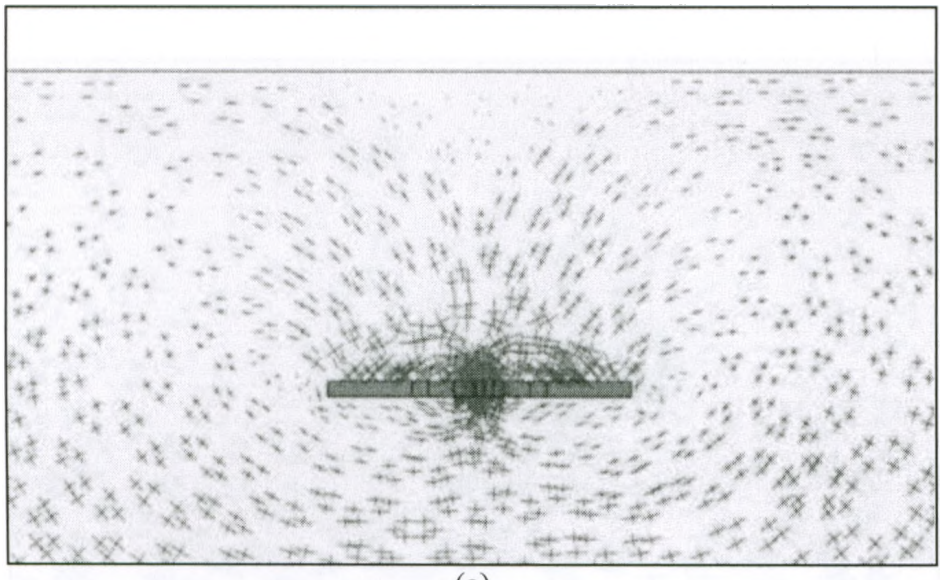

(a)

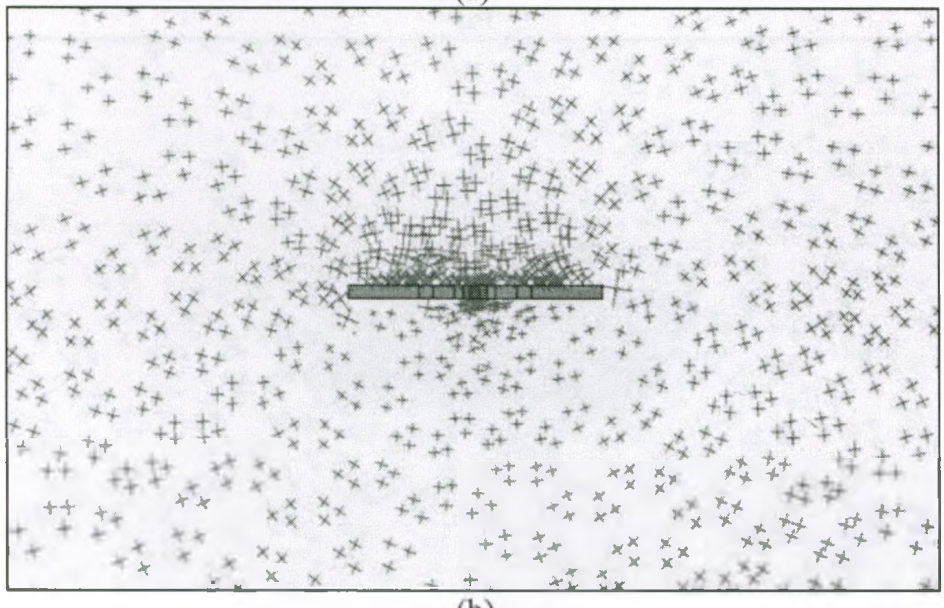

(b)

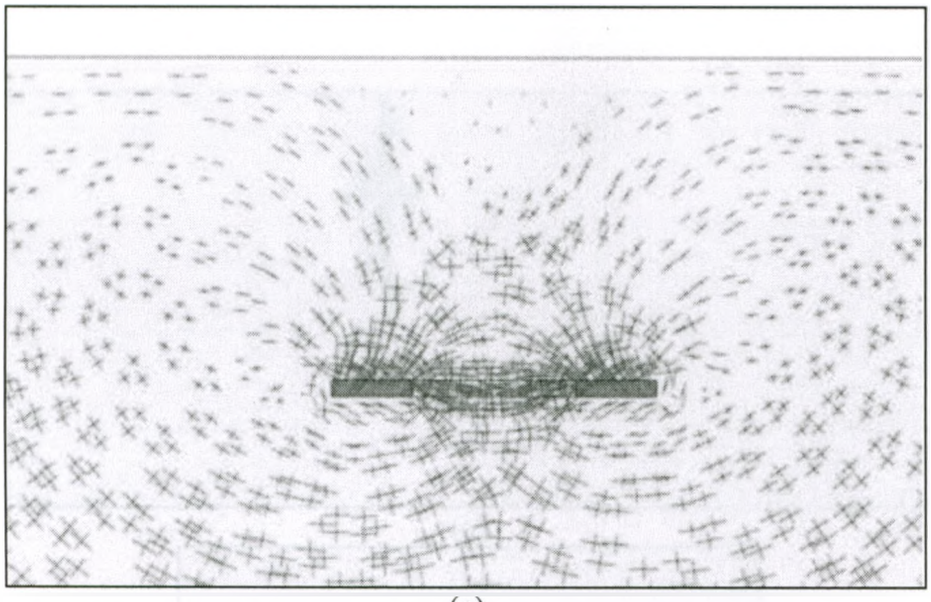

(c)

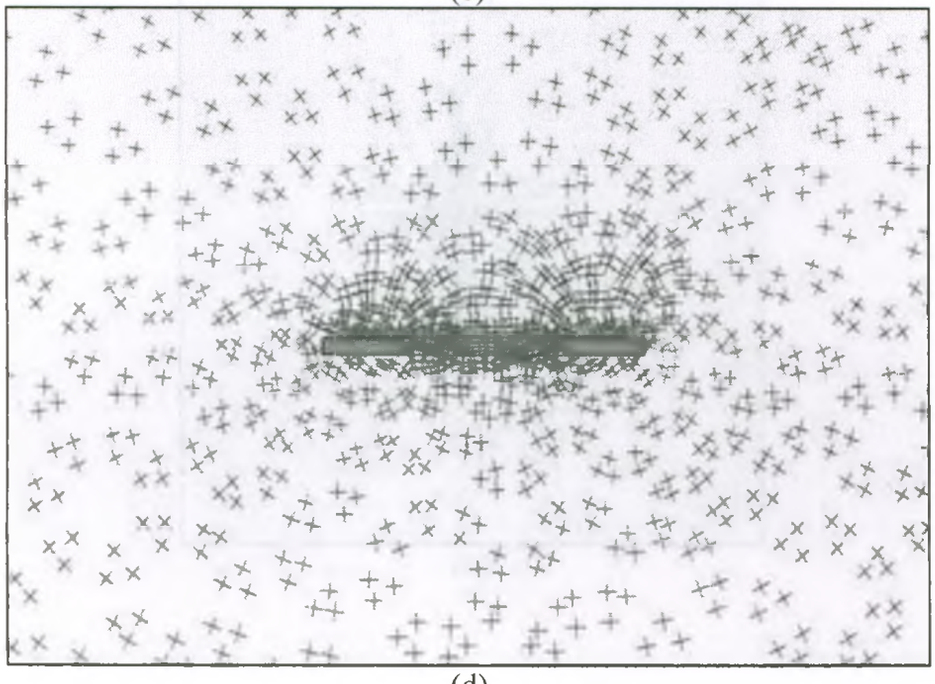

(d)

Figure B. 5: Incremental strain-principal stresses directions diagrams for fully bonded horizontal anchors subjected to 45° inclined loads for (a) $H/B = 1$, $S/b = 0.1$, (b) $H/B = 5$, $S/b = 0.1$, (c) $H/B = 1$, $S/b = 2$ and (d) $H/B = 5$, $S/b = 2$

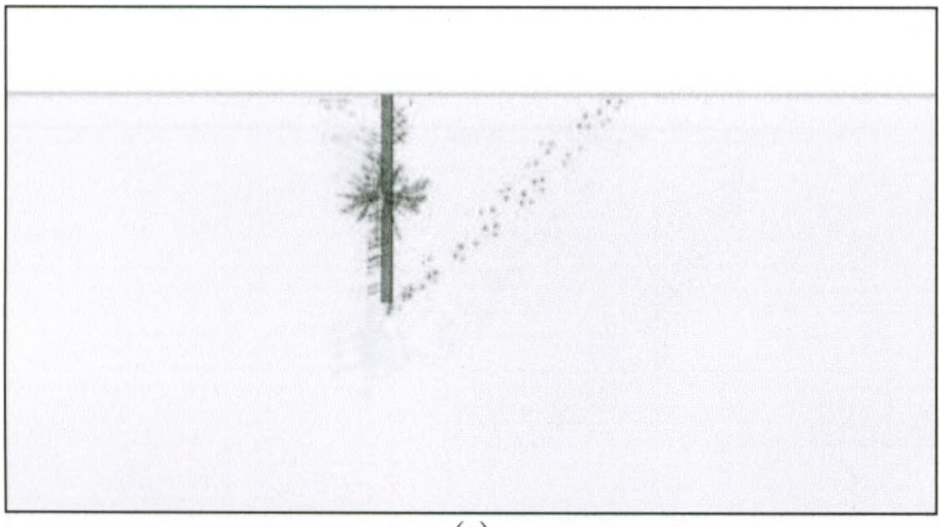

(a)

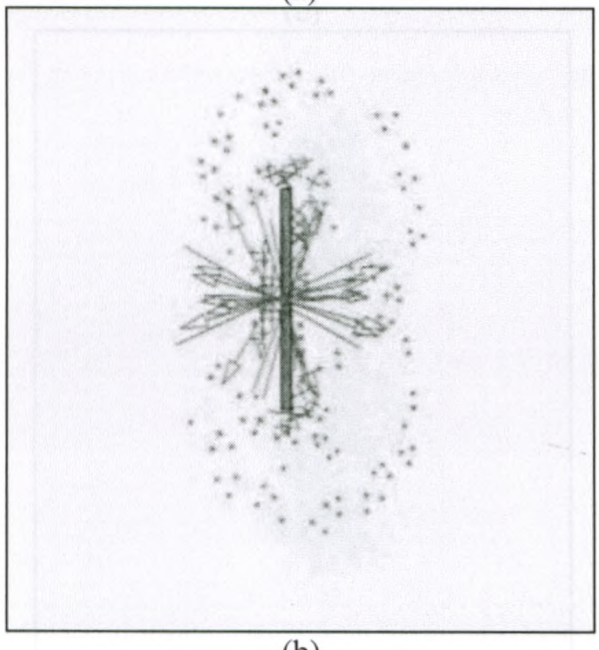

(b)

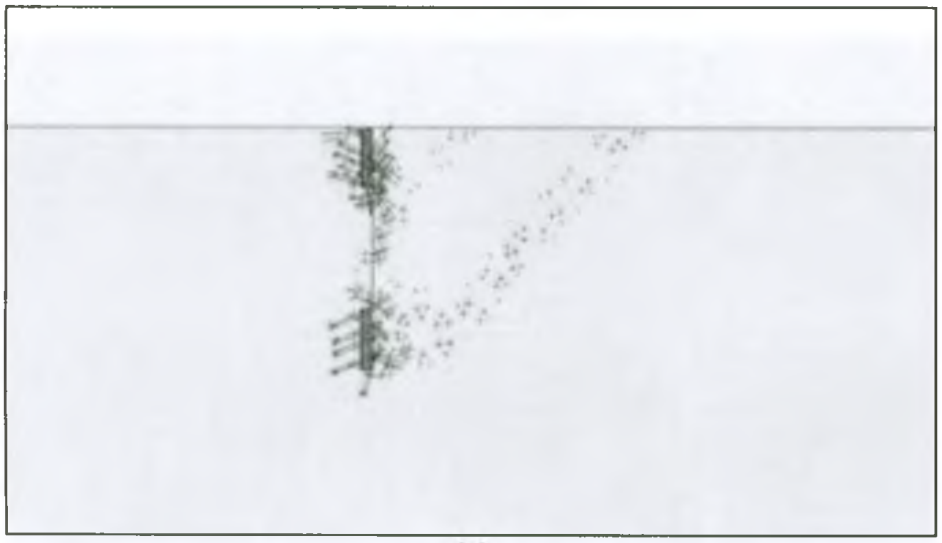

(c)

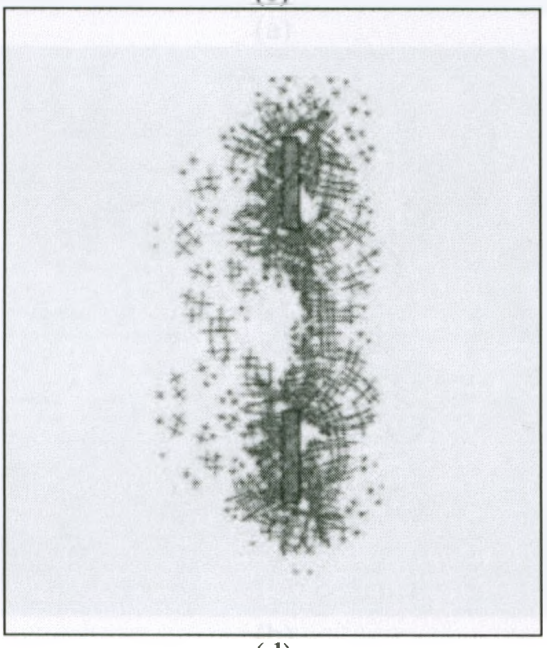

(d)

Figure B. 6: Incremental strain-principal stresses directions diagrams for fully bonded horizontal anchors subjected to 45° inclined loads for (a) $H/B = 1$, $S/b = 0.1$; (b) $H/B = 5$, $S/b = 0.1$ (c) $H/B = 1$, $S/b = 2$ and (d) $H/B = 5$, $S/b = 2$

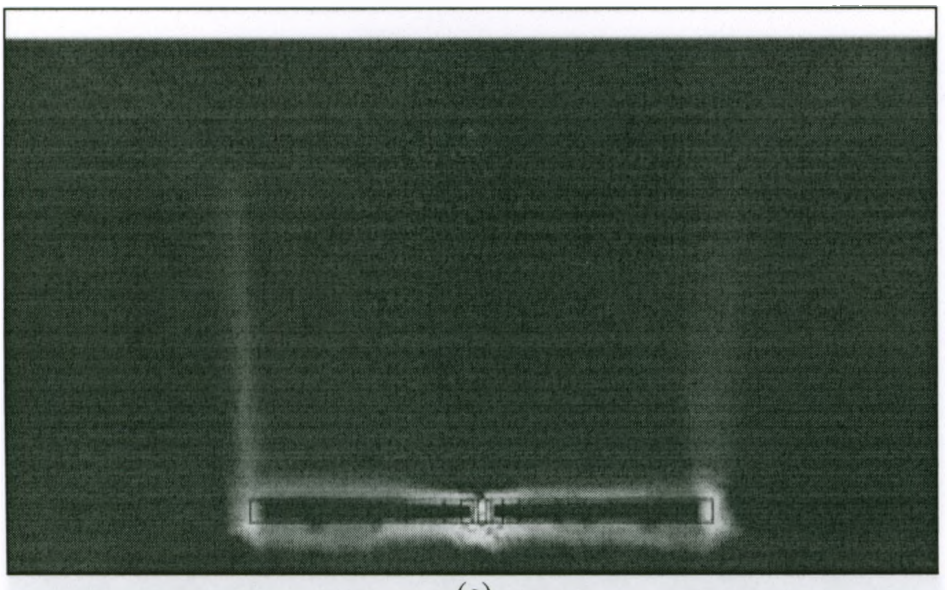

(a)

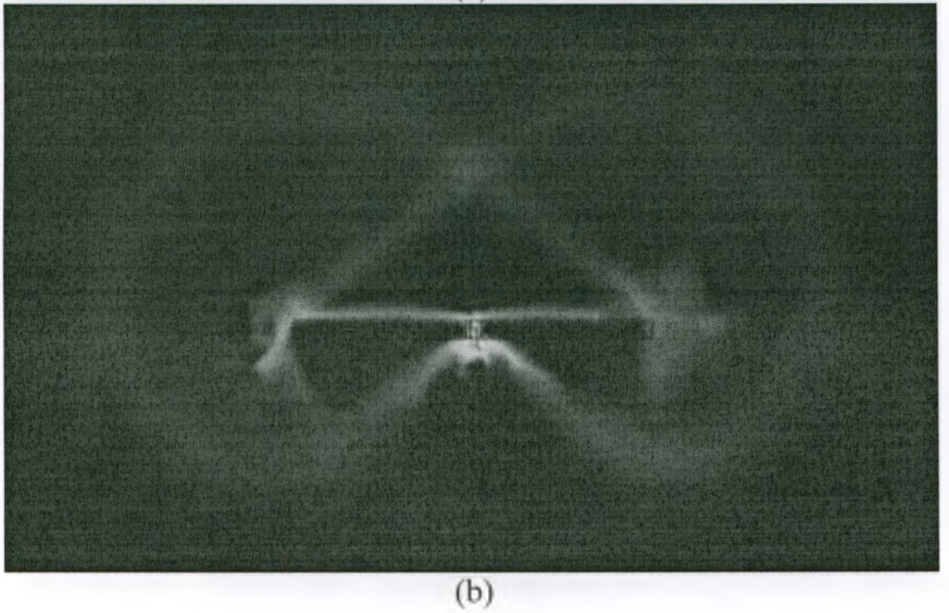

(b)

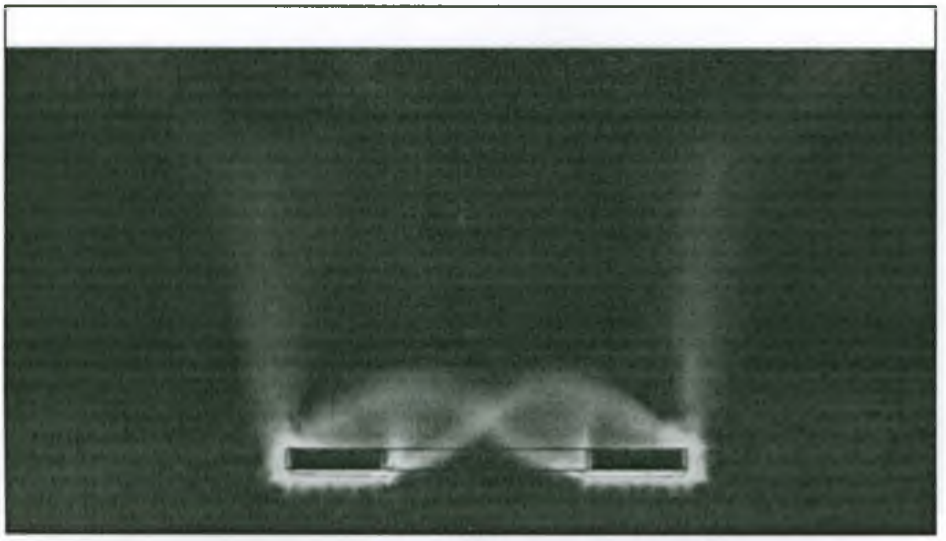

(c)

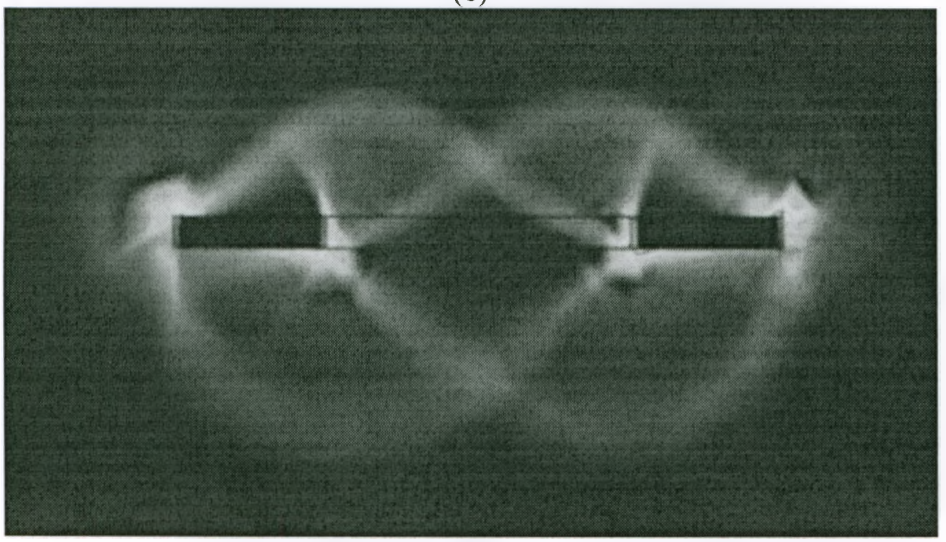

(d)

Figure B. 7: Incremental strain-shear shading diagrams for fully bonded horizontal anchors subjected to 45° inclined loads for (a) $H/B = 1$, $S/b = 0.1$, (b) $H/B = 5$, $S/b = 0.1$, (c) $H/B = 1$, $S/b = 2$ and (d) $H/B = 5$, $S/b = 2$

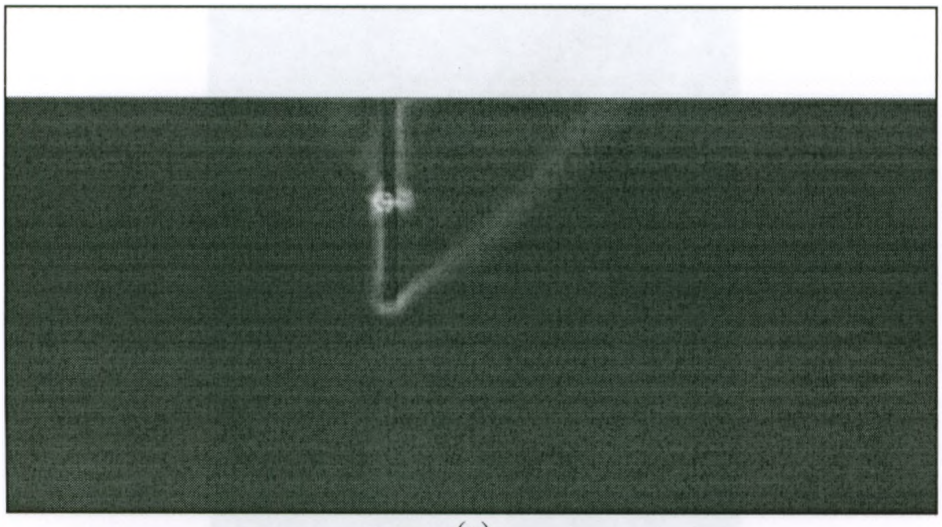

(a)

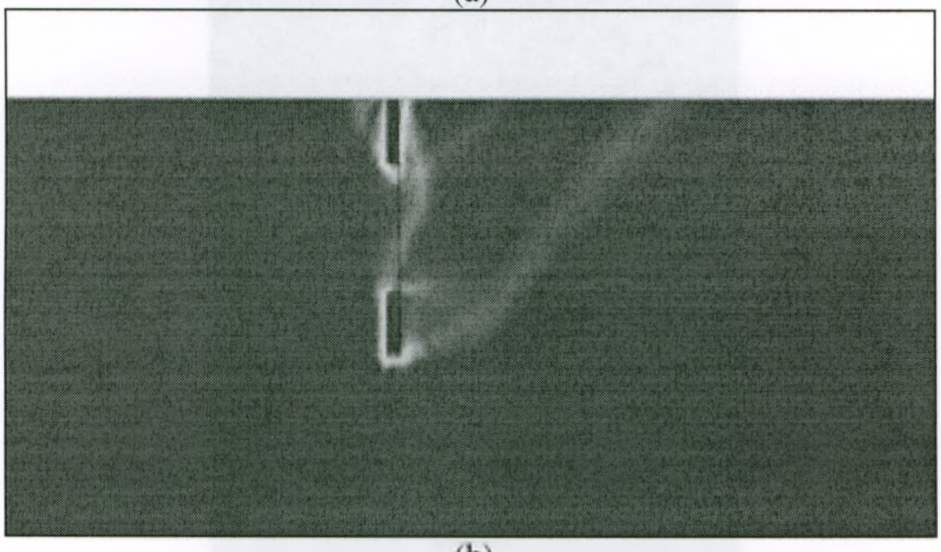

(b)

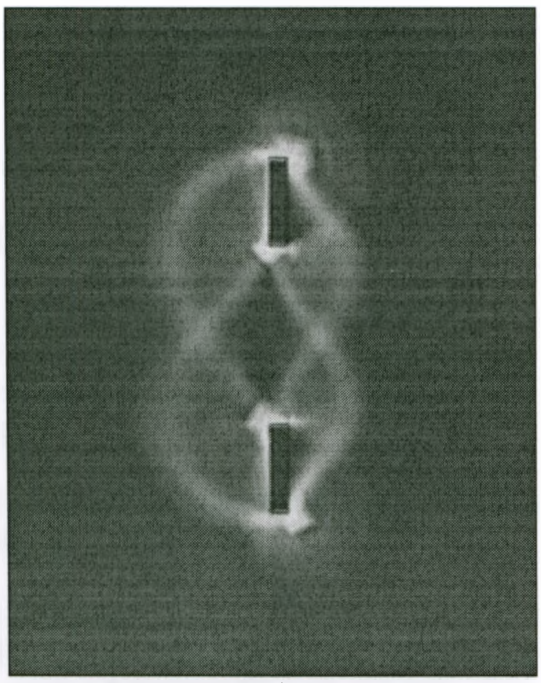

(c)

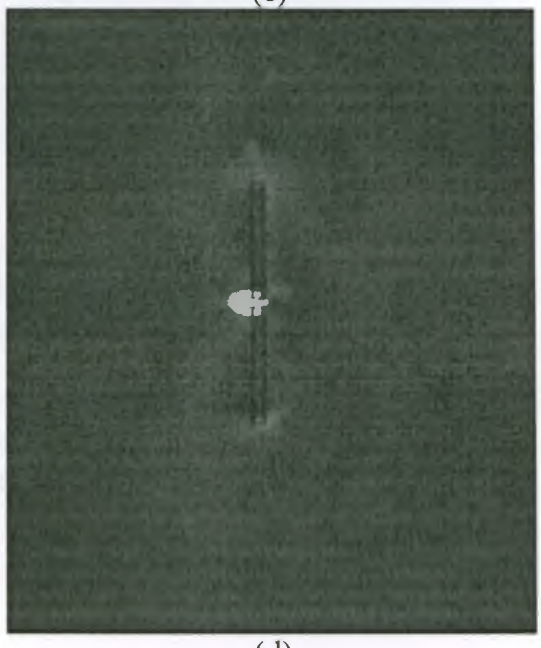

(d)

Figure B. 8: Incremental strain-shear shading diagrams for fully bonded horizontal anchors subjected to 45° inclined loads for (a) $H/B = 1$, $S/b = 0.1$; (b) $H/B = 5$, $S/b = 0.1$ (c) $H/B = 1$, $S/b = 2$ and (d) $H/B = 5$, $S/b = 2$